Compact seasonal PCM heat storage for solar heating systems

Dannemand, Mark; Furbo, Simon; Fan, Jianhua

Publication date:
2015

Document Version
Publisher's PDF, also known as Version of record

Compact seasonal PCM heat storage for solar heating systems

Mark Dannemand

PhD Thesis

Department of Civil Engineering
2015

DTU Civil Engineering Report R-344

DTU Civil Engineering
Department of Civil Engineering

Compact seasonal PCM heat storage for solar heating systems

Mark Dannemand

PhD Thesis

29/2/2016

DTU.BYG

Supervisors:
Associate Professor Simon Furbo, DTU Civil Engineering, Denmark
Associate Professor Jianhua Fan, DTU Civil Engineering, Denmark

Assessment Committee:
Associate Professor Toke Rammer Nielsen, DTU Civil Engineering
Senior Scientist Hermann Schranzhofer, Graz University of Technology, Austria
Principal Engineer, Louise Jivan Shah, Haldor Topsøe A/S, Denmark

Compact seasonal PCM heat storage for solar heating systems

Publisher: Department of Civil Engineering,
Technical University of Denmark,
Brovej, building 118, 2800
Kgs. Lyngby, Denmark

ISBN: 9788778774354
ISSN: 1601-2917

Report: BYG R-344

Preface

This thesis was submitted as a partial fulfilment of the requirements for the Degree of Doctor of Philosophy at the Technical University of Denmark, Department of Civil Engineering. The thesis is the result of three years of research in seasonal thermal energy storage with phase change materials for solar heating systems.

The thesis is based on a number of journal and conference articles and consists of two parts. Part I of the thesis summarizes the main methods and results of the research and provides a perspective for future development. Part II of the thesis consists of a number of published articles and submitted articles under review.

Acknowledgments

I would like to thank Simon Furbo and Jianhua Fan for always being open for supervision and scientific discussions.

I would like to thank the entire solar research group in the Section of Building Energy at the Department of Civil Engineering at Technical University of Denmark for being nice colleagues, for their friendship and sharp but well-meaning critique of my dissemination work.

I would like to thank the technical personnel at the Department of Civil Engineering at Technical University of Denmark including Martin Dandanell, Robert Svan, Claus Aagaard, Troels V. Kristensen, Lars Kokholm, and Christian Rasmussen for supporting me in building up experiments and recording data.

I would like to thank H.M. Heizkörper GmbH & Co. KG and Christian Muhr for supplying the cylindrical heat storage units for testing.

I would like to thank Nilan A/S and Henry Sørensen for building up flat prototype heat storage units for our testing.

I would like to thank all the colleagues in the COMTES consortium and especially Hermann Schranzhofer and the Christoph Moser from TU Graz for their collaboration in the development of the flat storage prototype units and discussions.

I would like to thank Ana Lazaro, Monica Delgado, Conchita Peñalosa, Mateo de Guadalfajara and the rest of GITSE research group at University of Zaragoza for hosting me during my 3 moths research stay, sharing knowledge and letting me use their laboratory.

I would like to thank Professor Svend Svendsen for supervising in scientific writing.

I would like to thank the experts in the IEA Task 42 network for fruitful discussions and sharing knowledge during the experts meeting.

I would like to thank the Danish Energy Agency for financing the PhD study.

Mark Dannemand

Kgs. Lyngby, February 29th, 2016.

Abstract

Space heating of buildings and preparation of domestic hot water accounts for a large part of the society's energy consumption. Solar radiation is an abundant and renewable energy source which can be harvested by solar collectors and used to cover heating demands in the built environment. The seasonal availability of solar energy does however not match with the heating demands in buildings which typically are large in winter periods when limited solar energy is available. Heat can be stored over a few days in water stores but continuous heat losses limits the storage periods. The possibility of storing heat from summer where solar energy is widely available to winter periods where the heating demands are large, allows for implementing more renewable energy in our energy system.

The phase change material (PCM) sodium acetate trihydrate (SAT) melts at 58 °C. The melting process requires a significant amount of energy. When completely melted, SAT can cool down below the melting temperature and remain in liquid state. When the SAT remains in this supercooled state at ambient temperature, the energy used for the melting process is stored without any additional heat losses occurring. When the solidification of the supercooled SAT is started, the temperature of the SAT rises to the melting temperature and the stored heat is released. Utilizing this principle makes it possible to store heat seasonally.

A number of problems, barriers and proposed solutions for operating a storage based on stable supercooled SAT have been identified. Key problems include phase separation of SAT which causes the heat storage potential to be reduced over repeated heating and cooling cycles. This problem can be reduced by making PCM composites of the SAT with extra water or thickening agents. Another key problem is achieving stable supercooling of the PCM in the storage period. The supercooling stability can be compromised by local high pressures in the storage tanks or by external particles coming in contact with the supercooled SAT. A closed PCM chamber which can operate with minimal pressure changes caused by the changing density of the SAT during heating and cooling have shown increased stability of supercooling.

Two differently designed heat storage prototypes in steel and stainless steel with different PCM composites have been tested under controlled laboratory conditions. One design was a flat rectangular unit consisting of a 5 cm high PCM chamber with heat exchangers on the outer surfaces. This design was tested with 200 kg SAT with extra water and with 220 kg of SAT with the thickening agent carboxymethyl cellulose. Supercooling was stable for up to two months in one test with this unit when an external expansion device allowed for operating the storage with minimal pressure built up. Stable supercooled failed in some test cycles.

Cylindrical shaped units with a height of 1.5 meters were tested with 116 kg SAT with extra water and with SAT with the thickening agent Xanthan rubber. Supercooling was achieved for shorter periods in these units in few of the test cycles. Spontaneous solidification started in these prototypes due to the design of the inner surfaces of the PCM chamber and the method for handling the expansion of the PCM.

By testing the prototype units it was found that the heat content of SAT with extra water was reduced over the repeated test cycles. The heat contents of the SAT mixtures with thickening agents were stable over the test cycles. Higher heat content and discharge powers were achieved in the units with SAT and thickening agents. The heat transfer was lower in the units with SAT and thickening agents during charge due to a reduced heat transfer by convection in the thickened PCM.

Investigations by a simple heat loss method on samples of 200 g SAT with additives have elucidated possible ways to avoid phase separation and optimize the heat stored in the supercooled SAT. It was found that composites of SAT with thickening agents or liquid polymers had the highest heat content of the investigated additives.

Investigations of SAT composites with extra water, thickening agents and graphite elucidated the thermal conductivity and the solidification behavior in bulk size samples. It was found that thickening agents had an effect on where cavities were formed during the solidification and cooling and the associated contraction of the PCM. Graphite flakes showed to have better effect on increasing thermal conductivity in SAT composites compared to graphite powder. The amount of thickening agents required to keep the graphite suspended and evenly distributed in the SAT composite was also elucidated.

Overall, the research has shown that it is possible to utilize stable supercooling of SAT for seasonal heat storage in actual application sized units. Furthermore, investigations have elucidated the potential for increasing the performance of a storage by using SAT composites with additives.

Resumé

Rumopvarmning i bygninger og opvarmning af brugsvand står for en stor del af samfundets energiforbrug. Solenergi er en rigt forekommende og vedvarende energikilde som kan opfanges af solfangere og bruges til at dække varmebehov i bebyggelser. Den sæsonmæssige tilgængelighed af solenergi passer ikke sammen med perioder med opvarmningsbehov i bygninger hvilke typisk er store i vinterperioden når kun begrænset solenergi er til rådighed. Varme kan lagres over få dage i varmelagre med vand men et kontinuerligt varmetab begrænser den mulige lagringstid. Muligheden for at lagre varme fra sommer hvor solenergi er rigt tilgængeligt, til vinter med store varmebehov, muliggør integration af mere vedvarende energi i vores energisystemer.

Faseændringsmaterialet (PCM) natriumacetat trihydrat (SAT) smelter ved 58 °C. Smelteprocessen optager en betydelig mængde energi. Når SAT er fuldt smeltet kan det køle ned under smeltepunktet og forblive i flydende tilstand. Når SAT forbliver i denne underafkølede tilstand ved samme temperatur som omgivelserne er den energi optaget i smelteprocessen lagret uden at der forekommer yderlige varmetab. Når størkningen af det underafkølede SAT startes stiger temperaturen af det til smeltepunktet og den lagrede energi friviges. Ved at udnytte dette princip er det muligt at lagre varme fra sommer til vinter.

En række problemer, barrierer og mulige løsninger til at styre et varmelager baseret på stabil underafkøling af SAT er blevet identificeret. Nøgleproblemer inkluderer faseseparation af PCM'et hvilket medfører at lagringspotentialet bliver reduceret over gentagende opvarmnings- og afkølingscykler. Dette problem kan reduceres ved at bruge PCM blandinger med ekstra vand eller fortykkelsesmidler. Et andet nøgleproblem er at opnå stabil underafkøling af PCM'et i lagringsperioden. Stabiliteten kan blive kompromitteret af lokale høje tryk i PCM lagertanken eller ved at partikler udefra kommer i kontakt med det underafkølede SAT. En lukket PCM beholder med minimale trykændringer forårsaget af densitetsændringen af SAT ved opvarmning og afkøling har vist øget stabilitet af underafkølingen.

To forskelligt designet varmelagerprototyper i stål og rustfrit stål med forskellige PCM blandinger er blevet testet under kontrollerede laboratorieforhold. Et design var en flad rektangulær enhed bestående af et 5 cm højt PCM kammer med varmevekslere på de ydre overflader. Dette design blev testet med 200 kg SAT med ekstra vand og med 220 kg SAT med fortykkelsesmidlet carboxymethyl cellulose. Underafkøling var stabil i op til to måneder i en test med enheden. En ekstern ekspansionstank tillod at et minimalt tryk blev opbygget i varmelageret ved opvarmningen. Stabil underafkøling mislykkedes i nogle testcykler.

Cylinderformede enheder med en højde på 1,5 meter blev testet med 116 kg SAT med ekstra vand og med SAT med fortykkelsesmidlet Xanthan gummi. Underafkøling blev opnået i kortere perioder med disse enheder i enkelte testcykler. Spontan størkning startede i disse prototyper pga. designet af de indre overfalder af PCM kammeret og metoden til at håndtere udvidelsen af PCM'et.

Ved at teste prototype enhederne blev det konstateret at varmeindholdet af SAT blandingen med ekstra vand blev reduceret over gentagende testcykler. Varmeindholdet af SAT blandinger med fortykkelsesmidler var stabile over gentagende testcykler. Højere varmeindhold og afladningseffekt blev opnået i enhederne med SAT og fortykkelsesmidler. Varmeoverføringsevnen var lavere i enhederne med SAT og fortykkelsesmidler pga. reduceret varmeoverføring ved konvektion i det fortykkede PCM.

Undersøgelser vha. en simpel varmetabsmetode med prøver af 200 g SAT blandinger med tilsætningsstoffer belyste hvordan det bedst var muligt at eliminere faseseparation og optimere varmeindholdet i underafkølet SAT. Det blev konstateret at blandinger med fortykkelsesmidler eller flydende polymerer havde det højeste varmeindhold.

Undersøgelser af SAT blandinger med ekstra vand, fortykkelsesmiddel og grafit belyste varmeledningsevnen i større prøvestørrelser og opførslen ved størkning. Det blev konstateret, at fortykkelsesmidlet havde indflydelse på hvor hulrum blev dannet ved størkning, afkøling og den tilhørende sammentrækning af PCM'et. Grafitflager viste sig at have en bedre effekt på at forbedre varmeledningsevnen i SAT blandinger sammenlignet med grafitpulver. Andelen af fortykkelsesmiddel som var nødvendig for at fastholde grafitten jævnt fordelt in SAT blandingerne er også blevet belyst.

Alt i alt har forskningen vist, at det er muligt at udnytte stabilt underafkølet SAT til sæsonvarmelagring i varmelagringsenheder i praktisk anvendelige størrelser. Ydermere har undersøgelserne belyst mulighederne for at forbedre ydeevnen af SAT i et varmelager vha. tilsætningsstoffer.

Table of Contents

Part I – Introduction, summary and perspective

1 Introduction

Solar energy has the potential to become a key energy source in future energy systems. It is a renewable energy source which can be converted into electrical energy or thermal energy. Integrating more renewable energy in our energy systems will reduce the need for fossil fuels. The use of fossil fuels emits greenhouse gasses and is associated with environmental pollution and destruction of wildlife habitats. A reduction of greenhouse gas emissions will reduce the risk of irreversible climate changes [1,2]. Shifting away from fossil fuels to renewable energy resources clearly has environmental value. Locally generated renewable energy also has the potential to make nations independent of imported resources from unstable regions of the world. This could also lead to stabile and more predictable energy prices.

1.1 Background

Production of heat accounts for approximately 50 % of the world's energy consumption [3]. A major part of this demand is for heating of buildings and preparation of domestic hot water. The temperature requirements for these heating purposes are relatively low and can easily be supplied by already marketed solar collectors with a high efficiency. There is however a mismatch between the periods where solar energy is abundant, typically in summer, and when heating demand in buildings is large, typically in winter. Heat storage is needed to solve this mismatch between supply of solar energy and heating demands. Sensible heat water storage is typically used to bridge shorter gaps between fluctuating supply and demand. This could be heat storage from day to night or storage over a few days.

Solar combi-systems for space heating and domestic hot water preparation can cover up to 30 % of the heating demand in single family houses in Denmark with smaller sized water stores [4]. Alternative storage technologies are needed for longer storage periods. If heat is stored long-term, for example from summer to winter in a seasonal heat storage, the solar fraction of the single family house can be increased. Theoretically, houses can be self-sufficient with solar energy for heating when the seasonal heat storage is efficient and large enough. In passive houses seasonal heat storage has been shown to be economical feasible [5].

In larger centralized systems, where heat is supplied to buildings by district heating networks, very large sensible water pit stores have shown to be a feasible storage technology [6–8]. However, in decentralized heating systems, for example in single family households, sensible water stores need to be impractical large to work as seasonal heat storages.

Latent heat storages with phase change materials (PCM) are being researched extensively as an alternative to the sensible heat storage technology [9–56]. The PCM for a store is chosen based on the melting point and the required temperature levels for the application. The phase change process takes up a significant amount of energy compared to the sensible heat of a material, especially if the applied temperature range is narrow. The latent heat stores can therefore have higher energy densities compared to sensible heat water stores because the latent heat of fusion is utilized. This can lead to better performing stores and an increased coverage of the demand by the solar heating system [57–59].

1.2 State of the art

Thermal energy storage has been identified to play an important role in achieving the European Union's targets for renewable energy and energy efficiency. The European Commission has therefore funded several large research projects through the Seventh Framework Programme for Research and Technological Development running between 2012 and 2016. These project aims to develop and demonstrate new heat storage technologies. The SAM.SSA project aims to develop new materials with better thermal properties than existing PCMs [60]. SoTherCo aims to demonstrate thermo-chemical storage based on hydration/dehydration of salt in large scale [61]. MERITS aims is to build a prototype of a fully functioning compact rechargeable heat battery that would fit in for example a cellar also based on thermo-chemical reactions [62]. The COMTES project has three development lines [63]. Line A focuses on thermochemical storage with zeolite, Line B focuses on storage based on liquid absorption and Line C focuses on storage with supercooled sodium acetate trihydrate. Common for all projects is that the technologies have the potential to be used for compact seasonal heat storage of solar energy.

1.3 Storage with supercooling

The inorganic salt hydrate sodium acetate trihydrate (SAT) has the chemical formula $NaCH_3C00\cdot 3H_2O$. It is a low cost material and it is non-harmful to the environment. This PCM has been investigated extensively because it has a relative high latent heat of fusion at a temperature level which works well with space heating and preparation of domestic hot water and the melting temperature fits well with solar heating systems [64–110].

Sodium acetate trihydrate melts at 58 °C. The latent heat of fusion at the melting point is 264 kJ/kg [13]. When SAT is completely melted, it has the ability of cool down below the melting point without solidifying, hence not releasing the latent heat of fusion. When the melted SAT remains in this supercooled state in temperature equilibrium with the ambient, the latent heat of fusion is stored without a continuous heat loss. The crystallization of supercooled SAT will start when a seed SAT crystal is present in the solution. The solidification will spread rapidly from this nucleation point to the entire volume of PCM. The latent heat of fusion is then released and the temperature of the SAT increases. This released heat can be utilized for heating purposes. When SAT is melted by solar heat in the summer and stored in supercooled state until winter and then used for heating, seasonal heat storage of solar heat is realized. The storage principle has been described in previous research [111–116].

The supercooled state is a metastable state and can be affected by various external factors. Spontaneous nucleation in the storage period needs to be avoided and the stability of the supercooling over long periods of time is essential for the storage principle.

In many previous research projects this supercooling has been seen as an undesired effect in PCMs as it kept the latent heat of fusion from being released when the PCM storage was discharged. Various ways to avoid supercooling or to initiate nucleation have been investigated by several researchers [112–115].

1.4 Aim and scope

The aim of the research carried out within this PhD study was to elucidate the potential of seasonal heat storage by utilizing the concept of stable supercooling of sodium acetate trihydrate in storage unit sizes which can be used in applications for heating of single family houses. This includes:

- Identify or develop and investigate PCM composites based on sodium acetate trihydrate with optimized thermal properties including:
    - Testing the cycling and thermal stability of the PCM composites related high stable energy content.
    - Testing the stability of the supercooling of the PCM composites over long periods.
- Elucidate parameters which affect heat transfer in bulk PCM composites including:
    - Solidification behavior in bulk sized PCM composites.
    - Additives for enhancing thermal conductivity.
- Identify problems and test solutions for obtaining stable supercooling in large unit sizes.
- Evaluate the performance of heat storage prototype units with SAT composites under controlled conditions in a laboratory including:
    - Heat content measurements and cycling stability.
    - Heat exchange capacity rates.
    - Stability of supercooling.
- Identify areas that can improve the performance of the tested storage prototypes.
- Show that it is possible to achieve complete melting and stable supercooling of SAT composites in heat storage prototype units with heat generated by solar collectors.

The research was partly done by experiments on small sample sizes with 100 to 1300 g of PCM. The small scale investigations resulted in development of PCM composites with desired characteristics which were tested in large heat storage prototype units with 100 to 220 kg of PCM.

The research included the development of a heat storage prototype unit. Several unit designs were built and tested. A number of design iterations led to the final tested design. The performance of the prototype units under controlled laboratory test conditions was elucidated and characterized. After the laboratory testing the developed units were implemented in a demonstration system in order to show if full melting and stable supercooling could be achieved with solar collectors as heat source.

A second heat storage unit design, supplied from an external partner, was likewise tested and characterized under laboratory conditions. Two units from the external partner were tested.

Further, numerical investigations were done with TRNSYS and CFD simulations.

1.5 Structure of the thesis

Part I present an introduction, a summary of the methods and main results of the research and include possibilities for future development and an application perspective.

Part II consists of a number of published and submitted journal and conference articles with details of the research.

Paper 1: *Long term thermal energy storage with stable supercooled sodium acetate trihydrate*, Mark Dannemand, Jørgen M. Schultz, Jakob Berg Johansen, Simon Furbo, Applied Thermal Engineering, Vol. 91 pp. 671–678, 2015, doi:10.1016/j.applthermaleng.2015.08.055.

Paper 2: *Solidification behaviour and thermal conductivity of bulk sodium acetate trihydrate mixtures with thickening agents and graphite powder*, Mark Dannemand, Jakob Berg Johansen, Simon Furbo, Solar Energy Materials and Solar Cells, Vol 145, Part 3, pp. 287–295, 2016, doi:10.1016/j.solmat.2015.10.038.

Paper 3: *Experimental investigations on prototype heat storage units utilizing stable supercooling of sodium acetate trihydrate mixtures,* Mark Dannemand, Janne Dragsted, Jianhua Fan, Jakob Berg Johansen, Weiqiang Kong, Simon Furbo*,* Applied Energy, Vol 169, pp. 72-80, 2016, doi:10.1016/j.apenergy.2016.02.038.

Paper 4: *Experimental investigations on cylindrical latent heat storage units with sodium acetate trihydrate composites utilizing supercooling,* Mark Dannemand, Jakob Berg Johansen, Weiqiang Kong, Simon Furbo, Submitted to Applied Energy.

Paper 5: *Experimental investigations on heat content of supercooled sodium acetate trihydrate by a simple heat loss method,* Weiqiang Kong, Mark Dannemand, Jakob Berg Johansen, Jianhua Fan, Janne Dragsted, Gerald Englmair, Simon Furbo, Submitted to Solar Energy Materials and Solar Cells.

Paper 6: *Validation of a CFD model simulating charge and discharge of a small heat storage test unit based on a sodium acetate water mixture,* Mark Dannemand, Jianhua Fan, Simon Furbo, Janko Reddi, ISES Solar World Congress 2013, Energy Procedia, 57 pp. 2451 – 2460, 2014, doi:10.1016/j.egypro.2014.10.254.

Paper 7: *Testing of PCM heat storage units with solar collectors as heat source,* Gerald Englmair, Mark Dannemand, Jakob B. Johansen, Weiqiang Kong, Janne, Dragsted, Simon Furbo, Jianhua Fan, International Conference on Solar Heating and Cooling for Buildings and Industry 2015, Energy Procedia .

2 Theoretical heat content

The theoretical heat storage potential of supercooled SAT can be calculated from its material properties. Equations (1) to (5) elucidate the theoretical heat content of SAT in a storage unit.

The theoretical change of heat content of a heat storage unit for a given charge $E_{charge,theoretical}$ is given by (1). The expression includes the sensible heat of the PCM in solid and liquid phase, the latent heat of fusion of the PCM and the sensible heat of the storage unit heated from a temperature below melting point T_{start} to above the melting point T_{max}.

$$E_{charge,theoretical}(T_{start}, T_{max}) = m \cdot \left((T_{melt} - T_{start}) \cdot c_p(s) + L_f + (T_{max} - T_{melt}) \cdot c_p(l)\right) + C_{module} \cdot (T_{max} - T_{start}) \quad (1)$$

where m is the mass of the PCM, T_{melt} is the melting temperature of the PCM of 58 °C, T_{start} is the storage temperature at the start of the charge, T_{max} is the temperature the heat storage unit reaches during a charge, $c_p(s)$ is the specific heat of the solid PCM, $c_p(l)$ is the specific heat of the liquid PCM, L_f is the latent heat of fusion of the PCM and C_{unit} is the heat capacity of the storage unit including the heat transfer fluid in the heat exchangers.

The theoretical heat content $E_{discharge,theoretical}$ of a heat storage unit for a discharge from melted state at temperature T_{max} to supercooled state at temperature $T_{supercool}$ is given by (2). Just the sensible heat of the liquid PCM and the storage unit material is discharged when discharging without the PCM crystallizing. This assumes that the specific heat of the PCM in supercooled state is similar to the specific heat of the PCM in liquid state.

$$E_{discharge,theoretical}(T_{max}, T_{supercool}) = (m \cdot c_p(l) + C_{unit}) \cdot (T_{max} - T_{supercool}) \quad (2)$$

Equation (3) express the thermal energy stored in the supercooled state $E_{supercool,theoretical}$ at a temperature $T_{supercool}$. This is derived from (1) and (2).

$$E_{supercool,theoretical}(T_{supercool}) = m \cdot \left(L_f - (T_{melt} - T_{supercool}) \cdot (c_p(l) - c_p(s))\right) \quad (3)$$

This shows that energy stored in supercooled state is lower than the latent heat of fusion at the melting temperature and depends on the temperature of the supercooled SAT. The lower the storage temperature of the supercooled SAT, the lower the stored energy.

The storage potential can be calculated from (3) if the temperature of the storage unit at supercooled state $T_{supercool}$ and the final discharge temperature T_{end} after the solidification and discharge are the same.

If the storage is discharged to a different temperature than the supercooled temperature, the discharged energy is corrected for the sensible heat of the storage unit material and the PCM in solid state. This correction is shown by (4).

$$E_{correct,theoretical}(T_{supercool}, T_{end}) = (T_{supercool} - T_{end}) \cdot (C_{unit} + m \cdot c_p(s)) \quad (4)$$

The storage temperature $T_{supercool}$ will be similar to the surrounding temperature of the storage when remaining in supercooled state over a long period. The final discharge temperature T_{end} will depend on the application and may be higher or lower than the supercooled temperature when used for space heating or

domestic hot water preparation. When considering different supercooled storage temperature and final discharge temperature, the theoretical heat content per unit mass of PCM in a storage unit is expressed by (5).

$$E_{content,theoretical}(T_{supercool}, T_{end}) = \frac{E_{supercool,theoretical} - E_{correct,theoretical}}{m} \quad (5)$$

The sensible heat of the of the storage unit material C_{unit} is included in this expression. This must be considered when storage and discharge temperature are different.

The energy content per unit of mass of PCM from 20-90 ˚C is displayed in Figure 1 for the solid, melted and supercooled states. A specific heat capacity for the solid state SAT $c_p(s)$ of 2.1 kJ/kgK, a specific heat capacity for the liquid SAT $c_p(l)$ of 3.0 kJ/kgK [100] and a latent heat of fusion of 264 kJ/kg [13] at the melting temperature of 58 ˚C is used. The used specific heat capacities are averaged to constants at the temperature range derived from Araki [100]. In reality the specific heat capacities vary with temperature.

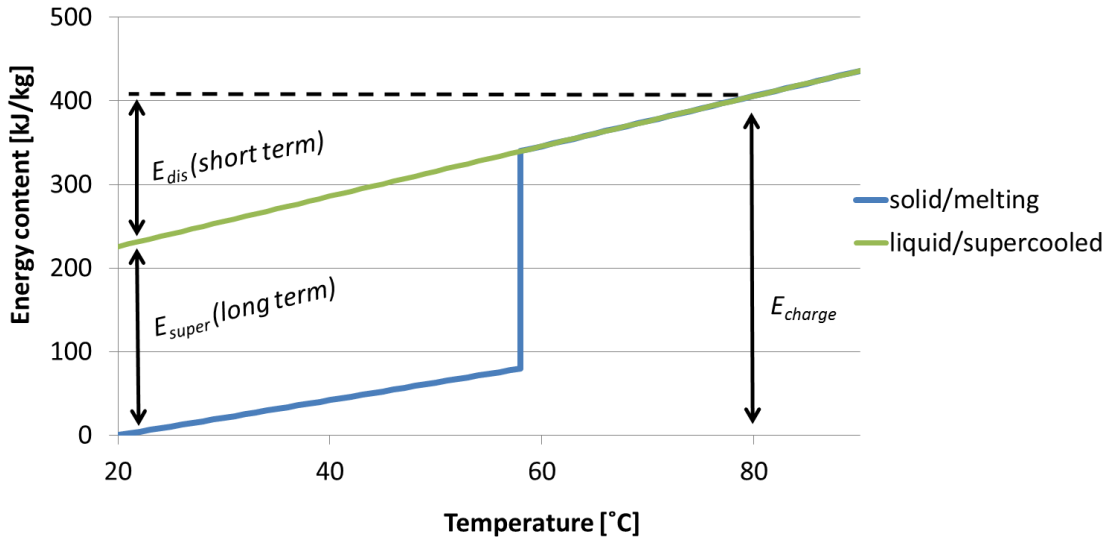

Figure 1. Principle of long term heat storage utilizing stable supercooling and storage potential for sodium acetate trihydrate.

The theoretical heat storage potential of SAT in supercooled state at 20 °C if discharged back down to 20 °C $E_{supercool,theoretical}$ (20 ˚C, 20 ˚C) is 230 kJ/kg. If the SAT is stored in supercooled state at 10 ˚C and discharged down to 30 ˚C after solidification, the theoretical heat storage potential $E_{supercool,theoretical}$ (10 ˚C, 30 ˚C) is 179 kJ/kg. In this case some additional heat will be lost to heating the storage unit material from 10 ˚C to 30˚C. This indicates that a storage unit with as low thermal mass as possible is desired.

3 Experimental and numerical investigations

Experimental investigations were carried out on different scales. The characteristics of SAT mixtures in sample sizes of 100-1300 g were investigated and suggestions of optimized compositions were given. The performance of prototype heat storage units containing 100-220 kg SAT mixtures were investigated under laboratory conditions. A demonstration solar combi-system elucidated the potential to achieve stable supercooling of storage units with SAT mixtures under realistic conditions with solar collectors as heat source. Simulation software elucidated the potential performance of a solar heating combi-system for a single family house including heat storage units with SAT able to supercool. Comparison between experimental investigations and numerical CFD calculations of heating and cooling including phase change of SAT in a small test unit were made.

The experimental setups and the reasoning for the path of development are described in the following sections.

3.1 Composites of sodium acetate trihydrate

One of the key problems of utilizing sodium acetate trihydrate as a heat storage material is phase separation of the incongruently melting phase change material. Phase separation is caused by the fact that the solubility of sodium acetate in water at the melting point of 58 °C is not high enough to dissolve all the sodium acetate in the corresponding crystal water from the sodium acetate trihydrate composition. Therefore, melted SAT just above the melting point consists of a saturated solution of sodium acetate dissolved in water and undissolved sodium acetate. Due to the density difference, the undissolved salt will settle to the bottom of the container if no measure is taken to prevent it. When SAT suffering from phase separation solidifies, all potential SAT crystals will not be formed due to the physical distance between the sodium acetate in the bottom of the container and the water it needs to bind with in the top of the container. This reduces the heat of fusion in practice.

Another key problem of using PCM in heat storage is the relative low thermal conductivity of the PCM itself. The thermal conductivity affects how fast heat is transferred in the PCM especially in the solid state, and will therefore to a high extent influence the charge time and the discharge power of a PCM storage.

Both phase separation and low thermal conductivity may cause the PCM storage to perform worse than it potentially could. The possibility of developing composites of SAT with different additives has therefore been investigated. The research was focused on maximizing the heat content of SAT composites by reducing losses due to phase separation and elucidated a method to enhance the thermal conductivity of SAT composites.

3.1.1 Heat content measurements

The highest possible heat content of the supercooled SAT mixtures is desired in this application. The heat released after solidification of the supercooled SAT mixtures may be lower than the theoretical maximum due to the phase separation. This part of the investigations focused on developing SAT mixtures where the loss of heat storage potential due to phase separation was reduced. A variety of additives to the SAT was tested.

Adding extra water to the SAT may allow for all sodium acetate to dissolve in the water at melted state and thereby possibly avoid phase separation. By studying the phase diagram of the sodium acetate – water mixture [100,121], it can be realized that a composition of approximately 42% water and 58% sodium acetate (SAT with 4% extra water) is required for all sodium acetate to dissolve in the solution at the melting point of 58 °C. In supercooled state at 20 °C a composition of approximately 45% water and 55% sodium acetate (SAT with 10% extra water) is required for all sodium acetate to be dissolved.

Another solution for avoiding phase separation is adding thickening agents to the SAT. These increase the viscosity of the solution, so that the precipitated sodium acetate stays suspended in the solution and does not settle to the bottom. This allows potentially for formation of all SAT crystals after solidification, when the sodium acetate stays near the water it needs to bind with at crystallization. The thickening agents Carboxymethyl Cellulose (CMC) and Xanthan rubber were investigated as additives to SAT.

Figure 2 (a) shows a sample of SAT in supercooled state at ambient temperature which suffers from phase separation. A layer with crystals can be seen in the lower part of the glass jar and a transparent solution can be seen in the upper part of the glass jar. Figure 2 (b) shows a sample of SAT with 10% extra water in supercooled state at ambient temperature. The entire solution is transparent. Figure 2 (c) shows a sample of SAT thickened with 0.5% Xanthan rubber in supercooled state at ambient temperature. The precipitated sodium acetate is suspended in the full height of the sample.

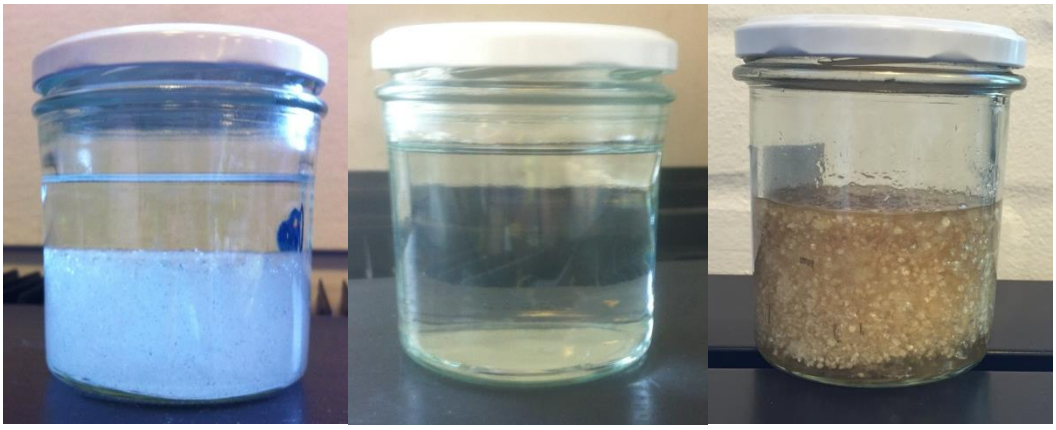

Figure 2. (a) SAT with phase separation.(b) SAT with extra water. (c) SAT with the thickening agent Xanthan rubber

Samples with different percentages of extra water, CMC or Xanthan rubber were prepared in 350 mL glass jars closed with metal lids. A suitable mixing method was necessary when mixing the thickening agents especially Xanthan Gum into the SAT. The Xanthan rubber binds very fast with the water when it is mixed into the samples and jelly chunks were easily formed. To have the Xanthan rubber evenly dispersed in the composite, 90% of the SAT was melted in an oven; the remaining 10% of the SAT was in cold solid granular

state mixed with the Xanthan rubber powder before it was added to the melted SAT little by little while stirring with an overhead mixer. This ensured a uniform mixture. Unwanted air bobbles were easily trapped inside the mixture when stirring the thickened SAT composite in the melted state. Mixing was carried out carefully to avoid this.

The samples of the SAT composites of approximately 200 g each were melted in the oven at 80-90 ˚C. The height of the PCM sample in the glass jars were 5 cm. After the heating they were placed in the ambient temperature at 20-25 °C to cool down to supercooled state.

The samples were then placed in an insulated box and the solidification was initiated by dropping a SAT crystal into the supercooled composite. The temperature developments of the samples were recorded after the solidification.

Beforehand, heat loss coefficients of the glass jars placed in the insulated boxes were determined by having the glass jars with heated water as a reference material cool down to ambient temperature. When the heat loss coefficient of the glass jars in the box was determined, the heat content of the SAT samples could then be determined by recording the temperature development as they cool down.

Figure 3 shows an open box with insulation and hole for placing the glass jars.

Figure 3. Well insulated box for heat content measurements by heat loss method.

Both short and long periods in supercooled state were investigated for the SAT samples with extra water.

An example of the cooling down progress of a SAT mixture is shown in Figure 4. At a temperature of approximately 80 ˚C the sample is placed in the in box. During the first 60 hours the sensible heat of the sample is released and the sample reached ambient temperature. At the 85th hour the solidification of the SAT mixture is initiated and the temperature increases. The heat generated from the solidification of the supercooled SAT sample is released during the following 40 hours.

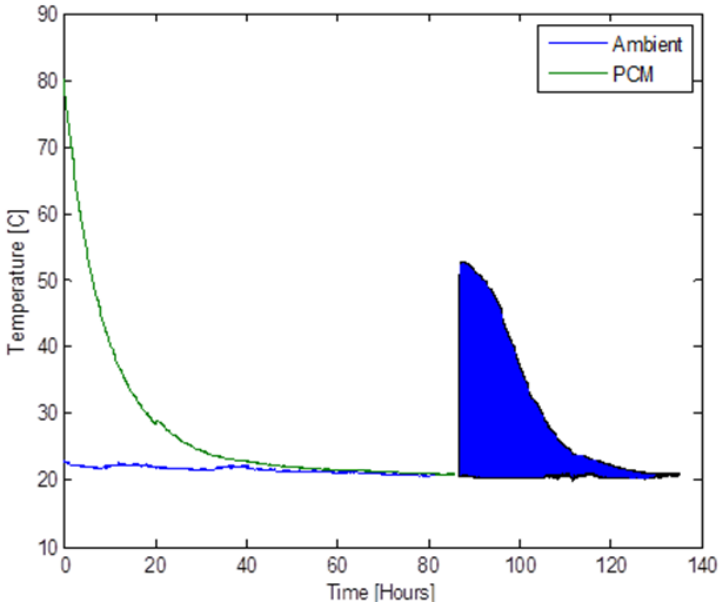

Figure 4. Temperature development of SAT composite sample inside insulated box.

The theoretical maximum heat content of supercooled SAT at 20 ˚C without phase separation calculated by equation (3) is 230 kJ/kg.

The heat loss experiments showed that SAT (40% water, 60% sodium acetate) without additives suffering from phase separation released 162 kJ/kg of heat with short storage periods. With a storage period of 100 days the heat content was further reduced to 100 kJ/kg. Samples of SAT with 4% extra water (42% water, 58% sodium acetate) showed a heat content of 190 – 200 kJ/kg for short storage periods and approximately 160 kJ/kg for longer storage periods. Samples with SAT and 10% extra water (45% water, 55% sodium acetate) showed to have a heat content of 160 – 170 kJ/kg, independent of the storage period.

Samples of SAT with CMC or Xanthan rubber as thickening agents showed to have heat contents up to 215-220 kJ/kg for short storage periods. Mixtures of SAT with 0.3-1.0% Xanthan rubber or 0.4-2.0% CMC resulted in the highest heat content.

The released heat after solidification of supercooled SAT samples with thickening agent was up to 95% of the theoretical potential of SAT.

Further details and results are given in Paper 5 - *Experimental investigations on heat content of supercooled sodium acetate trihydrate by a simple heat loss method*. Kong et al.

3.1.2 Suspension of graphite in thickened SAT composites

Low thermal conductivity of PCMs is a typical limitation when using PCMs in heat stores as it limits the heat transfer between the PCM and the heat transfer fluid [23,27,49,122]. One solution to increase the thermal conductivity of PCMs is to create composites with highly conductive additives. Many researchers have investigated the potential of graphite as additive to PCMs [39]. Some researchers investigated the potential for impregnating graphite matrices with PCM [19,37]. A more simple way is to make a PCM composite with small particles of graphite. In this case the PCM composites can easily be handled and filled into stores even with complex geometries. The characteristics of a PCM composite need to remain relatively homogeneous over its lifetime so that the performance is stable. If small sized particles are part of a PCM composite, it is necessary that the additive stays evenly distributed in the composite and does not settle to the bottom of the container or float to the top of the PCM.

A suspension test for evaluating the ability of different quantities of thickening agents to suspend graphite particles in SAT composites was carried out. Mixtures of SAT and graphite were placed on top of SAT composites with different percentages of thickening agents. The samples were heated to 90 ˚C in an oven and the ability for the thickened composited to keep the graphite suspended on top was evaluated. It was assumed that if the graphite stayed suspended on top of the thickened composite, there was enough thickening agent to keep a uniform mixture. Carboxymethyl cellulose (CMC) and Xanthan rubber were applied as thickening agents. Graphite powder and graphite flakes were used as the highly conductive compound in the investigations. Figure 5 shows three samples of thickened SAT with a SAT and graphite powder layer on top before being placed in the oven.

Figure 5. Three samples of SAT with thickening agent with a layer of graphite and SAT on top.

Figure 6 shows SAT samples with 0.25%, 0.5% and 1% Xanthan rubber with graphite powder on top after 14 days in the oven at 90 ˚C.

Figure 6. SAT samples with 0.25%, 0.5% and 1% Xanthan rubber with graphite powder on top after 14 days at 90 ˚C.

Figure 7 shows SAT samples with 1%, 2.5% and 5% CMC with graphite flakes on top after 14 days in an oven at 90 ˚C.

Figure 7. SAT samples with 1%, 2.5% and 5% CMC with graphite flakes on top after 14 days at 90 ˚C.

The suspension test showed that either 5% CMC or 1% Xanthan rubber was required for composites of SAT to keep graphite powder or graphite flakes suspended on top of the sample over a 14 days period at 90 ˚C.

Further details are given in Paper 2 - *Solidification behaviour and thermal conductivity of bulk sodium acetate trihydrate mixtures with thickening agents and graphite powder*. Dannemand et al.

3.1.3 Thermal conductivity and cavities of SAT composites

The density of solid SAT is 1280 kg/m^3 and the density of liquid SAT is 1450 kg/m^3 [123]. This density difference between the solid and liquid PCM may cause cavities forming in the PCM storage during solidification. These cavities may have an insulating effect reducing the effective thermal conductivity in bulk PCM. The speed at which the solidification of the PCM takes place may also have an effect on the crystal structure, as the PCM contracts in the process. When supercooled SAT solidifies the crystallization happens with a fast moving crystallization front from the point of nucleation. When SAT solidifies without supercooling the crystallization front moves slower as the heat is being released and the temperature drops below the melting point [105]. The crystal structure and the density of the solid may affect the thermal conductivity of the SAT composite. Therefore, in a storage the way the heat exchanger is designed and the cooling rate which is applied may also affect the effective thermal conductivity of the PCM.

The formation of cavities and the effective thermal conductivity of SAT in bulk size samples with 1.3 kg of SAT with different additives were investigated. Samples which had solidified from a supercooled state and samples which solidified without supercooling were compared. Composites with extra water, the thickening agents carboxymethyl cellulose and Xanthan rubber plus graphite powder and graphite flakes were investigated.

Figure 8 shows a solidified 1.3 kg SAT sample with extra water as additive. The samples were prepared by heating the SAT composites in glass jars. One sample of each type of composite was let to supercool to ambient temperature after which the solidification was initiated by opening the jar and dropping a SAT crystal. Other samples of each type cooled down to ambient with the lid open and a SAT crystal was added when the melting temperature of the SAT of 58 ˚C was reached to avoid supercooling. The solidified samples were removed from the glass jars and cut into three layers. The contraction and formation of cavities was observed and the thermal conductivity in the different layers was measured.

Figure 8. 1.3 kg SAT composite sample.

The thermal conductivities were measured with an ISOMET heat transfer analyzer from the company Applied Precision. Figure 9 shows the surface measuring probe on a layer of SAT composite.

Figure 9. Applied Precision surface probe for measuring thermal conductivity on SAT sample.

The location of cavities in the SAT composites after solidification varied depending on the type of additive and whether it solidified with or without supercooling. Single large cavities were typically formed away from the heat transfer surface in the samples without thickening agent and with CMC. When Xanthan rubber was used as thickening agent, minor cavities were typically spread out in the PCM volume. Samples that had solidified from a supercooled state tended to form fewer and smaller cavities.

Figure 10 (a) shows a SAT sample with 1% CMC solidified without supercooling. Figure 10 (b) shows a sample of SAT with 1% CMC which solidified from supercooled state.

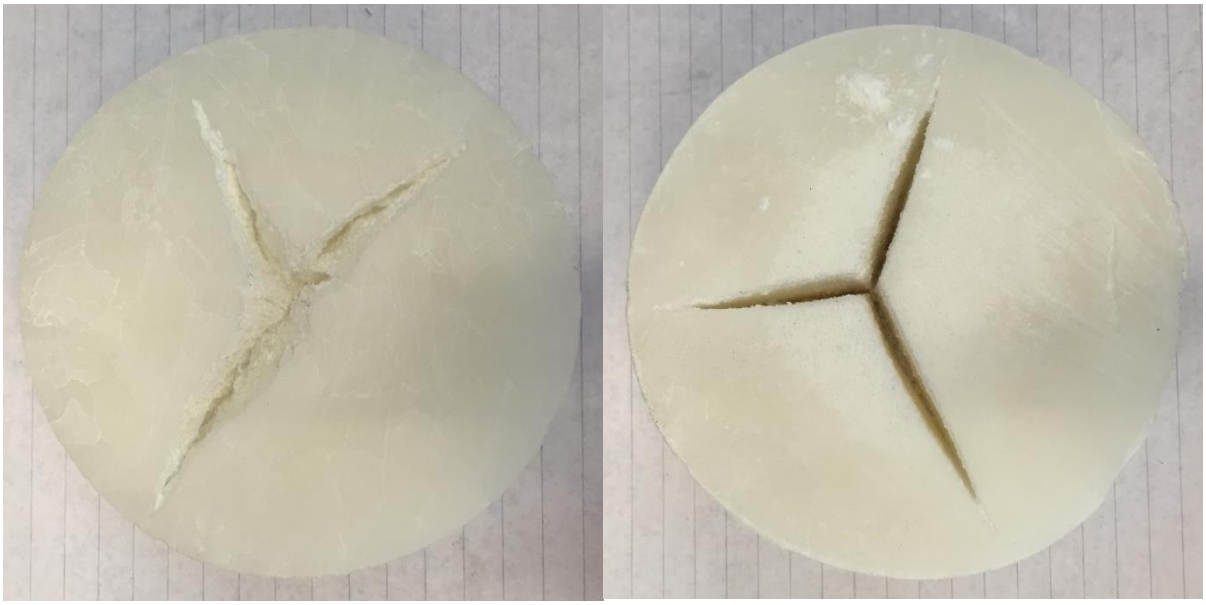

Figure 10. (a) SAT with 1% CMC solidified without supercooling. (b), SAT with 1% CMC solidified from supercooled state.

Figure 11 (a) shows a sample of SAT with 0.5% Xanthan rubber solidified without supercooling. Figure 11 (b) shows a sample of SAT with 0.5% Xanthan rubber which solidified from supercooled state.

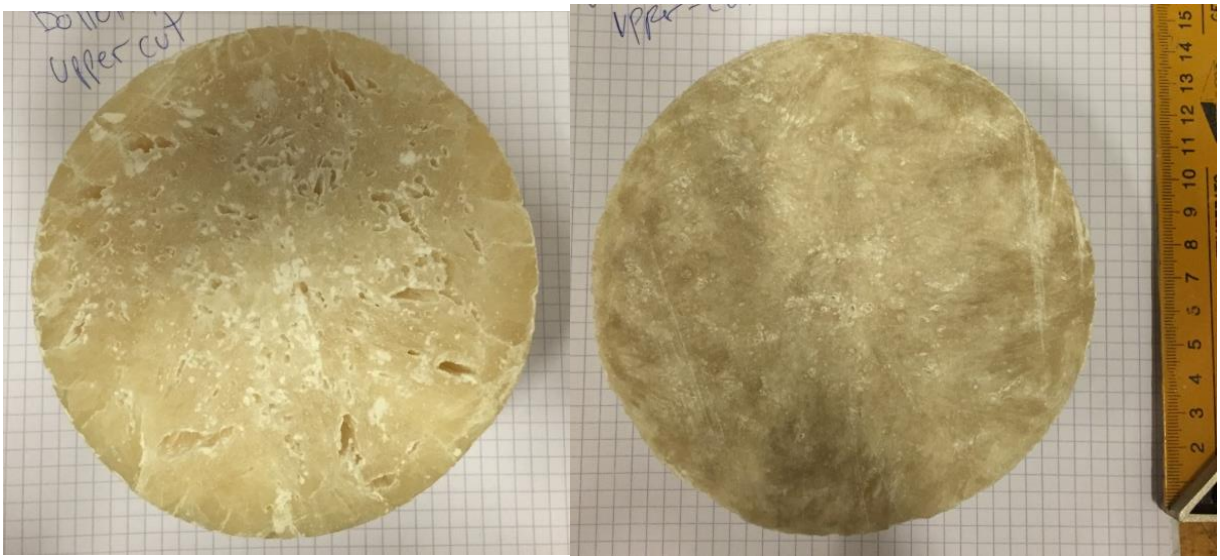

Figure 11. (a) SAT with 0.5% Xanthan rubber solidified without supercooling. (b) SAT with 0.5% Xanthan rubber solidified from supercooled state.

The measured thermal conductivity depended on whether the samples had solidified from supercooled state or without supercooling. The thermal conductivity was up to 0.64-0.67 W/m K in the solid parts of the SAT composites without graphite which had solidified without supercooling,. The samples of SAT without graphite which had solidified from supercooled state had thermal conductivities of 0.56-0.65 W/m K. The spread out cavities in the samples of SAT with Xanthan rubber gave in practice significantly lower thermal conductivities due to the cavities working as thermal resistances.

Graphite flakes showed to increase the thermal conductivity in the SAT composites more than graphite powder. In SAT composites with Xanthan rubber and 5% graphite flakes the thermal conductivity was up to 1.12 W/m K in the sample that solidified without supercooling and up to 0.95 W/m K in the sample that solidified from supercooled state.

Further details and results are given in Paper 2 - *Solidification behaviour and thermal conductivity of bulk sodium acetate trihydrate mixtures with thickening agents and graphite powder.* Dannemand at al.

3.2 Simulations and numerical calculations

3.2.1 Comparison of measurements on test unit with CFD calculations

A box shaped test unit of steel with the dimensions 302 x 302 x 55 mm was filled with 4.6 kg of SAT with 4% extra water (42% water, 58% sodium acetate). The steel box was heated and cooled under controlled conditions by placing it in a thermostatic bath. The temperatures of the surface and in the center of the PCM were measured. Figure 12 shows the steel box with thermocouples attached.

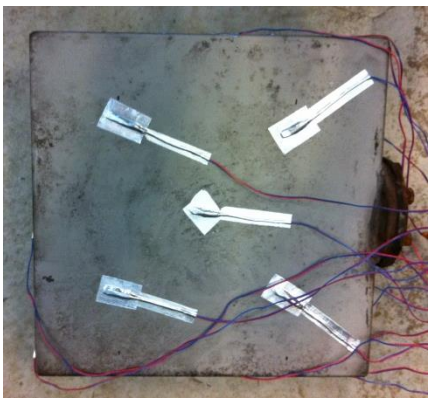

Figure 12. Steel unit containing 4.6 kg SAT with 4% extra water and thermocouples attached.

Figure 13 (a) shows the steel box placed in the thermostatic bath without water. Figure 13 (b) shows the thermostatic bath closed with lid and the controller.

Figure 13. (a) Steel unit placed the thermostatic bath. (b) Closed thermostatic bath with controller.

A computational fluid dynamics (CFD) model of the box was developed in Ansys Fluent. The measured surface temperatures were used as input parameters for the CFD model. The measured temperature development of the probe inside the steel box was compared to the temperature of the probe tip calculated by the CFD model.

Figure 14 shows part of the mesh of the CFD model of the steel box.

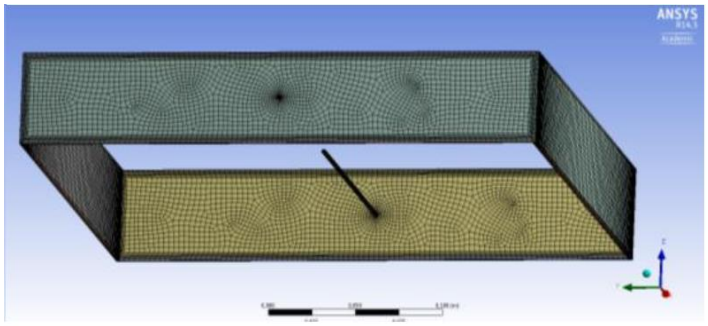

Figure 14. Part of mesh for CFD model of 302x302x55 mm steel box with SAT mixture.

Different heating and cooling scenarios were applied. Assumptions on formation of cavities affecting the heat transfer were made. The measured temperature in the center of the box was compared to the calculated values by the CFD model.

The agreement between the CFD calculations and the measurement was excellent in the cases which did not include phase change of the PCM. In the case where phase change occurred, some deviations were observed. In the CFD calculations the heating and melting happened faster than in the experiment. The reason may be the material properties of the SAT mixture used in the model. Especially the thermal conductivity may cause the deviation. Also the formation of cavities in the steel box may be different from what was expected and therefore gave larger resistance than assumed in the first case.

Figure 15 (a) shows the good agreement between the measured and calculated temperature developments of the probe in the steel box when heated from 22 ˚C to 52 ˚C. Figure 15 (b) shows the poor agreement between the measured and calculated temperature development of the probe in the steel box when heated across the phase change from 22 ˚C to 82 ˚C.

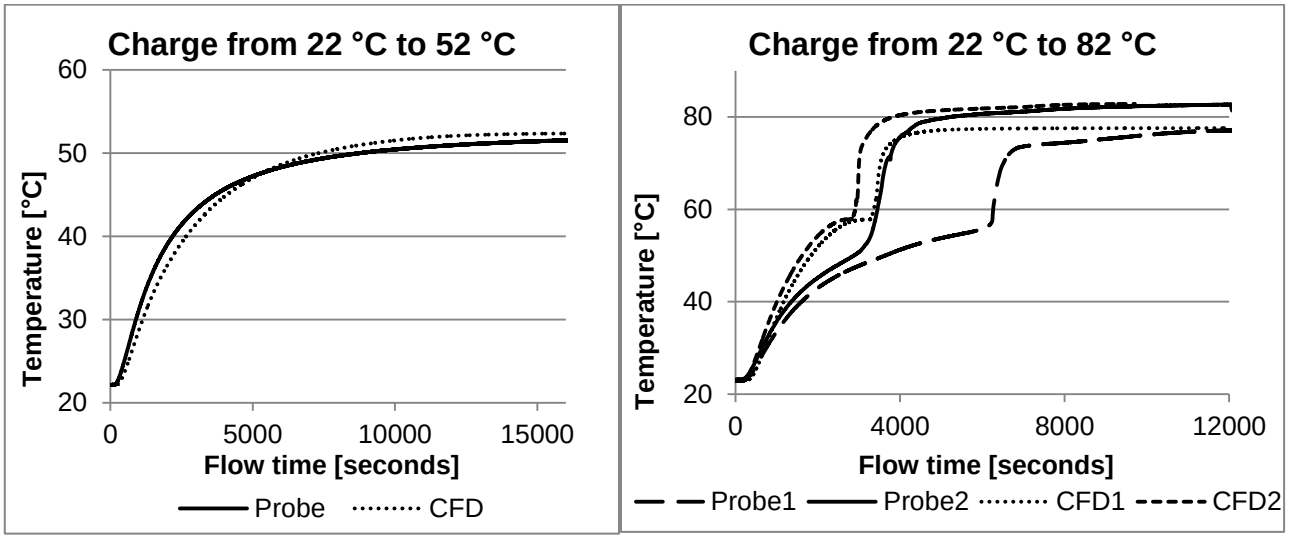

Figure 15. (a) Measured and calculated temperature development of probe in steel box heated from 22 ˚C to 52 ˚C. (b) Measured and calculated temperature development of probe in steel box heated from 22 ˚C to 82 ˚C.

Further details on the CFD model and the experiments are given in Paper 6 - *Validation of a CFD model simulating charge and discharge of a small heat storage test unit based on a sodium acetate water mixture*. Dannemand et al.

3.2.2 TRNSYS system simulation

A TRNSYS model of a solar heating combi-system with PCM storage previously developed by Schultz et al. [124] was adapted to fit the dimensions of the flat heat storage unit prototypes with a PCM volume of approximately 150 liters. The simulations were carried out for the system with 36 m^2 flat plate solar collectors facing south with a tilt of 75˚, a 180 liter domestic hot water tank, a space heating system and auxiliary heating. The solar collectors had a start efficiency of 0.82 and 1st and 2nd order heat loss coefficients of 2.44 W/(m^2 K) and 0.005 W/(m^2 K^2). The daily consumption of domestic hot water (DHW) was 99 liters per day. The DHW temperature was 50 ˚C and the cold water temperature was 10 ˚C, resulting in a yearly energy consumption of DHW of 1677 kWh. A space heating demand of 2008 kWh/year corresponding to the space heating demand of a passive house was assumed. The heat exchange capacity rate of the storage units was an input parameter to the TRNSYS model. Heat exchange capacity rate of the PCM storage units were varied to show the effect on the yearly system performance. Figure 16 shows the schematic of the system simulated in the TRNSYS model.

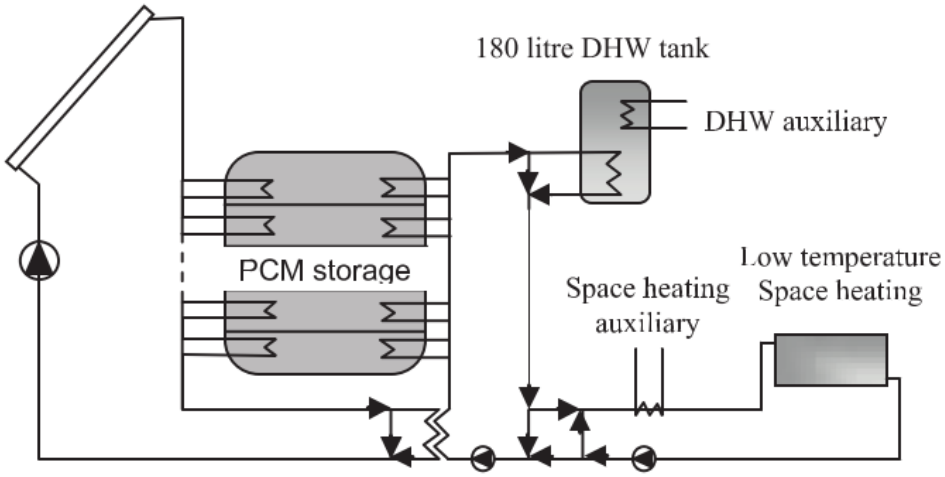

Figure 16. Schematic of demonstration system in TRNSYS model.

The TRNSYS simulations showed that the heat exchange capacity rate (HXCR) had significant influence on the yearly solar fraction of a solar combi-system with supercooled thermal energy storage. Figure 17 shows the yearly solar fraction of the simulated solar combi-system with varying number of storage units and HXCR.

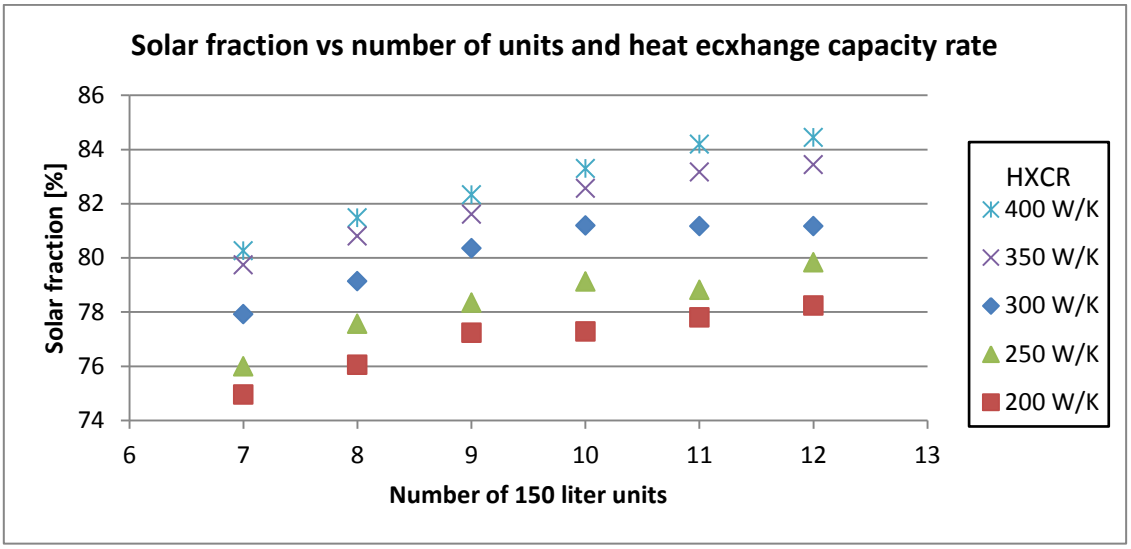

Figure 17. TRNSYS simulation results, effect of HXCR on solar fraction of solar combi system in single family house.

Further results are given in *Paper 1 - Long term thermal energy storage with stable supercooled sodium acetate trihydrate.* Dannemand et al.

3.3 Prototype heat storage units

The SAT mixtures should be contained in a closed container to avoid loss of water vapor from the PCM when it is melted. Loss of water from the SAT mixtures will change its composition and most likely reduce the performance over time. Also a closed container will provide more stable supercooling as external particles will not enter and initiate nucleation.

It is also recommended to design the inner surfaces of the PCM chamber, which is in contact with the supercooled PCM, to be as smooth as possible. Cracks, joining segments or penetrating tubes poses a risk of uncontrolled solidification of the supercooled PCM. In a similar way as bending a metal disc with cracks will start the solidification in the pocket sized hand warmers [108], solidification could be started at cracks in the unit if affected by internal or external pressure changes or impacts.

The density difference between the liquid SAT and the solid SAT is approximately 12% [123]. SAT expands when it melts. Preliminary investigations on early storage unit prototypes showed, that heating and melting SAT in a closed chamber caused deformations of the heat storage unit and sometimes leakage from the lids closing the PCM chamber due to a pressure built-up. Consequently supercooling failed. It was necessary to implement means for allowing the SAT mixture to expand and contract with minimal pressure changes in the PCM chamber to achieve stable supercooling. Filling approximately 85% of the PCM chamber of the storage units and connecting the air volume above the PCM to an external expansion device allowed for heating and melting the PCM with only slight pressure built up. Thereby no deformations of the storage unit occurred and stable supercooling was achieved.

As the PCM needs to be fully melted to achieve stable supercooling, a heat exchanger that provides relatively uniform heating and melting of the PCM is desired. The thermal conductivity of SAT is relatively

low; therefore the maximum distance between heat exchanger and PCM should be short to allow for faster complete melting of the PCM.

A number of barriers and problems for operating a heat storage based on stable supercooling of sodium acetate trihydrate in a large storage unit are discussed in *Paper 1 - Long term thermal energy storage with stable supercooled sodium acetate trihydrate*. Dannemand at al.

3.3.1 Flat heat storage unit

A heat storage unit design was developed at DTU with the partners in the COMTES project (see section 1.2 State of the art). The developed heat storage unit consisted of a flat PCM chamber with an internal height of 5 cm with heat exchangers on the outer surface of the PCM chamber. Manifolds were located along the side of the unit and 14 parallel channels covered the top surface of the PCM chamber and 16 channels covered the bottom surface. In this way heat could be transferred through the PCM chamber walls into the PCM. The length on the storage unit was 240 cm and the width was 120 cm (see Figure 18). One unit was constructed in steel and another unit with the inner chamber in stainless steel. There should be no risk of corrosion or chemical reactions happening with SAT in contact with steel and stainless steel [106].

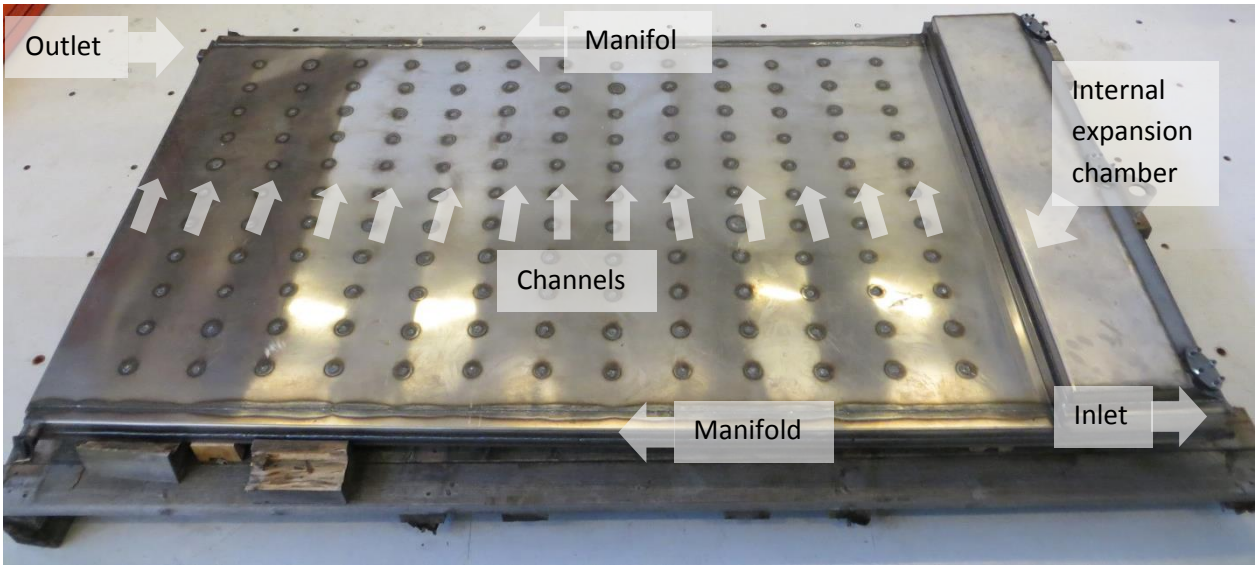

Figure 18. Flat heat storage unit with the dimensions 240 cm x 120 cm, internal expansion.

An expansion chamber was located in one end of the unit to accommodate for the density change of the SAT. An external expansion vessel without pre-pressure or an inflatable plastic bag allow for the expansion of the PCM in the unit with minimal pressure built-up (Figure 19)

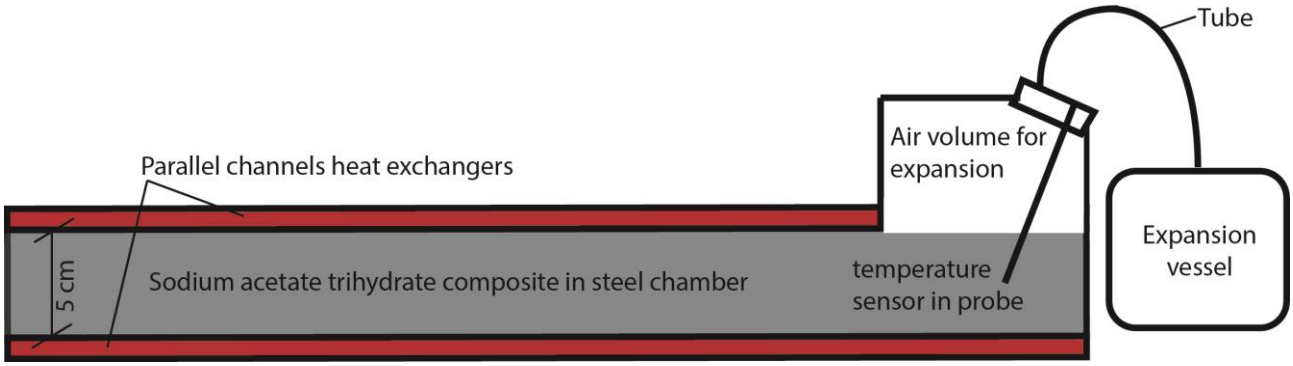

Figure 19. Principal diagram of flat heat storage unit with expansion.

The units were filled with 199.5 kg SAT with 9% extra water (44.8% water, 55.2% sodium acetate) and with 220 kg SAT with 1% CMC.

A 100 ml chamber was mounted on one side PCM chamber. When solidification was required, pressurized CO_2 was flushed through the chamber, and as the CO_2 evaporated the nearby PCM was cooled below its maximum degree of supercooling of about -15 ˚C [125]. This initiated the solidification of the supercooled PCM during laboratory testing.

Further details are given *in Paper 1 - Long term thermal energy storage with stable supercooled sodium acetate trihydrate* and *Paper 3 - Experimental investigations on prototype heat storage units utilizing stable supercooling of sodium acetate trihydrate mixtures.* Dannemand et al.

3.3.2 Cylindrical heat storage unit

Two cylindrical heat storage units in stainless steel were tested. The units were 150 cm high. The diameter was 30 cm. The units were insulated with 4 cm expanded polypropylene. Figure 20 shows the cylinder with insulation. One of the units had inspection windows to observe the state of the PCM inside the unit if needed. The heat exchangers consisted of 16 tubes located in a circular formation running from top to bottom. Thin aluminum plates were attached to the tubes as fins to increase heat transfer area. Figure 21 shows part of the steel tubes and the attached fins.

Figure 20. Cylindrical heat storage unit with insulation.

Figure 21. Internal heat exchanger of stainless steel pipes and aluminum fins.

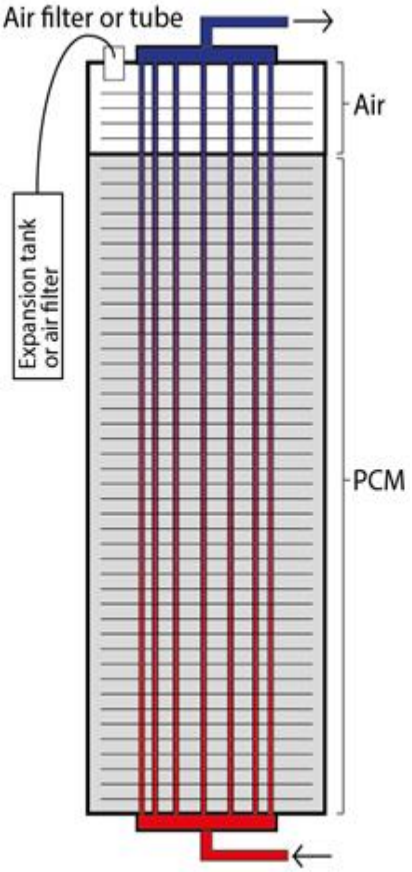

Figure 22. Principal diagram of PCM unit

The units were filled approximately 90% with the PCM to allow for the expansion. The units were tested with external expansion tanks and with an airlifter instead of the expansion. Figure 22 shows the principle diagram of the cylindrical unit with the expansion devices.

The cylindrical units were tested with 91 kg of water as a reference material; with 116 kg of SAT with 6.4% extra water (43.5 % water, 56.5% sodium acetate) and with 116.3 kg of SAT with 0.5% Xanthan rubber and 4.4% graphite powder. Paraffin oil was added to the PCM chamber of the unit with SAT, Xanthan rubber and graphite after some test cycles. This was done as an attempt to increase the heat transfer in the PCM when it was in solid phase. If oil filled the cavities formed during solidification of the PCM instead of air or vacuum it could enhance the heat transfer.

Further details are given in *Paper 4 - Experimental investigations on tall cylindrical latent heat storage units with sodium acetate trihydrate composites utilizing supercooling.* Dannemand at al.

3.3.3 Storage unit test description

The performance of PCM heat storage prototype units was investigated under controlled conditions in the heat storage test facilities to verify the working concept. The scale of the units represents a size which could be installed as part of a solar heating combi system in a single family house. The measured heat contents over a number of charge and discharge cycles were measured and compared to theoretical values.

The heat storage units were connected to a heat storage test facility. The test facility allowed for circulating water as the heat transfer fluid through the heat exchangers of the units and through an electric heating element and a heat exchanger for cooling. The power and temperatures for charge was set by a controller. The discharge power and temperature was controlled by adjusting the flow conditions of the heat sink side of the heat exchanger for the cooling. Flow rates were set by string values to represent desired test conditions.

The units were heated to a temperature of 80-90 ˚C to ensure supercooling during cooling down. Preliminary investigations showed that a minimum temperature of the PCM of 80 ˚C helped to achieve supercooling. The sensible heat was either actively or passively discharged from the units by cooling down to the ambient temperature of 20-25 ˚C. After solidification the units were actively discharged to determine the heat released after a supercooled period.

The units were charged with a high flow rate during a period long enough to ensure complete melting of the PCM and a minimum temperature in all parts of the storage units of 80 ˚C. During discharge the flow rates were relatively low in order to have high a temperature increase of the heat transfer fluid.

Five junction thermopiles based on copper/constantan type TT thermocouples with counter flow sensors measured the temperature difference across the inlet and outlet of the units. The accuracy of the temperature difference measured by the thermopile was 0.1 K. Absolute flow temperatures were measured with thermocouples. Temperatures on the outside of the units were measured at key locations. All thermocouples were copper/constantan type TT with accuracy of 0.5 K. In some cases the PCM temperature was determined by thermocouples in probes inserted into the PCM. The flow rate was measured by the inlet to the units with Clorius or Brunata HGQ1-R0 flow meters which had been calibrated to have an accuracy of ± 1 % in the relevant flow range. Solartron cards with a PC were used to log the measurements at respective intervals. Figure 23 shows the principle of the heat storage test facility.

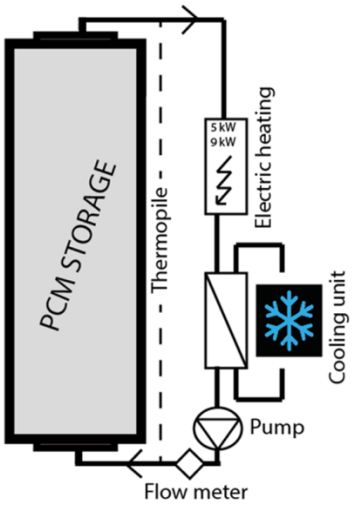

Figure 23. Principle diagram of heat storage test facility.

The charge and discharge powers $\dot{Q}$ [W] when heating and cooling the units were determined by:

$$\dot{Q} = \dot{V} \cdot c_p \cdot \rho \cdot (T_i - T_o) \qquad (6)$$

where, T_i is the inlet temperature, T_o is the outlet temperature, $\dot{V}$ is the volume flow rate of the heat transfer fluid measured at the inlet, c_p is the specific heat capacity of the heat transfer fluid at mean temperature between T_i and T_o, ρ is the density of the heat transfer fluid at T_i.

The heat loss coefficients H_{loss} [W/K] of the storage units were measured by heating the units to a high stable temperature. The heat balance of the system was used to determine the heat loss experimentally, that is, the heat added to the system was equal to the heat loss, when the storage temperature was stable over a period. In this way a simplified heat loss coefficient with a constant value was determined by:

$$H_{loss} = \dot{Q} \ /(T_s - T_{amb}) \quad (7)$$

where T_s is the mean temperature of the surface of the unit and T_{amb} is the ambient temperature. The heat loss coefficient for the storage unit was used when calculating the heat content of the unit based on the measured data. The heat content in the storage unit after a charge E_{charge} [J] or the heat discharged from the unit $E_{discharge}$ [J] over a specific time period t was determined by:

$$E_{charge/discharge}(t) = \int_0^t (\dot{Q} - H_{loss} \cdot (T_s - T_{amb}))dt \quad (8)$$

The heat content of the PCM per unit mass at a specific storage temperature T_s above a defined start temperature T_{start} excluding the specific heat of the tank material C_{unit} was calculated by the following expression:

$$E_{PCM}(T_s, T_{start}) = \frac{E_{charge/discharge}(T_s, T_{start}) - C_{unit} \cdot (T_s - T_{start})}{m} \quad (9)$$

where $E_{charge/discharge}\ (T_s, T_{start})$ is the measured heat content of the storage at a storage temperature T_s above a start temperature T_{start} and m is the mass of the PCM. This allows for comparing the heat content of the different PCMs disregarding the heat capacities of the unit material and comparing the measurement to a theoretical storage capacity of the PCMs with given sensible heat and latent heat.

The heat exchange capacity rate (HXCR) is an expression related to how fast heat is transferred between the heat transfer fluid and the heat storage material in the storage. It indicates how well the heat exchanger of the storage performs. The HXCR is affected by multiple factors such as the storage temperature, the power charged to or discharged from the storage, the flow rate, the heat exchanger design and material properties. The heat exchange capacity rate was expressed by the following equation which can be derived from the heat transfer rate and log mean temperature difference.

$$HXCR = \dot{V} \cdot c_p \cdot \rho \cdot ln\left(\frac{T_i - T_s}{T_o - T_s}\right) \quad (10)$$

A number of test cycles with each unit were carried out. This was done to evaluate the cycling stability of the PCM material, that is, if the heat content in first test cycles was similar to later test cycles or if this changed over the number of cycles. Also test cycles where the PCMs were kept in supercooled state for different periods were carried out to evaluate any potential heat loss over long storage periods. The performance of the different PCMs in the application sized units was determined so the heat content could be compared to the results from the investigations of heat content in the glass jars in the insulated boxes (section 3.1.1 Heat content measurements).

3.3.4 Measurements on flat units

The temperature development of a selected charge and discharge test cycle with the flat unit can be seen in Figure 24. During the charge period the temperature of the storage increased as more energy was stored in the unit. The unit was kept with a stable temperature of approximately 90 ˚C for a period. In this period the heat loss coefficient of the unit was determined to be 8 W/K. After the stable hot period the sensible heat was discharged. The PCM remained in liquid state and remained supercooled for approximately 3 days. After the supercooled period the solidification was initiated by the cooling technique and the latent heat released during solidification was discharged. Figure 24 also the shows the thermal energy content of the unit throughout the test cycle.

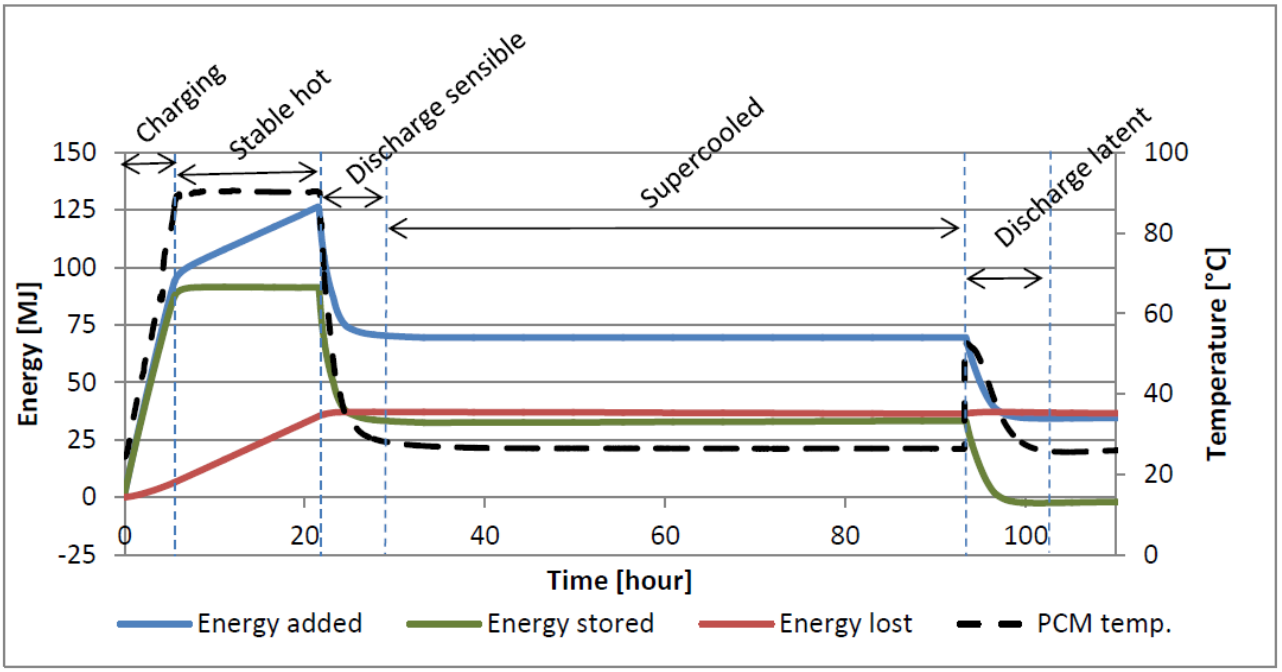

Figure 24. Test cycle with flat unit with SAT with 9% extra water.

The energy released after solidification of the supercooled SAT with 9% extra water was in the first test cycle 194 kJ/kg of PCM. In the 5th test cycle 188 kJ/kg was discharged. After 20 test cycles the measured energy content was 179 kJ/kg of PCM. The drop in heat content over the test cycles shows that the PCM mixture was not cycling stable. The heat content of the SAT with 9% extra water tested in this unit was slightly higher that what was expected from the heat content measurement of SAT with 10% extra water in the glass jars form section 3.1.1 Heat content measurements.

The energy released from the unit with SAT and 1% CMC after solidification of the supercooled was consistent around 205 kJ/kg of PCM over the six test cycles. The determined heat content in the glass jars similar SAT mixtures slightly higher than in the prototype unit tests.

The determined heat exchange capacity rate for the flat storage units during selected charges with similar charge powers are shown in Figure 25. It can be seen that the HXCR is higher for the bottom heat exchanger compared to the top heat exchanges. This is partly due to the larger heat transfer surface but possibly also due to better contact between PCM and heat exchanger in the bottom than in the top due to gravity. Also the buoyancy effect in the liquid PCM will favor the heat transfer of the bottom heat

exchanger. It can also be seen that the HXCR is significantly higher for the unit with SAT and extra water compared to the unit with SAT and 1% CMC. This is due to a lower heat transfer by convection in the unit with CMC due to the fact that the PCM was thickened.

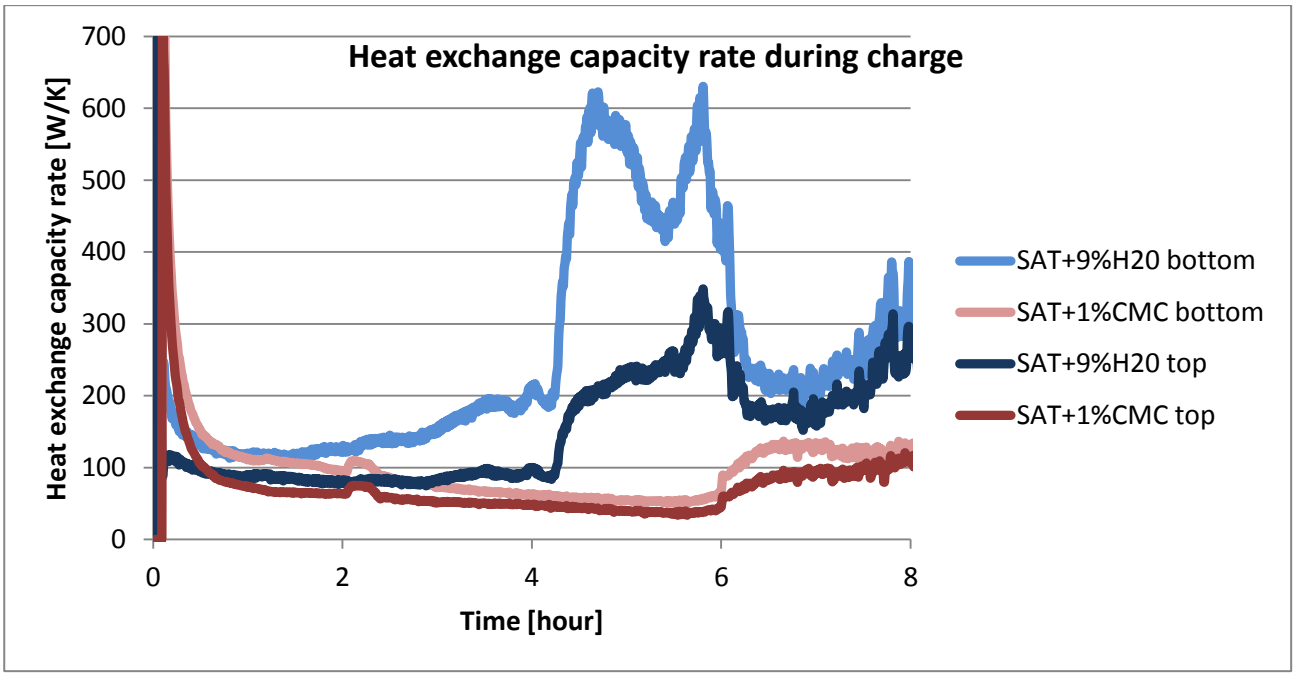

Figure 25. Heat exchange capacity rate during charge.

The unit with SAT and extra water was kept in supercooled state for up to 8 weeks and the unit with SAT and CMC was kept in supercooled state for up to 5 weeks before solidification was intentionally initiated and the units were discharged.

After solidification the discharge power of the modules peaked at approximately 5 kW in the beginning of the discharge. The heat transfer fluid temperature was raised from approximately 25 ˚C to 45 ˚C in the start of the discharge. This was with a flow rate of 2 l/min in each heat exchanger. A lower flow rate of 0.5 l/min gave a 2-3 K higher outlet temperature. The PCM temperature after solidification peaked at 58 ˚C in the SAT mixture with CMC whereas the PCM temperature in the SAT mixture with extra water peaked at 53 ˚C.

Further details are given in *Paper 3 - Experimental investigations on prototype heat storage units utilizing stable supercooling of sodium acetate trihydrate mixtures.* Dannemand et al.

3.3.5 Measurements on cylindrical units

Comparing the HXCR during charge of the cylindrical unit with the two different SAT mixtures showed similar tendency as for the flat storage units. The HXCR was significantly lower for the unit with the thickened SAT compared to the unit with SAT and extra water. Adding oil to the PCM chamber gave minimal improvement to the HXCR during charge. The amount of oil was however very small and larger amount of oil may show better improvements.

The released heat after solidification in the unit with SAT and 6.4% extra water was 177 kJ/kg in the first test cycles dropping to 140 kJ/kg after 17 test cycles. Severe phase separation was observed in the unit and the reason for the loss of storage potential. The heat content per kg SAT measured in the cylindrical unit was somewhat lower than for the flat storage unit. This may indicate that the risk of phase separation is higher in a tall unit compared to a unit of lower height.

The heat released after solidification of the SAT mixture with Xanthan rubber was stable at 205-210 kJ/kg in the cylindrical storage unit over the 40 test cycles carried out. This was similar to the heat content measured in the flat unit with SAT thickened with CMC.

Figure 26 shows the theoretical thermal energy content of the SAT mixture with Xanthan rubber and graphite over a selected temperature interval. The theoretical energy content is shown with blue curves, where the dotted curve represents the supercooled state. Measurements from two selected test cycles where stable supercooling was achieved are also shown. The areas marked with circles are the states where the temperature of the storage and PCM was considered uniform and the comparison between the measurements and calculations area valid.

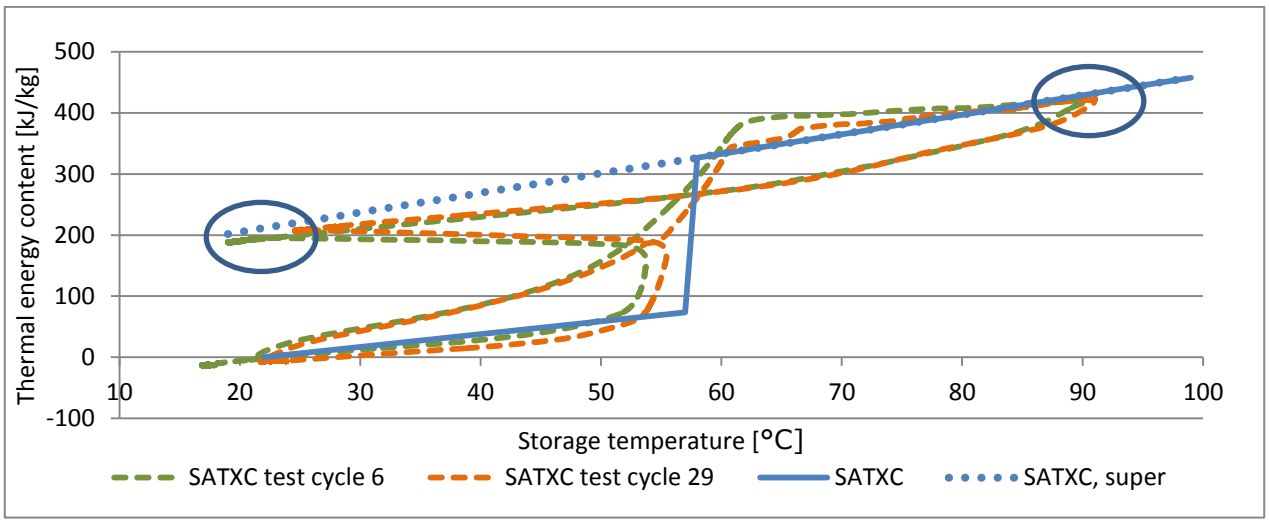

Figure 26. Theoretical and measured thermal energy content of SAT with Xanthan rubber in cylindrical unit.

In the cylindrical units, supercooling was unstable in most test cycles where solidification started spontaneously during the active or passive discharge of the sensible heat. Only short periods of stable supercooled PCM were achieved in the cylindrical units.

Further details are given in *Paper 4 - Experimental investigations on tall cylindrical latent heat storage units with sodium acetate trihydrate composites utilizing supercooling.* Dannemand et al.

3.4 Demonstration system

After laboratory testing the flat heat storage unit prototypes were installed as part of a full scale demonstration system. The scope of this thesis is just the unit which was filled with SAT with 1% CMC. Whether it was possible to completely melt the SAT mixture in the heat storage and thereafter achieve supercooling was investigated. The main components of the demonstration system were 22.4 m^2 of evacuated tubular collectors, a 735 liter tank in tank water buffer store and four flat heat storage units covered with insulation. Figure 27 shows a principle diagram of the demonstration system.

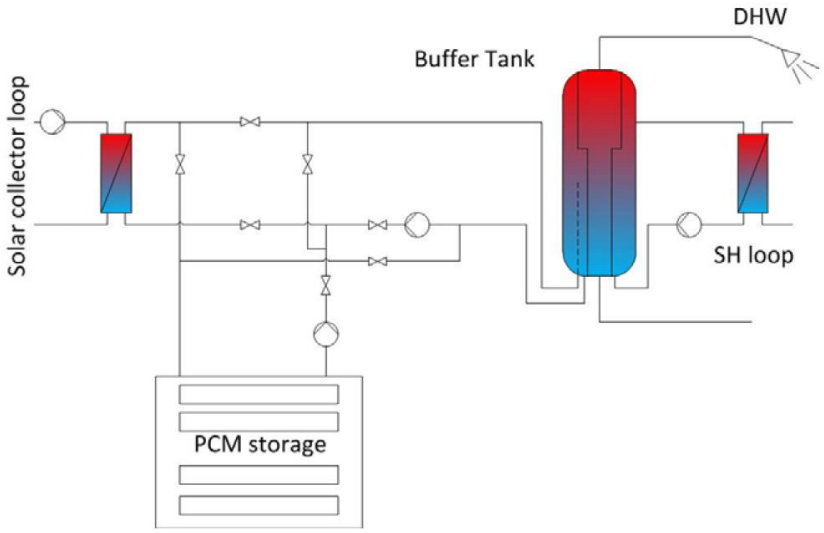

Figure 27. Principle diagram of demonstration system with PCM storage, pipes loops, water buffer storage [126]**.**

Figure 28 (a) shows the 22.4 m^2 of solar collectors of the demonstration system which charge the PCM storage units. Figure 28 (b) shows the insulated water buffer storage for the demonstration system.

Figure 28. (a) Evacuated solar collectors for demonstration system. (b) 735 liters water buffer storage for demonstration system.

Figure 29 shows the development of the PCM temperature in the unit over a 12 days period in August 2015. With the heat from the solar collector the PCM temperature was increased from 25 ˚C to 85 ˚C over the first 3 days in Figure 29. Several units were heated in parallel. It would therefore be possible to heat the

unit from 25 ˚C to 85 ˚C in one day if only one unit was charged. After the third day the unit was let to passively cool down to ambient temperature. After another 7 days the PCM inside the unit had reached 29 ˚C and the solidification was intentionally initiated and discharged.

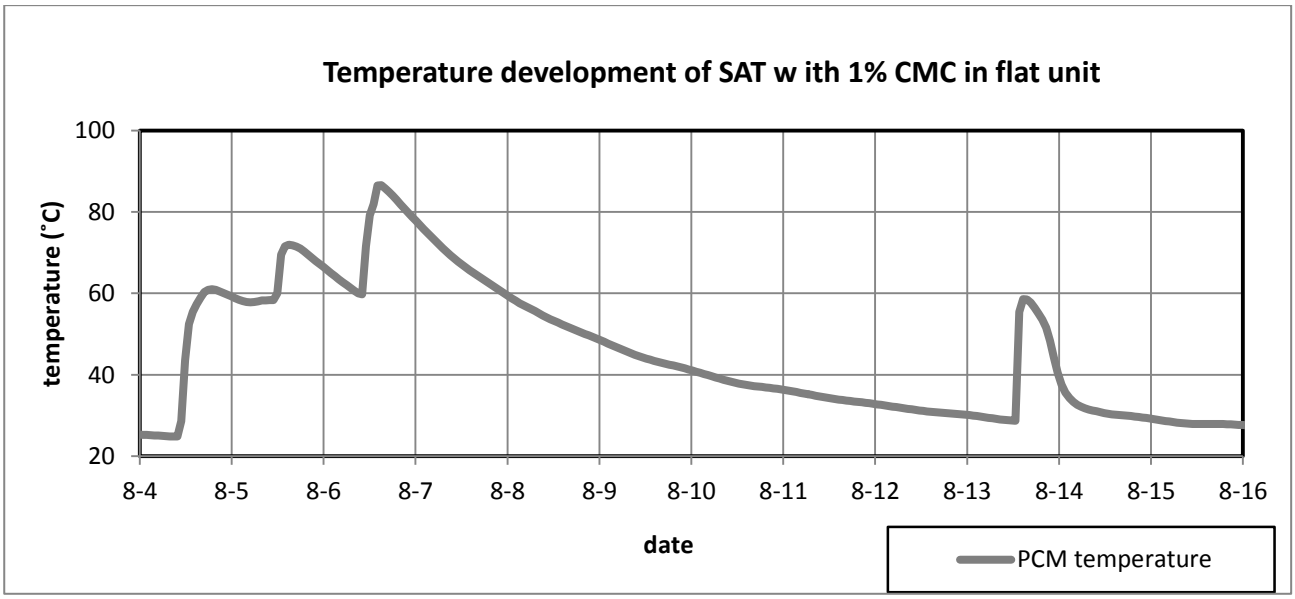

Figure 29. PCM temperature in flat heat storage unit charged with heat from solar collectors and cool down period.

Further details on the operation of the demonstration system are given in Paper 7 - *Testing of PCM heat storage units with solar collectors as heat source.* Englmair et al.

4 Discussions and perspectives

4.1 SAT composites

The SAT mixtures with thickening agents tested in the prototype units showed to have a heat content in the supercooled state of 205-210 kJ/kg, which is 90% of the theoretical maximum heat content of SAT of 230 kJ/kg at 20 °C. Further increasing the heat content may be possible by optimizing the ratio of the thickening agent in the SAT mixture or by refining the mixing method. As an alternative to the thickening agents, liquid polymers, additives with chelating effect or additives which increase the solubility of the sodium acetate in water may also be a solution.

One major drawback of using a thickening agent for solving phase separation in SAT is the increased viscosity which causes lower heat transfer by convection during charge. The liquid polymers as additives have the potential to reduce phase separation without increasing the viscosity of the PCM. In that case heat transfer during charge may be as high as for SAT. However, in the solidified state when discharging the SAT after a storage period, the PCM is entirely in solid state and the heat transfer is dominated by thermal conduction. In this case heat transfer of the SAT mixture with thickening agent and other additives may be the same. To increase the discharge power after solidification it is therefore necessary to increase the thermal conductivity of the PCM mixture. This could be by adding graphite to the PCM composite. As the investigation showed, it was required to thicken the SAT to keep the graphite suspended in the mixture. In this case the thickening agents solved both the phase separation problem and kept the graphite suspended in the solution. Higher discharge powers after solidification may therefore be achieved in PCM mixtures with thickening agents and graphite compared to PCM composites with liquid additives. Graphite flakes showed to have a better effect on increasing the thermal conductivity compared to graphite powder. The size of the graphite flakes may show to have an influence of the effect or there may be other graphite additives which prove to be even better. These may be graphite fibers or expanded graphite.

The performances of heat storage units in a solar heating system will to a high extend depend on the design of the systems, the supply of solar energy and the demand profiles. Whether the system as a whole will perform better with a higher heat transfer during the charge which will be possible with the liquid additives or if the system will perform better with a higher discharge power from the thickened PCM mixtures with graphite is a complex matter. Further simulations must clarify this but as the storage concept aims to deliver heat when solar energy is not available it is likely that higher discharge power is desired.

Adding oil to the PCM chamber of a storage unit potentially increases the heat transfer as the oil fills in the gaps that are formed when the SAT solidifies and contracts. When the PCM is in liquid state, the oil should float on top of the PCM. When PCM solidifies and contracts, the oil should be sucked into the cavities formed in the PCM to increase heat transfer. When the PCM again is melted, the oil should then again float to the top of the PCM to be ready for the next cycle. In a thickened PCM composite there is, however, a risk that the oil will not float to the top when the PCM is melted, but stay trapped in the thickened PCM in a similar way as air bubbles are trapped. Therefore, oil as an effective way to enhance heat transfer in thickened PCM mixtures may not be cycling stable over repeated test cycles. It is unknown if a PCM mixture is thick enough to avoid phase separation and to keep graphite suspended and at the same time allows for oil to escape and float op top.

In the research the general practice was to heat the SAT mixtures to 80 °C to achieve the stable supercooling. Some more detailed investigations of the required temperature and heating duration to achieve the supercooling can be carried out. Especially SAT mixtures with additives could be investigated as the additives may influence this temperature requirement. If a lower temperature is sufficient to achieve stable supercooling, this will have an effect on system performance and give more options for implementation of the storage technology.

4.2 Heat storage unit designs

The investigations showed that stable supercooling was not achieved in every test cycle with the prototype heat storage units. It is of course necessary that the supercooling is controlled in every cycle for such storage system. In some cases the supercooling failed in the first couple of test cycles and was afterwards achieved.

It was observed that in some cases the solidification of the SAT started from the bottom of the cylindrical unit. This was most likely due to the way the sides of the cylinder were joined with the bottom which formed a crevice or crack along the assembly line. Another critical point in the bottom of the cylinder was the location where the tubes for the heat exchanger penetrated the bottom. In both areas there was a risk of crystals being trapped under high pressure in the cracks and with a slight movement of the cylinder the trapped crystals could be released to initiate crystallization of the entire PCM volume. In the flat unit critical areas were when inner stabilizing supports of the PCM chamber were constructed where cracks could form between parts and when the lid closing the PCM chamber was in contact with the PCM. A design of the heat storage units and especially the inner surface of PCM chamber being smooth could possibly lead to increased supercooling stability. A coating on the inner surfaces could possible eliminate the problem with cracks. Alternatively, if the PCM chamber was made from a softer material, the risk of high pressures at cracks causing crystallization may be reduced.

It was shown, that the stores needed some expansion devices to handle the expansion and contraction of the PCM without causing too high pressures and deformation of the units to obtain stable supercooling in the rigid storage units. An inner expansion volume connected to an external expansion device seemed to work in many cases. In some cases, however, the tube connecting the internal and external expansion volumes was blocked after a number of test cycles leading to spontaneous solidification. The blockage was possibly by caused by SAT had migrated from the storage to the tube. An integrated expansion device in the PCM unit could avoid the need for the external expansion device and eliminate the risks associated with that. An air volume in the PCM chamber where the expansion of the PCM could be taken up by compressing the air will most likely need to be impractically large to avoid too high pressures. A flexible membrane in the top of the storage unit above the PCM which could move as the PCM expanded and contracted could be a solution. This could be a solution when the storage units are of rigid material such as steel. Alternatively, the outer shell of the PCM chamber could be of a flexible material which could take up the density changes. An outer shell of a soft plastic material could be a solution. Plastic containers casted of softer material could possibly be made with smooth inner surfaces without any joining of parts where a potential crack could pose a risk of trapped crystals. This could be a design that supports more stable supercooling. A heat exchanger spiral with or without fins could be inserted into the PCM from the top of the container with the joining parts being in a minor air gap above the PCM.

In some cases the spontaneous solidification started from the top of the cylindrical unit and from the end of the flat unit with the expansion chamber. Nucleation possibly started at the upper surface of the PCM. This nucleation could be caused by airborne SAT crystals or other particles in the air inside the expansion volume. When these particles land on the PCM surface, the solidification may start. Alternatively, particles or un-melted SAT crystals could be stuck on the inner surface of the PCM chamber above the supercooled SAT and at one point when they fall down and land on the surface of supercooled PCM and crystallization is initiated. If this is the case, having a layer on top of the SAT mixture which neutralizes the particle causing the spontaneous crystallization may be a solution.

4.3 Heat storage implementation

It is clear that a high heat transfer rate between the PCM and the heat transfer fluid is of key importance in this storage. As argued the material properties of the PCM affect the heat transfer. However, the heat exchanger design and system design have equal importance. Smarter and possible more complex designs of the heat exchangers should be considered to increase the performance of the storages units. More complex heat exchange designs are likely to be more costly therefore some parametric analysis optimizing the heat exchanger design and the PCM properties as well as the applications must be considered. Another consideration of implementing the storage is to have a water buffer store as part of the system. This buffer storage could cover the demands of a high discharge power over short time, while the PCM storage units are discharged into the water buffer with lower power but with high temperatures over longer periods. In a system with a water buffer storage the demand for HXCR for the PCM storage may not be so high.

The cost of the storage units does naturally play a vital role for the extent of implementation. Considering the life time of the storage and the number of cycles over its lifetime, the storage should provide high storage capacity at a low cost. Where this type of storage is justifiable to install, depends on the lifecycle cost of the full heating system of the house compared with alternative technologies. This storage principle may not prove to be economically feasible in areas with district heating. However, in more rural areas where few other sustainable energy sources are available this concept may be feasible.

The storage principle with supercooling of SAT is relatively simple. SAT is a simple low cost material which is easy to handle and there are low requirements for the containers. Potentially, stores can therefore be designed in a simple way at a low cost, for instance of plastic. For the two investigated storage designs, the cost was significantly lower for the cylindrical unit compared to the flat unit due to the production methods and amount of material for the tanks. The main reason for designing the unit flat was to reduce the risk of phase separation but as this problem was solved with thickening agents even in tall units, there is no longer incentive to design the units flat.

The number and sizes of the PCM storage units which has to form the PCM storage will depend on the demands of the system. What size water buffer storage will give the best performance and how it works with the PCM storage will depend on the system and demands. Optimizing this relationship including solar collector area is complex and can be done by simulations.

The scope of this work was to consider the storage as part of a solar heating system. The storage principle may also be used combined with other technologies or in other systems for example with heat pumps and utilizing periods with cheap electricity. Also future systems relying on solar heating and cheap electricity in winter are of interest, because the needed heat storage volume can be strongly reduced if the storage is

heated during winter. Or it could be in applications which runs more but shorter cycles, for example waste heat of industrial applications.

4.4 Sustainability

The storage concept allows for implementing more renewable energy in our energy systems. One of the arguments for doing this was the reduction of environmental pollution. It is assumed that the storage made from steel and with SAT as the storage material has little environmental footprint when the steel is considered to be recyclable and the SAT as the pure material is non-harmful to the environment. In order not to just exchange the negative impact of fossil fuels usage with a negative impact related to the production or recycling of the SAT storage, it is essential to consider the recyclability of the developed storage materials as well as ways of disposal or recyclability of the PCM mixtures. This is to consider if the additives mixed into the SAT are of low environmental impact in the production and disposal. Further, if there is a need for separating the SAT from additives after end life time, then the footprint related to this must likewise be considered. Life cycle analysis of the SAT storage including the PCM additives must be considered in future development to make sure that the storage concept is fully sustainable.

5 Conclusions

The thermal conductivity of SAT can be increased by adding graphite to the PCM mixture. It was shown that 1% Xanthan rubber or 5% CMC was required to keep a uniform composite where the graphite did not settle to the bottom of the sample container. Graphite flakes had a much better effect on increasing the thermal conductivity compared to graphite powder.

The thermal conductivity of the bulk SAT composites was influenced by whether the SAT solidified from a supercooled state or if it solidified without supercooling. Solidification without supercooling resulted in a denser crystal structure with higher thermal conductivity and cavities formed away from the heat transfer area. Solidification from supercooled state resulted in fewer large cavities in the bulk SAT samples and a lower thermal conductivity. The type of thickening agent added to the SAT composited affected the formation of cavities.

Phase separation reduced the storage potential of SAT significantly. Adding water to the SAT can limit the loss in heat content of supercooled SAT due to phase separation. In large storage unit sizes the heat content is however reduced over repeated charge and discharge cycles. This was especially evident in a 1.5 m tall storage unit. SAT composites with 1% CMC or 0.5% Xanthan rubber as thickening agents showed to have a high stable heat content also over repeated charge and discharge cycles in the storage unit. The heat content of the SAT composite with Xanthan rubber was stable over repeated cycles in a 1.5 meter tall storage unit.

The storage principle of utilizing stable supercooled sodium acetate trihydrate for long-term heat storage worked in unit sizes large enough for systems for single family houses. The supercooling in the tested prototypes units was however not stable in all cycles. Uncontrolled solidification occurred in a number of test cycles. This was caused by improper handling of the expansion, inner surface design of PCM chamber with cracks and operation of the units. In rigid storage units of steel and stainless steel it was necessary to operate the units with minimal pressure built up in the PCM chamber during charge and discharge due to risk on uncontrolled crystallization. An expansion volume inside the PCM chamber connected to an external expansion tank allow for having the SAT remain stable in supercooled state.

Under laboratory test conditions prototype heat storage units were in supercooled state for up to two months after which the solidification was intentionally initiated and the latent heat of fusion discharged.

Simulations showed that the heat exchange capacity of the heat storage units significantly affected the yearly performance of a solar heating combi-system for a single family passive house.

6 References

[1] P. Arce, M. Medrano, A. Gil, E. Oró, L.F. Cabeza, Overview of thermal energy storage (TES) potential energy savings and climate change mitigation in Spain and Europe, Appl. Energy. 88 (2011) 2764–2774. doi:10.1016/j.apenergy.2011.01.067.

[2] L.F. Cabeza, L. Miró, E. Oró, A. de Gracia, V. Martin, A. Krönauer, et al., CO2 mitigation accounting for Thermal Energy Storage (TES) case studies, Appl. Energy. 155 (2015) 365–377. doi:10.1016/j.apenergy.2015.05.121.

[3] International Energy Agency, Heating without global warming, Paris, 2014.

[4] E. Andersen, L.J. Shah, S. Furbo, Thermal performance of Danish solar combi systems in practice and in theory, J. Sol. Energy Eng. 126 (2004) 744–749. doi:10.1115/1.1688381.

[5] J. Persson, M. Westermark, Low-energy buildings and seasonal thermal energy storages from a behavioral economics perspective, Appl. Energy. 112 (2013) 975–980. doi:10.1016/j.apenergy.2013.03.047.

[6] A. V Novo, J.R. Bayon, D. Castro-Fresno, J. Rodriguez-Hernandez, Review of seasonal heat storage in large basins: Water tanks and gravel-water pits, Appl. Energy. 87 (2010) 390–397. doi:10.1016/j.apenergy.2009.06.033.

[7] G.K. Pavlov, B.W. Olesen, Thermal energy storage—A review of concepts and systems for heating and cooling applications in buildings: Part 1—Seasonal storage in the ground, HVAC&R Res. 18 (2012) 515–538. doi:10.1080/10789669.2012.667039.

[8] D. Bauer, R. Marx, J. Nußbicker-Lux, F. Ochs, W. Heidemann, H. Müller-Steinhagen, German central solar heating plants with seasonal heat storage, Sol. Energy. 84 (2010) 612–623. doi:10.1016/j.solener.2009.05.013.

[9] M.M. Farid, A.M. Khudhair, S.A.K. Razack, S. Al-Hallaj, A review on phase change energy storage: materials and applications, Energy Convers. Manag. 45 (2004) 1597–1615. doi:10.1016/j.enconman.2003.09.015.

[10] S.D. Sharma, K. Sagara, Latent Heat Storage Materials and Systems: A Review, Int. J. Green Energy. 2 (2005) 1–56. doi:10.1081/GE-200051299.

[11] F. Agyenim, N. Hewitt, P. Eames, M. Smyth, A review of materials, heat transfer and phase change problem formulation for latent heat thermal energy storage systems (LHTESS), Renew. Sustain. Energy Rev. 14 (2010) 615–628. doi:10.1016/j.rser.2009.10.015.

[12] H. Mehling, L.F. Cabeza, Materials used as PCM in thermal energy storage in buildings: A review, Renew. Sustain. Energy Rev. (2011) 1675–1695. doi:10.1016/j.rser.2010.11.018.

[13] B. Zalba, J.M. Marín, L.F. Cabeza, H. Mehling, Review on thermal energy storage with phase change: materials, heat transfer analysis and applications, Appl. Therm. Eng. 23 (2003) 251–283. doi:10.1016/S1359-4311(02)00192-8.

[14] R. Baetens, B.P. Jelle, A. Gustavsen, Phase change materials for building applications: A state-of-the-art review, Energy Build. 42 (2010) 1361–1368. doi:10.1016/j.enbuild.2010.03.026.

[15] A.A. Al-abidi, S. Bin Mat, K. Sopian, M.Y. Sulaiman, A.T. Mohammed, CFD applications for latent heat thermal energy storage: a review, Renew. Sustain. Energy Rev. 20 (2013) 353–363. doi:10.1016/j.rser.2012.11.079.

[16] M.J. Hosseini, A.A. Ranjbar, K. Sedighi, M. Rahimi, A combined experimental and computational study on the melting behavior of a medium temperature phase change storage material inside shell and tube heat exchanger, Int. Commun. Heat Mass Transf. 39 (2012) 1416–1424. doi:10.1016/j.icheatmasstransfer.2012.07.028.

[17] C. Barreneche, A. de Gracia, S. Serrano, M. Elena Navarro, A.M. Borreguero, a. Inés Fernández, et al., Comparison of three different devices available in Spain to test thermal properties of building materials including phase change materials, Appl. Energy. 109 (2013) 421–427. doi:10.1016/j.apenergy.2013.02.061.

[18] D. Zhou, C.Y. Zhao, Y. Tian, Review on thermal energy storage with phase change materials (PCMs) in building applications, Appl. Energy. 92 (2012) 593–605. doi:10.1016/j.apenergy.2011.08.025.

[19] X. Py, R. Olives, S. Mauran, Paraffin/porous-graphite-matrix composite as a high and constant power thermal storage material, Int. J. Heat Mass Transf. 44 (2001) 2727–2737. doi:10.1016/S0017-9310(00)00309-4.

[20] P. Verma, S. Singal, Review of mathematical modeling on latent heat thermal energy storage systems using phase-change material, Renew. Sustain. Energy Rev. 12 (2008) 999–1031. doi:10.1016/j.rser.2006.11.002.

[21] J.F. Belmonte, P. Eguía, A.E. Molina, J.A. Almendros-Ibáñez, R. Salgado, A simplified method for modeling the thermal performance of storage tanks containing PCMs, Appl. Therm. Eng. 95 (2016) 394–410. doi:10.1016/j.applthermaleng.2015.10.111.

[22] S. Canbazoğlu, A. Şahinaslan, A. Ekmekyapar, Ý.G. Aksoy, F. Akarsu, Enhancement of solar thermal energy storage performance using sodium thiosulfate pentahydrate of a conventional solar water-heating system, Energy Build. 37 (2005) 235–242. doi:10.1016/j.enbuild.2004.06.016.

[23] A. Sari, A. Karaipekli, Thermal conductivity and latent heat thermal energy storage characteristics of paraffin/expanded graphite composite as phase change material, Appl. Therm. Eng. 27 (2007) 1271–1277. doi:10.1016/j.applthermaleng.2006.11.004.

[24] A. Lázaro, E. Günther, H. Mehling, S. Hiebler, J.M. Marín, B. Zalba, Verification of a T-history installation to measure enthalpy versus temperature curves of phase change materials, Meas. Sci. Technol. 17 (2006) 2168–2174. doi:10.1088/0957-0233/17/8/016.

[25] A. Castell, C. Solé, M. Medrano, J. Roca, L.F. Cabeza, D. García, Natural convection heat transfer coefficients in phase change material (PCM) modules with external vertical fins, Appl. Therm. Eng. 28 (2008) 1676–1686. doi:10.1016/j.applthermaleng.2007.11.004.

[26] X. Sun, Q. Zhang, M.A. Medina, K.O. Lee, Experimental observations on the heat transfer enhancement caused by natural convection during melting of solid–liquid phase change materials (PCMs), Appl. Energy. 162 (2016) 1453–1461. doi:10.1016/j.apenergy.2015.03.078.

[27] S.-Y. Lee, H.K. Shin, M. Park, K.Y. Rhee, S.-J. Park, Thermal characterization of erythritol/expanded graphite composites for high thermal storage capacity, Carbon N. Y. 68 (2014) 67–72. doi:10.1016/j.carbon.2013.09.053.

[28] C. Peñalosa, A. Lázaro, M. Delgado, B. Zalba, Looking for " low cost " Phase Change Materials and their application, (2012) 1–10.

[29] A. de Gracia, E. Oró, M.M. Farid, L.F. Cabeza, Thermal analysis of including phase change material in a domestic hot water cylinder, Appl. Therm. Eng. 31 (2011) 3938–3945. doi:10.1016/j.applthermaleng.2011.07.043.

[30] W.-B. Ye, D.-S. Zhu, N. Wang, Fluid flow and heat transfer in a latent thermal energy unit with different phase change material (PCM) cavity volume fractions, Appl. Therm. Eng. 42 (2012) 49–57. doi:10.1016/j.applthermaleng.2012.03.002.

[31] S. Jegadheeswaran, S.D. Pohekar, Performance enhancement in latent heat thermal storage system: A review, Renew. Sustain. Energy Rev. 13 (2009) 2225–2244. doi:10.1016/j.rser.2009.06.024.

[32] P. Dolado, A. Lazaro, J.M. Marin, B. Zalba, Characterization of melting and solidification in a real scale PCM-air heat exchanger: Numerical model and experimental validation, Energy Convers. Manag. 52 (2011) 1890–1907. doi:10.1016/j.enconman.2010.11.017.

[33] P. Charvát, L. Klimeš, M. Ostrý, Numerical and experimental investigation of a PCM-based thermal storage unit for solar air systems, Energy Build. 68 (2014) 488–497. doi:10.1016/j.enbuild.2013.10.011.

[34] F.L. Tan, S.F. Hosseinizadeh, J.M. Khodadadi, L. Fan, Experimental and computational study of constrained melting of phase change materials (PCM) inside a spherical capsule, Int. J. Heat Mass Transf. 52 (2009) 3464–3472. doi:10.1016/j.ijheatmasstransfer.2009.02.043.

[35] C. Arkar, S. Medved, Influence of accuracy of thermal property data of a phase change material on the result of a numerical model of a packed bed latent heat storage with spheres, Thermochim. Acta. 438 (2005) 192–201. doi:10.1016/j.tca.2005.08.032.

[36] D. MacPhee, I. Dincer, Thermodynamic Analysis of Freezing and Melting Processes in a Bed of Spherical PCM Capsules, J. Sol. Energy Eng. 131 (2009) 031017. doi:10.1115/1.3142822.

[37] A. Mills, M. Farid, J.R. Selman, S. Al-Hallaj, Thermal conductivity enhancement of phase change materials using a graphite matrix, Appl. Therm. Eng. 26 (2006) 1652–1661. doi:10.1016/j.applthermaleng.2005.11.022.

[38] A. Sharma, V. V Tyagi, C.R. Chen, D. Buddhi, Review on thermal energy storage with phase change materials and applications, Renew. Sustain. Energy Rev. 13 (2009) 318–345. doi:10.1016/j.rser.2007.10.005.

[39] P. Zhang, X. Xiao, Z.W. Ma, A review of the composite phase change materials: Fabrication, characterization, mathematical modeling and application to performance enhancement, Appl. Energy. 165 (2016) 472–510. doi:10.1016/j.apenergy.2015.12.043.

[40] T. Kousksou, P. Bruel, A. Jamil, T. El Rhafiki, Y. Zeraouli, Energy storage: Applications and challenges, Sol. Energy Mater. Sol. Cells. 120 (2014) 59–80. doi:10.1016/j.solmat.2013.08.015.

[41] A. López-Navarro, J. Biosca-Taronger, J.M. Corberán, C. Peñalosa, A. Lázaro, P. Dolado, et al., Performance characterization of a PCM storage tank, Appl. Energy. 119 (2014) 151–162. doi:10.1016/j.apenergy.2013.12.041.

[42] A. de Gracia, L.F. Cabeza, Phase change materials and thermal energy storage for buildings, Energy

Build. 103 (2015) 414–419. doi:10.1016/j.enbuild.2015.06.007.

[43] A. García-Romero, G. Diarce, J. Ibarretxe, A. Urresti, J.M. Sala, Influence of the experimental conditions on the subcooling of Glauber's salt when used as PCM, Sol. Energy Mater. Sol. Cells. 102 (2012) 189–195. doi:10.1016/j.solmat.2012.03.003.

[44] C. Barreneche, A. Solé, L. Miró, I. Martorell, A.I. Fernández, L.F. Cabeza, Study on differential scanning calorimetry analysis with two operation modes and organic and inorganic phase change material (PCM), Thermochim. Acta. 553 (2013) 23–26. doi:10.1016/j.tca.2012.11.027.

[45] V.D. Bhatt, K. Gohil, A. Mishra, Thermal Energy Storage Capacity of some Phase changing Materials and Ionic Liquids, Int. J. ChemTech Res. 2 (2010) 1771–1779. file:///C:/Users/Janko/Desktop/Uni/Thesis/CT=62 (1771-1779).pdf.

[46] M.K.A. Sharif, A.A. Al-Abidi, S. Mat, K. Sopian, M.H. Ruslan, M.Y. Sulaiman, et al., Review of the application of phase change material for heating and domestic hot water systems, Renew. Sustain. Energy Rev. 42 (2015) 557–568. doi:10.1016/j.rser.2014.09.034.

[47] J.N.W. Chiu, V. Martin, Submerged finned heat exchanger latent heat storage design and its experimental verification, Appl. Energy. 93 (2012) 507–516. doi:10.1016/j.apenergy.2011.12.019.

[48] A. Erek, I. Dincer, An approach to entropy analysis of a latent heat storage module, Int. J. Therm. Sci. 47 (2008) 1077–1085. doi:10.1016/j.ijthermalsci.2007.08.002.

[49] L. Fan, J.M. Khodadadi, Thermal conductivity enhancement of phase change materials for thermal energy storage: A review, Renew. Sustain. Energy Rev. 15 (2011) 24–46. doi:10.1016/j.rser.2010.08.007.

[50] F. Frusteri, V. Leonardi, G. Maggio, Numerical approach to describe the phase change of an inorganic PCM containing carbon fibres, Appl. Therm. Eng. 26 (2006) 1883–1892. doi:10.1016/j.applthermaleng.2006.01.018.

[51] P.D. Silva, L.C. Goncalves, L. Pires, Transient behaviour of a latent-heat thermal- energy store: numerical and experimental studies, Appl. Energy. 73 (2002) 83–98.

[52] F. Samara, D. Groulx, P.H. Biwole, Natural Convection Driven Melting of Phase Change Material : Comparison of Two Methods, (n.d.). file:///C:/Users/Janko/Desktop/Uni/Thesis/Modelling of heat transfer.pdf.

[53] Z. Zhang, X. Fang, Study on paraffin/expanded graphite composite phase change thermal energy storage material, Energy Convers. Manag. 47 (2006) 303–310. doi:10.1016/j.enconman.2005.03.004.

[54] M. Rostamizadeh, M. Khanlarkhani, S. Mojtaba Sadrameli, Simulation of energy storage system with phase change material (PCM), Energy Build. 49 (2012) 419–422. doi:10.1016/j.enbuild.2012.02.037.

[55] P. Pinel, C.A. Cruickshank, I. Beausoleil-Morrison, A. Wills, A review of available methods for seasonal storage of solar thermal energy in residential applications, Renew. Sustain. Energy Rev. 15 (2011) 3341–3359. doi:10.1016/j.rser.2011.04.013.

[56] J. Xu, R.Z. Wang, Y. Li, A review of available technologies for seasonal thermal energy storage, Sol. Energy. 103 (2013) 610–638. doi:10.1016/j.solener.2013.06.006.

[57] D. Aydin, Z. Utlu, O. Kincay, Thermal performance analysis of a solar energy sourced latent heat storage, Renew. Sustain. Energy Rev. 50 (2015) 1213–1225. doi:10.1016/j.rser.2015.04.195.

[58] D. Haillot, V. Goetz, X. Py, M. Benabdelkarim, High performance storage composite for the enhancement of solar domestic hot water systems, Sol. Energy. 85 (2011) 1021–1027. doi:10.1016/j.solener.2011.02.016.

[59] M. Mazman, L.F. Cabeza, H. Mehling, M. Nogues, H. Evliya, H.Ö. Paksoy, Utilization of phase change materials in solar domestic hot water systems, Renew. Energy. 34 (2009) 1639–1643. doi:10.1016/j.renene.2008.10.016.

[60] SAM.SSA, (n.d.). http://samssa.eu/ (accessed February 12, 2016).

[61] SOTHERCO, (n.d.). http://www.sotherco.eu/index.php (accessed February 12, 2016).

[62] MERITS, (n.d.). http://www.merits.eu/ (accessed February 12, 2016).

[63] COMTES, (n.d.). http://comtes-storage.eu/ (accessed February 12, 2016).

[64] J. Guion, M. Teisseire, Nucleation of sodium acetate trihydrate in thermal heat storage cycles, Sol. Energy. 46 (1991) 97–100. doi:10.1016/0038-092X(91)90021-N.

[65] K. Seo, S. Suzuki, T. Kinoshita, I. Hirasawa, Effect of Ultrasonic Irradiation on the Crystallization of Sodium Acetate Trihydrate Utilized as Heat Storage Material, Chem. Eng. Technol. 35 (2012) 1013–1016. doi:10.1002/ceat.201100680.

[66] J.-H. Li, J.-K. Zhou, S.-X. Huang, An investigation into the use of the eutectic mixture sodium acetate trihydrate-tartaric acid for latent heat storage, Thermochim. Acta. 188 (1991) 17–23. doi:10.1016/0040-6031(91)80200-3.

[67] S. Nagata, Study on Solidification Process of Sodium Acetate from Supercooled State Trihydrate, 2 (2008) 105–111.

[68] Y. Yoshii, M. Kuraoka, K. Sengoku, T. Ohachi, Induction time and three-electrode current vs. voltage characteristics for electrical nucleation of concentrated solutions of sodium acetate trihydrate, J. Cryst. Growth. 237-239 (2002) 414–418. doi:10.1016/S0022-0248(01)01823-1.

[69] T. Wada, R. Yamamoto, Y. Matsuo, Heat storage capacity of sodium acetate trihydrate during thermal cycling, Sol. Energy. 33 (1984) 373–375. doi:10.1016/0038-092X(84)90169-5.

[70] K. Saita, F. Goto, M. Ishida, H. Hamamatsu, A crystallographic study on the deactivation temperature of crystal nucleating agents for supercooled sodium acetate trihydrate, J. Chem. Eng. Japan. 40 (2007) 36–43.

[71] T. Inagaki, T. Isshiki, Thermal Conductivity and Specific Heat of Phase Change Latent Heat Storage Material Sodium Acetate Trihydrate and Heat Transfer of Natural Convection in a Horizontal Enclosed Rectangular Container, Kagaku Kogaku Ronbunshu. 39 (2013) 33–39. doi:10.1252/kakoronbunshu.39.33.

[72] X. Jin, S. Zhang, M.A. Medina, X. Zhang, Experimental study of the cooling process of partially-melted sodium acetate trihydrate, Energy Build. 76 (2014) 654–660. doi:10.1016/j.enbuild.2014.02.059.

[73] T. Wada, H. Yoneno, Studies on salt hydrates for latent heat storage. VII. The relation between activation process of crystal nucleation catalysts for sodium acetate trihydrate and their

deactivation temperatures, Bull. Chem. Soc. Jpn1. 58 (1985) 919–925.

[74] A. Pebler, Dissociation vapor pressure of sodium acetate trihydrate, Thermochim. Acta. 13 (1975) 109–114.

[75] J. Mao, J. Li, G. Peng, J. Li, A Selection and Optimization Experimental Study of Additives to Thermal Energy Storage Material Sodium Acetate Trihydrate, 2009 Int. Conf. Energy Environ. Technol. (2009) 14–17. doi:10.1109/ICEET.2009.11.

[76] T. Wada, R. Yamamoto, STUDIES ON SALT HYDRATE FOR LATENT-HEAT STORAGE .1. CRYSTAL NUCLEATION OF SODIUM-ACETATE TRIHYDRATE CATALYZED BY TETRASODIUM PYROPHOSPHATE DECAHYDRATE, Bull. Chem. Soc. Jpn. 55 (1982) 3603–3606.

[77] R. Tamme, Behaviour of Sodium Acetate Trihydrate in a Dynamic Latent Heat Storage System, in: AIAA 19th Thermophys. Conf., 1984.

[78] T. Manakata, S. Nagata, Study on Solidification Process of Sodium Acetate Trihydrate from Supercooled State, Japan Soc. Mech. Eng. (2008).

[79] Y. Ouchi, S. Someya, T. Munakata, H. Ito, Visualization of the phase change behavior of sodium acetate trihydrate for latent heat storage, Appl. Therm. Eng. 91 (2015) 547–555. doi:10.1016/j.applthermaleng.2015.08.056.

[80] T. Wada, Y. Matsuo, Studies on salt hydrates for Latent heat storge. VI. Preheating effect on crystallization of sodium acetate trihydrate from aqueous solution with a small amont of disodium hydrogenphosphate, Bull. Chem. Soc. Jpn. 57 (1984).

[81] B. Garay-Ramírez, A. Cruz-Orea, E. San Martín-Martínez, Effect of Silver Nanoparticles on the Thermal Properties of Sodium Acetate Trihydrate, Int. J. Thermophys. 36 (2015) 1164–1172. doi:10.1007/s10765-015-1837-z.

[82] X. Jin, M.A. Medina, X. Zhang, S. Zhang, Phase-Change Characteristic Analysis of Partially Melted Sodium Acetate Trihydrate Using DSC, Int. J. Thermophys. 35 (2014) 45–52. doi:10.1007/s10765-014-1560-1.

[83] J.-H. Li, G. Zhang, J.-Y. Wang, Investigation of a eutectic mixture of sodium acetate trihydrate and urea as latent heat storage, Sol. Energy. 47 (1991) 443–445. doi:10.1016/0038-092X(91)90112-A.

[84] A. Uman, B. Valentin, INVESTIGATIONS OF SODIUM ACETATE TRIHYDRATE FOR SOLAR LATENT HEAT STORAGE, CONTROLLING THE MELTING POINT, Sol. Energy Mater. 9 (1983) 177–181.

[85] C.S. Chang, H.Y. Yeh, L.J. Fang, Freezing and melting behaviour og sodium acetate trihydrate, in: Natl. Heat Transf. Conf., 1989: pp. 37–43.

[86] T. Wada, K. Matsunaga, Y. Matsuo, Studies on salt hydrates for latent heat storage V. preheating effect on crystallization of sodium Acetate Trihydrate from aqueous solution with a small amount of sodium pyrophosohate decahydrate, Bull. Chem. Soc. Jpn. 57 (1984) 557–560.

[87] H.K. Shin, M. Park, H.-Y. Kim, S.-J. Park, Thermal property and latent heat energy storage behavior of sodium acetate trihydrate composites containing expanded graphite and carboxymethyl cellulose for phase change materials, Appl. Therm. Eng. 75 (2015) 978–983. doi:10.1016/j.applthermaleng.2014.10.035.

[88] H. Kimura, J. Kai, Phase change stability of sodium acetate trihydrate and its mixtures, Sol. Energy. 35 (1985) 527–534. doi:10.1016/0038-092X(85)90121-5.

[89] A.-M.A. El-Bassuoni, A.M. Tayeb, N.H. Helwa, A.M. Fathy, Modification of urea–sodium acetate trihydrate mixture for solar energy storage, Renew. Energy. 28 (2003) 1629–1643. doi:10.1016/S0960-1481(02)00052-6.

[90] L.F. Cabeza, G. Svensson, S. Hiebler, H. Mehling, Thermal performance of sodium acetate trihydrate thickened with different materials as phase change energy storage material, Appl. Therm. Eng. 23 (2003) 1697–1704. doi:10.1016/S1359-4311(03)00107-8.

[91] P. Hu, D.-J. Lu, X.-Y. Fan, X. Zhou, Z.-S. Chen, Phase change performance of sodium acetate trihydrate with AlN nanoparticles and CMC, Sol. Energy Mater. Sol. Cells. 95 (2011) 2645–2649. doi:10.1016/j.solmat.2011.05.025.

[92] B.M.L. Garay Ramirez, C. Glorieux, E.S. Martin Martinez, J.J.A. Flores Cuautle, Tuning of thermal properties of sodium acetate trihydrate by blending with polymer and silver nanoparticles, Appl. Therm. Eng. 61 (2013) 838–844. doi:10.1016/j.applthermaleng.2013.09.049.

[93] J.M. Schultz, S. Furbo, Heat of Fusion Storage with High Solar Fraction for Solar Low Energy Buildings, Eurosun 2006. (2006).

[94] M.A. Rogerson, S.S.S. Cardoso, Solidification in heat packs: II. Role of cavitation, AIChE J. 49 (2003) 516–521. http://doi.wiley.com/10.1002/aic.690490221.

[95] J. Fan, S. Furbo, E. Andersen, Z. Chen, B. Perers, M. Dannemand, et al., Thermal behavior of a heat exchanger module for seasonal heat storage, Energy Procedia. 30 (2012) 244–254. doi:10.1016/j.egypro.2012.11.029.

[96] M.A. Rogerson, S.S.S. Cardoso, Solidification in heat packs: I. Nucleation rate, AICHE J. 49 (2003) 505–515. doi:10.1002/aic.690490220.

[97] W. Li, J. Mao, L. Wang, L. Sui, Effect of the Additive on Thermal Conductivity of the Phase Change Material, Adv. Mater. Res. 399-401 (2011) 1302–1306. doi:10.4028/www.scientific.net/AMR.399-401.1302.

[98] K.K. Meisingset, F. Grønvold, Thermodynamic properties and phase transitions of salt hydrates between 270 and 400 K III. CH3CO2Na·3H2O, CH3CO2Li·2H2O, and (CH3CO2)2Mg·4H2O, J. Chem. Thermodyn. 16 (1984) 523–536. doi:10.1016/0021-9614(84)90003-X.

[99] J. Fan, S. Furbo, Z. Chen, E. Andersen, B. Perers, HEAT TRANSFER CAPACITY OF A HEAT EXCHANGER MODULE FOR SEASONAL HEAT STORAGE, (2010).

[100] N. Araki, M. Futamura, A. Makino, H. Shibata, Measurements of Thermophysical Properties of Sodium Acetate Hydrate, Internaltional J. Thermophys. 16 (1995) 1455–1466. doi:10.1007/BF02083553.

[101] H.W. Ryu, S.W. Woo, B.C. Shin, S.D. Kim, Prevention of supercooling and stabilization of inorganic salt hydrates as latent heat storage materials, Sol. Energy Mater. Sol. Cells. 27 (1992) 161–172. doi:10.1016/0927-0248(92)90117-8.

[102] S.K. Sharma, C.K. Jotshi, S. Kumar, Kinetics of dehydration of sodium salt hydrates, Thermochim. Acta. 184 (1991) 9–23. doi:10.1016/0040-6031(91)80130-B.

[103] U.N. Hatkar, P.R. Gogate, Ultrasound Assisted Cooling Crystallization of Sodium Acetate, Ind. Eng. Chem. Res. 51 (2012) 12901–12909. doi:10.1021/ie202220q.

[104] L. Dietz, J.S. Brukner, C.A. Hollingsworth, LINEAR CRYSTALLIZATION VELOCITIES OF SODIUM ACETATE IN SUPERSATURATED SOLUTIONS, J. Phys. Chem. 61 (1957) 944–948.

[105] E. Günther, H. Mehling, S. Hiebler, Modeling of subcooling and solidification of phase change materials, Model. Simul. Mater. Sci. Eng. 15 (2007) 879–892. doi:10.1088/0965-0393/15/8/005.

[106] L.F. Cabeza, J. Roca, M. Nogués, H. Mehling, S. Hiebler, Immersion corrosion tests on metal-salt hydrate pairs used for latent heat storage in the 48 to 58 C temperature range, Mater. Corros. 53 (2002) 902–907. doi:10.1002/maco.200290004.

[107] T. Ohachi, M. Hamanaka, H. Konda, S. Hayashi, I. Taniguchi, ELECTRICAL NUCLEATION AND GROWTH OF NaCH3COO 3H2O, J. Cryst. Growth. 99 (1990) 72–76.

[108] M.A. Rogerson, S.S.S. Cardoso, Solidification in Heat Packs : III . Metallic Trigger, AIChE J. 49 (2003) 522–529. doi:10.1002/aic.690490222.

[109] S.K. Sharma, C.K. Jotshi, S. Kumar, Thermal stability of sodium salt hydrates for solar energy storage applications, Sol. Energy. 45 (1990) 177–181. doi:10.1016/0038-092X(90)90051-D.

[110] P. Moreno, L. Miró, A. Solé, C. Barreneche, C. Solé, I. Martorell, et al., Corrosion of metal and metal alloy containers in contact with phase change materials (PCM) for potential heating and cooling applications, Appl. Energy. 125 (2014) 238–245. doi:10.1016/j.apenergy.2014.03.022.

[111] J.B. Johansen, M. Dannemand, W. Kong, J. Fan, J. Dragsted, S. Furbo, Thermal Conductivity Enhancement of Sodium Acetate Trihydrate by Adding Graphite Powder and the Effect on Stability of Supercooling, Energy Procedia. 70 (2015) 249–256. doi:10.1016/j.egypro.2015.02.121.

[112] S. Furbo, J. Dragsted, Z. Chen, J. Fan, E. Andersen, B. Perers, Towards seasonal heat storage based on stable super cooling of sodium acetate trihydrate, in: EUORSUN Congr. Prodeedings, 2010.

[113] J. Schultz, S. Furbo, Solar heating systems with heat of fusion storage with 100% solar fraction for solar low energy buildings, in: ISES Sol. World Congr. 2007 Proc., 2007: pp. 2721–2725.

[114] P.F. Barrett, B.R. Best, K.B. Oldhan, Thermal Energy Storage in Supersaturated Salt Solutions, Mater. Chem. Phys. 10 (1984) 39–49.

[115] B. Sandnes, J. Rekstad, Supercooling salt hydrates: Stored enthalpy as a function of temperature, Sol. Energy. 80 (2006) 616–625. doi:10.1016/j.solener.2004.11.014.

[116] P.F. Barrett, B.R. Best, Thermal energy storage in supercooled salt mixtures, Mater. Chem. Phys. 12 (1985) 529–536.

[117] M. Telkes, Nucleation of Supersaturated Inorganic Salt Sloutions, Ind. Eng. Chem. 44 (1952) 1308–1310.

[118] A.E.M. Anthony, P.F. Barrett, B.K. Dunning, Verification of mechanism for nucleating crysrallization of supercooled liquids, Mater. Corros. 25 (1990) 199–205.

[119] L. Wei, K. Ohsasa, Supercooling and Solidification Behavior of Phase Change, ISIJ Int. 50 (2010) 1265–1269. doi:10.2355/isijinternational.50.1265.

[120] P.F. Barrett, D.K. Benson, A mechanism for nucleating supercooled liquids, Mater. Chem. Phys. 20 (1988) 171–178.

[121] W.F. Green, The “Melting-Point” of Hydrated Sodium Acetate : Solubility Curves, J. Phys. Chem. 12 (1908) 655–660.

[122] A. Hernández-Guerrero, S.M. Aceves, E. Cabrera-Ruiz, R. Romero-Méndez, Effect of Cell Geometry on the Freezing and Melting Processes inside a Thermal Energy Storage Cell, J. Energy Resour. Technol. 127 (2005) 95. doi:10.1115/1.1789517.

[123] G. Lane, Solar heat storage latent heat material Vol 2, CRC, Boca Raton, Florida, United states, 1986.

[124] J. Schultz, System Simulation Report System: PCM with supercooling, A Report of IEA Solar Heating and Cooling programme - Task 32 Advanced storage concepts for solar and low energy buildings, 2008.

[125] S. Furbo, J. Fan, E. Andersen, Z. Chen, B. Perers, Development of seasonal heat storage based on stable supercooling of a sodium acetate water mixture, in: Energy Procedia, 2012: pp. 1–10.

[126] J.B. Johansen, G. Englmair, M. Dannemand, W. Kong, J. Fan, B. Peres, et al., Laboratory Testing of Solar Combi System with Compact Long Term PCM Heat Storage, Energy Procedia. (2015).

List of symbols

$c_p(s)$	specific heat capacity (solid)	[kJ/kg K]
$c_p(l)$	specific heat capacity (liquid)	[kJ/kg K]
c_p	specific heat capacity	[kJ/kg K]
C_{unit}	heat capacity of storage unit material	[kJ/K]
E_{charge}	measured heat content after charge	[J]
$E_{charge,theoretical}$	theoretical heat content after charge	[J]
$E_{correct,theoretical}$	theoretical correction of heat content	[J]
$E_{content,theoretical}$	theoretical heat capacity of PCM	[kJ/kg]
$E_{discharge}$	measured discharged heat	[J]
$E_{discharge,theoretical}$	theoretical discharged heat	[J]
E_{PCM}	heat capacity of the PCM	[kJ/kg]
$E_{supercool,theoretical}$	theoretical heat content in supercooled state	[J]
H_{loss}	heat loss coefficient	[W/K]
$HXCR$	heat exchange capacity rate	[W/K]
L_f	latent heat of fusion	[kJ/kg]
m	mass	[kg]
$\dot{Q}$	charge/discharge power	[W]
t	time	[s]
T_{end}	storage temperature at the end of a cycle	[˚C]
T_{amb}	ambient temperature	[˚C]
T_i	inlet temperature	[˚C]
T_{max}	maximum storage temperature	[˚C]
T_{melt}	melting temperature	[˚C]
T_o	outlet temperature	[˚C]
T_s	storage mean temperature	[˚C]
T_{start}	storage temperature at the beginning of a cycle	[˚C]
$T_{supercool}$	temperature of the storage with the PCM in supercooled state	[˚C]
$\dot{V}$	volume flow rate	[m^3/h]
ρ	density	[kg/m^3]

Abbreviations

SAT	sodium acetate trihydrate
HXCR	heat exchange capacity rate
DHW	domestic hot water
CFD	computational fluid dynamics
PCM	phase change material
CMC	carboxymethyl cellulose

List of figures

Part II - Papers

Paper 1 - Long term thermal energy storage with stable supercooled sodium acetate trihydrate

Mark Dannemand, Jørgen M. Schultz, Jakob Berg Johansen, Simon Furbo

Applied Thermal Engineering, Vol. 91 pp. 671–678. 2015

doi:10.1016/j.applthermaleng.2015.08.055.

Applied Thermal Engineering 91 (2015) 671–678

Contents lists available at ScienceDirect

Applied Thermal Engineering

journal homepage: www.elsevier.com/locate/apthermeng

Research paper

Long term thermal energy storage with stable supercooled sodium acetate trihydrate

Mark Dannemand [a, *], Jørgen M. Schultz [b], Jakob Berg Johansen [a], Simon Furbo [a]

[a] Department of Civil Engineering, Technical University of Denmark, Brovej 118, Kgs. Lyngby, DK 2800, Denmark
[b] Steensen Varming, Ryesgade 23, DK-2200 Copenhagen N, Denmark

HIGHLIGHTS

- A compact seasonal heat storage utilizing stable supercooling of sodium acetate trihydrate is described.
- Solutions for key obstacles for reliable operation are suggested.
- A TRNSYS model of a solar heating combi system elucidates the performance.

ARTICLE INFO

Article history:
Received 9 March 2015
Accepted 18 August 2015
Available online 1 September 2015

Keywords:
Compact seasonal heat storage
Long term thermal energy storage
Phase change material
PCM
Supercooling
Sodium acetate trihydrate

ABSTRACT

Utilizing stable supercooling of sodium acetate trihydrate makes it possible to store thermal energy partly loss free. This principle makes seasonal heat storage in compact systems possible. To keep high and stable energy content and cycling stability phase separation of the storage material must be avoided. This can be done by the use of the thickening agents carboxymethyl cellulose or xanthan rubber. Stable supercooling requires that the sodium acetate trihydrate is heated to a temperature somewhat higher than the melting temperature of 58 °C before it cools down. As the phase change material melts it expands and will cause a pressure built up in a closed chamber which might compromise stability of the supercooling. This can be avoided by having an air volume above the phase change material connected to an external pressure less expansion tank. Supercooled sodium acetate trihydrate at 20 °C stores up to 230 kJ/kg. TRNSYS simulations of a solar combi system including a storage with four heat storage modules of each 200 kg of sodium acetate trihydrate utilizing stable supercooling achieved a solar fraction of 80% for a low energy house in Danish climatic conditions.

1. Introduction

Space heating of buildings and domestic hot water supply account for a large part of our energy use. Solar energy is more abundant in summer than in winter periods when heating demands are much larger. Thermal energy storage technologies are therefore needed to match the intermittent supply of solar energy with varying heating demands if solar heating systems should fully cover our heat demand. Currently available heat storage systems that use water as the storage medium work well but mainly for short term storage, as their continuous heat losses limit the storage period. With a very large water storage, it is possible to store heat enough for a whole winter for a single family house but implementation is limited due to practicalities. For long storage periods in compact storages alternative technologies are needed. For this study long term storage is considered as biannually or longer periods which are required for seasonal heat storage.

Heat storages utilising latent heat of fusion of a phase change material (PCM) has been suggested for improving the performance compared to heat storage of sensible heat by several authors. Sharma and Sagara made an extensive review on latent heat storage materials and systems [1]. Nkwetta et al. did a review on the experimental and theoretical studies including PCMs in storages and solar collectors [2]. Sharif et al. also did a review on application of PCM for hot water and heating system [3] Sole et al. showed that including PCM in a water storage can improve its performance [4]. Wada et al. investigated several promising mixtures for solar energy storage [5]. Canbazoglu et al. investigated how hydrated salts

* Corresponding author.
E-mail address: markd@byg.dtu.dk (M. Dannemand).

http://dx.doi.org/10.1016/j.applthermaleng.2015.08.055
1359-4311/

can enhance the thermal energy storage performance of solar water heating systems [6]. Nagano et al. did experimental investigations in a latent heat storage considered for waste heat utilization and found that available enthalpy was more than double compared to a water storage [7]. López-Navarro et al. presented the design of a latent cold storage with a paraffin and characterized its performance [8]. Arce et al. elucidates how thermal energy storage can reduce energy consumptions with theoretical calculations [9]. Abhat introduces some fundamental considerations for both sensible and latent heat storages related to material properties and storage design [10].

Supercooling, subcooling or undercooling is when a phase change material in liquid state cools down below its melting point without solidifying; leaving it in a metastable state where the latent heat of fusion is not released. In latent heat storage supercooling has traditionally been seen as an undesired effect that had to be avoided as it prevented the heat of fusion from being released when the melting point of the storage material was reached during the discharge process [11]. This can be done by using various nucleation agents such as Aluminium Nitride Nanoparticles [12] or various salts [13]. The idea of utilizing supercooled salt hydrates for long term storage has however been known since the late 1920s [14] and pocket-sized heat packs storing heat in supercooled sodium acetate trihydrate were patented in 1978 [15]. This principle makes long term thermal energy storage possible by letting the melted salt hydrate remain in supercooled state at ambient temperature in the storage period. Once the heat is needed the solidification of the supercooled solution is triggered and the latent heat of fusion is released as it crystalizes. Investigations have previously shown that there is a potential in utilizing stable supercooling as a storage technique. Hirano and Saitoh showed by numerical simulations that latent heat storages utilizing supercooling have higher efficiencies than latent heat storages not utilizing supercooling and that the efficiency increases with longer storage periods [16] and is effected by the operating temperature [17]. The same authors tested a storage unit utilizing supercooling of 36–39 kg PCM [18]. Sandnes and Rekstad made measurement of energy released from supercooled samples of salt hydrates and gives recommendation for storage design [19]. Barrett and Best showed that some PCM mixtures can remain in supercooled state well below its melting point [20].

Sodium acetate trihydrate (SAT) has a melting point of 58 °C and a relatively high heat of fusion of 264 kJ/kg [21], supercool consistently down to temperatures well below 0 °C [22]. Rogerson and Cardoso investigated the relation between nucleation pressure and temperature and found via experiments that sodium acetate trihydrate spontaneously crystalizes at −14 °C or lower [23]. Wei and Ohsasa investigated supercooling and solidification of sodium acetate trihydrate and found that there may be a link between the time and level of heating above the melting point and the stability of the supercooling [24]. Wada also reports that SAT crystalizes at a temperature of −30 °C or below [25]. When considering the application of space heating and domestic hot water preparation and solar collectors as the heat source, sodium acetate trihydrate has suitable thermal properties as storage material for long term heat storage [26].

Well-functioning heat storage prototypes utilizing supercooled PCM which can serve as seasonal heat storage for single family houses have not yet been reported. The primary barriers to achieve an operating storage based on stable supercooling of sodium acetate trihydrate are listed in this article along with proposed solutions. Suggested solutions are based on a series of laboratory experiments in small scale and on prototype storage modules. The theoretical storage potential for sodium acetate trihydrate is calculated based on a simple theory of specific heat capacities and latent heat of fusion of the PCM. A TRNSYS model simulating a solar combi system including a PCM storage utilizing stable supercooling of sodium acetate trihydrate covering the heat demand for a passive house in Danish climatic conditions elucidates the potential for the storage concept.

2. Barriers, problems and solutions

To achieve a reliable operating heat storage utilizing the principle of stable supercooling of sodium acetate trihydrate a number of problems need to be considered and solved. Problems are phase separation; expansion and contraction of the PCM during melting and solidifying, stable supercooling, heat transfer to and from the PCM and triggering the crystallization. A series of small scale test with sample sizes of 200–500 g in glass jars and testing of prototype storages containing PCM masses of 100–220 kg have been carried out in order to find solutions for these problems.

2.1. Phase separation

Sodium acetate trihydrate is an incongruently melting salt hydrate and will suffer from phase separation especially over repeated heating and cooling cycles. This will reduce the heat storage capacity as the energy released after crystallization of a supercooled sample is reduced when anhydrate sodium acetate segregates and settles to the bottom of the container so that the reformation of the trihydrate crystal is prevented as mentioned by Kimura [13] and Lane [14]. Furbo and Svendsen did extensive experimental testing of storages with salt hydrates [27], [28]. They suggest that adding extra water to the salt hydrate so the salt water mixture composition is always at a point where all salt is dissolved in the water when it is in liquid and supercooled state as a solution. This solution does however reduce the energy density of the storage as shown by Araki [29]. Also the melting temperature of the sodium acetate water mixtures will drop with increasing water content which may reduce the performance of the storage [30]. The extra water principle requires soft mixing of the salt water mixture to avoid phase separation which can possibly be achieved by the convection during heating, depending on the storage and heat exchanger design. However, as the phase separation happens mainly in the supercooled state before crystallization is triggered, there will still be a loss of latent heat of fusion when using the extra water principle for long term thermal energy storage with supercooling of sodium acetate trihydrate, if the mixing is not applied in another way.

Another method to solve the problem with phase separation is to add a thickening agent to the salt hydrate to keep the segregated salt from settling to the bottom of the container. Several additives such as carboxyl methyl cellulose (CMC) and Xanthan rubber have been researched previously. Hu worked with CMC [12]. Lane reports on some early research in search for cycling stable thickeners [14]. Cabeza et al. found starch and bentonite to be an appropriate thickener for sodium acetate trihydrate. Also Cellulose was tested but showed not to be stable above 65 °C [31]. Wada et al. reports improvement of cycling stability of sodium acetate trihydrate when thickened with a mixture including polyvinyl alcohol [32]. Ryu et al. tested a super absorbent polymer and CMC as thickeners and found them effective [33]. Garay Ramirez et al. reports that a mixture of polymers of CMC and Silica Gel reduce phase separation [34].

Requirements for the thickening agent are inherently that it is stable over the temperature range of which the storage operates and the life time of the storage. The drawback of using thickening agents can be reduced storage density and reduced convection of the melted PCM in the storage, which will reduce the heat exchange capacity rate in the PCM during the charging process. In small scale

tests 200 g samples were heated to 90 °C in an oven until fully melted and let to passively cool to room temperature. A mixture of sodium acetate trihydrate and 1 wt% of CMC or 0.5 wt% for Xanthan rubber well mixed into the PCM has in small scale test shown to be sufficient to change the viscosity enough to keep anhydrate crystals suspended in the supercooled solution. Thickening agents may have viscosity changing ability varying over temperatures. To solve the phase separation problem with a thickening agent, it must be able to keep segregated salt suspended in the supercooled state, not necessarily in the hot melted state where all salt is dissolved in the water.

2.2. Expansion of the PCM

With a density of 1280 kg/m^3 [26] [35]of the liquid sodium acetate trihydrate and 1450 kg/m^3 of the solid, a volume difference of more than 10% has to be considered when designing the storage tanks. One problem related to this expansion is the strains it put on the storage tank during the heating and cooling cycling. The tank material should be able to withstand the pressure changes and deformations over the lifetime of the storage if this is not solved in another way. Testing of a prototype module in steel containing 100 kg sodium acetate trihydrate showed a pressure difference of 1.2 bars in the PCM chamber between the crystalized state at room temperature and the fully melted state at 90 °C.

A soft container for the PCM could be a solution if the container material can remain flexible over a life time of the storage. Also a flexibility of the connection for the storage may possibly be required. A rigid storage design with an expansion device that allows for the expansion and contraction of the PCM without pressure built up can eliminate the problems with changing strains in the storage tank material and possibly fatigue over time. In such system a fluid or gas can work as the medium going in and out of the expansion while the PCM stays in the primary chamber. The principle of how the expansion issue was solved for the prototype testing is illustrated in Fig. 1 where an expansion vessel without pre-pressure is connected to an air volume above the PCM.

2.3. Supercooling and cycling stability

To achieve supercooling of the sodium acetate trihydrate it is necessary that all crystals of the bulk are melted so that it will not crystallise as it cools down. There appears to be a link between the level of heating above the melting point and the stability of supercooling as investigated by Wei [24] and Wada [36]. This was also investigated by Jin [37] who found that heating 8 g sodium acetate trihydrate in a test tube to 62 °C for 80 min would result in no crystallization when it was cooled to ambient temperatures. There was no information if the samples crystalized after some time. Our investigations have shown that for both small scale tests and prototype module tests showed a temperature of around 20 K above melting point in the entire volume helps to achieve stable supercooling over time. When the ever-present impurities in the salt hydrate work as nucleation agents, large PCM volumes may show reduced stability of supercooling, as the chance of a spontaneous nucleation caused by an impurity increases with the volume [23].

Heating the salt hydrate to a high temperature will cause some evaporation of the water; therefore a closed container with no loss of water through the tank material over the lifetime of the storage unit is essential to avoid changing the composition of the PCM. As the metastable state of the supercooled salt hydrate could easily be interrupted by external influences, a closed container is inherently more stable. Diffusion of the heat transfer fluid from the heat exchanger into the PCM should be avoided. When considering the choice of tank material, corrosion and chemical reactions between the salt and the tank material must be considered. Steel and stainless steel in combination with sodium acetate trihydrate has been shown to be stable over long periods as shown by Furbo et al., [27,28]. Cabeza et al. investigated corrosion of metals immersed in salt hydrates and also recommends sodium acetate trihydrate in combination with steel and stainless steel [38].

If using rigid constructions such as steel the density change between the cold solid and the warm liquid salt hydrate must be considered, as the volume change of the PCM in a closed container can cause pressure changes and deformations of the tank. Just as bending a metal disk with cracks works as a triggering mechanism for the pocket sized heat packs by creating a local high pressure [39], small cracks on the inside of the PCM chamber can in combination with pressure changes and deformations work as an uncontrolled activation mechanism e.g. at joints or welds [40,41]. So if the storage tanks material is of rigid material operating it with constant pressure will provide better stability of the supercooling. Coating of inner surfaces to eliminate cracks or creating a softer inner surface may be a solution for rigid materials and at cracks and joints.

2.4. Effective heat transfer from PCM to heat transfer fluid

The volume reduction that takes place in sodium acetate trihydrate when changing from the liquid to the solid phase will form cavities inside the tank. These cavities will reduce the thermal conduction of the bulk PCM and heat exchange capacity rate between the PCM and the heat transfer fluid of the heat exchangers in a rigid storage [21,42]. Depending on the heat exchanger design these cavities could be a significant resistance in heat transfer as the cavities work as thermal resistances. Designing a soft container where the heat exchangers move along with the expansion and contraction of the PCM can be a solution but this requires a lot of the tank material in terms of flexibility and lifetime.

Another well-known problem of heat transfer in phase change materials is their low thermal conductivity [43]. To increase the

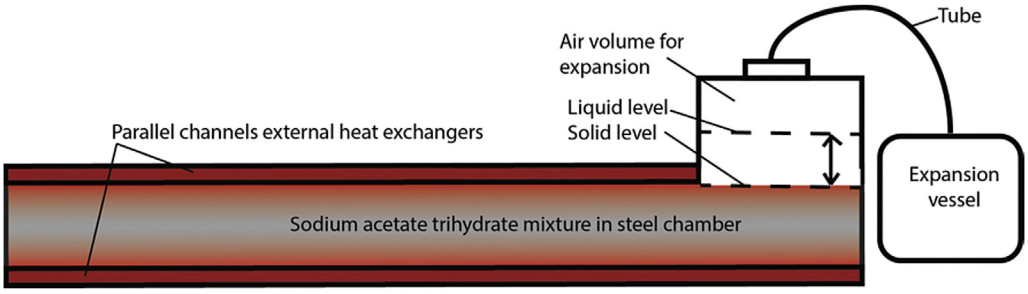

Fig. 1. Principle of heat storage module with expansion vessel to solve expansion of the PCM.

heat transfer and the charge and discharge power of PCM storages, the thermal conductivity of the PCM has been sought increased by adding high conducting material such as graphite powder, expanded graphite or fibres to the PCM with good results. Heinz showed that adding graphite to a sodium acetate mixture will reduce the internal temperature difference in a sample especially during heating [44]. Li et al. made investigations of the effect on adding expanded graphite to sodium acetate trihydrate [45]. Frusteri et al. showed that adding about 8% by volume graphite fibres can increase the thermal conductivity of a composite PCM by a factor of 4 [46]. Shin et al. investigated thermal properties of sodium acetate trihydrate mixed with expanded graphite and CMC [47]. Cabeza et al. investigated heat transfer enhancement in PCM thermal energy storages and found that a graphite matrix was very effective for heat flux enhancement [48]. Nkwette did numerical investigations showing the effect of having PCM integrated in a hot water storage. One of the investigated PCMs was sodium acetate trihydrate with 10% graphite [49]. A thickening agent that is stable for the operating temperature range which may be as high as up to 95 °C is required to keep the graphite powder dispersed and evenly distributed in the PCM mixture and avoiding that the graphite powder segregates. Test with 300 g samples of sodium acetate trihydrate and fine graphite powder with up to 4% CMC have shown that at a temperature of 90 °C the thickening effect of the CMC is reduced and the graphite powder settles to the bottom. Samples with Xanthan rubber has shown to be stable in temperatures up to 90 °C.

When operating with supercooling and the rapid crystallization happening from supercooled state, the PCM may not contract in a uniform way and therefore cavities inside the PCM could form which would further enhance the problem of low conduction of the PCM. A high conductive liquid possibly oil that does not mix with the PCM and with a lower density so it floats on top when the PCM is in liquid state could work as an enhancer for the heat transfer. It could fill the cavities in the PCM and between the PCM and the heat exchanger. This would lead to a higher effective heat transfer when the PCM solidifies and contracts. This heat transfer liquid could possibly be considered when designing the expansion device. When the PCM is heated the oil can be pushed out to the expansion volume of the module.

With the low thermal conductivity of the PCM and no convection in the sold phase, the heat exchangers has to be designed to have good heat transfer, possibly by having large heat transfer areas short distances to the PCM. When designing the heat exchanger the requirements for a minimum temperature in all parts of the PCM to obtain supercooling should be considered.

2.5. Triggering the crystallization

As the entire volume will solidify once the crystallization is started, it is desirable to divide the storage unit into a number of separate modules that can be operated individually. The size and number of modules would depend on the application into which it is integrated and an economic evaluation.

The crystallization and release of the heat of fusion from the supercooled sodium acetate trihydrate is initialised when the first seed crystal of a certain size is present in the solution. From the point of activation the crystallization will spread to the entire volume and the temperature will rise to close to the melting point of 58 °C [23]. Supplying the seed crystal to trigger the crystallization in a reliable and controllable way is essential for such a system. Ultra-sonic sound has been tried and found reliable as an activation mechanism [50]. The metallic disc of the pocket sized heat packs also works reliably but needs moving parts submerged in the solution and therefore introduce a risk of uncontrollable activation. Mechanically providing a crystal to the supercooled solution might also be a viable solution. Lastly, it has been shown that cooling supercooled sodium acetate trihydrate to a low temperature will eventually cause crystallization of the supercooled solution [22]. Experiments have shown that 100 g samples of sodium acetate trihydrate can stay supercooled down to temperatures of −15 °C to −25 °C before it crystalizes. Solutions where cooling is used to trigger the formation of the seed crystal could be made using peltier elements or cooling by the evaporation of liquid CO_2 [22]. One benefit of the cooling method is that there are no moving parts inside the PCM chamber and that reduces the risk of spontaneous crystallization. Evaporating liquid CO_2 under pressure has a large cooling power and can be done through the tank wall from the outside of the tank. The loss of thermal energy by cooling can be considered negligible if just a tiny part of the PCM is cooled by a high cooling power. Cooling with CO_2 has been a reliable activation technique in the prototype testing.

3. Theoretical calculations

The theoretical energy content of the sodium acetate trihydrate is determined by the specific heat capacity of the solid and liquid phases as well as the latent heat of fusion. The following calculations assume an ideally performing material without losses due to phase separation; without problems related to stability of the supercooling, expansion of the PCM, heat transfer and triggering the crystallization. If these problems are not solved or only partly solved the performance will be worse that described. The theory describes the thermal energy content in a simple way, assuming that the sodium acetate trihydrate mixture behaves as an ideal compound that changes phase from solid to liquid at a specific melting temperature. In reality the phase change may happen over a temperature range especially if extra water is added to the salt hydrate [27]. When the focus is on the stable initial, fully charged, supercooled and discharged state, this simple theory provides a sufficient basis for estimation of energy content.

3.1. Material storage potential

The following equations show the theoretical change of thermal energy in the heat storage module for a given charge. The equation consists of the sensible heat of the salt hydrate in solid and liquid state, the latent heat of fusion of the salt hydrate and the sensible heat of the storage module material.

$$E_{charge,theo} = m\cdot\Big((T_{melt} - T_{start})\cdot c_p(s) + L_f + (T_{max} - T_{melt})\cdot c_p(l)\Big) + C_{module}\cdot(T_{max} - T_{start}) \quad (1)$$

where m is the mass of the PCM, T_{melt} is the melting temperature of the PCM of 58 °C, T_{start} is the mean storage temperature at the start of the charge, $c_p(s)$ is the specific heat of the PCM in solid phase, $c_p(l)$ is the specific heat of the PCM in liquid phase, L_f is the latent heat of fusion of the PCM, C_{module} is the heat capacity of the storage module material including the heat transfer fluid in the heat exchangers, and T_{max} is the mean maximum temperature the heat storage module reaches during a charge.

When the storage module is discharged from the fully charged state at T_{max} to a temperature $T_{supercool}$ without crystallising, just the sensible heat of the module and the liquid sodium acetate mixture is discharged. Assuming the specific heat of the supercooled sodium acetate mixture is the same as the liquid sodium acetate mixture, the discharged energy E_{dis} can be expressed by:

$$E_{dis,theo} = (m \cdot c_p(l) + C_{module}) \cdot \left(T_{max} - T_{supercool}\right) \quad (2)$$

where $T_{supercool}$ is the storage temperature at supercooled state.

The stored thermal energy at supercooled state can be expressed using Eq. (3). Here the discharged energy expressed in Eq. (2) is subtracted from the charged energy expressed by Eq. (1).

$$E_{supercool,theo} = E_{charge,theo} - E_{dis,theo} \quad (3)$$

If the temperature of the storage module at supercooled state $T_{supercool}$ and end temperature T_{end} after the activation and discharge are the same, then the thermal energy stored at supercooled state $E_{supercool,\ theo}$ at a temperature $T_{supercool}$ can be expressed by:

$$E_{supercool,theo} = m \cdot \left(L_f - \left(T_{melt} - T_{supercool}\right) \cdot \left(c_p(l) - c_p(s)\right)\right) \quad (4)$$

If the storage is discharged to a temperature that is different from that of the supercooled state, the discharged energy is corrected for the difference in sensible heat of the module material and the PCM mixture in solid state.

$$E_{correct,theo} = \left(T_{supercool} - T_{end}\right) \cdot \left(C_{module} + m \cdot c_p(s)\right) \quad (5)$$

The energy released per unit mass of PCM from activating a supercooled sodium acetate mixture at a specific temperature, corrected for a difference between the final discharge temperature and the temperature of the supercooled PCM mixture before activation is:

$$E_{cont,theo}\left(T_{supercool}\right) = \frac{E_{supercool,theo} - E_{correct,theo}}{m} \quad (6)$$

With the specific heat for the solid state sodium acetate trihydrate of 2.1 kJ/kgK and 3.0 kJ/kgK [29] for the liquid state, a latent heat of fusion of 264 kJ/kg at the melting point of 58 °C; the energy content per unit of mass at a temperature range relevant for solar heating systems are displayed in Fig. 2. The listed specific heat capacities are averaged to a constant at the temperature range. In reality the specific heat capacities vary with temperature [29].

3.2. System performance by TRNSYS modelling

A TRNSYS model [51] of a solar combi system with a PCM storage was used for a parametric study to determine the PCM storage size and solar collector area to obtain a solar fraction of 80% of the yearly heat demand for a passive house in Danish climatic conditions. The solar fraction (SF) was defined as

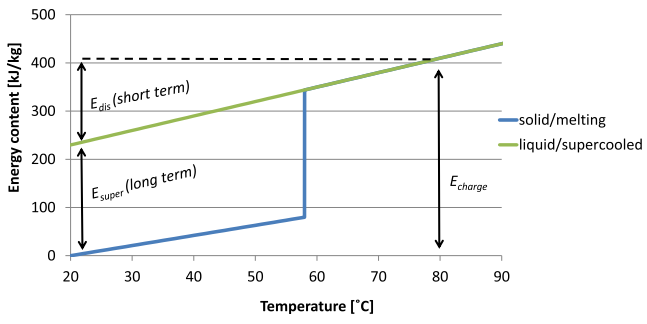

Fig. 2. Principle of long term heat storage utilizing stable supercooling and storage potential for sodium acetate trihydrate.

$$SF = 1 - \frac{Q_{aux}}{Q_{Spa} + Q_{DHW}},$$

where Q_{aux} is the auxiliary heating for the system, Q_{Spa} is the energy used for space heating and Q_{DHW} is the energy used for domestic hot water (DHW) preparation.

A principle diagram of the solar heating system design is shown in Fig. 3.

The system included the PCM storage and a 180 L DHW tank. The DHW tank was required to fulfil the power demand related to hot water draw offs, which would be difficult to fulfil with direct discharge of the PCM storage. Energy from the solar collectors could either be used for direct charge of the PCM storage or transferred to the demand loop through the heat exchanger connecting the solar collector loop and the demand loop. Here the energy could either be used for heating of the DHW tank or for space heating. The PCM storage was made up of a number of subsections that can be individually controlled with respect to charging, discharging and activation of solidification. The sub sectioning of the PCM storage makes it possible to activate a small part of the total storage volume to match the demand and saving the rest of the supercooled sections for later activation. Previous analyses [52] have shown that the optimum control strategy for charging was first to heat up the DHW tank if the forward temperature from the collector was sufficient. When the DHW tank had reached a temperature of 70 °C the PCM storage was thereafter charged one section at the time until fully melted if the forward temperature from the collector was high enough. Otherwise the section with the highest temperature that could be further heated was chosen. In case of space heating demand the necessary forward temperature to the space heating loop was secured by controlling the flow rate through the DHW heat exchanger if relevant or by discharging a section in the PCM storage that resulted in the necessary forward flow temperature to the heat exchanger. When discharging the PCM storage the section that just had the sufficient temperature for covering the actual demand was chosen. A supercooled section was activated if no liquid or solidified section had the required temperature level.

The PCM storage with sodium acetate trihydrate including the control had been modelled in a TRNSYS type and a series of parametric studies was carried out in TRNSYS with the system design shown in Fig. 3. The solar collectors were flat plate collectors with a start efficiency of 0.82, 1st and 2nd order heat loss coefficients of 2.44 W/(m^2·K) and 0.005 W/(m^2·K^2). The collectors were facing south with a collector tilt of 75°. The PCM storage and the DHW tank were in the reference case insulated corresponding to an effective heat loss coefficient of 0.4 W/(m^2·K). The flow rate in the solar collector loop was set to 1800 kg/hr. The heat exchange capacity rate between the PCM in the storage module and the heat transfer fluid is affected by the design of the heat exchanger and the properties of the PCM. Simulations with different values for heat exchange capacity rates are made to show how the system size is related to the heat exchange capacity rate. The heat exchange capacity rate for charge and discharge of the PCM storage was varied between 200 and 400 W/K in this parameter variation. The volume of the modules was set to 150 L. The thermal conductivity of the PCM in both solid and liquid state was set to 0.6 W/mK. The daily DHW consumption was set to 99 L/day (33 L draw off at 7.00, 12:00 and 18:00). The DHW temperature was 50 °C and the cold water temperature was 10 °C resulting in an annual DHW energy consumption of approximately 1677 kWh. The space heating demand was calculated on hourly basis with the building energy simulation tool, tsbi3 [53] for a low energy house built according to the passive

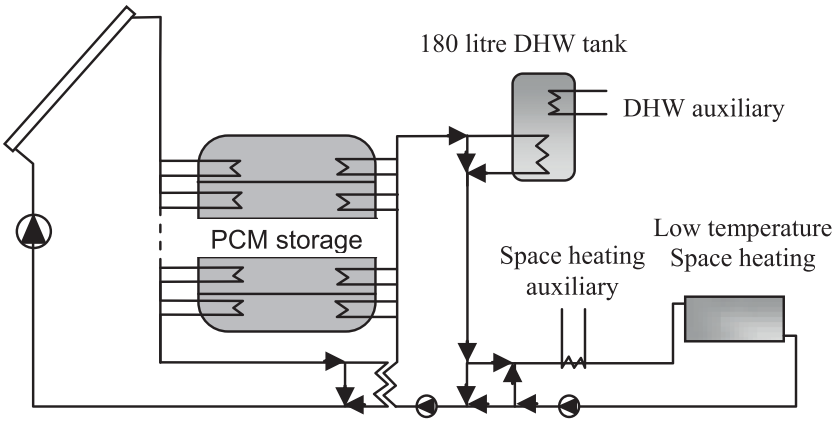

Fig. 3. Principle diagram of TRNSYS model for solar heating combi system.

house standard [54] located in a Danish climate (~3000° days; horizontal solar radiation: ~1020 kWh/m^2/year). The space heating system was a low temperature system, e.g. floor heating with a heating demand of 2008 kWh per year.

Previous calculations [55] have been carried out simulating a low energy house with a heating demand of 2010 kWh per year and an annual DHW consumption of 2540 kWh. The heat exchange capacity rate for charge and discharge of the PCM storage was 500 W/K in these calculations. It was shown that it was possible to achieve a 100% solar fraction for a solar heating system with a 36 m^2 collector area and 6 m^3 sodium acetate trihydrate divided into 24 subsections. A Module size of 250 L had showed to be the optimal size in this simulation. For this calculation it was assumed that the heat loss form the storage was utilized for space heating e.g. by having the storage located inside the building. Overheating of the house in the summer should be considered in this case. A PCM volume of 10 m^3 was required if the losses were considered not utilized. The previous study showed that this volume was less than 25% of the required volume for a water storage to cover 100%.

4. Results and discussion

Based on the theory in section 3.1 it is possible to store 230 kJ/kg of thermal energy in a supercooled solution of sodium acetate trihydrate at a temperature of 20 °C if discharged to 20 °C after crystallization. This assumes no losses due to phase separation. Activating the supercooled PCM at 15 °C and discharging it to 30 °C will release 194 kJ/kg. Some additional energy will in the case, where storage and final discharge temperature differs, be lost as it is used to heat up the storage tank material.

When operating with PCM in bulk sizes that are needed for storing enough energy for heating building and long storage periods, the material may act differently compared to small sample sizes. Phenomena like phase separation and local cavities resulting in thermal resistances may not be obvious in small sample sizes normally used in material characterization such as T-history and differential scanning calorimetry (DSC) measurements. The key material property for making a heat of fusion storage with supercooling is the latent heat of fusion as this determines the storage capacity. The highest heat of fusion for the sodium acetate trihydrate is assumed to be of the pure material if phase separation is avoided. Additives such as thickening agents for stabilizing the PCM or thermal conductivity enhancers will reduce the latent heat of fusion per unit of mass but may be necessary to have the system perform reliable.

4.1. TRNSYS simulation

The parametric studies carried out were aimed at achieving 80% solar fraction of both DHW and space heating in a passive house in a Danish climate. The heat exchange capacity rate of a PCM module will depend on multiple variables such as heat exchanger design and thermal properties of the PCM and heat transfer fluid as well as operating conditions. Values ranging from 200 W/K to 400 W/K for the heat exchange capacity rate were included in the parameter variation. From Fig. 4 where the solar collector area of the system was fixed to 36 m^2, it can be seen that the heat exchange capacity rate of each module highly affects the solar fraction achieved by the system. With a heat exchange capacity rate of 400 W/K it was possible the reach 80% solar fraction with 7 modules of 150 L. If the heat exchange capacity rate was 250 W/K 12 modules were required to obtain 80% solar fraction.

The sizes of the individual modules have also shown to have an effect on the yearly performance of the system even if the total PCM volume was kept. Doubling the PCM volume of the modules and assuming the heat exchange capacity rate also doubles due to a larger heat exchanger showed to increase the solar fraction by 7 percentage points. Doubling the PCM volume without increasing the heat exchange capacity rate had almost no effect of the system performance as may be seen in Fig. 5. This indicates that there is a relation between the operation strategy, energy demand and system design which can be optimized for each case.

The results shown in Fig. 6 are for systems reaching 80% solar fraction. Values of 250 W/K and 400 W/K for the heat exchange capacity rate were selected. The solar collector area and the number of modules were varied. Based on the cost of the PCM modules and

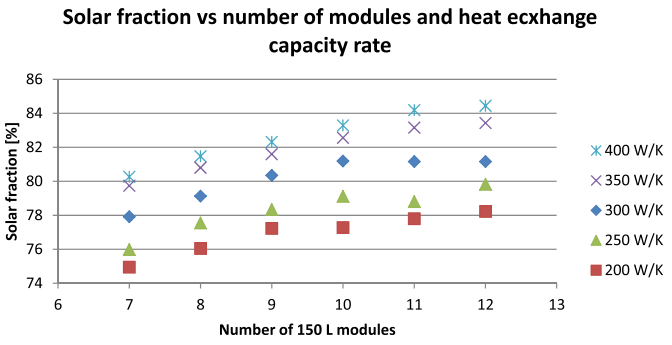

Fig. 4. Solar fraction vs number of modules and heat exchange capacity rate for solar combi system with 36 m^2 collector area.

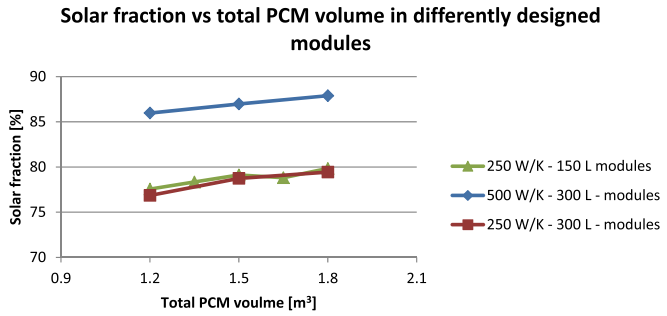

Fig. 5. Solar fraction vs. total PCM volume in differently designed modules.

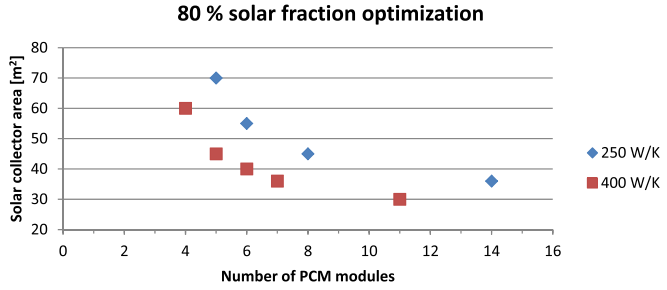

Fig. 6. 80% solar fraction for systems with heat exchange capacity rate for the PCM storage of 250 W/K and 400 W/K.

of the solar collectors an evaluation can be made to choose the optimum system design and size.

Installation of such PCM storage systems in already built houses also leads to considerations related practically installation, possibilities of access and handling. This could lead to restrictions of module size.

5. Conclusions

To have a reliable long term heat storage based on stable supercooling of sodium acetate trihydrate a number of problems have to be solved. Capacity loss due to phase separation can be solved by using thickening agents such as carboxyl methyl cellulose (CMC) and Xanthan rubber. The density difference of the sodium acetate trihydrate from the coldest to the hottest state is associated with pressure changes in a storage module. To obtain stable supercooling in large bulks of sodium acetate trihydrate in closed rigid tanks it is essential to operate the PCM chamber with minimal pressure changes. This can e.g. be done by having an expansion volume in the PCM chamber connected to an external expansion vessel without pre-pressure. The heat exchange capacity rate to and from the PCM can be improved by adding a highly conductive compound such as graphite powder to the PCM combined with a temperature stable thickening agent. The thickening agent has to be stable in the entire temperature interval the storage operates. Xanthan rubber has shown to keep its thickening ability up to 90 °C. Cavities in the PCM are formed when the PCM contracts during crystallization. A heat transfer fluid inside the PCM chamber that does not react with the PCM can fill in these gaps and increase the heat exchange capacity rate. Triggering the crystallization of the supercooled sodium acetate can be done by providing a seed crystal or by cooling a small part of the PCM to its minimum level of supercooling e.g. by evaporating CO_2 in a small chamber adjacent to the PCM chamber.

From theoretical consideration it is possible to store up to 230 kJ/kg of supercooled sodium acetate trihydrate at 20 °C if all sensible heat down to 20 °C can be utilized. A TRNSYS simulation showed that for a passive house in Danish climate it was possible to achieve a solar fraction of 80% by a solar heating system with 36 m^2 solar collector area and 7 PCM modules of 150 L if the heat exchange capacity rate was 400 W/K. If the heat exchange capacity rate was 250 W/K 12 modules were required to achieve 80% solar fraction. Based on this parametric study including system size and heat exchange capacity rate of the module it was obvious that a high heat exchange capacity rate is desired to reach a high solar fraction with smaller system sizes.

Acknowledgements

This research was partly funded by the European Commission (Grant Agreement N° 295568) as part of the Seventh Framework Programme of the European Community for Research, Technological Development and Demonstration Activities under the funding scheme of "Collaborative Project" through the COMTES consortium. Partly by the Danish Energy Agency supporting the joint IEA SHC Task 42/ECES Annex 29 programme on Compact Thermal Energy Storage. We thank our partners Henry Sørensen from Nilan A/S and Hermann Schranzhofer and Christoph Moser from Graz University of Technology for sharing knowledge and discussions.

References

[1] S.D. Sharma, K. Sagara, Latent heat storage materials and systems: a review, Int. J. Green Energy 2 (2005) 1–56, http://dx.doi.org/10.1081/GE-200051299.
[2] D.N. Nkwetta, F. Haghighat, Thermal energy storage with phase change material – a state-of-the art review, Sustain. Cities Soc. 10 (2014) 87–100, http://dx.doi.org/10.1016/j.scs.2013.05.007.
[3] M.K.A. Sharif, A.A. Al-abidi, S. Mat, K. Sopian, M.H. Ruslan, Review of the application of phase change material for heating and domestic hot water systems, Renew. Sustain. Energy Rev. 42 (2015) 557–568, http://dx.doi.org/10.1016/j.rser.2014.09.034.
[4] C. Solé, M. Medrano, A. Castell, M. Nogue, H. Mehling, L.F. Cabeza, Energetic and exergetic analysis of a domestic water tank with phase change material, Int. J. Energy Res. 32 (2008) 204–214, http://dx.doi.org/10.1002/er.
[5] T. Wada, F. Kimura, R. Yamamoto, Studies on salt hydrates for latent heat storage. II. Eutectic mixture of pseudo-binary system, Bull. Chem. Soc. Jpn. (1983) 1223–1226.
[6] S. Canbazoğlu, A. Şahinaslan, A. Ekmekyapar, Ý.G. Aksoy, F. Akarsu, Enhancement of solar thermal energy storage performance using sodium thiosulfate pentahydrate of a conventional solar water-heating system, Energy Build. 37 (2005) 235–242, http://dx.doi.org/10.1016/j.enbuild.2004.06.016.
[7] K. Nagano, K. Ogawa, T. Mochida, K. Hayashi, H. Ogoshi, Performance of heat charge/discharge of magnesium nitrate hexahydrate and magnesium chloride hexahydrate mixture to a single vertical tube for a latent heat storage system, Appl. Therm. Eng. 24 (2004) 209–220, http://dx.doi.org/10.1016/j.applthermaleng.2003.09.002.
[8] A. López-navarro, J. Biosca-taronger, J.M. Corberán, C. Peñalosa, A. Lázaro, P. Dolado, et al., Performance characterization of a PCM storage tank, Appl. Energy 119 (2014) 151–162, http://dx.doi.org/10.1016/j.apenergy.2013.12.041.
[9] P. Arce, M. Medrano, A. Gil, E. Oró, L.F. Cabeza, Overview of thermal energy storage (TES) potential energy savings and climate change mitigation in Spain and Europe, Appl. Energy 88 (2011) 2764–2774, http://dx.doi.org/10.1016/j.apenergy.2011.01.067.
[10] A. Abhat, Short term thermal energy storage, Energy Build. 3 (1981) 49–76.
[11] J. Guion, M. Teisseire, Nucleation of sodium acetate trihydrate in thermal heat storage cycles, Sol. Energy 46 (1991) 97–100.
[12] P. Hu, D.-J. Lu, X.-Y. Fan, X. Zhou, Z.-S. Chen, Phase change performance of sodium acetate trihydrate with AlN nanoparticles and CMC, Sol. Energy Mater. Sol. Cells 95 (2011) 2645–2649, http://dx.doi.org/10.1016/j.solmat.2011.05.025.
[13] H. Kimura, J. Kai, Phase change stability of sodium acetate trihydrate and its mixtures, Sol. Energy 35 (1985) 527–534, http://dx.doi.org/10.1016/0038-092X(85)90121-5.
[14] G.A. Lane, Solar Heat Storage Latent Heat Material, vol. 1, 1983. Boca Raton, Florida, United states.
[15] J. Stanley, G.L. Hoerner, Reusable Heat Pack Containing Supercooled Solution and Means for Activating Same, 1978. www.google.com/patents/US4077390 (accessed 28.05.15).
[16] S. Hirano, T.S. Saitoh, Heat balance of long-term supercooled thermal energy storage, Nihon Enerugi Gakkaishi/J. Jpn. Inst. Energy 80 (2001) 1050–1059.
[17] S. Hirano, S. Takeo, INFLUENCE of operating temperature on efficiency of supercooled thermal energy storage, in: IECEC 2002 Pap, 2002, pp. 684–689. No. 20040.

[18] S. Hirano, T.S. Saitoh, Performance of supercooled thermal energy storage unit with practial demensions, in: 3rd Int. Energy Convers. Eng. Conf. 2, 2005, pp. 1293–1300.
[19] B. Sandnes, J. Rekstad, Supercooling salt hydrates: stored enthalpy as a function of temperature, Sol. Energy 80 (2006) 616–625, http://dx.doi.org/10.1016/j.solener.2004.11.014.
[20] P.F. Barrett, B.R. Best, Thermal energy storage in supercooled salt mixtures, Mater. Chem. Phys. 12 (1985) 529–536.
[21] B. Zalba, J.M. Marin, L.F. Cabeza, H. Mehling, Review on thermal energy storage with phase change: materials, heat transfer analysis and applications, Appl. Therm. Eng. 23 (2003) 251–283.
[22] S. Furbo, J. Fan, Heat Storage Based on a NaCH3COO Water Mixture for Solar Heating Systems, DTU Civil Engineering, Report SR-12–10 (UK), Kgs. Lyngby, Denmark, 2012.
[23] M.A. Rogerson, S.S.S. Cardoso, Solidification in heat packs: I. Nucleation rate, AIChE J. 49 (2003) 505–515, http://dx.doi.org/10.1002/aic.690490220.
[24] L. Wei, K. Ohsasa, Supercooling and solidification behavior of phase change, ISIJ Int. 50 (2010) 1265–1269.
[25] T. Wada, F. Kimura, Y. Matsuo, Studies on salt hydrates for latent heat storage. IV. Crystallization in the binary system, Bull. Chem. Soc. Jpn. 56 (1983) 3827–3829.
[26] H. Mehling, L.F. Cabeza, Materials used as PCM in thermal energy storage in buildings: a review, Renew. Sustain. Energy Rev. (2011) 1675–1695, http://dx.doi.org/10.1016/j.rser.2010.11.018.
[27] S. Furbo, S. Svendsen, Report on Heat Storage in a Solar Heating System Using Salt Hydrates, Therm. Insul. Labotatory, DTU, Kgs. Lyngby, Denmark, 1977. Rep. 70.
[28] S. Furbo, Investigations of Heat Storages with Salt Hydrate as Storage Medium Based on the Extra Water Principle, Therm. Insul. Labotatory, DTU, Kgs, Lyngby, Denmark, 1978. Rep. 80. Meddelelse.
[29] N. Araki, M. Futamura, A. Makino, H. Shibata, Measurements of thermophysical properties of sodium acetate hydrate, Int. J. Thermophys. 16 (1995) 1455–1466.
[30] L. Desgrosseilliers, P. Allred, D. Groulx, M.A. White, Determination of enthalpy-temperature-composition relations in incongruent-melting phase change materials, Appl. Therm. Eng. 61 (2013) 193–197, http://dx.doi.org/10.1016/j.applthermaleng.2013.07.019.
[31] L.F. Cabeza, G. Svensson, S. Hiebler, H. Mehling, Thermal performance of sodium acetate trihydrate thickened with different materials as phase change energy storage material, Appl. Therm. Eng. 23 (2003) 1697–1704, http://dx.doi.org/10.1016/S1359-4311(03)00107-8.
[32] T. Wada, R. Yamamoto, Y. Matsuo, Heat storage capacity of sodium acetate trihydrate during thermal cycling, Sol. Energy 33 (1984) 373–375, http://dx.doi.org/10.1016/0038-092X(84)90169-5.
[33] H.W. Ryu, S.W. Woo, B.C. Shin, S.D. Kim, Prevention of supercooling and stabilization of inorganic salt hydrates as latent heat storage materials, Sol. Energy Mater. Sol. Cells 27 (1992) 161–172, http://dx.doi.org/10.1016/0927-0248(92)90117-8.
[34] B.M.L. Garay Ramirez, C. Glorieux, E.S. Martin Martinez, J.J.A. Flores Cuautle, Tuning of thermal properties of sodium acetate trihydrate by blending with polymer and silver nanoparticles, Appl. Therm. Eng. 61 (2013) 838–844, http://dx.doi.org/10.1016/j.applthermaleng.2013.09.049.
[35] G. Lane, Solar Heat Storage Latent Heat Material, vol. 2, CRC, Boca Raton, Florida, United states, 1986.
[36] T. Wada, Studies on Sodium Acetate Trihydrate for Latent Heat Storage, Osaka University, Japan, 1985. hdl.handle.net/11094/2830.
[37] X. Jin, S. Zhang, M.A. Medina, X. Zhang, Experimental study of the cooling process of partially-melted sodium acetate trihydrate, Energy Build. 76 (2014) 654–660, http://dx.doi.org/10.1016/j.enbuild.2014.02.059.
[38] L.F. Cabeza, J. Roca, M. Nogués, H. Mehling, S. Hiebler, Immersion corrosion tests on metal-salt hydrate pairs used for latent heat storage in the 48 to 58 8C temperature range, Mater. Corros. 53 (2002) 902–907.
[39] M.A. Rogerson, S.S.S. Cardoso, Solidification in heat Packs: III. Metallic trigger, AIChE J. 49 (2003) 522–529.
[40] A.E.M. Anthony, P.F. Barrett, B.K. Dunning, Verification of mechanism for nucleating crysrallization of supercooled liquids, Mater. Corros. 25 (1990) 199–205.
[41] P.F. Barrett, D.K. Benson, A mechanism for nucleating supercooled liquids, Mater. Chem. Phys. 20 (1988) 171–178.
[42] W.-B. Ye, D.-S. Zhu, N. Wang, Fluid flow and heat transfer in a latent thermal energy unit with different phase change material (PCM) cavity volume fractions, Appl. Therm. Eng. 42 (2012) 49–57, http://dx.doi.org/10.1016/j.applthermaleng.2012.03.002.
[43] M. Medrano, M.O. Yilmaz, M. Nogués, I. Martorell, J. Roca, L.F. Cabeza, Experimental evaluation of commercial heat exchangers for use as PCM thermal storage systems, Appl. Energy 86 (2009) 2047–2055, http://dx.doi.org/10.1016/j.apenergy.2009.01.014.
[44] A. Heinz, Application of Thermal Energy Storage with Phase Change Materials in Heating Systems, Graz University of Technology, Austria, 2007.
[45] W. Li, J. Mao, L. Wang, L. Sui, Effect of the additive on thermal conductivity of the phase change material, Adv. Mater. Res. 399–401 (2011) 1302–1306, http://dx.doi.org/10.4028/www.scientific.net/AMR.399-401.1302.
[46] F. Frusteri, V. Leonardi, G. Maggio, Numerical approach to describe the phase change of an inorganic PCM containing carbon fibres, Appl. Therm. Eng. 26 (2006) 1883–1892, http://dx.doi.org/10.1016/j.applthermaleng.2006.01.018.
[47] H.K. Shin, M. Park, H.-Y. Kim, S.-J. Park, Thermal property and latent heat energy storage behavior of sodium acetate trihydrate composites containing expanded graphite and carboxymethyl cellulose for phase change materials, Appl. Therm. Eng. 75 (2015) 978–983, http://dx.doi.org/10.1016/j.applthermaleng.2014.10.035.
[48] L.F. Cabeza, H. Mehling, S. Hiebler, F. Ziegler, Heat transfer enhancement in water when used as PCM in thermal energy storage, Appl. Therm. Eng. 22 (2002) 1141–1151, http://dx.doi.org/10.1016/S1359-4311(02)00035-2.
[49] D.N. Nkwetta, P.-E. Vouillamoz, F. Haghighat, M. El-Mankibi, A. Moreau, A. Daoud, Impact of phase change materials types and positioning on hot water tank thermal performance: using measured water demand profile, Appl. Therm. Eng. 67 (2014) 460–468, http://dx.doi.org/10.1016/j.applthermaleng.2014.03.051.
[50] K. Seo, S. Suzuki, T. Kinoshita, I. Hirasawa, Effect of ultrasonic irradiation on the crystallization of sodium acetate trihydrate utilized as heat storage material, Chem. Eng. Technol. 35 (2012) 1013–1016, http://dx.doi.org/10.1002/ceat.201100680.
[51] W. Streicher, J. Bony, S. Citherlet, A. Heinz, P. Pusching, H. Schranzhofer, et al., Simulation Models of PCM Storage Units, IEA Solar Heating and Cooling Programme – Task 32 "Advanced Storage concepts For Solar and Low Energy, Report C5 of Subtask C buildings,", Institute of Thermal Engineering Graz University of Technology, Austria, 2008.
[52] J.M. Schultz, S. Furbo, Investigation of heat of fusion storage for solar low energy buildings, in: Proc. Sol. World Congr. 2005 Bringing Water to World, Incl. Proc. 34th Ases Annu. Conf. Proc. 30th Natl. Passiv. Sol. Conf, Proc. Sol. World Congr. Bringing Water World, Incl. Proc. Ases Annu, vol. 3, 2005, pp. 1833–1838.
[53] Statens Byggeforskningsinstitut, tsbi3, 1993. www.sbi.dk.
[54] Passive House Institute, Passive House Institute, www.passiv.de/en/index.php (accessed 28.05.15).
[55] J. Schultz, S. Furbo, Solar heating systems with heat of fusion storage with 100% solar fraction for solar low energy buildings, in: ISES Sol. World Congr. 2007 Proc, 2007, pp. 2721–2725.

Paper 2 - Solidification behaviour and thermal conductivity of bulk sodium acetate trihydrate mixtures with thickening agents and graphite powder

Mark Dannemand, Jakob Berg Johansen, Simon Furbo

Solar Energy Materials and Solar Cells, Vol 145, Part 3, pp. 287–295, 2016
doi:10.1016/j.solmat.2015.10.038.

Solar Energy Materials & Solar Cells 145 (2016) 287–295

Contents lists available at ScienceDirect

Solar Energy Materials & Solar Cells

journal homepage: www.elsevier.com/locate/solmat

Solidification behavior and thermal conductivity of bulk sodium acetate trihydrate composites with thickening agents and graphite

Mark Dannemand *, Jakob Berg Johansen, Simon Furbo

Technical University of Denmark, Department of Civil Engineering, Kgs. Lyngby 2800, Denmark

ARTICLE INFO

Article history:
Received 23 September 2015
Received in revised form
20 October 2015
Accepted 24 October 2015
Available online 6 November 2015

Keywords:
Phase change material
Sodium acetate trihydrate
Solidification
Thermal conductivity
Supercooling
Thickening agent

ABSTRACT

Sodium acetate trihydrate is a promising phase change material for long term storage of solar thermal energy if supercooling is actively utilized. Well performing thermal energy storages need to be able to charge and discharge energy at a high rate. The relatively low thermal conductivity of the phase change material limits the heat exchange capacity rate to and from the storage. Another factor that limits the heat transfer is the contraction and expansion of the salt hydrate during the phase change. This density change causes formation of cavities inside the solid storage material. Investigations of the solidification behavior, the formation of cavities and thermal conductivity of composites based on sodium acetate trihydrate crystalizing with or without supercooling are presented in this paper. The thermal conductivity was measured with an ISOMET hot disc surface measurement probe. Samples that crystalized without supercooling tended to form solid crystals near the heat transfer surface and cavities away from the heat transfer surface. The measured thermal conductivity was up to 0.7 W/m K in solid sodium acetate trihydrate. Samples that crystalized from supercooled state formed fewer large cavities but had a lower thermal conductivity. A composite with sodium acetate trihydrate, thickening agent and 5% graphite flakes had a thermal conductivity of up to 1.1 W/m K.

1. Introduction

The phase change material (PCM) sodium acetate trihydrate (SAT) is a promising material for heat storages. It has a relatively high latent heat of fusion of 264 kJ/kg at a melting point of 58 °C [1]. This melting point makes it suitable for applications for space heating and domestic hot water preparation combined with solar thermal energy [2]. SAT has the ability to supercool in a stable way down to ambient temperature and is therefore a candidate material for long term heat storage. Long term or seasonal heat storage is possible by melting SAT by solar energy and then letting it remain in supercooled state at ambient temperature in the storage period [3]. Once the crystallization of the supercooled SAT is initialized, the latent heat of fusion is released and can be discharged for heating purposes. Dannemand et al. describe a number of barriers and solutions for operating a seasonal heat storage based on stable supercooling of SAT as well as some numerical calculations elucidating the potential [4]. One of the limiting factors in using PCMs in a heat storage is the low thermal conductivity of the PCM itself, which limits the heat exchange capacity rate and discharge power of the storage [5].

The enhancement of the thermal conductivity of PCMs has been investigated by several researchers. One method is to create PCM composites with enhanced thermal properties by mixing additives in the PCM. Another method is to have fixed highly conductive structures or fins inside the PCM storage or to impregnate a highly conductive porous media with the PCM. Li et al. investigated the effect of adding powdered expanded graphite (EG) into SAT and found that the thermal conductivity could be almost doubled by adding 10% EG to the SAT mixture, which also contained Carboxymethyl cellulose (CMC) [6]. Lee et al. investigated composites of EG and erythritol and found that EG as an additive is a highly promising material for improving heat transfer in heat storages with PCMs [7]. Cabeza et al. studied the effect of adding steel pipes or copper pieces as fins in a storage with water as PCM to increase heat transfer, but found that a graphite matrix was better [8]. Sari and Karaipekli showed that the thermal conductivity of a paraffin could be increased significantly by adding a few percentage of EG and this would decrease the melting time of the PCM [9]. Mills et al. also showed that the thermal conductivity of a graphite matrix impregnated with PCM is a viable choice for enhancing thermal conductivity [10]. Also Py et al. showed that paraffin impregnated in compressed expanded natural graphite significantly increased the thermal conductivity compared to the paraffin alone [11]. Zhang and Fang carried out investigations on paraffin and EG composites and likewise found this an effective way of increasing thermal

* Corresponding author.
E-mail address: markd@byg.dtu.dk (M. Dannemand).

http://dx.doi.org/10.1016/j.solmat.2015.10.038
0927-0248/

conductivity [12]. Fan and Khodadadi did a review on thermal conductivity enhancement of PCMs for thermal energy storage [13]. Jegadheeswaran and Pohekar did a review on several other techniques for enhancing the performance of latent heat storages [5]. Kousksou et al. also did a review listing some important characteristics of energy storage including latent heat storages with salt hydrates [14]. Considering a storage with stable supercooling of SAT, Johansen et al. had SAT samples mixed with graphite powder in stable supercooled condition for five months after it had been heated to 85 °C for 12 h [15]. They concluded that it is possible to have stable supercooled composites of SAT and graphite powder at ambient temperature.

1.1. Phase separation and additives

SAT is an incongruently melting salt hydrate and suffers from phase separation especially over repeated melting and solidification cycles [16]. The problem has been sought to be solved by adding extra water [17] or thickening agents to the SAT. Ramirez et al. studied the use of CMC and silica gel to avoid phase separation of SAT and reported thermal cycling stability in cycles from 30 °C to 72 °C by use of differential scanning calorimetry (DSC) [18]. Hu et al. investigated the reduction of supercooling by the use of Aluminum Nitride nanoparticles in the SAT composite with 4% CMC and found the thickening agent suitable to avoid phase separation and suspend the nucleation agent in the mixture [19]. Ryu et al. investigated several salt hydrates and found that for some salt hydrates a super absorbent polymer (SAP) was an effective thickening agent however CMC was more effective for SAT [20]. Shin et al. investigated the combination of CMC and expanded graphite as additives for SAT and found that composites with 2.5 wt% EG and 5 wt% CMC had a thermal conductivity of 1.85 W/m K [21]. Meisingset and Grønvold investigated thermodynamic properties of salt hydrates and suggested that 0.5–1% xanthan rubber can solve the problem of phase separation in SAT [22]. A suitable thickening agent could both solve phase separation and keep small sized conduction enhancers evenly distributed in the PCM composite at the temperature the storage is meant to operate at and over its lifetime.

1.2. Solidification

The density difference between the solid and liquid SAT is approximately 10% [23]. The resulting volume change of the PCM in a rigid storage tank will cause formation of cavities [24]. These cavities act as thermal resistances, reducing the effective thermal conductivity of the bulk PCM. This was also reported by Choi et al., who investigated heat transfer in storages with SAT [25]. Once a supercooled PCM is nucleated, it crystalizes almost instantly [26]. A PCM that solidifies without supercooling crystalizes at a slower rate as the crystallization front moves with the heat being released and the temperature drops below the melting point. Whether the PCM solidifies without supercooling or with a high degree of supercooling may affect the formation of the solid PCM and the location of the cavities, which affect the thermal conductivity of the bulk PCM. Additives such as extra water and thickening agents added to avoid phase separation may also affect the thermal conductivity of the PCM.

1.3. Applications

In designing and planning thermal systems including heat storages, numerical simulation models are an important tool. To do numerical calculations of PCM storages, an accurate value for the thermal conductivity of the PCM in bulk sizes that resemble the usage in full scale applications is desired. Lele et al. found the importance of investigating the effective thermal conductivity of the storage material using a measuring setup representative of the considered application [27]. They found that a self-made guarded hot cartridge method gave results more representative for the real storage compared to DSC measurements.

Literature values for the thermal conductivity of solid SAT range from 0.17 W/m K [21] to 0.7 W/m K [28,29]. In previous literature there was no distinction between the thermal conductivity of SAT composites crystalizing from supercooled state or without supercooling.

This article reports the investigations by a simple suspension test on how well different concentrations of the thickening agents CMC and xanthan rubber suspend graphite particles in SAT composites. The second part of this article reports on the solidification behavior and the formation of cavities. Additionally, the thermal conductivity in bulk size SAT composites, which are meant to resemble the conditions in an actual heat storage with or without utilizing supercooling, were investigated. Measurements showed how extra water, thickening agents and graphite powder or graphite flakes affected the thermal conductivity of bulk size PCM composites.

2. Method

Sodium acetate trihydrate was purchased from the company IG Chemicals GmbH. Carboxymethyl cellulose and xanthan rubber was received as samples from the company CP Kelco under the product names Cekol 30000 and Keltrol Advanced performance-F. Fine graphite powder with a particle size less than 50 μm and graphite flakes mesh size 10 (see Fig. 1) were purchased from the company VWR International.

2.1. Suspension of graphite in PCM mixture

To ensure a PCM composite with graphite uniformly distributed in the sample simple suspension tests were carried out. The aim was to investigate the ability of the thickening agents to suspend the graphite in the PCM composite at a temperature of 90 °C which could be the maximum operating temperature of a PCM storage with SAT in a solar combi system. Graphite powder and flakes have a higher density than SAT. The graphite will separate from the PCM and settle to the bottom of the container if no precautions are taken. Mixtures of 200 g SAT with 1%, 2.5% and 5% CMC and SAT with 0.25%, 0.5% and 1% xanthan rubber (all wt%) were prepared without graphite. Then a layer of 40 g graphite powder or graphite flakes mixed with SAT in the ratio 1:10 was placed on top of the thickened PCM mixture.

The samples were heated in an oven to 90 °C for 14 days. During this period the samples inspected to see if the graphite settled to the bottom of the sample or remained suspended on the top of the sample. It was assumed that if the graphite stayed suspended on the top of the sample, the viscosity of the thickened PCM mixture would also be high enough to keep a uniform composite. On the other hand, if the graphite would fall through the thickened PCM mixture during the test period, it would also eventually settle to the bottom of a container in an application intended to function for years. In this case the graphite would not give the desired effect of increasing the thermal conductivity in the entire bulk.

Shaking the samples would also affect the mixing, therefore the sample were carefully handled when being inspected.

2.2. Solidification and thermal conductivity sample preparation

To evaluate the thermal conductivity and the formation of cavities in PCM composites based on SAT in bulk size, a series of 1.3 kg samples were prepared in glass jars with airtight lids (see

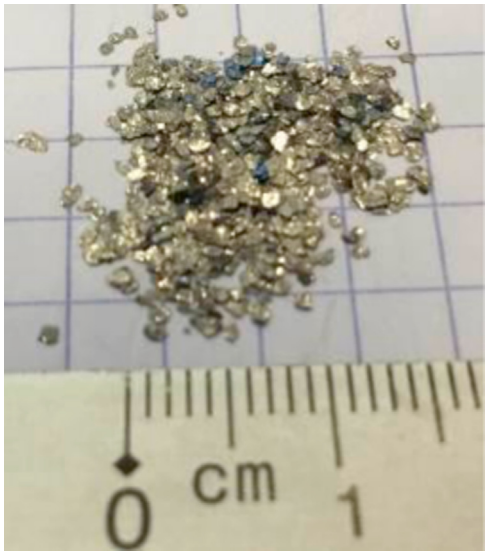

Fig. 1. Graphite flakes mesh size 10.

Fig. 2. 1.3 kg PCM composite based on SAT in glass jar.

Fig. 2). The PCM samples were 90–100 mm high and had a diameter of 120 mm.

To elucidate the different behavior of samples that crystalized from supercooled state or with minimal supercooling, two of each PCM composites were prepared. For most of the samples multiple repetitions were made to confirm repeatability. The following types of PCM composites were prepared.

1) Sodium acetate trihydrate.
2) Sodium acetate trihydrate plus 9% extra water.

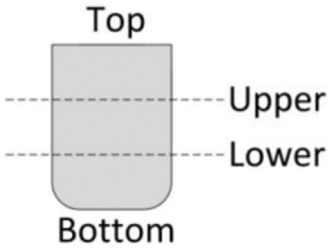

Fig. 3. Cut in PCM sample.

3) Sodium acetate trihydrate plus 0.5% xanthan rubber.
4) Sodium acetate trihydrate plus 0.5% xanthan rubber and 5% graphite powder.
5) Sodium acetate trihydrate plus 1% xanthan rubber and 5% graphite flakes.
6) Sodium acetate trihydrate plus 1% CMC.
7) Sodium acetate trihydrate plus 1% CMC and 2% graphite powder.

The PCM composites were prepared by melting the SAT in an oven at 90 °C for 24 h in the closed glass jars. For samples with graphite, the graphite was mixed into the SAT before placing in the oven. For samples with CMC, the thickening agent was added to the melted SAT while stirring with an overhead mixer until a uniform mixture was achieved. For samples thickened with xanthan rubber, the thickening agent was mixed with 130 g of the SAT in crushed solid state at ambient temperature. The xanthan rubber and SAT mixture was then added to the melted SAT little by little while stirring with an overhead mixer to ensure a uniform mixture. At temperatures around 90 °C the SAT composite with xanthan rubber became a thick jelly that easily trapped air bubbles. It was therefore necessary to stir the PCM composite carefully to avoid trapping air bubbles in the PCM. After adding the additives, the samples were placed in the oven for 4 h to obtain a uniform temperature, before they were removed from the oven and placed in the ambient at a temperature of about 22 °C.

One of each sample type was set to cool in the closed glass jar to ambient temperature for 24 h. This left the samples in supercooled state after which the crystallization was started by opening the jar and adding a seed crystal of SAT. In other samples of each type the lid was opened as they cooled down and the temperatures of the samples were monitored. As the temperature of the sample dropped close to the melting temperature of 58 °C, a seed crystal was added to ensure crystallization without supercooling. This passive cooling and crystallization without supercooling is referred to as natural cooling in this article. The samples reached ambient temperature approximately 24 h after crystallization was started. One heating and cooling cycle for each sample was carried out over 48–72 h. After the samples were crystalized and cooled to ambient temperature, the samples were removed from the jars. The samples were cut horizontally at approximately 1/3 and 2/3 of their height, as indicated in Fig. 3. Each layer of the samples had a thickness of 25–30 mm. The solidification behavior and the formation of cavities in each layer of the samples were inspected visually and measurements of thermal conductivity were carried out.

2.3. Measuring procedure

Measurements of the thermal conductivity at top and bottom as well as on the surface of the cut layers of the samples were carried out with an ISOMET model 2104 Heat Transfer Analyzer from Applied Precision Ltd. The accuracy of the thermal conductivity measurements are stated to be 5% for values up to 0.7 W/m K and 10% for values above 0.7 W/m K [30]. The tool utilizes the hot disc

principle, so the thermal conductivity of the sample was measured at the surface. The tool requires a flat surface with at least the same diameter as the probe of 60 mm and a minimal thickness of the material of 10–15 mm. Before the measurements were carried out, the surfaces of the samples were made level with sandpaper to ensure a good thermal contact between the probe and the sample. The measurements were made in the center of the samples or where it was possible to place the probe on a uniform surface without too large cavities. The measurements were repeated 2–5 times with slight offsets between each measurement. Averages of these measurements are presented in the result chapter.

3. Results and discussion

3.1. Suspension of graphite in the PCM mixture

Pictures of the samples from before starting the suspension test and after being in the oven at 90 °C at selected time intervals are shown in Tables 1 and 2. The samples were inspected to observe the suspension of the graphite.

It is clear from the pictures in Table 1 that both the graphite powder and the graphite flakes started to settle to the bottom of the samples thickened with 1% and 2.5% CMC after one day at 90 °C. The graphite remained suspended on the top of the PCM composites with 5% CMC during the test period of 14 days. This indicates that to keep a uniform PCM composite where graphite particles stays suspended, the SAT needs to be thickened with at least 5% CMC.

From the pictures it can also be seen that the color of the PCM mixtures darkened over the heating period. This might indicate that the CMC breaks down over time and it could lose its thickening ability when applied at this temperature. A longer test period is needed to clarify this.

Inspection of the SAT samples thickened with xanthan rubber showed that after one day in the oven at 90 °C graphite flakes began to fall through the PCM composite with 0.25% and 0.5% xanthan rubber. In the sample with 0.25% xanthan rubber and graphite powder the layer of graphite started to segregate after 2 days and for the sample with 0.5% xanthan rubber slight segregation was observed after 7 days. The composite with 1% xanthan rubber maintained the graphite suspended on the top of the sample throughout the test period.

Similarly to the composites with CMC, the color of the mixtures darkened over the heating period, which might indicate degradation of the xanthan rubber.

Table 1
Samples of SAT with 1%, 2.5% and 5% CMC from left to right with graphite SAT mix on top.

	1%, 2.5%, 5% CMC+graphite powder	1%, 2.5%, 5% CMC+graphite flakes
Start		
15 h		
2 days	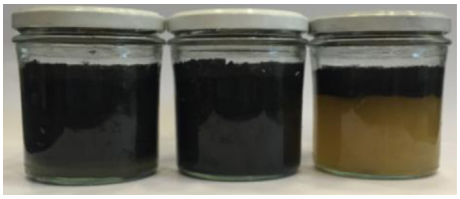	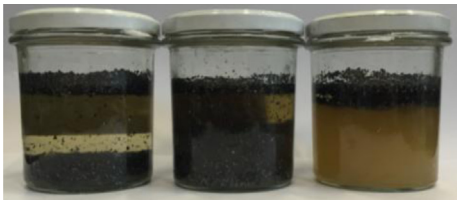
7 days		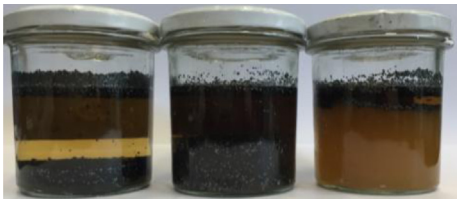
14 days		

Table 2
Samples of SAT with 0.25%, 0.5% and 1% xanthan rubber with graphite SAT mix on top.

	0.25%, 0.5%, 1% xanthan rubber+graphite powder	0.25%, 0.5%, 1% xanthan rubber+graphite flakes
start		
15 h	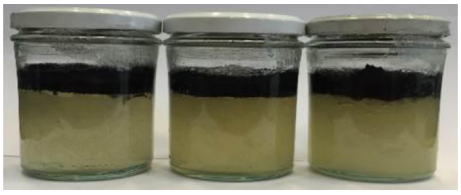	
2 days		
7 days		
14 days	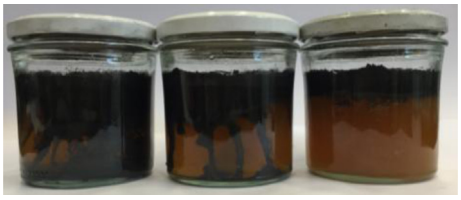	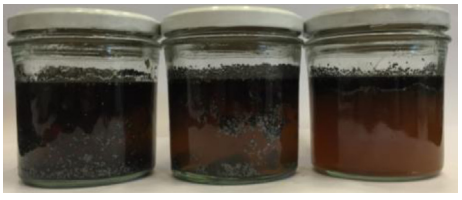

Although handling of the samples was done carefully, some shaking of the samples may have influenced the segregation of graphite.

3.2. Formation of cavities and thermal conductivity

The solidification behaviors of the PCM samples were inspected visually at the cuts through the samples. Pictures of the layers of the PCM samples with the formed cavities can be seen in Table 3. Averaged values of the measurements of the thermal conductivity at different layers are also listed in Table 3.

Values in parentheses are measurement where the probe was placed on top of obvious cavities. Here the individual measurement varied with up to ± 0.15 W/m K depending on placement of the probe. Numbers listed without parentheses indicate a measuring point on an apparently solid surface, where the variations between measurements were ± 0.02 W/m K. No measurements were made if there was a large cavity where the probe had to be placed. "NA" in the table is representing large cavities in the samples where no measurements were made.

The samples of SAT without additives that crystalized during cooling down formed solid crystals in the bottom and near the sides of the glass jar and the cavities were concentrated in the upper central part of the sample. The sample of SAT without additives that crystalized from supercooled state formed a whiter softer crystal structure without large visual cavities, most likely due to the fast crystallization speed. The thermal conductivity of the lower and bottom layers representing the densest solid was significant lower in the sample that had solidified from the supercooled state compared to the sample that solidified without supercooling. The sample that crystalized with supercooling appeared with a more easily breakable crystal structure and a whiter color.

The supercooled SAT composite with 9% extra water (consisting of 45% water and 55% Sodium acetate) was clearly moist. The extra water increased the thermal conductivity throughout the sample compared to the sample of SAT without extra water for the supercooled case. The sample with extra water which solidified during cooling down without supercooling pushed the extra water away from the crystallization front. This left a pool of saturated salt water solution in upper central part of the sample when ambient temperature was reached. In this case the measured thermal conductivity was similar to the sample without extra water in to bottom layer.

Solidified SAT samples that were thickened with CMC appeared to have one large star shaped cavity in the center of the sample with long straight partition lines splitting the sample. The lengths of the cavities were up to 90 mm long and 40 mm wide. The mixture with SAT and CMC that crystalized from supercooled state showed similar contraction and splitting behavior, but a smaller cavity was formed. The average thermal conductivity was slightly higher for the sample that had not been supercooled.

Table 3
View of cavities and measured thermal conductivity in different layers of the SAT composites.

	Top	Upper	Lower	Bottom
SAT natural	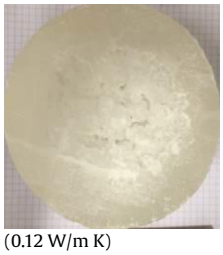 (0.12 W/m K)	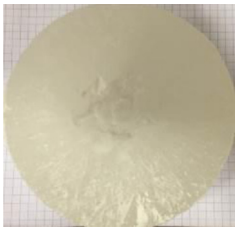 (0.07 W/m K)	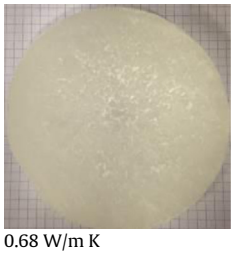 0.68 W/m K	 0.67 W/m K
SAT supercool	 0.38 W/m K	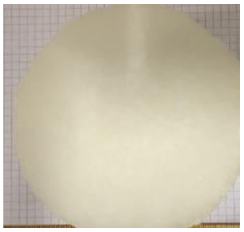 0.31 W/m K	 0.59 W/m K	 0.56 W/m K
SAT 9% extra water natural	 NA	 NA	 NA	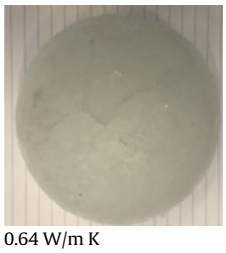 0.64 W/m K
SAT 9% extra water supercool	 0.53 W/m K	 0.46 W/m K	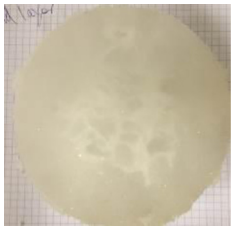 0.59 W/m K	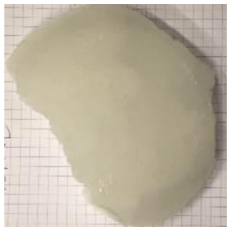 0.65 W/m K
SAT 1% CMC natural	 (0.58 W/m K)	 0.65 W/m K	 0.64 W/m K	 0.64 W/m K
SAT 1% CMC supercool	 0.59 W/m K	 (0.57 W/m K)	 0.65 W/m K	 0.63 W/m K
SAT 1% CMC 2% graphite powder Natural	 (0.43 W/m K)	 NA	 (0.74 W/m K)	 0.85 W/m K

Table 3 (*continued*)

	Top	Upper	Lower	Bottom
SAT 1% CMC 2% graphite powder Supercool	 0.60 W/m K	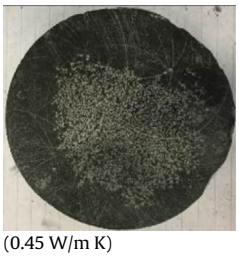 (0.45 W/m K)	 0.83 W/m K	 0.84 W/m K
SAT 0.5% xanthan rubber natural	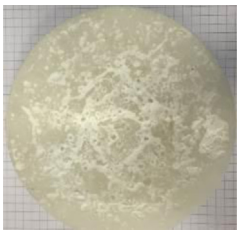 (0.50 W/m K)	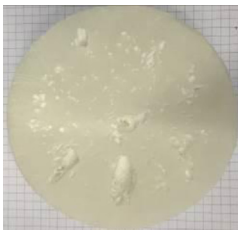 (0.57 W/m K)	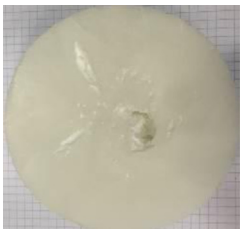 (0.54 W/m K)	 0.65 W/m K
SAT 0.5% xanthan rubber supercool	 (0.52 W/m K)	 (0.59 W/m K)	 (0.57 W/m K)	 0.59 W/m K
SAT 0.5% xanthan rubber 5% graphite powder natural	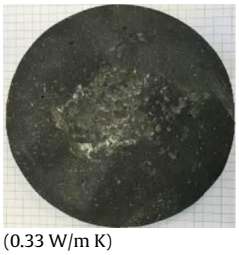 (0.33 W/m K)	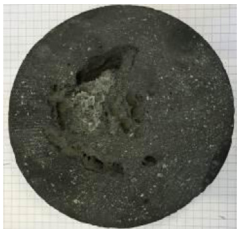 NA	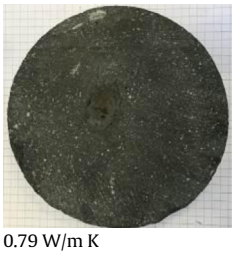 0.79 W/m K	 0.79 W/m K
SAT 0.5% xanthan rubber 5% graphite powder supercool	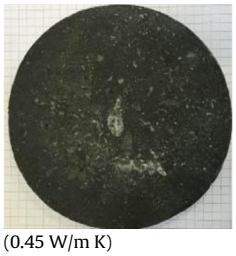 (0.45 W/m K)	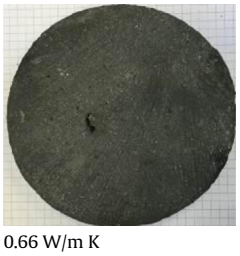 0.66 W/m K	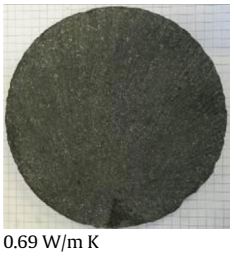 0.69 W/m K	 0.71 W/m K
SAT 1% xanthan rubber 5% graphite flakes natural	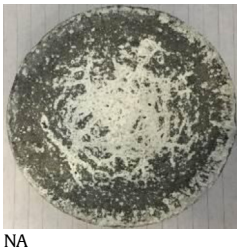 NA	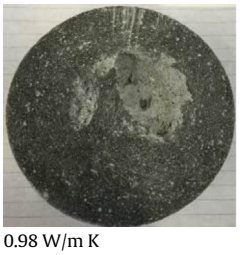 0.98 W/m K	 1.01 W/m K	 1.12 W/m K
SAT 1% xanthan rubber 5% graphite flakes supercool	 0.95 W/m K	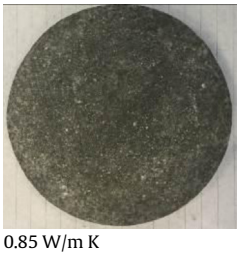 0.85 W/m K	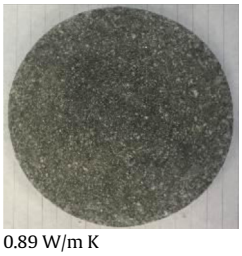 0.89 W/m K	 0.81 W/m K

The samples that were thickened with xanthan rubber and solidified without supercooling formed multiple oblong cavities across the majority of the two middle layers except from very near the perimeter of the sample. The cavities were up to 40 mm long and 12 mm wide, most of the cavities were smaller. The sample thickened with xanthan rubber which crystalized after supercooling formed minor clustered cavities with diameters up to 3 mm. Some circular cavities may be due to air bobbles trapped in the PCM mixture from the mixing process.

The bottom layer of the samples with SAT, 1% CMC and 2% graphite powder had a thermal conductivity 31% higher than of the sample with SAT and CMC. In the top surface of the sample the thermal conductivity was similar to that of the SAT sample with CMC. This indicates that the concentration of graphite powder may have been larger in the bottom of the sample in coherence with the findings in Section 3.1.

Samples with SAT, 0.5% xanthan rubber and 5% graphite powder had thermal conductivities 20–22% higher than the sample with SAT and xanthan rubber. The cavities formed tended to be larger but fewer compared to the mixture of SAT and xanthan rubber without graphite. Only few obvious cavities can be observed in the supercooled sample of SAT and 0.5% xanthan rubber and 5% graphite powder. Consistently with the other findings, the crystals formed from solidifying without supercooling had higher thermal conductivity than from crystallization from supercooled state.

The solidification behavior and formation of cavities were similar for the composite with SAT, xanthan rubber and graphite flakes as for the sample with SAT, Xanthan rubber and graphite powder. Both samples consisted of 5% graphite, but the graphite flakes improved the thermal conductivity of up to 72% for the naturally cooled sample and 50% for the supercooled sample compared the sample with SAT and 0.5% xanthan rubber. This can be explained by the larger graphite particles giving longer distances for the heat to conduct and fewer transitions between SAT and graphite.

The investigated samples underwent only one heating and cooling cycle. As phase separation might worsen over repeated cycles, it is expected that the composition in the layers of the SAT samples without thickening agents would change with repeated cycles. This may influence the thermal conductivity in the different layers. Phase separation is avoided and the suspension of graphite is sustained in the composites containing thickening agents, as long as sufficient thickening agent is added and it does not degrade. In this case, it is expected that the composition in the layers will remain constant over repeated heating and cooling cycles. Results from Table 1 indicated that the composites with 5% CMC or 1% xanthan rubber were stable for 14 days at 90 °C. Repeated heating and cooling cycles or heating periods longer than 14 days may destabilize the composite. Future cycling tests must clarify this.

Considering solidification behavior and formation of cavities in repeated thermal cycles, it is suggested that in composites where the viscosity in the melted state is low enough to let air bobbles escape from the sample, there will be no difference in solidification behavior with repeated cycles. For composites with a high viscosity that may trap air bobbles in the PCM, an effect of increasing the air trapped inside the PCM may occur with repeated cycles, if new air is sucked into the PCM each time the PCM solidifies and contracts. Future cycling tests should elucidate this.

The measured values of thermal conductivity of samples mixed with graphite were significantly lower than what was found by Shin et al., who investigated a SAT composite with 2.5% expanded graphite and 5% CMC which had a thermal conductivity of 1.85 W/m K [21]. The difference could be due to better performance of EG compared to the graphite types used in this article.

As the samples cooled from the heated state to the ambient temperature, the heat flux was away from the center of the samples and through the outer surface. In the naturally cooled samples the first part of the samples to reach the crystallization temperature would be the PCM by the perimeter of the sample where the solidification would start. When the PCM crystalizes at a slow speed during cooling the formation of crystals has time to form dense crystals. When there is a contraction of the PCM as it crystalizes and the possibility for the liquid PCM to move/float, the cavities forming, due to the contraction, would appear in the central and upper part of the samples, where the temperature drops last. On the contrary, when a sample crystalizes with a high speed from a supercooled state, the PCM does not have time to contract and form a cavity in the center of the sample, but will create less dense crystals over the entire section and with smaller cavities or with no visual cavities at all. From a heat transfer point of view, the formation of the cavity in the center of the sample will give the best heat transfer ability as no heat stored in the cavity in the center has to be transferred away. Minor cavities spread out over the sample will give an insulating affect and there will be heat stored in the center which needs to be conducted longer distances compared to the samples with cavities in the center.

Considering actual applications, these investigations indicated whether a PCM storage operating with or without supercooling would affect the location of cavities formed due to contraction. Also the geometry of an actual storage including the heat exchanger design may influence the location of the cavities. In the cases where the contraction of the PCM causes a large central cavity and dense PCM near the heat transfer area, the insulating effect of the cavities may be minimal. In this case the values of thermal conductivity without parentheses listed in Table 3 could be averaged and used for calculations and simulation tools.

In the cases where cavities are spread out or crystallization occurs from a supercooled state, the effective thermal conductivity of the bulk PCM is significantly lower than for dense PCM. In this case the thermal conductivity for the bulk PCM used for calculations and simulations tools can be approximated by the averages of the values in Table 3, with and without parentheses.

4. Conclusions

The suspension test with composites of SAT and different quantities of thickening agents showed that to keep graphite powder or graphite flakes suspended on top of the mixture, the SAT had to be thickened with at least 5% CMC or 1% xanthan rubber.

In SAT composites that solidified without supercooling, the contraction of the PCM during solidification caused formation of cavities in the central upper part of the samples. Samples that solidified from supercooled state formed smaller or no visual cavities. The type of thickening agent affected the solidification and the formation of the cavities. PCM mixtures thickened with Carboxymethyl cellulose formed one large cavity in the center of the sample, no matter if it was supercooled or not. The PCM composite thickened with Xanthan rubber that solidified without supercooling formed smaller cavities spread out in the entire volume of the sample except very close to the perimeter in the sample. PCM mixtures thickened with xanthan rubber has a risk of trapping air bobbles in the sample due to their jelly consistency even at temperatures up to 90 °C

The location of the cavities affected the measured thermal conductivity of the bulk PCM. The measured thermal conductivity was generally lower in the PCM composite that had solidified from a supercooled state compered to composites that had solidified without supercooling except for the sample with extra water.

The thermal conductivity was up to 0.68 W/m K in the areas without visual cavities in the SAT samples without graphite that crystalized without supercooling. In a PCM composite with SAT, 1% xanthan rubber and 5% graphite flakes, the thermal conductivity was up to 1.1 W/m K.

Acknowledgment

This research was funded by the Danish Energy Agency (64012-0220) supporting the joint IEA SHC Task 42/ECES Annex 29 programme on Compact Thermal Energy Storage.

References

[1] B. Zalba, J.M. Marin, L.F. Cabeza, H. Mehling, Review on thermal energy storage with phase change: materials, heat transfer analysis and applications, Appl. Therm. Eng. 23 (2003) 251–283.
[2] A. Sharma, V.V. Tyagi, C.R. Chen, D. Buddhi, Review on thermal energy storage with phase change materials and applications, Renew. Sustain. Energy Rev. 13 (2009) 318–345, http://dx.doi.org/10.1016/j.rser.2007.10.005.
[3] B. Sandnes, J. Rekstad, Supercooling salt hydrates: Stored enthalpy as a function of temperature, Sol. Energy 80 (2006) 616–625, http://dx.doi.org/10.1016/j.solener.2004.11.014.
[4] M. Dannemand, J.M. Schultz, J.B. Johansen, S. Furbo, Long term thermal energy storage with stable supercooled sodium acetate trihydrate, Appl. Therm. Eng. 91 (2015) 671–678, http://dx.doi.org/10.1016/j.applthermaleng.2015.08.055.
[5] S. Jegadheeswaran, S.D. Pohekar, Performance enhancement in latent heat thermal storage system: a review, Renew. Sustain. Energy Rev. 13 (2009) 2225–2244, http://dx.doi.org/10.1016/j.rser.2009.06.024.
[6] W. Li, J. Mao, L. Wang, L. Sui, Effect of the additive on thermal conductivity of the phase change material, Adv. Mater. Res. 399–401 (2011) 1302–1306, http://dx.doi.org/10.4028/www.scientific.net/AMR.399-401.1302.
[7] S.-Y. Lee, H.K. Shin, M. Park, K.Y. Rhee, S.-J. Park, Thermal characterization of erythritol/expanded graphite composites for high thermal storage capacity, Carbon 68 (2014) 67–72, http://dx.doi.org/10.1016/j.carbon.2013.09.053.
[8] L.F. Cabeza, H. Mehling, S. Hiebler, F. Ziegler, Heat transfer enhancement in water when used as PCM in thermal energy storage, Appl. Therm. Eng. 22 (2002) 1141–1151, http://dx.doi.org/10.1016/S1359-4311(02)00035-2.
[9] A. Sari, A. Karaipekli, Thermal conductivity and latent heat thermal energy storage characteristics of paraffin/expanded graphite composite as phase change material, Appl. Therm. Eng. 27 (2007) 1271–1277, http://dx.doi.org/10.1016/j.applthermaleng.2006.11.004.
[10] A. Mills, M. Farid, J.R. Selman, S. Al-Hallaj, Thermal conductivity enhancement of phase change materials using a graphite matrix, Appl. Therm. Eng. 26 (2006) 1652–1661, http://dx.doi.org/10.1016/j.applthermaleng.2005.11.022.
[11] X. Py, R. Olives, S. Mauran, Paraffin/porous-graphite-matrix composite as a high and constant power thermal storage material, Int. J. Heat Mass Transf. 44 (2001) 2727–2737, http://dx.doi.org/10.1016/S0017-9310(00)00309-4.
[12] Z. Zhang, X. Fang, Study on paraffin/expanded graphite composite phase change thermal energy storage material, Energy Convers. Manag. 47 (2006) 303–310, http://dx.doi.org/10.1016/j.enconman.2005.03.004.
[13] L. Fan, J.M. Khodadadi, Thermal conductivity enhancement of phase change materials for thermal energy storage: a review, Renew. Sustain. Energy Rev. 15 (2011) 24–46, http://dx.doi.org/10.1016/j.rser.2010.08.007.
[14] T. Kousksou, P. Bruel, A. Jamil, T. El Rhafiki, Y. Zeraouli, Energy storage: Applications and challenges, Sol. Energy Mater. Sol. Cells 120 (2014) 59–80, http://dx.doi.org/10.1016/j.solmat.2013.08.015.
[15] J.B. Johansen, M. Dannemand, W. Kong, J. Fan, J. Dragsted, S. Furbo, Thermal conductivity enhancement of sodium acetate trihydrate by adding graphite powder and the effect on stability of supercooling, Energy Procedia 70 (2015) 249–256, http://dx.doi.org/10.1016/j.egypro.2015.02.121.
[16] M.M. Farid, A.M. Khudhair, S.A.K. Razack, S. Al-Hallaj, A review on phase change energy storage: materials and applications, Energy Convers. Manag. 45 (2004) 1597–1615, http://dx.doi.org/10.1016/j.enconman.2003.09.015.
[17] S. Furbo, Investigations of Heat Storages with Salt Hydrate as Storage Medium Based on the Extra Water Principle, Thermal Insulation Labotatory, DTU, Kongens Lyngby, Denmark, 1978, Rep. 80. Meddelelse.
[18] B.M.L. Garay Ramirez, C. Glorieux, E.S. Martin Martinez, J.J.A. Flores Cuautle, Tuning of thermal properties of sodium acetate trihydrate by blending with polymer and silver nanoparticles, Appl. Therm. Eng. 61 (2013) 838–844, http://dx.doi.org/10.1016/j.applthermaleng.2013.09.049.
[19] P. Hu, D.-J. Lu, X.-Y. Fan, X. Zhou, Z.-S. Chen, Phase change performance of sodium acetate trihydrate with AlN nanoparticles and CMC, Sol. Energy Mater. Sol. Cells 95 (2011) 2645–2649, http://dx.doi.org/10.1016/j.solmat.2011.05.025.
[20] H.W. Ryu, S.W. Woo, B.C. Shin, S.D. Kim, Prevention of supercooling and stabilization of inorganic salt hydrates as latent heat storage materials, Sol. Energy Mater. Sol. Cells 27 (1992) 161–172, http://dx.doi.org/10.1016/0927-0248(92)90117-8.
[21] H.K. Shin, M. Park, H.-Y. Kim, S.-J. Park, Thermal property and latent heat energy storage behavior of sodium acetate trihydrate composites containing expanded graphite and carboxymethyl cellulose for phase change materials, Appl. Therm. Eng. 75 (2015) 978–983, http://dx.doi.org/10.1016/j.applthermaleng.2014.10.035.
[22] K.K. Meisingset, F. Grønvold, Thermodynamic properties and phase transitions of salt hydrates between 270 and 400 K III. $CH_3CO_2Na \cdot 3H_2O$, $CH_3CO_2Li \cdot 2H_2O$, and $(CH_3CO_2)2\,Mg \cdot 4H_2O$, J. Chem. Thermodyn. 16 (1984) 523–536, http://dx.doi.org/10.1016/0021-9614(84)90003-X.
[23] G. Lane, Solar Heat Storage Latent Heat Material, Vol 2, CRC, Boca Raton, Florida, United states, 1986.
[24] N. Shamsundar, Similarity rule for solidification heat transfer with change in volume, J. Heat Transfer. 103 (1981) 173–175.
[25] J.C. Choi, S.D. Kim, G.Y. Han, Heat transfer characteristics in low-temperature latent heat storage using salt-hyrate, Sol. Energy Mater. Sol. Cells 40 (1996) 71–87.
[26] L. Dietz, J.S. Brukner, C.A. Hollingsworth, Linear crystallization velocities of sodium acetate in supersaturated solutions, J. Phys. Chem. 61 (1957) 944–948.
[27] A. Fopah Lele, K.E. N'Tsoukpoe, T. Osterland, F. Kuznik, W.K.L. Ruck, Thermal conductivity measurement of thermochemical storage materials, Appl. Therm. Eng. 89 (2015) 916–926, http://dx.doi.org/10.1016/j.applthermaleng.2015.06.077.
[28] T. Inagaki, T. Isshiki, Thermal conductivity and specific heat of phase change latent heat storage material sodium acetate trihydrate and heat transfer of natural convection in a horizontal enclosed rectangular container, Kagaku Kogaku Ronbunshu 39 (2013) 33–39, http://dx.doi.org/10.1252/kakoronbunshu.39.33.
[29] N. Araki, M. Futamura, A. Makino, H. Shibata, Measurements of thermophysical properties of sodium acetate hydrate, Int. J. Thermophys. 16 (1995) 1455–1466.
[30] User's Guide ISOMET Heat Transfer Analyser Model, 2104. (n.d.).

Paper 3 - Experimental investigations on prototype heat storage units utilizing stable supercooling of sodium acetate trihydrate mixtures

Mark Dannemand, Janne Dragsted, Jianhua Fan, Jakob Berg Johansen, Weiqiang Kong, Simon Furbo

Applied Energy, Vol 169, pp. 72-80, 2016

doi:10.1016/j.apenergy.2016.02.038

Applied Energy 169 (2016) 72–80

Contents lists available at ScienceDirect

Applied Energy

journal homepage: www.elsevier.com/locate/apenergy

Experimental investigations on prototype heat storage units utilizing stable supercooling of sodium acetate trihydrate mixtures

Mark Dannemand *, Janne Dragsted, Jianhua Fan, Jakob Berg Johansen, Weiqiang Kong, Simon Furbo

Department of Civil Engineering, Technical University of Denmark, Brovej 118, Kgs. Lyngby DK 2800, Denmark

HIGHLIGHTS

- Heat storage based on stable supercooling of sodium acetate trihydrate is demonstrated.
- Thermal energy is stored partly loss free for two months.
- Heat exchange capacity rate and discharge power are evaluated.
- Energy contents of storage units with two different PCM mixtures are determined.
- Supercooling and thermal cycling stability are evaluated.

ARTICLE INFO

Article history:
Received 28 October 2015
Received in revised form 4 February 2016
Accepted 5 February 2016

Keywords:
Compact thermal energy storage
Seasonal heat storage
Supercooling
Sodium acetate trihydrate
Phase change material

ABSTRACT

Laboratory tests of two heat storage units based on the principle of stable supercooling of sodium acetate trihydrate (SAT) mixtures were carried out. One unit was filled with 199.5 kg of SAT with 9% extra water to avoid phase separation of the incongruently melting salt hydrate. The other unit was filled with 220 kg SAT mixture thickened with 1% carboxymethyl cellulose. The heat exchange capacity rate during the charging of the unit with the extra water was significantly higher than for the unit with the thickening agent due to the different levels of convection. The SAT mixtures in the units were stable and supercooled at indoor ambient temperatures for up to two months, after which the units were discharged. The energy discharged after solidification of the supercooled SAT and water mixture was 194 kJ/kg in the first test cycle, dropping to 179 kJ/kg after 20 test cycles. The energy discharged from the unit with SAT and the thickening agent after solidification was stable at 205 kJ/kg over 6 test cycles.

1. Introduction

Heating of buildings and domestic hot water represent a large part of society's energy demand. Heating demands are especially high in winter. Solar energy is available all year round in most regions on earth, but it is limited in high-latitude regions in winter. It is more abundant in summer, when it can easily be harvested as low-grade thermal energy using solar collectors.

Thermal energy storage integrated in energy systems can help to optimize the use of energy resources by peak-shaving and making it possible to implement more renewable energy sources in our energy infrastructure [1]. This can lead to a reduction in greenhouse gas emissions from our thermal energy use and a reduction in environmental pollutants. Implementing more thermal energy storage may lead to more sustainable energy systems and may help to reduce climate change.

1.1. State of the art

Short-term storage of solar thermal energy for space heating and domestic hot water is typically done in small water stores, where continuous heat loss limits the storage period. With very large water stores, it is possible to store enough thermal energy to heat a single-family house during a winter. Alternatively, a form of thermal energy storage without continuous heat losses would allow for a more compact storage, where thermal energy could be stored from summer to winter in a seasonal heat storage. Large water stores for centralized systems are based on a relativity mature technology. Bauer et al. reported on various types of seasonal sensible heat stores for central solar heating plants in Germany [2], and Novo et al. did a review seasonal heat storage in large water tanks and pits for centralized heating systems [3]. In

* Corresponding author.
E-mail address: markd@byg.dtu.dk (M. Dannemand).

http://dx.doi.org/10.1016/j.apenergy.2016.02.038
0306-2619/

both cases, the authors find the use of large sensible heat storage units feasible in centralized heating systems. On the smaller scale of individual buildings, Colclough and McGrath made a life cycle analysis of a low-energy single-family house with a solar combi system with a 23 m^3 water seasonal thermal energy storage [4]. They found that implementing seasonal heat storage in the combi system would reduce the carbon emissions and life cycle energy consumption of the system in the long term. Persson and Westermark looked at the financial aspect of seasonal thermal energy stores for individual houses and found that more competitive investment and annual costs could be offered if they were applied to passive houses [5]. Xu et al. did a review on available technologies for seasonal heat storage and reported that sensible heat storage technology has been implemented in many large-scale plants [6]. Their review also covered latent heat and chemical stores, which are still at the stage of material investigations and lab-scale experiments. Pinel et al. reviewed methods for seasonal storage of solar heat in residential applications, mainly focusing on sensible heat stores [7]. Their paper also mentions chemical and latent thermal energy storage principles. These technologies could be used to store thermal energy over longer periods in more compact systems, but they need further development. Yan et al. have reviewed promising candidate reactions for chemical heat storage [8], and Aydin et al. have reviewed thermochemical heat storage systems, including comparison with other storage methods. Both reviews conclude that the chemical storage principle is a promising technology, but needs further development before it can reach the market. Zondag et al. reported on the development of a small-scale prototype thermochemical heat storage system [9], and Mette et al. presented a solar thermal combi system with a thermochemical energy storage for long-term heat storage [10]. Both these reports demonstrate the storage principles, although they need more research.

1.2. Phase change material heat storage

Stores that use the latent heat of fusion of a phase change material (PCM) have been suggested by many authors for improving performance compared to sensible heat stores. Nkwetta et al. carried out numerical investigations on incorporating PCM in water tanks and found that it could increase the energy stored [11]. López-Navarro et al. did experimental investigations on a storage tank with PCMs and made a full experimental characterisation of its performance [12]. Nkwetta and Haghighat [13] and Sharif et al. [14] have written reviews on thermal energy stores with PCMs. None of these authors report using the supercooling of a PCM for long-term heat storage. In fact, the supercooling of a PCM in a latent heat storage has usually been seen as an undesirable effect that needs be avoided by using various nucleation agents. This is because it prevents the heat of fusion from being released as desired during the discharge process when the melting point of the PCM is reached [15]. However, when a PCM is in a supercooled state in temperature equilibrium with the ambient, the melting enthalpy of the PCM is stored, but no continuous heat loss occurs, which makes long-term heat storage possible. Sandnes and Rekstad carried out laboratory investigations on the stored enthalpy in small samples of supercooled salt hydrates [16], but do not report investigations of constructed storage units. Dannemand et al. have previously reported a number of barriers and solutions for the reliable operation of a storage unit utilizing the principle of stable supercooling of sodium acetate trihydrate (SAT) mixtures and elucidated the theoretical storage potential with numerical calculations [17], but they did not investigate the actual measured performance of storage units. One of the problems they list is the phase separation of the SAT. In another article, Dannemand et al. investigated the performance of a prototype unit containing a SAT mixture with extra water. The extra water was added to solve the phase separation problem. They focused on cycling stability, discharge power and discharge temperatures [18], but they did not explore the heat exchange capacity rate. Another way of avoiding phase separation is to add a thickening agent to the SAT. This has been investigated by several authors in small sample sizes [19–22]. However, the performance of SAT mixtures with thickening agents actively being used for supercooling in large application-size heat storage units has not previously been reported.

1.3. Scope

This article reports on laboratory tests of two full-scale heat storage units for building heating purposes that use the principle of stable supercooling with two different PCM mixtures. The performance of a unit with a SAT mixture with extra water was compared with the performance a unit with a SAT mixture with carboxymethyl cellulose (CMC) – a thickening agent for avoiding phase separation. The experiments showed that the storage principle works in full-scale application-size units and that the unit with the SAT mixture with CMC as a thickening agent had the highest heat content. The heat exchange capacity rate of the heat storage prototypes, which is an important factor in system performance, was measured and compared. We also measured the energy released after the solidification of the supercooled PCMs, the discharge temperatures after solidification of the supercooled PCMs, and the cycling stability of the two units. The results verify the functionality of the storage concept in real application-size units and give an indication of the performance that can be expected from the first prototype storage units.

2. Experimental setup

The primary storage medium in the prototypes tested was sodium acetate trihydrate (SAT), which has a melting point of 58 °C and a latent heat of fusion of 264 kJ/kg [23]. It has been shown to supercool consistently down to temperatures well below 0 °C [24]. SAT is an incongruently melting salt hydrate and suffers from phase separation, especially over repeated heating and cooling cycles, where segregated anhydrous sodium acetate settles to the bottom of the PCM container and the water concentration in the upper part increases due to the density differences. When a PCM sample suffering from phase separation solidifies, not all possible trihydrate crystals will be formed because of the physical separation of water molecules in the upper part of the sample and segregated anhydrous sodium acetate in the lower part. This will reduce the effective latent heat of fusion of the bulk PCM and thereby also its storage capacity [25]. One solution that has been proposed is to add extra water to the salt hydrate so that the salt water mixture composition is always at a point where all salt is dissolved in the water when it is in supercooled liquid phase [26]. This requires soft mixing of the salt water mixture to avoid phase separation and reduces the energy density of the storage [27]. Another proposed solution for avoiding phase separation is to add a thickening agent to the PCM mixture. A suitable thickening agent will keep segregated anhydrous sodium acetate from settling to the bottom and keep the anhydrous salt suspended in the solution near the water it can recombine with at solidification.

2.1. PCM mixtures and material properties

A sodium acetate water mixture was prepared by melting the solid SAT in a closed barrel in a large oven for several days. To increase the water weight content from 39.7% of the SAT composi-

Table 1
Thermal properties of the PCM mixtures.

Material property	Solid specific heat $c_p(s)$ (kJ/kgK)	Liquid specific heat $c_p(l)$ (kJ/kgK)	Latent heat of fusion L (kJ/kg)
SAT + 9% H_2O	2.2	3.1	189.4
SAT + 1% CMC	2.1	3.0	250

tion to 44.8% water, 9 wt% extra water was added. The other PCM was a mixture of SAT with 1% carboxymethyl cellulose (CMC) which was prepared by initially melting the SAT and then, with the SAT in a hot melted state, mixing in the CMC little by little, while mechanically stirring to ensure a uniform PCM mixture. CMC was chosen as the thickening agent due to the positive experience of several authors [19–22]. The ratio of CMC and SAT chosen was based on recommendations from the supplier of the additive. A series of tests with smaller sample sizes showed that 1% CMC was the minimum quantity for a stable uniform mixture.

The specific heat capacities for the solid and liquid phases and the latent heat of fusion of the PCM mixtures were determined using the findings of Araki [28]. Non-temperature-dependent specific heat capacities for the solid and liquid phase PCM mixtures were determined as the average over the relevant temperature intervals. The latent heat of fusion and the specific heat capacities for the SAT and 1% CMC mixture were estimated to be the same as for SAT without extra water in Araki's findings. The value for the latent heat of fusion of SAT without extra water determined by Araki's correlation is slightly lower than the values generally stated in the literature [23]. Material properties applied for theoretical calculations are listed in Table 1.

2.2. Heat storage units

The units were designed as flat rectangular chambers for the PCM with an internal height of 50 mm. The low height was to reduce the risk of phase separation. The width and length of the units were 1200 × 2400 mm. One unit was made from normal steel and the other had the inner chamber for the PCM made in stainless steel. Steel and stainless steel in combination with SAT have been shown to be stable over long periods with regard to corrosion and chemical reactions [29,30]. At one end of the units were 300 mm wide and 100 mm high extensions in the width of the units. These were incorporated to allow for expansion of the PCM mixture during heating. The units had separate heat exchangers at the top and bottom of the PCM chamber. The heat exchangers had manifolds along the sides of the units. Each manifold had a cross section of 30 × 30 mm. The bottom surface of the PCM chamber was covered by 16 parallel channels and 14 channels covered the top surface. The heat exchangers were incorporated on to the outer surfaces of the PCM chamber to transfer heat through the top and bottom surfaces of the PCM chamber, as shown in Figs. 1 and 2. This enabled the PCM to be heated to a relatively uniform temperature to obtain complete melting of all crystals. It also allowed mixing of the salt water mixture by convection during heating. The internal height of the heat exchanger channels was 4 mm and the width was 130 mm separated by 20 mm spacers. The internal volumes of the chambers were approximately 144 l for the PCM and another 30 l for the expansion volume. No heat exchangers were incorporated on top of the expansion volume. The thickness of the steel plates was 2 mm. The mass of each empty unit was 236 kg. The total volume of heat transfer fluid (water) in the heat exchangers including the manifolds was 32 l in each unit.

When rigid constructions such as steel are used, the density change between the cold solid and the warm liquid salt can cause pressure changes and deformations of the tank. Just as bending a metal disk with cracks work as a triggering mechanism for pocket-sized heat packs [31], small cracks on the inside of the PCM chamber can in combination with pressure changes and deformations work as an uncontrolled activation mechanism, e.g. at joints or welds. To reduce the pressure changes in the PCM chamber during heating and cooling, an inflatable plastic bag or an expansion vessel without pre-pressure was connected to the expansion volume via a tube to allow for expansion of the PCM mixture without pressure build-up inside the PCM chamber. This closed design made it possible to heat the salt hydrate to a high temperature without loss of water vapour from the PCM. Moreover, the metastable state of the supercooled salt hydrate is easily interrupted by external disturbances, so a closed container is naturally more stable.

The inner surfaces of the PCM chamber were designed and manufactured to be simple and smooth without cracks or gaps. This was to avoid spontaneous nucleation caused by possible movement of cracks. Thirty pipe segments of 50 mm length were welded inside the PCM chamber to the top and bottom surfaces functioning as supports and to provide the unit with a rigid construction. One support inside the PCM chamber can be seen in Fig. 3.

Three openings to the PCM chamber were provided for filling the chamber with PCM and for installing the tube for the expansion tank and a probe to measure the temperature of the PCM. These filling necks were closed with lids and 3 mm thick rubber gaskets, as shown in Fig. 4. The filling necks were located in the upper part of the expansion volume to avoid contact between the PCM and the lids and gaskets.

2.3. Activation of solidification

Crystallization and the release of the heat of fusion from the supercooled SAT initiate when the first seed crystal of a certain size appears in the solution. After that, the crystallization will spread to the entire volume and the temperature will rise approximately to the melting point of the PCM. It has been shown that cooling a supercooled SAT mixture to a low temperature eventually causes crystallization of the supercooled solution [32]. To utilize this cooling technique to initiate the crystallization of the supercooled PCM, a 100 ml chamber was welded to the outside of each unit in good thermal contact with the PCM chamber at the opposite end to the expansion volume, as shown in Fig. 5. Liquid CO_2 with a pressure of 5–6 bars could then be flushed through this chamber to cool a small part of the PCM through the chamber wall to a low temperature as the CO_2 evaporated, and thus initiate nucleation.

2.4. Filling

The units were filled with the melted PCM mixture at a temperature of approximately 80 °C in a slightly tilted position to achieve complete filling of the PCM chamber. The unit was filled until the level of PCM was 2–4 cm higher in the expansion volume than elsewhere in the unit. This would allow for some contraction of the PCM during solidification while keeping a height of 5 cm in solid state at 25 °C in the entire unit, if the crystallization occurred homogeneously without air pockets in the PCM chamber.

Being handmade, the geometry of the units differed somewhat. The densities of the PCM mixtures also differed slightly due to dif-

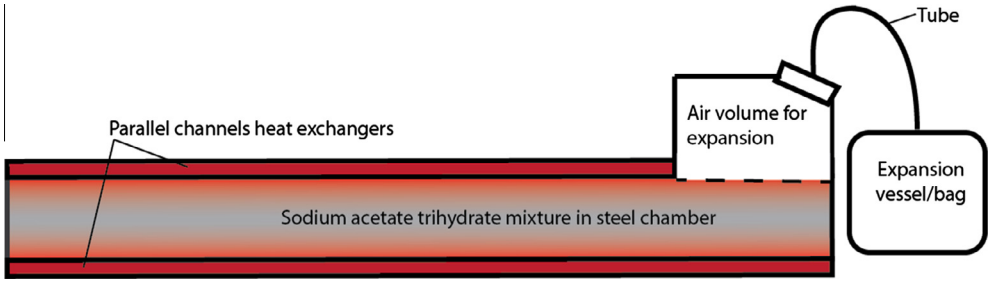

Fig. 1. Diagram of unit with PCM chamber, heat exchangers on top and bottom surfaces, and integrated and external expansion.

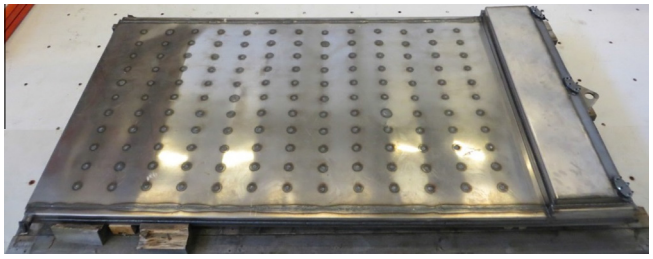

Fig. 2. 1200 × 2400 × 60 mm unit with heat exchangers on the top and bottom surfaces, and integrated expansion volume.

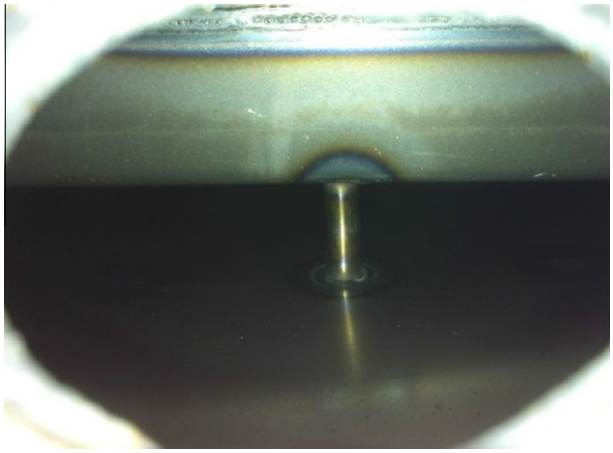

Fig. 3. View of a round stabilizer through filling neck.

Fig. 4. Expansion volume with filling necks, rubber gaskets and lids.

Fig. 5. CO_2 chamber for activating solidification of supercooled PCM mixture by cooling.

Table 2
Unit chamber material and PCM mixture and masses.

	Unit 1	Unit 2
PCM mixture	SAT + 9% H_20	SAT + 1% CMC
PCM mass	199.5 kg	220 kg
PCM chamber material	Steel	Stainless steel

ferent additives, which meant the units ended up containing different PCM masses. The steel unit contained 199.5 kg of SAT with 9% extra water (44.8 wt% water and 55.2 wt% sodium acetate). The unit with the inner chamber in stainless steel contained 220 kg of SAT thickened with 1% CMC. During testing the units were supported on a bed of 100 mm insulating material and a layer of 100 mm insulation was placed on the top and around the sides of each unit. An overview of the two units is given in Table 2.

Copper/constantan thermocouples were used to measure the surface temperature of the units on the outside of the heat exchangers, at the front and back of each unit, near the lids, and at the CO_2 chamber. One thermocouple in a probe was inserted through one of the filling necks to measure the temperature of the PCM. Thermopiles were used to measure the temperature difference across the inlets and outlets of the heat exchangers. Two Brunata HGQ1 flow meters were used to measure the flow rate to the heat exchangers. Solartron cards were used with a PC to record data every 10 s.

3. Test procedure and calculations

The units were connected to a heat storage test facility so that they could be heated and cooled under controlled conditions. Twenty test cycles with different flow rates, charge and discharge powers, temperatures settings and durations were carried out with

the unit with extra water. Six test cycles were carried out with the unit containing SAT and CMC.

To achieve supercooling of the SAT mixture, it is necessary that all crystals of the bulk PCM are melted, so that the PCM will not crystallise when it cools down. There appears to be a link between the level of heating above the melting point and the stability of the supercooling, as reported by Wei [33]. Our initial investigations showed that a temperature of at least 20 K above melting point in the entire volume helped to achieve stable supercooling.

The power of the heating element used for charging the units in the test facility was 6–9 kW. The units were charged for a period of 10–22 h with an inlet temperature of 90–94 °C and a flow rate of 10–11 l/min in each heat exchanger. Inlet, outlet and storage temperatures were typically stable after approximately 8 h of charging. After a stable hot period, the units were discharged with the aim of achieving a supercooled state with a flow rate of 2 l/min in each heat exchanger and an inlet temperature of approximately 25 °C. This temperature could represent the return temperature of a low-temperature heating system. The heat sink was the central cooling system of the test facility connected via a heat exchanger and controlled by a thermostatic valve. The response time of the valve caused the discharge temperature to vary somewhat throughout the discharge period. In some tests the aim was to keep the PCM stable in a supercooled state over a long period. In these tests, the units passively cooled towards the ambient temperature and were not actively discharged.

After the PCM had remained in a supercooled state for a period of time, crystallization was started by flushing CO_2 through the CO_2 chamber to cool a small part of the PCM. The energy released after solidification was discharged with a flow rate of 2 l/min in each heat exchanger.

The charge and discharge powers of the storage unit were determined by:

$$\dot{Q}_{charge} = \dot{V} \cdot c_p \cdot \rho \cdot (T_{in} - T_{out}) \quad (1)$$

where $\dot{V}$ is the volume flow rate of the heat transfer fluid measured at the inlet, T_{in} is the inlet temperature, T_{out} is the outlet temperature, c_p is the specific heat capacity of the heat transfer fluid at mean temperature between T_{in} and T_{out}, and ρ is the density of the heat transfer fluid at T_{in}.

The heat loss coefficient of the storage unit was determined by heating the unit to a stable temperature over a long period. The energy balance of the system was used to determine the heat loss experimentally. The energy added to the system was equal to the heat loss when the storage temperature remained stable over a period. In this way a heat loss coefficient with a constant value could be determined for the specific temperatures by:

$$H_{loss} = \dot{Q}_{charge}/(T_s - T_{amb}) \quad (2)$$

where T_s is the average surface temperature of the unit in a stable hot period, and T_{amb} is the ambient temperature. The heat loss coefficient for the storage unit was used to calculate the energy content of the storage unit based on the measured data.

The change of heat content in the unit over a specific time period during a charge was determined by:

$$E_{charge,measured} = \int_0^{t_c} \left[\dot{Q}_{charge} - H_{loss} \cdot (T_s - T_{amb})\right] dt \quad (3)$$

where T_s is the average surface temperature of the unit in the relevant time step, and t_c is the duration of the charge period. A similar procedure was used to determine discharged energy.

The heat exchange capacity rate (HXCR) expresses the ability to transfer thermal energy from a heat transfer fluid to the PCM material in the storage unit. It depends on the design of the heat exchanger of the storage unit, the operating conditions, and the thermophysical properties of the PCM. The HXCR is derived from the heat transfer rate and the log mean temperature difference [34,35]:

$$HXCR = \dot{V} \cdot c_p \cdot \rho \cdot ln\left(\frac{T_{in} - T_{PCM}}{T_{out} - T_{PCM}}\right) \quad (4)$$

where T_{PCM} is the PCM temperature measured by the probe inserted in the PCM. A high HXCR is desirable, so that the storage unit can be charged fast, e.g. when solar thermal energy is available, and so that it can be discharged with sufficient power to meet a given demand.

Finally, the measured heat per unit mass of PCM released after solidification of the supercooled PCM was determined for the test cycles to evaluate its cycling stability and storage potential, and to compare the two different PCMs.

With a specific heat of steel of 500 J/kgK and 32 l of water in the heat exchangers, the theoretical heat capacity C_{unit} of the storage unit was determined to be 252 kJ/K.

3.1. Theoretical calculations

The measured thermal energy charged to and discharged from the storage units was compared to the theoretical energy content calculated by Dannemand et al. [17] for a PCM storage with stable supercooling taking into account the latent heat of fusion, the specific heat capacities of the solid and liquid PCM, and the sensible heat of the storage tank material and heat transfer fluid. Their theoretical model indicates that the energy released from supercooled SAT at ambient temperature will be lower than the latent heat of fusion at the melting point, because the specific heat of the supercooled SAT is higher than the specific heat of the solid SAT. Their model also assumes that the PCM behaves like an ideal compound, which changes phase from solid to liquid at a specific melting temperature. When extra water is added to salt hydrates, phase change happens over a temperature range [26]. In our investigations, the focus was on the differences in energy content between the initial, the fully heated, the supercooled, and the discharged conditions. The simple theory with a specific melting temperature therefore provides a sufficient basis for comparison.

These sets of formulae were applied when calculating the theoretical energy content of the storage units with different start, maximum, supercooled and end temperatures, so that the measured values could be compared to theoretical values over the same temperature intervals.

4. Results and discussion

4.1. Test cycle energy content

The following section summarizes the results for the 13th test cycle of the unit with SAT and extra water. The 13th test cycle was typical for the test series. From a starting temperature of 24.6 °C, the unit was charged with a flow rate of 21 l/min for both heat exchangers combined. Stable conditions with an average heat storage temperature of 90.1 °C were reached after approximately 8 h of charging. The heat loss coefficient was experimentally determined using Eq. (2) to be H_{loss} = 8 W/K at 90 °C over a 12-h period.

The total energy stored in the unit, including PCM mixture and steel, for this temperature interval was 91.4 MJ, calculated from Eq. (3). The accumulated heat loss from this 8-h charge period was 10.8 MJ. Fig. 6 shows the accumulated heat loss over time, the energy stored in the unit, the total energy charged into the unit including the heat loss, and the PCM temperature during the test cycle. This illustrates the energy content of the unit during the test cycle and the different stages of the cycle.

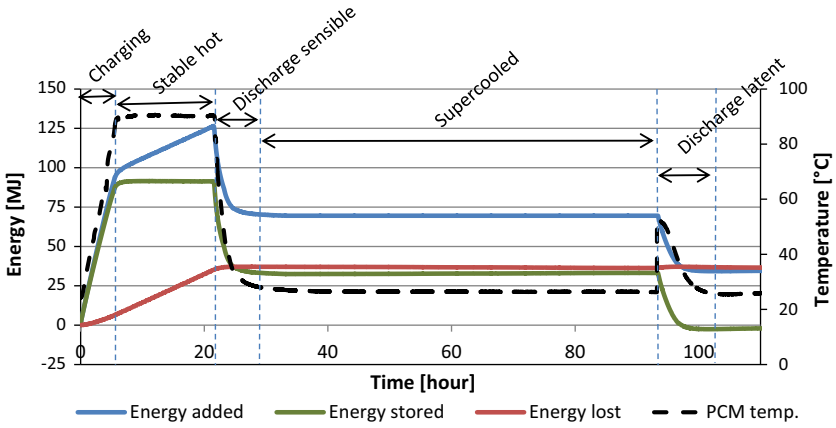

Fig. 6. Energy content of unit with SAT and extra water, accumulated heat loss and total energy added during a test cycle.

The theoretical thermal energy change in the unit for this temperature set and for the material properties in Table 1 was calculated to be 88.7 MJ. The measured energy content was 3% higher than the theoretical energy content. The measured energy discharged from the stable hot state to the supercooled state was 58.2 MJ. This is 5% higher than the theoretical discharged energy of 55.3 MJ.

After the unit had remained in supercooled state for three days at a storage temperature of 26.4 °C, the crystallization was started using the CO_2 cooling technique. The temperature on the outside of the CO_2 container reached −34 °C before the activation was registered as a temperature increase on a nearby thermocouple. The unit was discharged with a flow rate of 2 l/min in each heat exchanger to a temperature of 24.8 °C. After eight hours, all surface temperature sensors had stabilized and the unit was fully discharged. The total thermal energy discharged 8 h after solidification was 35.7 MJ. The theoretical thermal energy discharged for this temperature set and properties of SAT with 9% extra water listed in Table 1 was 33.2 MJ. So, the measured energy discharged after solidification of the supercooled sodium acetate water mixture was 7.5% higher than the theoretical.

Table 3 gives a summary of charge, discharge and solidification energies for the test cycle with SAT and extra water and for a test cycle with SAT and 1% CMC, along with the respective temperature intervals.

The deviation between the theoretical energy content and the measured values could indicate that incorrect values were used for the PCM properties in the theoretical calculations. A value for the latent heat of fusion of 202 kJ/kg instead of 189.4 kJ/kg for the SAT–water mixture, and of 242 kJ/kg instead of 250 kJ/kg for the SAT–CMC mixture would minimize deviations between the theoretical calculations and measured values.

4.2. Cycling stability

With a temperature of the supercooled storage and a final discharge temperature of approximately 25 °C, the energy released after solidification of the supercooled SAT with extra water in the first test cycle was 194 kJ/kg of PCM. In the 5th test cycle, 188 kJ/kg was discharged. After 20 test cycles, the measured discharged energy was 179 kJ/kg of PCM. This indicates that the problem of phase separation was not completely solved by adding 9% extra water, because the discharged energy declined over the test cycles. Mixtures with larger water content may show better cycling stability.

The energy released from the supercooled PCM in the unit with 1% CMC was consistently around 205 kJ/kg of PCM over the six test cycles.

In one test cycle, the unit with SAT and extra water was kept in supercooled state for eight weeks, while the unit with thickening agent was kept in supercooled state for five weeks before solidification was activated by cooling with CO_2. There was no significant difference in the energy discharged after a short or a long storage period.

In 13 of the 20 test cycles with the unit with SAT and extra water, the crystallization started spontaneously during discharge. In some tests, this was probably due to too low temperatures in the SAT caused by too short charge periods. In later test cycles, the PCM solidified spontaneously in three consecutive test cycles, after which the expansion bag was dismounted and it was observed that the tube between the unit and the expansion bag had been blocked with SAT. After cleaning the tube and remounting the expansion vessel, stable supercooling was again achieved. This indicates that the solution to the problem of the expansion of the PCM using a tube connected to an external expansion vessel may not be durable in the long run. In the unit with SAT and CMC, the crystallization started spontaneously in two of the six test cycles. In the remaining test cycles, the solidification was triggered by cooling with CO_2 after the PCM had remained supercooled and stable at ambient temperatures.

4.3. Heat exchange capacity rate

Fig. 7 shows the heat exchange capacity rates for the top and bottom heat exchangers for selected charges with similar test conditions for the two units. The HXCR for the unit with extra water

Table 3
Energy content of PCM in units during charge, discharge and activation.

	199.5 kg SAT with 9% extra water			220 kg SAT with 1% CMC		
	Temperature range (°C)	Theoretical (MJ)	Measured (MJ)	Temperature range (°C)	Theoretical (MJ)	Measured (MJ)
Charge	24.6–90.2	88.7	91.4	26.1–92.5	109.1	108
Discharge	90.2–26.4	55.3	58.2	92.5–26.2	60.4	59.8
Solidification	26.4–24.8	33.2	35.7	23.6–24.2	47.8	45.2

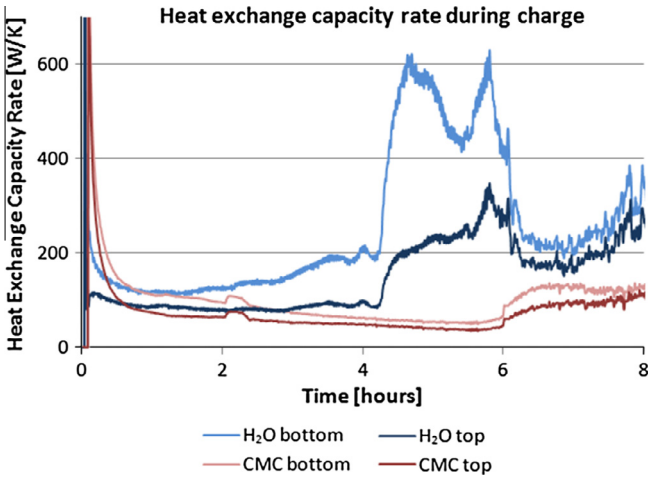

Fig. 7. Heat exchange capacity rate during charging for top and bottom heat exchangers for units with PCM mixtures with extra water and CMC.

increased during the charging period and the HXCR for the unit with thickening agent decreased until the end of the charge period. Sudden increases in HXCR occurred after 4 h for the unit with SAT and extra water and after 6 h for the unit with SAT and CMC. This was when the PCMs were fully melted and convection could occur throughout the respective PCM chambers. The HXCR was higher for the bottom heat exchanger in both units, partly because of the larger surface area of bottom heat exchanger and partly because heating the PCM from the bottom induced convection in the melted PCM, while heating from the top did not. The main reason for the difference in HXCR between the two units was the different levels of convection in the two PCM mixtures. The melted SAT with water mixture had a lower viscosity and therefore more convection occurred than in the melted SAT mixture with CMC, where convection remained low even after melting due to its higher viscosity. Sun et al. also report that the convection in PCM has a significant effect on the heat transfer in a PCM storage [36].

Another factor that affects the HXCR of the exchangers is convection of the heat transfer fluid inside the heat exchangers, which in the case of charging enhances the heat transfer in the bottom heat exchangers.

After solidification of the supercooled PCMs and the following discharges, the HXCRs for the two units showed a similar tendency. At this time, both PCMs were in solid states and there was no convection in the PCMs. With a flow rate of 2 l/min, the HXCR started at 160–180 W/K and dropped during the discharge.

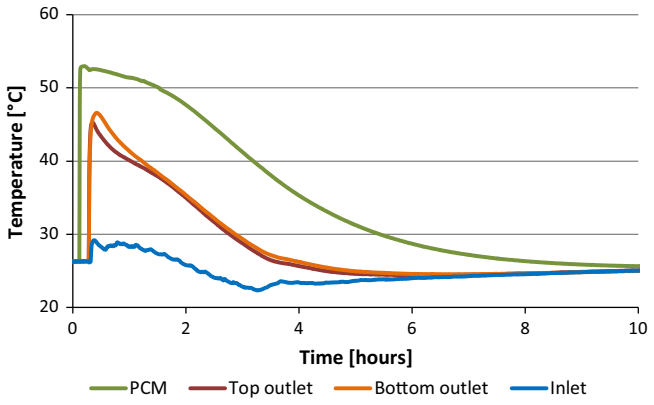

Fig. 8. PCM, inlet, top outlet and bottom outlet temperatures for the unit with extra water.

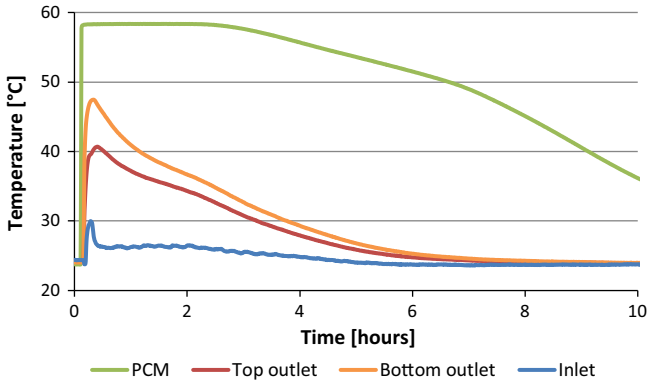

Fig. 9. PCM, inlet, top outlet and bottom outlet temperatures for the unit with thickening agent.

4.4. Solidification temperatures

Figs. 8 and 9 show the temperatures the PCMs reached after solidification from the supercooled state, the inlet and the outlet temperatures of the heat transfer fluid in the heat exchangers. The flow rates were 2 l/min in each heat exchanger. The maximum temperatures measured in the probes submerged in the PCMs after solidification were 53 °C for the SAT with extra water and 58 °C for the SAT with CMC. The higher outlet temperatures of the bottom heat exchangers were partially due to the larger area of the bottom heat exchangers. Another possible explanation could be non-optimal contact between the PCMs and the top heat exchangers caused by cavities or air bubbles formed during contraction of the PCMs as they cooled. The inlet temperatures during the discharge varied due to the response time of the thermostatic valve in the cooling loop.

A test with a discharge flow rate of 0.5 l/min increased the maximum average outlet temperature at the start of the discharge by 2–3 K.

4.5. Discharge power

The total discharge powers combining both top and bottom heat exchangers in each of the two units are shown in Fig. 10. The unit with SAT and CMC contained 10% more PCM mixture with a higher latent heat of fusion. This unit could therefore be discharged with a higher power and for a longer duration than the unit with SAT with extra water. The difference was especially clear in the second half of the discharge period. Discharging with a lower flow rate led to a lower initial power peak, but a longer discharge period. The discharge flow of the unit with extra water started with

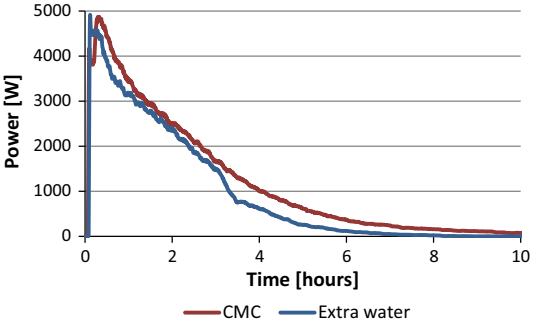

Fig. 10. Total discharge powers for units with sodium acetate trihydrate with extra water and CMC.

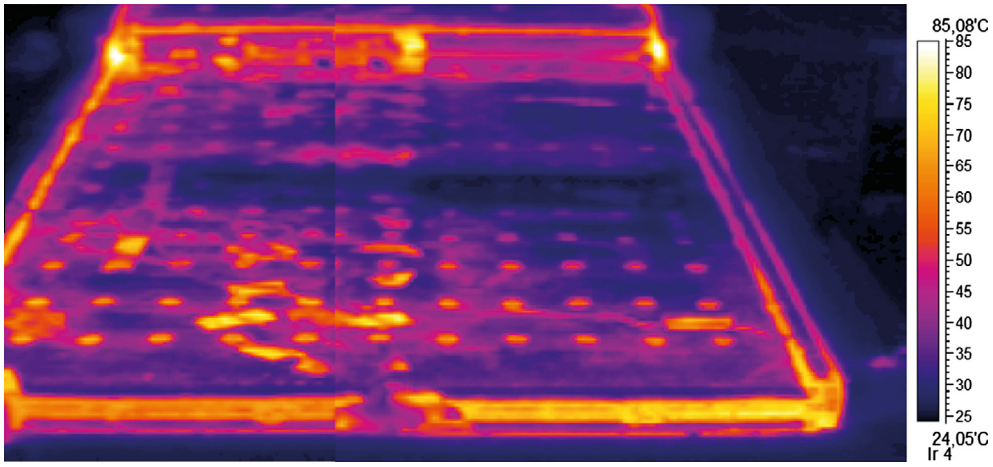

Fig. 11. Thermovision image of the top surface of a unit during charging.

a time delay after solidification of the supercooled PCM. In this case the water in the heat exchangers had more time to heat up before the flow started. This is the reason for the earlier peak in the discharge power for the unit with extra water in Fig. 10.

4.6. Unit and heat exchanger design

A thermovision image of the top surface of one of the units is shown in Fig. 11. The image was taken approximately 30 min after charging had begun. The inlet for the top heat exchanger was in the top left corner of the unit while the outlet is shown in the bottom right. The inlet manifold is on the left in the image and the outlet manifold is on the right. The flows in the channels across the top surface in the image are from left to right.

It can be seen from Fig. 11 that the temperature on the top surface was not uniform. A cooler area in the central channels can be observed. This indicates that the flow distribution was not uniform across the channels. Applying the theory for flow distribution in Z-configured solar collectors, the uneven flow distribution could be due to too high pressure drops in the manifolds compared to the pressure drop in the individual channels [37]. If so, increasing the cross section area of the manifolds by a factor of 3 might give a more even flow distribution. With an even flow distribution in the heat exchanger channels, we would expect shorter charge times and higher discharge powers and temperatures. The PCM in the space immediately below the expansion volume is furthest away from the heat exchangers and will therefore be the area where the full melting and discharge happens last.

The laboratory testing also showed that it was difficult to flush out air trapped in the heat exchangers in this flat unit design. Furthermore, the flat rectangular design limited the possible operation pressure in the heat exchangers, which might not be compatible with the operation pressure elsewhere in a solar heating system.

For design development, it is therefore recommended that the heat exchangers should allow relatively uniform heating and discharge of the PCM for optimal performance. The design should also make it easy for any air in either the heat exchanger or the PCM chamber to escape. This would help ensure optimal heat transfer between the PCM and the heat transfer fluid. And a design with flexible expansion integrated in the unit instead of the external expansion vessel would be an improvement.

The phase separation problem of the SAT was solved with thickening agents in this flat unit, so it should be investigated whether taller units would also allow for a stable SAT composite throughout multiple charge and discharge cycles. Other thickening agents or other additives may also prove functional. Cylindrical unit designs and heat exchangers made of tubes may cope better with internal pressures than the flat unit design presented in this article. Tall cylindrical shaped units might also reduce the cost of manufacture compared to the flat design.

4.7. Integration of heat storage units in solar heating system

The laboratory investigations showed that it was possible to fully melt SAT mixtures and obtain stable supercooled PCMs in 200 kg units using an inlet flow temperature of 90 °C. This temperature could be delivered by solar collectors. By placing a number of heat storage units in a utility room, e.g. in the basement of the house, the heat to melt the SAT mixtures could be transferred from the solar collectors to the units by a piping system. In the laboratory tests, the discharge temperature and power after solidification was high enough to cover the requirements of a low-temperature heating system in a single-family house, e.g. a floor-heating system. The heat could also be used for the preparation of domestic hot water. The number of units required to cover the heat demand can then be determined. With this seasonal heat storage technique, the heating demand of a single-family house could theoretically be covered 100% by solar energy.

5. Conclusions

Experimental investigations have shown that it is possible to store thermal energy in supercooled sodium acetate trihydrate mixtures in units of a size that could be used for real applications. One prototype unit contained 199.5 kg of SAT with 9% extra water and was stable in supercooled state at ambient temperature for up to 2 months before solidification was intentionally started. Another unit contained 220 kg of SAT thickened with 1% carboxymethyl cellulose and was stable in supercooled state at ambient temperature up to 5 weeks before solidification was intentionally started. This shows that CMC works as thickening agent for SAT in large-scale applications.

The heat exchange capacity rate during charging of the unit with SAT and extra water was significantly higher than for the unit with SAT and CMC due to the higher viscosity of the thickened PCM. Initiating the crystallization of the supercooled PCM was done by cooling a small part of the SAT mixture to its maximum degree of supercooling by flushing pressurized liquid CO_2 through a small chamber attached to the outside of the PCM chamber. The energy discharged after solidification of the supercooled SAT with 9% extra water was 194 kJ/kg of PCM in the first cycle, 188 kJ/kg after five test cycles and 179 kJ/kg after 20 test cycles. The energy

discharged after solidification of the SAT with CMC was stable at around 205 kJ/kg of PCM over six test cycles. The SAT with extra water reached 53 °C after solidification and the SAT mixture with CMC reached 58 °C after solidification. For both PCMs the outlet temperature reached approximately 45 °C at the beginning of the discharge with a flow rate of 2 l/min in each heat exchanger. The discharge power after solidification of the supercooled PCMs peaked at 4.5–5 kW at the beginning of the discharge and remained above 1 kW for approximately 4 h. Crystallization of the PCM mixtures happened spontaneously in some test cycles and stable supercooling was not always achieved.

Acknowledgements

This project was funded by the European Commission as part of the Seventh Framework Programme of the European Community for Research, Technological Development and Demonstration Activities under the funding scheme of "Collaborative Project" through the COMTES consortium, Grant Agreement N° 295568. We thank our partner Henry Sørensen from Nilan A/S for constructing the storage unit prototypes and our partners Hermann Schranzhofer and Christoph Moser from Graz University of Technology for discussions and sharing their knowledge. We thank our technicians Martin Dandanell and Claus Aagaard for constructing the test rig for the units.

References

[1] Cabeza LF, Miró L, Oró E, de Gracia A, Martin V, Krönauer A, et al. CO_2 mitigation accounting for Thermal Energy Storage (TES) case studies. Appl Energy 2015;155:365–77. http://dx.doi.org/10.1016/j.apenergy.2015.05.121.
[2] Bauer D, Marx R, Nußbicker-Lux J, Ochs F, Heidemann W, Müller-Steinhagen H. German central solar heating plants with seasonal heat storage. Sol Energy 2010;84:612–23. http://dx.doi.org/10.1016/j.solener.2009.05.013.
[3] Novo AV, Bayon JR, Castro-Fresno D, Rodriguez-Hernandez J. Review of seasonal heat storage in large basins: water tanks and gravel-water pits. Appl Energy 2010;87:390–7. http://dx.doi.org/10.1016/j.apenergy.2009.06.033.
[4] Colclough S, McGrath T. Net energy analysis of a solar combi system with Seasonal Thermal Energy Store. Appl Energy 2015;147:611–6. http://dx.doi.org/10.1016/j.apenergy.2015.02.088.
[5] Persson J, Westermark M. Low-energy buildings and seasonal thermal energy storages from a behavioral economics perspective. Appl Energy 2013;112:975–80. http://dx.doi.org/10.1016/j.apenergy.2013.03.047.
[6] Xu J, Wang RZ, Li Y. A review of available technologies for seasonal thermal energy storage. Sol Energy 2013;103:610–38. http://dx.doi.org/10.1016/j.solener.2013.06.006.
[7] Pinel P, Cruickshank CA, Beausoleil-Morrison I, Wills A. A review of available methods for seasonal storage of solar thermal energy in residential applications. Renew Sustain Energy Rev 2011;15:3341–59. http://dx.doi.org/10.1016/j.rser.2011.04.013.
[8] Yan T, Wang RZ, Li TX, Wang LW, Fred IT. A review of promising candidate reactions for chemical heat storage. Renew Sustain Energy Rev 2015;43:13–31. http://dx.doi.org/10.1016/j.rser.2014.11.015.
[9] Zondag H, Kikkert B, Smeding S, De Boer R, Bakker M. Prototype thermochemical heat storage with open reactor system. Appl Energy 2013;109:360–5. http://dx.doi.org/10.1016/j.apenergy.2013.01.082.
[10] Mette B, Kerskes H, Drück H, Müller-Steinhagen H. New highly efficient regeneration process for thermochemical energy storage. Appl Energy 2013;109:352–9. http://dx.doi.org/10.1016/j.apenergy.2013.01.087.
[11] Nkwetta DN, Vouillamoz P-E, Haghighat F, El-Mankibi M, Moreau A, Daoud A. Impact of phase change materials types and positioning on hot water tank thermal performance: using measured water demand profile. Appl Therm Eng 2014;67:460–8. http://dx.doi.org/10.1016/j.applthermaleng.2014.03.051.
[12] López-Navarro A, Biosca-Taronger J, Corberán JM, Peñalosa C, Lázaro A, Dolado P, et al. Performance characterization of a PCM storage tank. Appl Energy 2014;119:151–62. http://dx.doi.org/10.1016/j.apenergy.2013.12.041.
[13] Nkwetta DN, Haghighat F. Thermal energy storage with phase change material – a state-of-the art review. Sustain Cities Soc 2014;10:87–100. http://dx.doi.org/10.1016/j.scs.2013.05.007.
[14] Sharif MKA, Al-Abidi AA, Mat S, Sopian K, Ruslan MH, Sulaiman MY, et al. Review of the application of phase change material for heating and domestic hot water systems. Renew Sustain Energy Rev 2015;42:557–68. http://dx.doi.org/10.1016/j.rser.2014.09.034.
[15] Guion J, Teisseire M. Nucleation of sodium acetate trihydrate in thermal heat storage cycles. Sol Energy 1991;46:97–100. http://dx.doi.org/10.1016/0038-092X(91)90021-N.
[16] Sandnes B, Rekstad J. Supercooling salt hydrates: stored enthalpy as a function of temperature. Sol Energy 2006;80:616–25. http://dx.doi.org/10.1016/j.solener.2004.11.014.
[17] Dannemand M, Schultz JM, Johansen JB, Furbo S. Long term thermal energy storage with stable supercooled sodium acetate trihydrate. Appl Therm Eng 2015;91:671–8. http://dx.doi.org/10.1016/j.applthermaleng.2015.08.055.
[18] Dannemand M, Kong W, Fan J, Johansen JB, Furbo S. Laboratory test of a prototype heat storage module based on stable supercooling of sodium acetate trihydrate. In: Energy procedia. Elsevier B.V.; 2015. p. 172–81. doi:10.1016/j.egypro.2015.02.113.
[19] Hu P, Lu D-J, Fan X-Y, Zhou X, Chen Z-S. Phase change performance of sodium acetate trihydrate with AlN nanoparticles and CMC. Sol Energy Mater Sol Cells 2011;95:2645–9. http://dx.doi.org/10.1016/j.solmat.2011.05.025.
[20] Garay Ramirez BML, Glorieux C, Martin Martinez ES, Flores Cuautle JJA. Tuning of thermal properties of sodium acetate trihydrate by blending with polymer and silver nanoparticles. Appl Therm Eng 2013;61:838–44. http://dx.doi.org/10.1016/j.applthermaleng.2013.09.049.
[21] Dannemand M, Johansen JB, Furbo S. Solidification behavior and thermal conductivity of bulk sodium acetate trihydrate composites with thickening agents and graphite. Sol Energy Mater Sol Cells 2016;145:287–95. http://dx.doi.org/10.1016/j.solmat.2015.10.038.
[22] Shin HK, Park M, Kim H-Y, Park S-J. Thermal property and latent heat energy storage behavior of sodium acetate trihydrate composites containing expanded graphite and carboxymethyl cellulose for phase change materials. Appl Therm Eng 2015;75:978–83. http://dx.doi.org/10.1016/j.applthermaleng.2014.10.035.
[23] Zalba B, Marin JM, Cabeza LF, Mehling H. Review on thermal energy storage with phase change: materials, heat transfer analysis and applications. Appl Therm Eng 2003;23:251–83. http://dx.doi.org/10.1016/S1359-4311(02)00192-8.
[24] Rogerson MA, Cardoso SSS. Solidification in heat packs: I. Nucleation rate. AIChE J 2003;49:505–15. http://dx.doi.org/10.1002/aic.690490220.
[25] Kimura H, Kai J. Phase change stability of sodium acetate trihydrate and its mixtures. Sol Energy 1985;35:527–34. http://dx.doi.org/10.1016/0038-092X(85)90121-5.
[26] Furbo S, Svendsen S. Report on heat storage in a solar heating system using salt hydrates. Therm. Insul. Lab. DTU, Kgs. Lyngby, Denmark, Rep. 70.; 1977.
[27] Furbo S. Investigations of heat storages with salt hydrate as storage medium based on the extra water principle. Therm. Insul. Lab. DTU, Kgs. Lyngby, Denmark, Rep. 80. Meddelelse; 1978.
[28] Araki N, Futamura M, Makino A, Shibata H. Measurements of thermophysical properties of sodium acetate hydrate. Int J Thermophys 1995;16:1455–66. http://dx.doi.org/10.1007/BF02083553.
[29] Cabeza LF, Roca J, Nogués M, Mehling H, Hiebler S. Immersion corrosion tests on metal-salt hydrate pairs used for latent heat storage in the 48–58 °C temperature range. Mater Corros 2002;53:902–7. http://dx.doi.org/10.1002/maco.200290004.
[30] Moreno P, Miró L, Solé A, Barreneche C, Solé C, Martorell I, et al. Corrosion of metal and metal alloy containers in contact with phase change materials (PCM) for potential heating and cooling applications. Appl Energy 2014;125:238–45. http://dx.doi.org/10.1016/j.apenergy.2014.03.022.
[31] Rogerson MA, Cardoso SSS. Solidification in heat packs: III. Metallic trigger. AIChE J 2003;49:522–9. http://dx.doi.org/10.1002/aic.690490222.
[32] Furbo S, Fan J. Heat storage based on a NaCH3COO water mixture for solar heating systems. DTU Civil Engineering, Report SR-12-10 (UK), Kgs. Lyngby, Denmark; 2012.
[33] Wei L, Ohsasa K. Supercooling and solidification behavior of phase change. ISIJ Int 2010;50:1265–9. http://dx.doi.org/10.2355/isijinternational.50.1265.
[34] Cengel YA. Heat transfer: a practical approach. 2nd ed. McGraw-Hill; 2003.
[35] Furbo S. Heat storage for solar heating systems. Educational Note, ISSN 1396-4046, BYG.DTU, Kgs. Lyngby, Denmark; 2005.
[36] Sun X, Zhang Q, Medina MA, Lee KO. Experimental observations on the heat transfer enhancement caused by natural convection during melting of solid–liquid phase change materials (PCMs). Appl Energy 2016;162:1453–61. http://dx.doi.org/10.1016/j.apenergy.2015.03.078.
[37] Weitbrecht V, Lehmann D, Richter A. Flow distribution in solar collectors with laminar flow conditions. Sol Energy 2002;73:433–41. http://dx.doi.org/10.1016/S0038-092X(03)00006-9.

Paper 4 - Experimental investigations on tall cylindrical latent heat storage units with sodium acetate trihydrate composites utilizing supercooling

Mark Dannemand, Jakob Berg Johansen, Weiqiang Kong, Simon Furbo

Draft / Submitted to Applied Energy

Title: Experimental investigations on cylindrical latent heat storage units with sodium acetate trihydrate composites utilizing supercooling

Authors: Mark Dannemand, Jakob Berg Johansen, Weiqiang Kong, Simon Furbo

Corresponding email: markd@byg.dtu.dk

Affiliation: Department of Civil Engineering, Technical University of Denmark, Brovej 118, Kgs. Lyngby, DK 2800, Denmark

Abstract

Latent heat storage units utilizing stable supercooling of sodium acetate trihydrate (SAT) composites were tested in a laboratory. The stainless steel units were 1.5 m high cylinders with internal heat exchangers of tubes with fins. One unit was tested with 116 kg SAT with 6% extra water. Another unit was tested with 116.3 kg SAT with 0.5% Xanthan rubber as a thickening agent and 4.4% graphite powder. The heat exchange capacity rate during charge was significantly lower for the unit with SAT and Xanthan rubber compared to the unit with SAT and extra water. This was due to less convection in the thickened phase change material after melting. The heat content in the fully charged state and the heat released after solidification of the supercooled SAT mixtures at ambient temperature was higher for the unit with the thickened SAT mixture. The heat discharged after solidification of the supercooled SAT with extra water decreased, while the heat discharged from the SAT with Xanthan rubber remained stable, over the charge and discharge cycles. In both units, the solidification started spontaneously in the majority of the test cycles. This was due to the design of the unit or the method for handling the expansion and contraction of the SAT during charge and discharge.

Keywords: Compact Thermal Energy Storage; Latent Heat; Phase Change Material; Sodium Acetate Trihydrate; Supercooling.

1. Introduction

Large amounts of energy are used for heating of buildings. A significant part of the energy used to cover these demands is from fossil fuels. The burning of fossil fuels leads to climate change and other pollution. Clean energy free from greenhouse gas emissions can be produced by renewable resources such as solar. Solar irradiance can be harvested by solar collectors as thermal energy and used for heating purposes. The supply of solar energy is however intermittent and does often not meet demand patterns. Thermal energy storage is therefore needed as parts of solar heating systems to match the intermittent supply of solar energy with varying demands. Apart from heating of buildings, thermal energy storage is also used in other applications to make the energy systems more sustainable [1]. Thermal energy storage enables a more optimal use of energy resources and may reduce the use of fossil fuels [2].

Phase change materials (PCM) can be used to improve the volumetric storage capacity of a thermal energy storage compared to sensible heat storage by utilizing the latent heat of fusion [3], [4], [5]. Sodium acetate trihydrate (SAT) is an incongruently melting salt hydrate with a latent heat of fusion of 264 kJ/kg at the melting temperature of 58 °C [6]. These thermal properties make SAT a suitable material to integrate with solar heating systems, space heating and domestic hot water preparation. Furthermore, melted SAT has the ability to cool down to ambient temperatures without crystalizing [7]. Letting the SAT remain in this supercooled state allows for a partly loss-free storage, when the

latent heat of fusion of the SAT is stored in temperature equilibrium with the ambient. Solidification of the supercooled SAT can be initiated when a heat demand arises and the latent heat of fusion is released and used for the heating purpose. This principle of utilizing stable supercooling makes compact seasonal heat storage possible in decentralized systems for example in single family houses [8].

1.1 State of the art

A lot of research has previously been carried out aiming to find solutions for improving the performance of thermal energy storage. López-Navarro et al. did an experimental characterization of a PCM storage tank with paraffin [9]. Novo et al. did a review on large seasonal sensible heat storage [10]. Nkwetta and Haghighat did a review on available technologies including active systems for thermal energy storage with PCMs [11]. Sharif et al. likewise did a review on applications with PCMs for space heating and domestic hot water preparation [12]. None of these reviews included technologies that utilize supercooling of a PCM. Xu et al. [13] and Pinel et al. [14] did reviews on methods and available technologies for seasonal thermal energy storage and briefly touch on the concept of utilizing supercooling of SAT for compact seasonal heat storage. Persson and Westermark did an analysis of the economy of buildings with seasonal thermal energy storage and found that their relative competitiveness was higher when used for passive houses compared to houses with higher heat demands [15]. Colclough and McGrath did life cycle analysis of a low energy dwelling and found that over a long-term perspective, a solar combi-system with seasonal thermal energy storage had the lowest embodied energy and carbon [16].

Dannemand et al. presented in an article a number of practical solutions to barriers and problems for obtaining a functional heat storage based on stable supercooling of SAT [17]. They also describe how this concept can be used for seasonal heat storage of solar thermal energy.

1.2 Sodium acetate trihydrate composites

Phase separation is a key problem when using the incongruently melting SAT as a heat storage material. Melted SAT consists of sodium acetate dissolved in water [18]. The solubility of the sodium acetate is too low in the supercooled state to dissolve all the salt in the water from the melted SAT. Undissolved sodium acetate will therefore settle to the bottom of the container. All the potential SAT crystals cannot be formed when the SAT solidifies again due to the physical separation of the segregated sodium acetate at the bottom and the corresponding water in the top of the container [19]. This reduces in practice the latent heat of fusion and the heat storage potential [20]. One suggested solution for solving this problem has been adding extra water to the SAT. In this way all the sodium acetate can be dissolved in water [21]. Adding extra water to the PCM mixture will however reduce the heat storage capacity compared to SATs potential [22].

Another possible solution is adding a thickening agent to the SAT. The precipitated sodium acetate will then stay suspended in the thickened supercooled solution and does not settle to the bottom. In this case the sodium acetate can recombine with the nearby water molecules at crystallization to form SAT [23]. However, the heat transfer in a PCM storage is affected by the convection in the PCM as elucidated by Sun et al. and may be reduced when the viscosity increases [24]. Ryu et al. investigated several thickening agent for different salt hydrates [25]. Several authors found that an SAT composite with carboxymethyl cellulose (CMC) was stable through thermal cycling [26], [27], [28]. Meisingset and Grønvold suggested using Xanthan rubber as a thickening agent [23]. All of these investigations were on a small laboratory scale and not tested on a scale representing heat storage applications large enough to meet a heat demand of a single family house.

In laboratory experiments Dannemand et al. characterized the performance of two flat storage units with approximately 200 kg SAT mixtures with extra water or CMC [29], [30]. Their tested units had an internal height of the PCM chamber of 5 cm. The low height was to reduce the risk of phase separation. Higher units may result in aggravated phase separation but give fewer design constrictions. They found that the heat content was reduced over repeated charge and discharge cycles for the unit with SAT and extra water but it was stable for the unit with SAT and CMC. They also found that the heat exchange capacity rate was lower in the unit with the thickened SAT mixture.

1.3 Heat transfer

The heat transfer of PCM storage is highly affected by the design of the heat exchanger. Different designs were evaluated by Medrano et al [31]. Chiu and Martin investigated numerically and experimentally the performance of a finned heat exchanger heat storage unit [32]. The low thermal conductivity of PCMs is another typical challenge of using PCMs in heat storage [33]. This combined with no heat transfer by convection when the PCM is in solid state and limited heat transfer by convection in the melted PCM with high viscosity, may result in a low heat exchange capacity rate (HXCR) in a storage [34].

It was shown by Dannemand et al. through numerical simulations that the HXCR of a PCM storage had a significant impact on the system performance of a solar combi-system including a PCM storage utilizing supercooling [17].

As the thermal conductivity of the PCM in a store affects the HXCR, improvement of the thermal conductivity of PCMs has been investigated by several researchers. Enhancing the thermal conductivity of PCMs has for example been by adding expanded graphite to the PCM [28], [33] or by impregnating graphite matrixes with the PCM [35], [36]. Zhang et al. did a review on fabrication and characterization of composite PCMs for performance enhancement [37]. Dannemand et al. investigated the effect on the thermal conductivity by adding graphite powder or graphite flakes to thickened SAT composites [38]. Dannemand et al. also suggest adding oil to the PCM chamber to increase heat transfer as the oil could fill in insulating cavities in the solid PCM [17]. Cavities in the PCM will be formed due to the density difference between the solid and liquid SAT.

1.4 Scope

The performance of SAT with extra water in a 1.5-meter high heat storage unit utilizing supercooling has not previously been reported. The performance of SAT thickened with Xanthan rubber in real application sized units has not previously been reported. Further, the effect of adding oil to the PCM chamber to increase heat transfer, which is touched on in this article has not been reported previously.

The performances of two 1.5-meter high cylindrical heat storage units containing SAT with extra water or SAT with Xanthan rubber and graphite powder are characterized. The performance of the units when actively utilizing supercooling for long term heat storage has been elucidated. Also, the performance of a storage unit containing water is compared to the performance of a unit containing SAT with extra water in terms of heat content and HXCR. The size of the investigated units could be for an actual application in heating systems for a single family house if multiple units are installed. The heat exchange capacity rates of the storage units, heat contents over repeated cycles, the stability of the supercooling and the energy discharged after the supercooled periods has been measured and analysed.

2. Method

Laboratory tests were carried out with heat storage units containing water and the two different SAT composites.

2.1. Storage unit description

The heat storage units were designed as stainless steel cylinders to be placed vertically. The cylinders were 150 cm high with a diameter of 30 cm. The units were insulated with 4 cm expanded polypropylene during testing. One of the two units had inspection windows to visually observe the PCM inside the unit during operation, (see Figure 1).

Figure 1. Cylindrical heat storage units with and without inspection windows and insulation.

Internal heat exchangers consisted of 16 stainless steel pipes located in a circular formation in the length of the cylinder with thin aluminium plates attached as fins to increase the heat transfer. The distance between the aluminium plates was approximately 0.5-1 cm (see Figure 2). Manifolds with inlets and outlets were located on the top and bottom of the cylinder, see Figure 3.

Figure 2. Internal heat exchanger [39].

The units were filled approximately 90% with the storage mediums leaving an air space in the top of the cylinder to accommodate the expansion/contraction of the PCM (see Figure 3). In some tests, an air filter was installed either directly on the top of the tank or at the end of a tube connected to the PCM chamber. This was to allow for the PCM to expand/contract without pressure build-up in the PCM chamber while limiting the possibility of airborne particles to enter and disturb the stability of the supercooling. In other tests, the top of the PCM chamber was connected to an external expansion tank via a tube, hence having a closed PCM chamber where the PCM could expand with reduced pressure build-up. Water vapour could possibly escape from the unit when the air filter was installed, whereas this was avoided with the expansion tanks installed. Dannemand et al. previously showed that reducing pressure build-up was needed to achieve stable supercooling of SAT in a steel chamber [17][30].

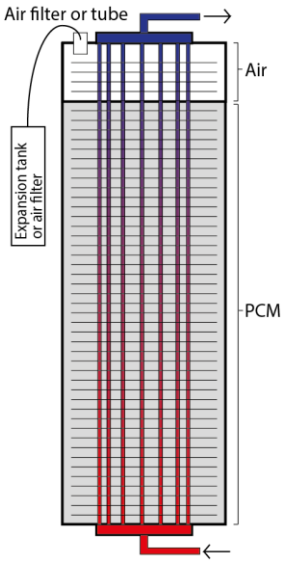

Figure 3. Diagram of cylindrical heat storage unit and heat exchanger.

The thermal capacity of the unit without the heat storage tank material C_{tank} was estimated to be 27.3 kJ/K for the unit without inspection windows and 40 kJ/K for the unit with inspection windows. These were determined by considering the masses and the materials of the empty units as well as the heat transfer fluid in the heat exchangers.

2.2. Storage materials

Water has often been used as the storage medium for short term storage and has therefore been tested as reference material for comparison with the PCMs. The heat storage unit with inspection windows was initially tested with water. Afterwards it was tested with a composite of 93.6% SAT and 6.4% extra water (SATH2O), equivalent to 56.5% sodium acetate and 43.5% water. All percentages are by weight. The other unit was tested with a mixture of 95.1% SAT, 0.5% Xanthan rubber as a thickening agent and 4.4% fine graphite powder for enhancing the thermal conductivity of the PCM (SATXC).

The PCM composites were prepared by melting the SAT in a closed barrel in a large oven. After melting the SAT, water or graphite was mixed into the barrel. The Xanthan rubber powder was mixed with 2-3 kg solid crushed SAT before it was added to the melted SAT little-by-little while stirring the melted PCM composite with a mortar mixer. This was done to ensure that the Xanthan rubber was properly dispersed in the mixture. The mixing of SAT with Xanthan rubber was done with a moderate intensity as the PCM mixture became a thick jelly even at high temperatures and air bubbles were easily trapped in the PCM. Air trapped in the PCM will reduce storage density and reduce heat transfer in the PCM.

Charging and discharging cycles were carried out with the units filled with 91 kg water, 116 kg SATH2O and 116.3 kg SATXC. With a density of SAT of 1280 kg/m^3 in liquid phase [40], all units were filled with approximately the same volume for all mediums.

2.3. Test cycles and test setup

The heat storage units were connected, via a pipe loop with water as the heat transfer fluid, to an electric heating element with a power of 3, 6 or 9 kW for charging and to a central cooling unit for discharging via a heat exchanger.

The inlet temperature of the heat transfer fluid during discharge was controlled with a thermostatic valve controlling the flow on the heat sink side of the heat exchanger, see Figure 4.

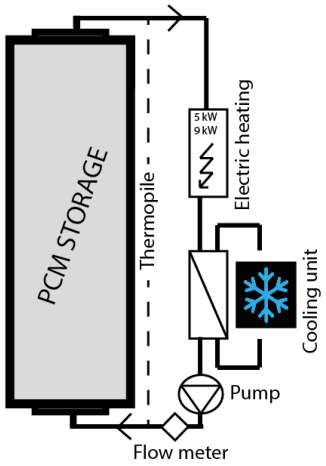

Figure 4. Schematic of charge and discharge loop for the PCM storage.

The flow direction through the unit was from bottom to top for both charge and discharge. During charging the thermostat of the electric heating element was set to 90-95 °C. During discharge, the inlet temperature was set to be 20-25 °C.

Six test cycles were carried out with water and 17 test cycles with SATH2O as the storage medium in the unit with inspection windows. A total of 40 test cycles were carried out with the unit with SATXC without inspection windows.

After the first 10 test cycles, 0.5 litres of paraffin oil was added to the PCM chamber of the unit with SATXC. After a number of test cycles, additional paraffin oil was added to the PCM chamber in steps until a total of 1.5 litre paraffin oil had been added. This was done as an attempt to enhance the heat transfer in the PCM. The oil is meant to float on top of the liquid state PCM due the density difference and the fact that the liquids do not mix. When the SAT solidifies and contracts the oil is then sucked into the PCM instead of air when passage allows. This may enhance the effective heat transfer of the PCM mixture as the cavities filled with oil will provide less thermal resistance compared to cavities with air.

A five junction thermopile based on copper/constantan type-TT thermocouples with counter flow sensors inside the inlet and outlet pipes measured the temperature difference across the inlet and outlet. The absolute flow temperatures were measured with thermocouples. All thermocouples were copper/constantan type-TT with an accuracy of 0.5 K. The accuracy of the temperature difference measured by the thermopile was 0.1 K. Temperatures on the outside of the tank were measured with 1 thermocouple on the bottom outer surface, 5 thermocouples distributed evenly on the outer side of the tank wall inside the insulation. A glass rod with 5 thermocouples evenly distributed in the height of the tank measured the temperatures in the centre of the unit with inspection windows. One thermocouple measured the ambient temperature. The flow rate was measured at the inlet with a Cloruis flow meter which had been calibrated to have an accuracy of ± 1 % in the relevant flow range. Solartron cards with a PC were used to log the measurements.

2.4. Calculations

The charge $\dot{Q}_{charge}$ [W] and discharge $\dot{Q}_{discharge}$ [W] powers were determined by:

$$\dot{Q}_{charge/discharge} = \dot{V} \cdot c_p \cdot \rho \cdot (T_i - T_o) \quad (1)$$

where, T_i is the inlet temperature, T_o is the outlet temperature, $\dot{V}$ is the volume flow rate of the heat transfer fluid measured at the inlet, c_p is the specific heat capacity of the heat transfer fluid at mean temperature between T_i and T_o, ρ is the density of the heat transfer fluid at T_i.

The heat loss coefficients H_{loss} [W/K] of the storage units were determined by heating the units to a stable temperature over a long period. The heat balance of the system was then used to determine the heat loss experimentally i.e. the heat added to the system was equal to the heat loss. In this way a simplified heat loss coefficient with a constant value was determined by:

$$H_{loss} = \dot{Q} / (T_s - T_{amb}) \quad (2)$$

where T_s is the mean temperature of the surface sensors and T_{amb} is the ambient temperature. The heat loss coefficient for the storage unit was used when calculating the heat content of the storage based on the measured data. The heat content in the storage unit after a charge E_{charge} [J] or the heat discharged from the unit $E_{discharge}$ [J] over a specific time period t was determined by:

$$E_{charge/discharge}(t) = \int_0^t (\dot{Q} - H_{loss} \cdot (T_s - T_{amb}))dt \quad (3)$$

where T_s and T_{amb} are for the relevant time steps. The heat content of the PCM per mass at a specific storage temperature T_s above a defined start temperature T_{start} excluding the specific heat of the tank material and heat transfer fluid C_{tank} was calculated by the following expression:

$$E_{PCM}(T_s, T_{start}) = \frac{E_{charge/discharge}(T_s, T_{start}) - C_{tank} \cdot (T_s - T_{start})}{m} \quad (4)$$

where $E_{charge/discharge}(T_s, T_{start})$ is the measured heat content of the unit at a temperature T_s above a start temperature T_{start} and m is the mass of the PCM. This allows for comparing the heat content of the different PCMs disregarding the heat capacities of the units and comparing the measurement to a theoretical storage capacity of the PCMs with given sensible and latent heats.

The heat exchange capacity rate was expressed by the following equation, which can be derived from the heat transfer rate and log mean temperature difference [41], [42].

$$HXCR = \dot{V} \cdot c_p \cdot \rho \cdot ln\left(\frac{T_i - T_s}{T_o - T_s}\right) \quad (5)$$

2.5. Material properties

Dannemand et al. described the theoretical heat content of supercooled SAT with melting at a specific temperature [17]. This approach has been adapted for the SATXC mixture. The specific heat capacity for the solid and liquid SATXC was estimated to be 2.0 kJ/kg K and 3.1 kJ/kg K, similar to SAT [43]. The latent heat of fusion of the SATXC mixture was estimated to be 251 kJ/kg at the melting point of 58 °C, which is equivalent to 95.1% of the heat of fusion of SAT [6]. The theory of Furbo and Svendsen has been adapted to the SATH2O mixture to describe the theoretical heat content of SATH2O as a function of temperature [21]. Adding extra water to SAT affects the melting behaviour of the SAT-

water mixture and reduces the latent heat of fusion of the PCM mixture as some SAT dissolves in the extra water. The melting takes place over a temperature range when extra water is added to SAT. The specific heat capacities for solid and liquid SATH2O were estimated to be 2.1 kJ/kg K and 3.2 kJ/kg K using the correlation of Araki [43]. Figure 5 shows the theoretical heat content of SATH2O and SATXC per mass as a function of the temperature from 20-90 °C. The heat contents in the supercooled states were estimated by extrapolating the lines representing the sensible heats in the melted states down to 20 °C. The dotted lines represent the heat contents in the supercooled states. The loss-free storage potential for storage at an ambient temperature of 20 °C is marked.

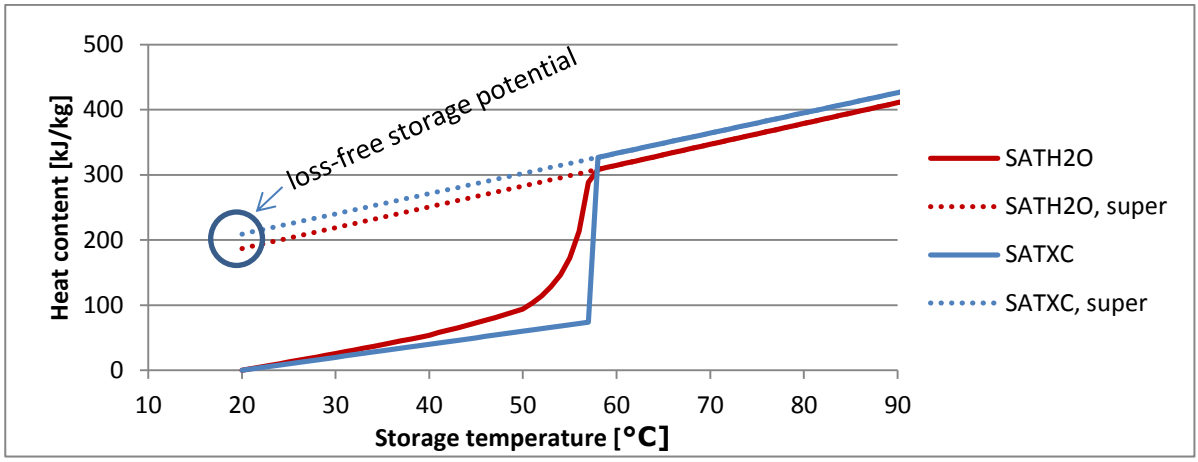

Figure 5. Theoretical heat content and storage potential of SATH2O and SATXC as a function of temperature.

The measured heat content per mass of the PCM calculated by equation (4) was compared to the theoretical heat content displayed in Figure 5. The PCM temperature was assumed to be the measured storage temperature. The measured storage temperatures may deviate from the actual PCM temperatures due to temperature gradients in the PCMs during charge and discharge. This was especially the case when the storage temperature was measured only on the outer surface of the tank. This caused either an overestimation or underestimation of the PCM temperature during charge and discharge. At the hot state and at the supercooled state where the temperatures were stable over a period of time, it was assumed, that the PCM temperatures were uniform in the storage unit and the temperatures were accurately measured by the sensors.

3. Results and discussions

Comparisons of the HXCRs, heat contents, and charge and discharge powers of the units with the three different storage mediums were made with various flow rates.

3.1. Charge

Charging of the unit filled with water was compared to charging the unit filled the SATH2O. The temperatures of the units before and after charging, the flow rates, heating element powers, inlet temperatures, the heat contents of the stores and the time for the full charges are listed in Table 1. The units were considered fully charged when the average storage temperatures were 0.5 K below the temperature at the stable hot states.

Table 1. Start and max storage temperature, flow rate, heating element power, inlet temperature, heat content and charge time for units with water and SATH2O.

Storage medium	Start temp. T_{start}	Max temp. T_{max}	Flow rate $\dot{V}$	Heating element $\dot{Q}$ / T_{in}	Heat content $E_{storage}$	Charge time t
Water	17.5 ˚C	85.5 ˚C	7.2 l/min	9 kW / 87 ˚C	28.6 MJ	128 min
SATH2O	15.0 ˚C	87.4 ˚C	7.3 l/min	9 kW / 89 ˚C	50.1 MJ	292 min

Figure 6 shows the HXCR and power $\dot{Q}_{charge}$ over the charge period for the units filled with water and SATH2O.

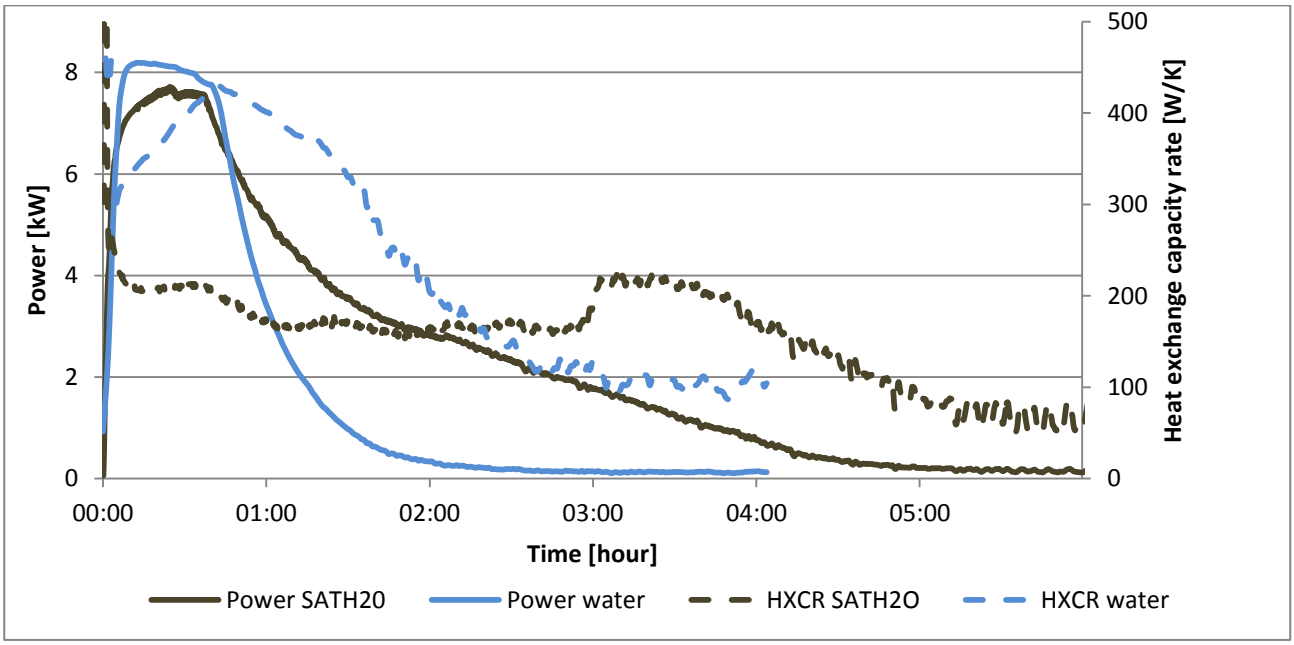

Figure 6. Typical charge powers and HXCRs for units with water and SATH20.

In Figure 6 can be seen, that the HXCR in the first hour of the charge was significantly higher for the unit with water compared to the unit with SATH2O, even though the charge powers were similar. This was due to a higher heat transfer by convection in the unit with water compared to the unit with SATH2O, in which the PCM was solid from the start. The power decreased earlier for the unit with water due to it being fully charged faster as a result of the lower heat capacity and a higher HXCR. At the third hour, the HXCR for the unit with SATH2O increased. At this time the last sensor on the outside of the tank had reached 58 ˚C which indicates that the SATH2O was fully melted. At this point no solid SATH2O remained and the heat transfer was dominated by convection.

Charging of the unit containing SATH2O was compared to charging the unit containing SATXC including one litre of paraffin oil. The conditions for the charges, the heat contents and charge times are listed in Table 2.

Table 2. Start and maximum storage temperature, flow rate, heating element power, inlet temperature, heat content and charge time for units with SATH2O and SATXC.

Storage medium	Start temp. T_{start}	Max temp. T_{max}	Flow rate $\dot{V}$	Heating element $\dot{Q}$/ T_{in}	Heat content E_{charge}	Charge time t
SATH2O	18.8 ˚C	85.6 ˚C	7.3 l/min	6 kW / 87 ˚C	45.8 MJ	308 min
SATXC + oil	23.2 ˚C	90.8 ˚C	7.4 l/min	6 kW / 95 ˚C	50.1 MJ	376 min

Figure 7 shows the HXCR and power $\dot{Q}_{charge}$ for the charge period for the units filled with SATH2O and SATXC with oil.

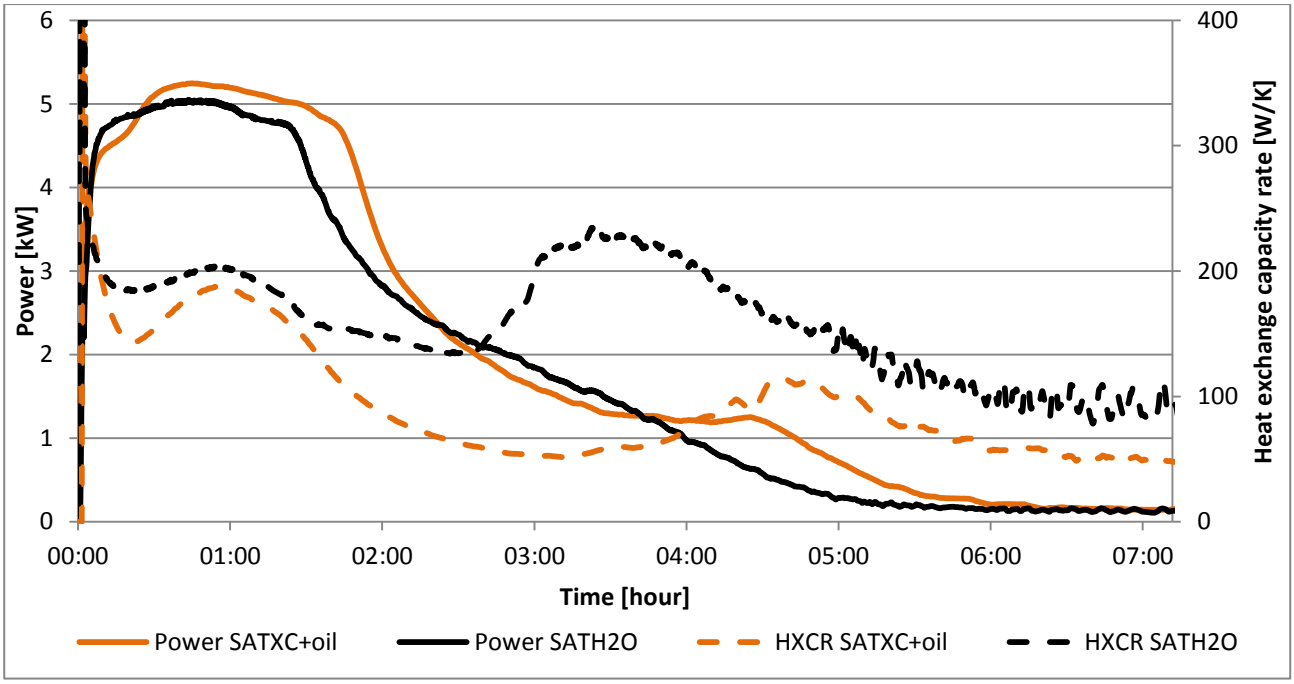

Figure 7. Typical charge powers and HXCRs for units with SATH2O and unit with SATXC with oil.

With similar conditions for charging, the HXCR for the unit with SATH2O was significantly higher compared to the unit with SATXC and oil. The heat content of the unit with thickened PCM was 9 % higher for the applied temperature intervals but the charge time was 22% longer. This was due to the better heat transfer by convection in the unit without a thickening agent. Again, at the third hour there was an increase in HXCR for the unit with SATH2O due to increased heat transfer by convection in the fully melted PCM. This increase is much less evident and occurring later in the unit with SATXC due to the higher viscosity of the SATXC in the melted state.

The HXCRs for charging the unit with SATXC with and without one litre of paraffin oil was compared. The charge conditions, the heat contents and charge times are listed in Table 3.

Table 3. Start and maximum storage temperature, flow rate, heating element power, inlet temperature, heat content and charge time.

Storage medium	Start temp. T_{start}	Max temp. T_{max}	Flow rate $\dot{V}$	Heating element $\dot{Q}$/ T_{in}	Heat content E_{charge}	Charge time t

SATXC	21.5 ˚C	90.4 ˚C	13.7 l/min	6 kW / 92 ˚C	50.9 MJ	395 min
SATXC + oil	20.8 ˚C	90.8 ˚C	13.7 l/min	6 kW / 92 ˚C	51.3 MJ	377 min

The charge powers $\dot{Q}_{charge}$ [W] and HXCRs for selected charges are displayed in Figure 8.

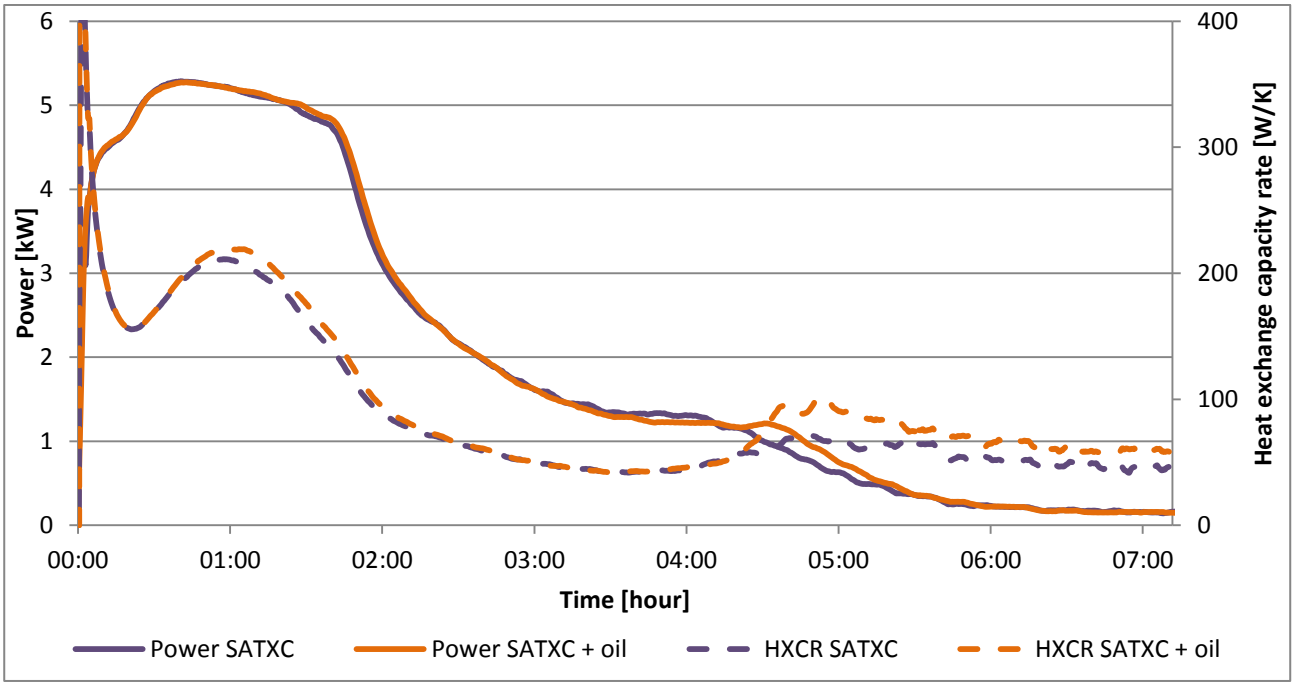

Figure 8. Charge powers and HXCRs for the unit with SATXC with and without 1 litre of paraffin oil.

Figure 9 shows a slight improvement of the HXCR by adding the one litre of paraffin oil. The effect was clearest from hour one to hour two of charging when the PCM was primary in the solid phase. In the last part of the charge temperature measurement uncertainties may cause the difference between the curves. After approximately 4h30 all temperature sensor on the outer surfaces of the tanks had reached 58 ˚C. At this point all the phase change was complete and the energy was transferred to the liquid PCM as sensible heat.

3.2. Discharge sensible heat

After the stable hot period, the sensible heats of the units were discharged. This left the units with PCMs in a supercooled state if the solidification did not start spontaneously. The temperature of the units at the stable hot states, the inlet temperatures of the heat transfer fluid, the flow rates, the discharged heat and the discharge times for typical cycles with units with water, SATH2O and SATXC with oil are listed in Table 4. The discharge was considered complete when the average storage temperature was 0.5 K higher than the inlet temperature. Temperature intervals are listed for the inlet temperature T_i because the temperature varied due to the response time of the thermostatic valve.

Table 4. Start storage temperature, inlet temperature, flow rate, discharged heat and discharge time for sensible heats.

Storage medium	Start temp. T_{max}	Inlet temp. T_i	Flow rate $\dot{V}$	Discharged heat $E_{discharge}$	Discharge time t
Water	82.4 ˚C	25-20 ˚C	5.7 l/min	25.3 MJ	177 min

SATH2O	85.5 ˚C	27-20 ˚C	5.7 l/min	26.9 MJ	288 min
SATXC + oil	90.9 ˚C	27-24 ˚C	6.2 l/min	26.3 MJ	370 min

The discharge powers and the HXCRs for the discharge periods can be seen in Figure 9.

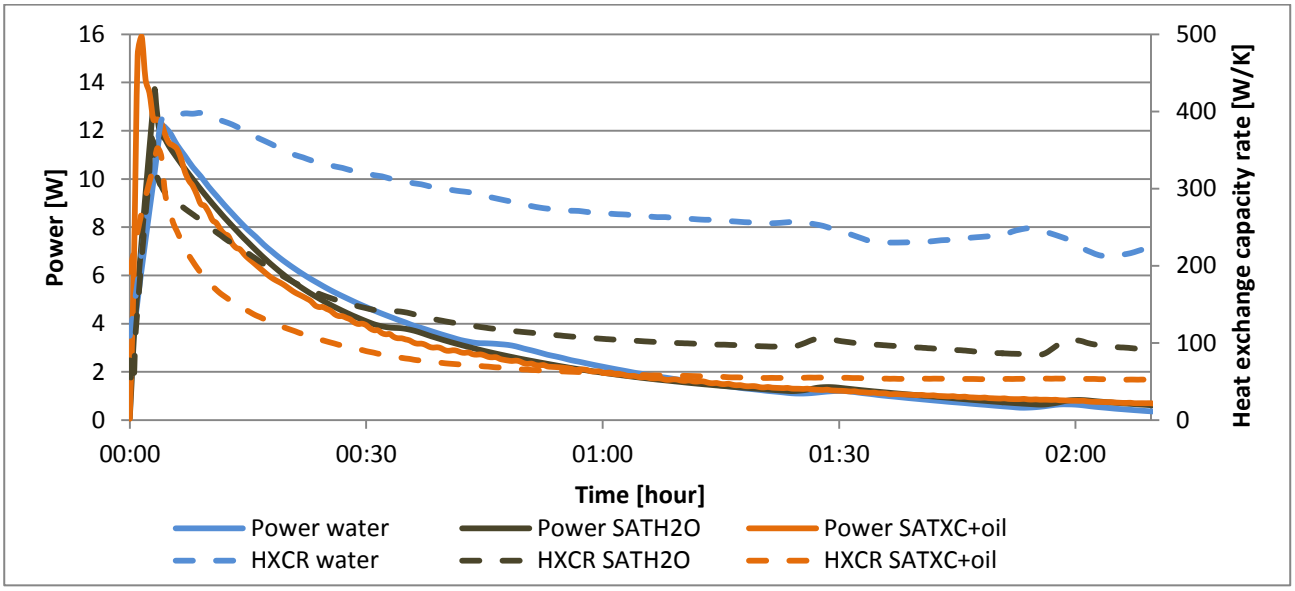

Figure 9. Typical discharge power and HXCR for the units with water, SATH2O and SATXC.

The majority of the heat was discharged during the first hour of discharge. The power and the HXCRs were the highest for the unit with water during this period. The discharge power of the unit with SATXC with oil had a higher peak at the beginning of the discharge due to a higher start storage temperature. The HXCR for the unit with SATXC was significantly lower compared to the unit with SATH2O. This was due to the higher viscosity of the thickened PCM which affected the heat transfer by convection. This is also reflected in the discharge times.

3.3. Discharge latent heat

After the sensible heats of the units with PCMs were discharged the PCMs were in a supercooled states at ambient temperature. The solidification was initialized by slightly shaking the unit or by dropping a seed crystal into the PCM. After solidification the latent heat of fusion was discharged. The temperatures of the units at the supercooled states, the inlet temperatures of the heat transfer fluid, the flow rates, the discharged heats for typical cycles with units with SATH2O and SATXC with oil are listed in Table 5.

Table 5. Start storage temperature, inlet temperature, flow rate and discharged heat for discharge of latent heat.

Storage medium	Start temp. T_{super}	Inlet temp. T_i	Flow rate $\dot{V}$	Discharged heat $E_{discharge}$
SATH2O	18.8 ˚C	27-20 ˚C	5.7 l/min	16.7 MJ
SATXC + oil	25.3 ˚C	27-24 ˚C	5.7 l/min	25.4 MJ

The discharge powers and HXCRs for the discharge period can be seen in Figure 10.

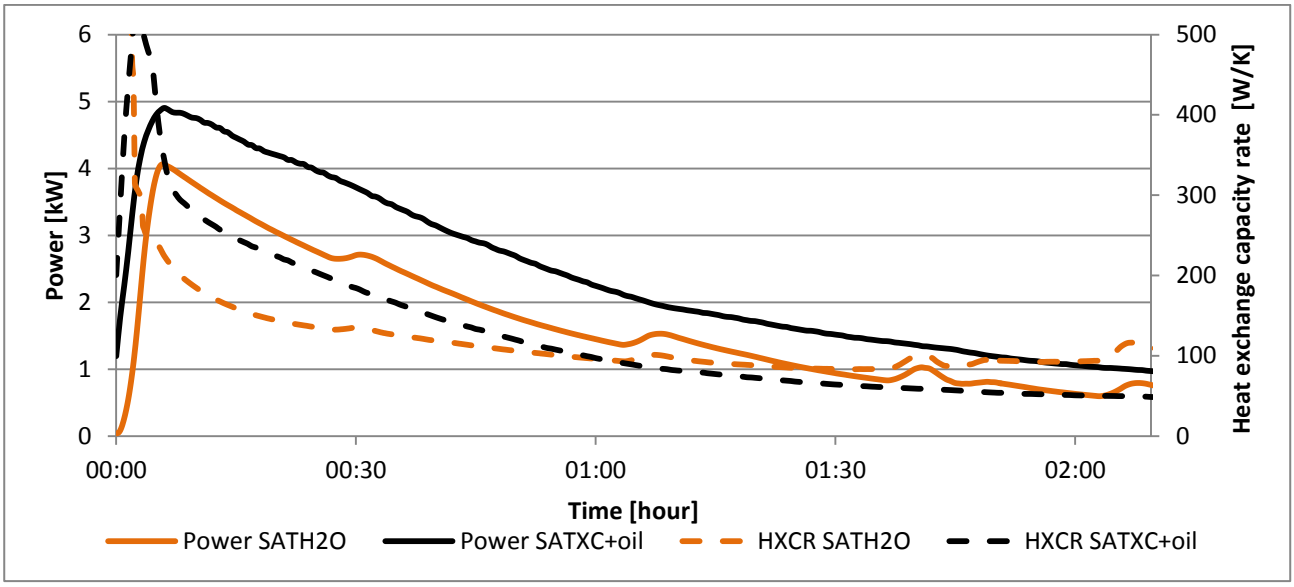

Figure 10. Typical discharge powers and HXCRs after solidification for units with SATH2O and SATXC.

Both the power and the HXCR were higher for the unit with SATXC compared to the unit with SATH2O. This was due to a higher heat content of the SATXC compared to the SATH2O. The thermal conductivity of the SATXC was assumed to be higher than for the SATH2O due to the addition of graphite and thereby also increasing the discharge power and HXCR. The higher storage temperature of the SATXC before solidification also resulted in a higher discharge power and heat content.

No significant difference was found when comparing discharge of sensible heat or latent heat from the unit with SATXC with or without one litre of paraffin oil. The amount of oil added was only 1-2% of the volume of the PCM. The density difference between the solid and liquid SAT is theoretically 12% [40]. A larger percentage of oil may have a better effect.

3.4 Discharge temperatures

The temperature increases from inlet to outlet during the discharge of latent heat for selected cycles are displayed in Figure 11. The units were discharged with an inlet temperature which stabilized at 18-20 ˚C. Discharge flow rates of approximately 2 l/min and 5.5 l/min were applied. Some fluctuations can be seen which was due to flow irregularities and the response time of the thermostatic valve.

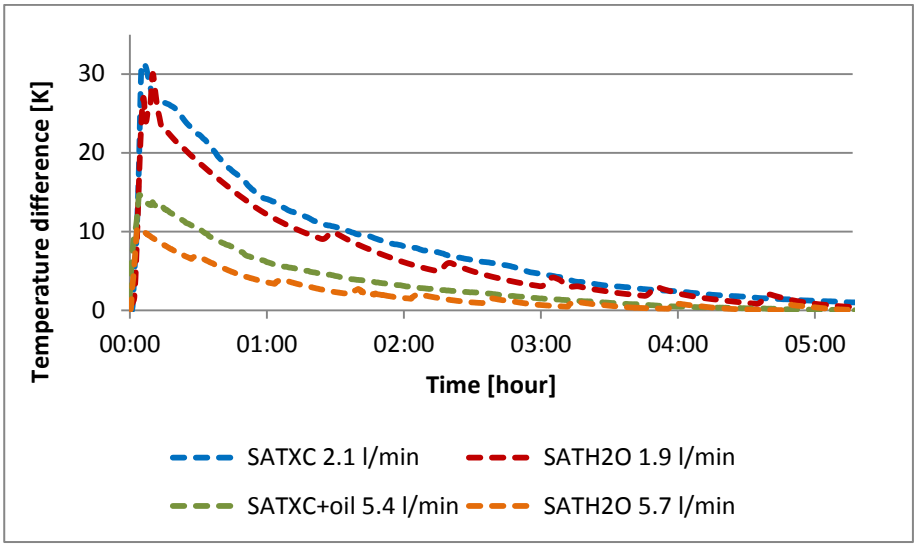

Figure 11. Temperature difference between inlet and outlet during discharge of latent heat.

The temperature increase of the heat transfer fluid during discharge was higher with lower flow rates. The unit with SATXC gave higher discharge temperatures compared to the unit with SATH2O at similar flow rates. With a discharge of 1.9 l/min and an inlet temperature of 22 ˚C, a maximum outlet temperature of 51 ˚C was reached at the start of the discharge of the unit with SATXC. Figure 12. Measured heat content of SATH2O compared to theoretical heat content.The measured surface temperature of the unit with SATXC after solidification was 1-2 K higher compared to the unit with SATH2O. This indicates a higher PCM temperature after solidification in the SATXC.

3.5. Heat content and cycling stability of SAT composites

The heat charged to the unit with SATH2O when heating from approximately 19 ˚C to 88 ˚C was stable at 45 – 48 MJ over the 17 test cycles. The heat discharged from the unit with SATH2O after solidification of the supercooled SATH2O at a temperature of 20 – 25 ˚C and discharging it back down to the same temperature was 20 MJ in the first cycle and 16.3 MJ in the 15th test cycle. The heat charged into the unit with SATXC when heating from approximately 21 ˚C to 91 ˚C was stable at 50 – 53 MJ over the 40 test cycles. The heat discharged after solidification of the supercooled SATXC at 20 – 25 ˚C and discharging back down to the same temperature was stable at 24 – 26 MJ for the test cycles where stable supercooled was achieved.

The heat content in the fully charged state was 9% higher in the unit with SATXC compared to the unit with SATH2O when including corrections for the slightly different the start, maximum and end temperatures. The discharged sensible heat was 1.5% lower from the unit with SATXC compared to the unit with SATH2O. The discharged latent heat after solidification of the supercooled PCMs was 20 – 36% higher for the unit with SATXC compared to the unit with SATH2O.

The measured heat contents per mass of PCM $E_{PCM}(T)$ for selected test cycles are displayed in Figure 12 for SATH2O and in Figure 15 for SATXC and compared to the theoretical values. The stable conditions where comparisons of theoretical and measured heat contents are valid are marked with circles.

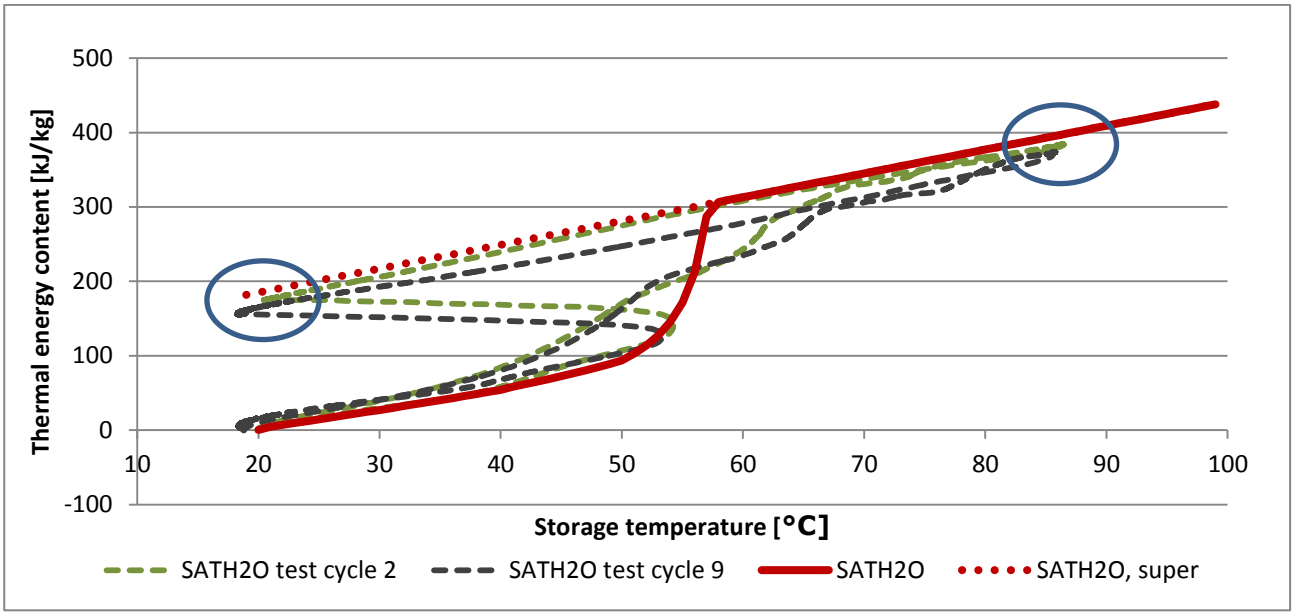

Figure 12. Measured heat content of SATH2O compared to theoretical heat content.

Figure 12 shows that the measured heat content in the 9th test cycle with SATH2O was lower compared to the heat content for the 2nd test cycle. The storage capacity of the SATH2O in the supercooled state at 20 ˚C was 177 kJ/kg in the first cycle decreasing to 140 kJ/kg after 17 cycles, a decrease of 21%.

Figure 13 and Figure 14 shows the top and bottom inspection windows of the unit after 17 cycles. There was a liquid solution layer of 20 – 22 cm in the top of the unit and a layer with whiter crystals in the bottom of the unit. This indicates a decreased salt concentration in the top and increased anhydrous salt at the bottom of the unit. The heat released after solidification of the supercooled SATH2O after a number of test cycles was decreased due to this phase separation.

In the research of Dannemand et al. where a flat unit was tested with 200 kg SAT with 9% extra water, the heat discharged after solidification the supercooled PCM at ambient temperature was 194 kJ/kg in the first test cycle and 179 kJ/kg after 14 test cycles [29][30]. This was a decrease of 8% from the first test cycle. This indicates that a tall unit is more likely to suffer from phase separation or that the higher water concentration in the SAT-water mixture better solved the phase separation.

Figure 13. Top inspection window of unit with SATH2O.

Figure 14. Bottom inspection window of unit with SATH2O.

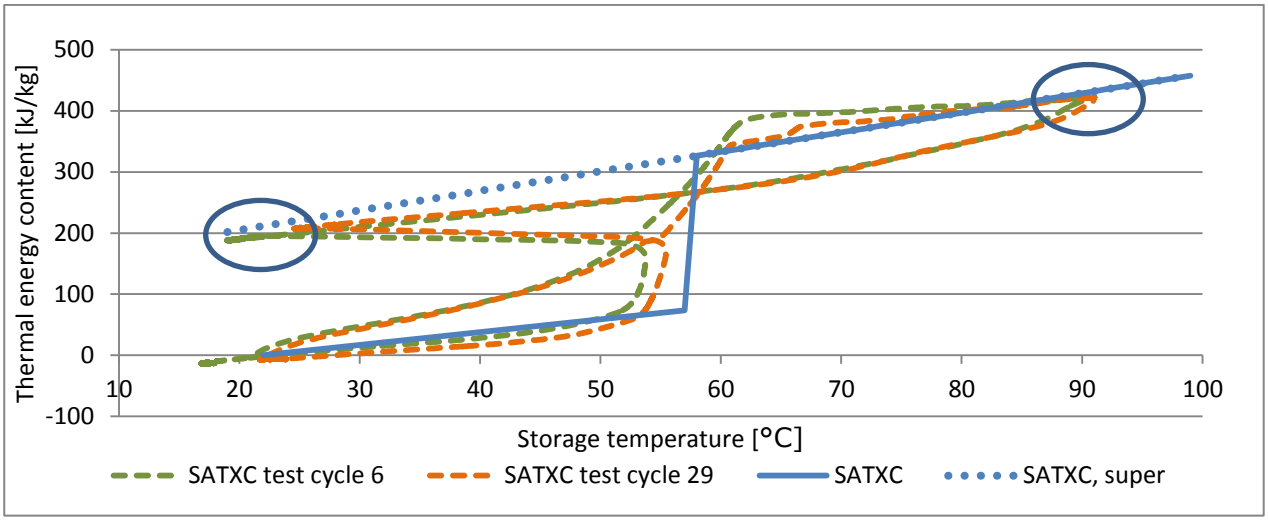

Figure 15. Measured heat content of SATXC compared to theoretical heat content.

Figure 15 shows that the measured heat content of the SATXC is close to the theoretical values and the heat contents were similar for the 6th and 29th test cycles. The storage capacity was 205 – 210 kJ/kg of SATXC in the supercooled state at 20 ˚C throughout the test cycles carried out. Dannemand et al. found in the investigations of a flat heat storage unit with SAT thickened with 1% CMC a stable heat content of the supercooled PCM of over 6 test cycles of 205 kJ/kg [29].

3.6. Supercooling stability

The SATH2O solidified spontaneously 10 times during discharge in the 17 test cycles. The stable supercooled state was reached 7 times. Slightly pushing the unit initialized the crystallization. The crystallization started from the bottom. It is assumed that a torque at a crack or joint at the bottom of the PCM chamber caused the starting of the solidification in a similar way as when flexing a metal disc in the hand warmers is a method for initializing crystallization [44]. The unit with SATXC solidified spontaneously 34 times of the 40 test cycles. In 6 cycles the unit reached a supercooled state at ambient temperature, it was activated manually by dropping a seed crystal into the PCM or shaking the unit. Three times the spontaneous solidification started from the bottom in the unit with SATXC, 22 times it started from the top and 9 times it was not possible to determine the starting point of crystallization. Crystallization starting from the bottom could be for the same reason as for the unit with SATH2O. Crystallization starting from the top may indicate that the solution for solving the expansion of the PCM by an air filter or expansion vessel may not be a viable solution. The solution did however seem to be working for the unit with SATH2O. Supercooled periods up to two days were achieved for the unit with SATXC with the air filter for two of the test cycles. However, the semi-open approach may lead to the loss of water vapour from the PCM chamber resulting in a change in PCM mixture composition and is therefore not a recommended solution.

Part of the spontaneous solidification on the SAT mixtures was most likely caused by the design of the inner surfaces of the PCM chamber. It is therefore recommended that the PCM chamber is designed with all inner surfaced being completely smooth with no cracks where surfaces are joining and no penetrations of the chamber wall with tubes where the SAT is in contact. Such areas pose a risk of spontaneous crystallization when crystals are trapped under high pressure and later released into the supercooled PCM if movement occurs.

The method for solving the expansion and contraction of the PCM was likewise not completely solved. Integrating a flexibility of the storage chamber itself may be a solution to avoid the external expansion. This could be a flexible membrane in the top of the PCM chamber or it could be by making the PCM chamber of a material which is relatively flexible for example a plastic material. Heat exchanger tubes could enter and exit in the top of the unit above the PCM.

5. Conclusions

Cylindrical heat storage units with water and with composites of SAT were experimentally investigated. It was found that the heat exchange capacity rates for the units with PCMs were lower than for the unit with water. The heat exchange capacity rate of a unit with SAT with 0.5% Xanthan rubber and 4.4% graphite was lower compared to a unit with SAT with 6.4 % extra water during charge. This was due to limited convection in the thickened PCM and resulted in a longer charge time. One litre of paraffin oil added to the PCM chamber gave a minor improvement of the heat exchange capacity rate during charge.

The heat discharged after solidification of the supercooled SAT with extra water at ambient temperature was 177 kJ/kg in the first cycle decreasing to 140 kJ/kg after 17 test cycles. Phase separation was visually observed in the unit and the reason for the decrease. For the applied test conditions phase separation of SAT was not solved by adding extra water. Stable supercooling to ambient temperatures was achieved in 7 out of 17 test cycles of the unit with SAT with extra water. The crystallization started from the bottom of the unit by a slight shaking most likely due to the design of inner surfaces of the PCM chamber of the unit.

The heat discharged after solidification of the supercooled SAT with Xanthan rubber and graphite powder at ambient temperature was stable around 205 – 210 kJ/kg over the 40 test cycles carried out. Stable supercooling to ambient temperatures was achieved in 6 out of 40 test cycles in the unit with SAT with Xanthan rubber and graphite powder. The spontaneous crystallization started mostly from the top of the PCM. Higher discharge powers, heat exchange capacity rates and temperatures were obtained after solidification of the unit with supercooled SAT with Xanthan rubber and graphite powder compared to the unit with SAT with extra water.

Overall these investigations have shown that the principle of utilizing stable supercooling for partly loss-free heat storage can work. SAT thickened with 0.5% Xanthan rubber did not suffer from phase separation over repeated charge and discharge cycles in a unit with a height of 1.5. However, accommodating for the expansion of the PCM during melting needs further research in order to always achieve stable supercooling.

Acknowledgement

The research was partly funded by H.M. Heizkörper GmbH & Co. KG who developed the heat storage unit prototypes and partly funded by the Danish Energy Agency supporting the joint IEA SHC Task 42/ ECES Annex 29 programme on Compact Thermal Energy Storage, Grant no. 64012-0220.

References

[1] Cabeza LF, Miró L, Oró E, de Gracia A, Martin V, Krönauer A, et al. CO2 mitigation accounting for Thermal Energy Storage (TES) case studies. Appl Energy 2015;155:365–77. doi:10.1016/j.apenergy.2015.05.121.

[2] Arce P, Medrano M, Gil A, Oró E, Cabeza LF. Overview of thermal energy storage (TES) potential energy savings

and climate change mitigation in Spain and Europe. Appl Energy 2011;88:2764–74. doi:10.1016/j.apenergy.2011.01.067.

[3] Najafian A, Haghighat F, Moreau A. Integration of PCM in Domestic Hot Water Tanks: Optimization for Shifting Peak Demand. Energy Build 2015;106:59–64. doi:10.1016/j.enbuild.2015.05.036.

[4] Sharma SD, Sagara K. Latent Heat Storage Materials and Systems: A Review. Int J Green Energy 2005;2:1–56. doi:10.1081/GE-200051299.

[5] Nkwetta DN, Vouillamoz P-E, Haghighat F, El-Mankibi M, Moreau A, Daoud A. Impact of phase change materials types and positioning on hot water tank thermal performance: Using measured water demand profile. Appl Therm Eng 2014;67:460–8. doi:10.1016/j.applthermaleng.2014.03.051.

[6] Zalba B, Marín JM, Cabeza LF, Mehling H. Review on thermal energy storage with phase change: materials, heat transfer analysis and applications. Appl Therm Eng 2003;23:251–83. doi:10.1016/S1359-4311(02)00192-8.

[7] Johansen JB, Dannemand M, Kong W, Fan J, Dragsted J, Furbo S. Thermal Conductivity Enhancement of Sodium Acetate Trihydrate by Adding Graphite Powder and the Effect on Stability of Supercooling. Energy Procedia 2015;70:249–56. doi:10.1016/j.egypro.2015.02.121.

[8] Sandnes B, Rekstad J. Supercooling salt hydrates: Stored enthalpy as a function of temperature. Sol Energy 2006;80:616–25. doi:10.1016/j.solener.2004.11.014.

[9] López-Navarro A, Biosca-Taronger J, Corberán JM, Peñalosa C, Lázaro A, Dolado P, et al. Performance characterization of a PCM storage tank. Appl Energy 2014;119:151–62. doi:10.1016/j.apenergy.2013.12.041.

[10] Novo A V, Bayon JR, Castro-Fresno D, Rodriguez-Hernandez J. Review of seasonal heat storage in large basins: Water tanks and gravel-water pits. Appl Energy 2010;87:390–7. doi:10.1016/j.apenergy.2009.06.033.

[11] Nkwetta DN, Haghighat F. Thermal energy storage with phase change material - A state-of-the art review. Sustain Cities Soc 2014;10:87–100. doi:10.1016/j.scs.2013.05.007.

[12] Sharif MKA, Al-Abidi AA, Mat S, Sopian K, Ruslan MH, Sulaiman MY, et al. Review of the application of phase change material for heating and domestic hot water systems. Renew Sustain Energy Rev 2015;42:557–68. doi:10.1016/j.rser.2014.09.034.

[13] Xu J, Wang RZ, Li Y. A review of available technologies for seasonal thermal energy storage. Sol Energy 2013;103:610–38. doi:10.1016/j.solener.2013.06.006.

[14] Pinel P, Cruickshank CA, Beausoleil-Morrison I, Wills A. A review of available methods for seasonal storage of solar thermal energy in residential applications. Renew Sustain Energy Rev 2011;15:3341–59. doi:10.1016/j.rser.2011.04.013.

[15] Persson J, Westermark M. Low-energy buildings and seasonal thermal energy storages from a behavioral economics perspective. Appl Energy 2013;112:975–80. doi:10.1016/j.apenergy.2013.03.047.

[16] Colclough S, McGrath T. Net energy analysis of a solar combi system with Seasonal Thermal Energy Store. Appl Energy 2015;147:611–6. doi:10.1016/j.apenergy.2015.02.088.

[17] Dannemand M, Schultz JM, Johansen JB, Furbo S. Long term thermal energy storage with stable supercooled sodium acetate trihydrate. Appl Therm Eng 2015;91:671–8. doi:10.1016/j.applthermaleng.2015.08.055.

[18] Lane GA. Solar heat storage latent heat material Vol 1. Boca Raton, Florida, United States: CRC; 1983.

[19] Kimura H, Kai J. Phase change stability of sodium acetate trihydrate and its mixtures. Sol Energy 1985;35:527–34. doi:10.1016/0038-092X(85)90121-5.

[20] Cabeza LF, Svensson G, Hiebler S, Mehling H. Thermal performance of sodium acetate trihydrate thickened with different materials as phase change energy storage material. Appl Therm Eng 2003;23:1697–704. doi:10.1016/S1359-4311(03)00107-8.

[21] Furbo S, Svendsen S. Report on heat storage in a solar heating system using salt hydrates. Kgs. Lyngby,

Denmark: 1977.

[22] Farid MM, Khudhair AM, Razack SAK, Al-Hallaj S. A review on phase change energy storage: materials and applications. Energy Convers Manag 2004;45:1597–615. doi:10.1016/j.enconman.2003.09.015.

[23] Meisingset KK, Grønvold F. Thermodynamic properties and phase transitions of salt hydrates between 270 and 400 K III. CH3CO2Na·3H2O, CH3CO2Li·2H2O, and (CH3CO2)2Mg·4H2O. J Chem Thermodyn 1984;16:523–36. doi:10.1016/0021-9614(84)90003-X.

[24] Sun X, Zhang Q, Medina MA, Lee KO. Experimental observations on the heat transfer enhancement caused by natural convection during melting of solid–liquid phase change materials (PCMs). Appl Energy 2016;162:1453–61. doi:10.1016/j.apenergy.2015.03.078.

[25] Ryu HW, Woo SW, Shin BC, Kim SD. Prevention of supercooling and stabilization of inorganic salt hydrates as latent heat storage materials. Sol Energy Mater Sol Cells 1992;27:161–72. doi:10.1016/0927-0248(92)90117-8.

[26] Garay Ramirez BML, Glorieux C, Martin Martinez ES, Flores Cuautle JJA. Tuning of thermal properties of sodium acetate trihydrate by blending with polymer and silver nanoparticles. Appl Therm Eng 2013;61:838–44. doi:10.1016/j.applthermaleng.2013.09.049.

[27] Hu P, Lu D-J, Fan X-Y, Zhou X, Chen Z-S. Phase change performance of sodium acetate trihydrate with AlN nanoparticles and CMC. Sol Energy Mater Sol Cells 2011;95:2645–9. doi:10.1016/j.solmat.2011.05.025.

[28] Shin HK, Park M, Kim H-Y, Park S-J. Thermal property and latent heat energy storage behavior of sodium acetate trihydrate composites containing expanded graphite and carboxymethyl cellulose for phase change materials. Appl Therm Eng 2015;75:978–83. doi:10.1016/j.applthermaleng.2014.10.035.

[29] Dannemand M, Dragsted J, Fan J, Johansen JB, Kong W, Furbo S. Experimental investigations on prototype heat storage units utilizing stable supercooling of sodium acetate trihydrate mixtures. Appl Energy 2016;169:72–80. doi:10.1016/j.apenergy.2016.02.038.

[30] Dannemand M, Kong W, Fan J, Johansen JB, Furbo S. Laboratory Test of a Prototype Heat Storage Module Based on Stable Supercooling of Sodium Acetate Trihydrate. Energy Procedia, vol. 70, Elsevier B.V.; 2015, p. 172–81. doi:10.1016/j.egypro.2015.02.113.

[31] Medrano M, Yilmaz MO, Nogués M, Martorell I, Roca J, Cabeza LF. Experimental evaluation of commercial heat exchangers for use as PCM thermal storage systems. Appl Energy 2009;86:2047–55. doi:10.1016/j.apenergy.2009.01.014.

[32] Chiu JNW, Martin V. Submerged finned heat exchanger latent heat storage design and its experimental verification. Appl Energy 2012;93:507–16. doi:10.1016/j.apenergy.2011.12.019.

[33] Sari A, Karaipekli A. Thermal conductivity and latent heat thermal energy storage characteristics of paraffin/expanded graphite composite as phase change material. Appl Therm Eng 2007;27:1271–7. doi:10.1016/j.applthermaleng.2006.11.004.

[34] Kousksou T, Bruel P, Jamil A, El Rhafiki T, Zeraouli Y. Energy storage: Applications and challenges. Sol Energy Mater Sol Cells 2014;120:59–80. doi:10.1016/j.solmat.2013.08.015.

[35] Py X, Olives R, Mauran S. Paraffin/porous-graphite-matrix composite as a high and constant power thermal storage material. Int J Heat Mass Transf 2001;44:2727–37. doi:10.1016/S0017-9310(00)00309-4.

[36] Mills A, Farid M, Selman JR, Al-Hallaj S. Thermal conductivity enhancement of phase change materials using a graphite matrix. Appl Therm Eng 2006;26:1652–61. doi:10.1016/j.applthermaleng.2005.11.022.

[37] Zhang P, Xiao X, Ma ZW. A review of the composite phase change materials: Fabrication, characterization, mathematical modeling and application to performance enhancement. Appl Energy 2016;165:472–510. doi:10.1016/j.apenergy.2015.12.043.

[38] Dannemand M, Johansen JB, Furbo S. Solidification Behavior and Thermal Conductivity of Bulk Sodium Acetate Trihydrate Composites with Thickening Agents and Graphite. Sol Energy Mater Sol Cells 2016;145:287–95. doi:10.1016/j.solmat.2015.10.038.

[39] Industrie anzeiger n.d. http://www.industrieanzeiger.de/technik/-/article/32571342/37619152 (accessed October 22, 2015).

[40] Lane G. Solar heat storage latent heat material Vol 2. Boca Raton, Florida, United States: CRC; 1986.

[41] Furbo S. Heat Storage for Solar Heating Systems, Educational Note, ISSN 1396-4046. Kgs. Lyngby, Denmark: BYG.DTU; 2005.

[42] Cengel YA. Heat Transfer: A Practical Approach. 2nd ed. McGraw-Hill; 2003.

[43] Araki N, Futamura M, Makino A, Shibata H. Measurements of Thermophysical Properties of Sodium Acetate Hydrate. Internaltional J Thermophys 1995;16:1455–66. doi:10.1007/BF02083553.

[44] Rogerson MA, Cardoso SSS. Solidification in Heat Packs : III . Metallic Trigger. AIChE J 2003;49:522–9. doi:10.1002/aic.690490222.

Paper 5 - Experimental investigations on heat content of supercooled sodium acetate trihydrate by a simple heat loss method

Weiqiang Kong, Mark Dannemand, Jakob Berg Johansen, Jianhua Fan, Janne Dragsted, Gerald Englmair, Simon Furbo

Draft / Submitted to Solar Energy Materials and Solar Cells

Experimental investigations on heat content of supercooled sodium acetate trihydrate by a simple heat loss method

Weiqiang Kong*, Mark Dannemand, Jakob Berg Johansen, Jianhua Fan, Janne Dragsted, Gerald Englmair, Simon Furbo

Technical University of Denmark, Department of Civil Engineering, Kgs. Lyngby 2800, Denmark

Abstract

Sodium acetate trihydrate is a phase change material that can be used for long term heat storage in solar heating systems because of its relatively high heat of fusion, a melting temperature of 58˚C and its ability to supercool stable. In practical applications sodium acetate trihydrate tend to suffer from phase separation which is the phenomenon where anhydrous salt settles to the bottom over time. This happens especially in supercooled state. The heat released from the crystallization of supercooled sodium acetate trihydrate with phase separation will be lower than the heat released from sodium acetate trihydrate without phase separation. Possible ways of avoiding or reducing the problem of phase separation were investigated. A wide variety of composites of sodium acetate trihydrate with additives including extra water, thickening agents, solid and liquid polymers have been experimentally investigated by a simple heat loss method. The aim was to find compositions of maximum heat released from the crystallization of supercooled sodium acetate trihydrate samples at ambient temperature. It was found that samples of sodium acetate trihydrate with 0.5% to 2% (wt.%) Carboxy-Methyl Cellulose, 0.3% to 0.5 % (wt.%) Xanthan Gum or 1% to 2% (wt.%) of some solid or liquid polymers as additives had significantly higher heat contents compared to samples of sodium acetate trihydrate suffering from phase separation.

Keywords: Sodium acetate trihydrate, Supercooling, Heat content measurement, Phase separation, Phase change material

1. Introduction

Solar energy along with other renewable energy sources can play an important role in clean energy utilization in modern society. However, solar energy has the characteristic of being intermittent on a daily basis and has an uneven seasonal distribution. Heat storage is one possible and effective way of solving the mismatch between heat demand and solar energy supply. Solar energy systems combined with long term heat storage are being widely studied in many projects. For example in the four EU funded projects SAM.SSA [2], MERITS [3], SOTHERCO [4], COMTES [5], and in IEA SHC Task 42 [6] and IEA ECES Annex 29 [7]. Phase change materials (PCMs) are considered as promising heat storage materials due to their latent heat of fusion which can possibly increase storage density compared to sensible heat storages. In some PCMs the latent heat of fusion can be preserved without heat loss for a long term storage period via the principle of stable supercooling [8–10].

Sodium acetate trihydrate (SAT), $NaCH_3COO \cdot 3H_2O$, consisting of 60.3% (wt.%) sodium acetate and 39.7% (wt.%) water, has the ability to supercool stable to ambient temperatures and has relatively high latent heat of fusion of 264 kJ/kg at the melting temperature of 58˚C [8]. Once the solidification of the supercooled SAT is activated the latent heat of fusion from the phase change will be released. This energy can be used for space heating and domestic hot water preparation. The ways of activating the solidification are easy and flexible such as cooling a part of the SAT to its maximum degree of

supercooling by either evaporating liquid CO_2 [11] or by a Peltier element cooling or by mechanically introducing a seed crystal. Therefore SAT is a promising phase change material which can be used for long term heat storage.

Fig. 1(a) shows one sample of supercooled sodium acetate water mixtures which have been in supercooled state for more than 2 years at indoor temperatures. Even impurities such as rusty iron immersed in the supercooled sodium acetate water mixture did not influence the stability of the supercooling, as can be seen in Fig. 1(b).

Phase separation/segregation is a key problem of using SAT for heat storage. It causes the heat content of the supercooled SAT to decrease over time. It is caused by the fact that SAT is an incongruently melting salt hydrate. An incongruently melting salt hydrate consists of an anhydrous salt with corresponding crystal water. The solubility of the anhydrous salt in water, which is given in [12] is not high enough at the melting point of 58 °C to dissolve all the anhydrous salt in the corresponding crystal water of the trihydrate composition. Therefore the molten salt hydrate at a temperature just above the melting point consists of a saturated salt solution and some anhydrous salt undissolved in the water [13]. When nothing is done to prevent it, the anhydrous salt settles to the bottom of the container as sediments due to its higher density, which can be seen in Fig. 1(a). In supercooled state below the melting point, even less anhydrous salt will be dissolved and the problem increases. This can be realized by observing the phase diagram for the sodium acetate - water system [14]. When the crystallization of a sample is initiated, the anhydrous salt at the bottom is unable to bind with the water in the top of the container. Therefore only a part of the anhydrous salt is active during phase change. The solidified salt hydrate with phase separation consists of three parts: At the bottom the solid salt hydrate crystals with additional anhydrous salt, in the middle a layer of salt hydrate crystals, and at the top the salt hydrate crystals with some additional water in which the some salt dissolves in. The amount of sediment increases with repeated cycles, and the heat storage capacity will therefore decrease with each melting/crystallization cycle. Therefore phase separation has to be avoided.

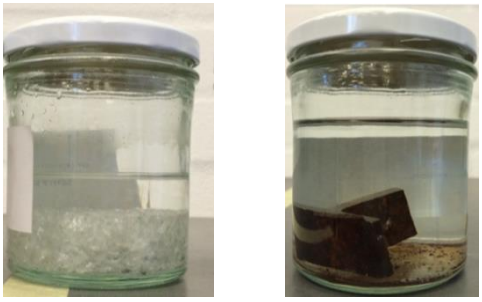

(a) (b)

Fig. 1. Long term supercooled samples of (a) SAT with extra water (b) SAT with extra water and immersed steel

Different possible ways of avoiding or reducing phase separation were investigated in previous studies. For example, the problem does not occur for the incongruently melting Glauber's salt, $Na_2SO_4 \cdot 10H_2O$, if the height of the container is smaller than 0.9 cm according to Kaufmann [15]. Glauber's salt has a much larger difference between the salt solubility at the melting point and the content of anhydrous salt in the salt hydrate compared to the difference between the salt solubility at the melting point and the content of anhydrous salt in SAT. Therefore, it could be possible that a low material height can avoid phase separation. Adding extra water is suggested a way to avoid phase separation and was studied by Furbo and

Svendsen [12]. The stored energy in SAT with extra water has however shown to decrease after a number of cycles in tests with prototype heat storage units with a PCM height of 5 cm [16][17]. Phase separation can also be reduced by adding thickening agents which were widely investigated in the literature. Peng Hu et al. [18] presented the mixture of SAT with 4% Carboxy-Methyl Cellulose (CMC) as thickening agent and 5% AIN nanoparticles as nucleating agent which had a high latent heat and avoids the supercooling. Similarly, Garay Ramirez et al. [19] used 0.5% AgNPs to reduce the supercooling and mixing silica gel with CMC to avoid phase separation and yielded an increment in the stability of the phase change behaviour. Nearly 95% of the latent heat of SAT was recovered in this study. In a study by Cabeza et al. [20], bentonite, starch and Cellulose were investigated for the thickening effect on SAT and they found an enthalpy decrease between 20% and 35% depending on the type and amount of thickening agents used. In a study by Ryu et al. [21], a super-absorbent polymer (SAP) made from acrylic acid copolymer and CMC-Na was investigated as thickening agent to avoid phase separation, together with K_2SO_4 as the nucleating agent. The combination of SAT with 1% SAP, 2% CMC-Na and 2% K_2SO_4 was used in a study by Choi et al. of heat storage systems [22].

Studies [18–22] focused on short term heat storage in which supercooling of the storage materials have to be avoided. Therefore nucleating agents which reduce the degree of supercooling were used in those studies. For seasonal heat storage using the principle of stable supercooling nucleating agents should be avoided

Suggested ways of reducing phase separation can be summarized in the following ways:

- Low height of material
- Adding extra water
- Adding thickening agent

Differential thermal analysis (DTA) and differential scanning calorimetry (DSC) methods [23] are conventional method for determining the latent heat of fusion and the specific heat of PCMs. However, DTA and DSC measurement facilities are complicated and expensive and the tested samples are usually very small (1-10 mg), which does not represent the bulk PCMs in actual storages [8]. Zhang et al. [24] proposed the T-history method, as a simple alternative to the DTA and DSC methods, to determine the melting point, heat of fusion, specific heat and thermal conductivity of the bulk PCMs with additives in a sealed tube. The T-history method was then widely recognized and used in studies. Further modification and improvement for the T-history method were proposed by researchers in order to remove unstable phase change, enhance the measurement accuracy and enlarge the range of applications [25–27].

In this study, a simple heat loss method was used to determine the heat contents of mixtures with supercooled SAT by measuring the heat released after the solidification of the supercooled SAT samples at ambient temperature with and without additives. This way of measuring the heat content represents how the storage material is used in a real application using the principle of stable supercooling for long term heat storage. The results are considered to be precise enough to be used for comparison of different combinations of SAT and additives and to find mixtures with high heat contents.

2. Method

2.1. Materials

Possible additives for reducing phase separation including extra water, thickening agents, solid and liquid polymers are investigated. All the mass of additives in the following paragraphs is given in weight percentage.

The following materials were used:

Sodium acetate trihydrate (analytical degree, purity>99%) produced by Shijiazhuang Haosheng Chemical Co. Ltd in China.

A variety of additives were tested including,

- Thickening agents provided as samples by the company of CP Kelco
  - Carboxymethyl Cellulose (CMC) under the product name CEKOL® 30000
  - Xanthan Gum (X-Gum) under the product name Keltrol® Advance Performance Carboxy-Methyl

The thickening agents are widely used in the food industry. The thickening agents increase the viscosity of the SAT and thereby possibly suspend the anhydrous salt in the container so that phase separation is reduced or avoided.

A selection of other additives with various effects on the phase separation was investigated. Effect on some of the additives could be to increase the solubility of anhydrous sodium acetate in crystal water.

- Acid modifier, tartaric acid (CAS number: 526-83-0)
- Glycerol ($C_3H_5(OH)_3$) (CAS number: 56-81-5)
- Chelating agent, EDTA, Disodium Ethylenediaminetetraacetic acid (CAS number: 139-33-3)
- Solid polymer AMPS, 2-Acrylamido-2-methylpropane sulfonic acid (CAS number: 15214-89-8)
- AquaKeep (10SH-NF) produced by SUMITOMO SEIKA Chemicals Co., Ltd.
- Liquid polymers HD 200 (PH: 4.5), HD 310 (PH: 4.0) and HD 500 (PH: 4.0) are liquid polymers with different lengths of molecular chains provided by Suzhou Hongde Co., Ltd. Jiangsu, China.

2.2. The simple heat loss method

The main assumption of the method is that the heat loss coefficient *UA* (W/K) of the glass jar in a well-insulated box can be determined by having hot water in the glass jar with known properties for cool down in the box towards ambient temperature. The heat content of SAT mixtures cooling down after solidification from supercooled state could then be calculated by applying the heat loss coefficient.

Glass jars with metal lids were used to contain the samples as shown in Fig. 2(a). The glass jars were placed in well insulated boxes after solidification of the SAT mixture; see Fig. 2(b). There were four thermocouple (Type T) temperature sensors for each box. Three of them were fixed outside of glass jar for measuring the temperature of the sample, see Fig. 2(c) and the fourth to measure the ambient temperature nearby.

(a) (b) (c)

Fig. 2 (a) Glass jar with lid (b)The well-insulated box (c) Locations of temperature sensors

The heat loss process can be described by the differential equation of Eq. (1). After solving Eq. (1), a logarithmic equation was derived for calculating *UA*, see Eq. (2).

$$mc\frac{dT}{dt} = -UA\cdot(T - T_a) \tag{1}$$

$$UA = \frac{mc}{\Delta t}\ln\frac{T_e - T_a}{T_b - T_a} \tag{2}$$

Where *mc* (J/K) is the total heat capacity of the reference consisting of glass, water and lid, *T* (K) is water temperature, T_b (K) and T_e (K) are start and end temperature of water, T_a (K) is ambient temperature, *t* (s) is time and Δt (s) is time period.

The *UA* value calculated by Eq. (2) is the average heat loss coefficient of the temperature range from T_b to T_e. The *UA* values were obtained for all temperature steps, a continuous *UA* curve was regressed by the scatter of *UA* values. A quadratic equation described the *UA* development.

The test procedure can be summarized as follows:

1. The heat loss coefficient of each box was determined by having the water reference cool down from 70 °C to ambient temperature.
2. The SAT samples were fully melted in the glass jars and then cooled down to ambient temperature leaving them in supercooled state.
3. The samples were placed in the boxes and the solidification was initiated by dropping a SAT crystal into them. The temperature development during the cooling process was recorded.
4. The heat contents *E* (kJ/kg) of the SAT samples were determined by using the heat loss coefficient and the recorded temperatures. See Eq. (3), where T_s is the SAT sample average temperature, *m* is the mass of the SAT sample.

$$E = \int_t^{t+\Delta t} UA(t)\cdot[T_s(t) - T_a(t)]\cdot dt / m \tag{3}$$

Fig. 3 shows the temperature development of a SAT sample cooling down to ambient temperature to supercooled state followed by activation of solidification and the cooling down to ambient temperature again. The green area is the heat content measured by this simple heat loss method.

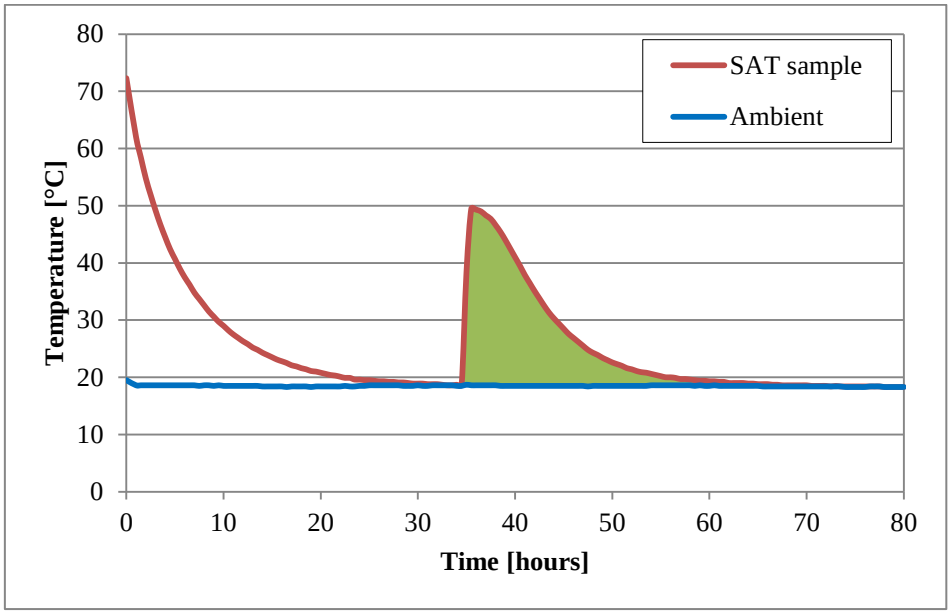

Fig. 3. An example of cooling process of PCM

2.3. Samples preparation

The heat content measurements were carried out with SAT and three types of additives; (1) different quantities of extra water, (2) thickening agents and (3) other polymer additives. All the samples were prepared with a height of 5 cm in liquid phase. All heat content results (kJ/kg) were calculated by considering the total mass of SAT including additives.

SAT contains approximately 40% water. Samples of sodium acetate water mixtures with the water content of 40% (205g SAT), 42% (196g SAT+7.8g water), 45% (185g SAT+17.8g water) and 46% (180g SAT+21g water) were prepared. Three repetitions of each sodium acetate water mixtures, in total of 12 samples, were made.

Samples of 200 g SAT with 0.1% to 2% CMC and Xanthan Gum were prepared. A proper mixing method was necessary for adding thickening agents into the SAT, especially Xanthan Gum. The Xanthan Gum powder binds very fast with the water when it is mixed into a sample and will easily form jelly chunks in the sample instead of dispersing evenly in the sample. To achieve uniformly mixed samples 90% of the SAT was melted in an oven, the remaining 10% of the SAT was in cold solid granular state mixed with the thickening agent powder before it was added to the melted SAT little by little while mixing with an overhead mixer. Mixing at hot state will easily trap unwanted air bobbles inside the mixture therefore the mixing was done carefully to avoid this [28].

Samples of 200 g SAT with different quantities of liquid or solid polymers were prepared. The liquid or solid polymers were added little by little into the melted SAT while stirring with an electronic stirrer.

2.4. Relating of the latent heat of fusion to the heat content

The heat content of a supercooled SAT sample is defined in this paper as the thermal energy dispersed to the ambient environment by the natural cooling process towards the ambient temperature after solidification of the supercooled SAT sample at ambient temperature. (The green area in Fig.3)

The definition of the latent heat of fusion is the enthalpy change resulting from heating a given quantity of a substance to change its state from a solid to a liquid at the temperature of the melting point [29].

The latent heat of fusion at the melting point is therefore somewhat different but related to the heat content of a supercooled sample. The heat loss method measures the heat content.

The following theory [17] explains the theoretical heat content of SAT in a simplified way as if the SAT behaves as an ideal compound which changes from solid to liquid phase at a specific melting temperature.

Eq. (4) and Eq. (5) show the theoretical change of thermal energy over a temperature increase where the melting temperature is passed for a heating and a cooling process.

$$E_{heating} = (T_{melt} - T_{start}) \cdot c_p(s) + L + (T_{\max} - T_{melt}) \cdot c_p(l) \tag{4}$$

$$E_{cooling} = (T_{\max} - T_{melt}) \cdot c_p(l) + L + (T_{melt} - T_{end}) \cdot c_p(s) \tag{5}$$

where T_{melt} is the melting point of 58 °C, T_{start} is the PCM temperature at the start of the charge, $c_p(s)$ is the specific heat of SAT in solid phase, $c_p(l)$ is the specific heat of SAT in liquid phase, L is the heat of fusion, T_{max} is the maximum temperature the PCM during heating, T_{end} is the temperature the PCM after the cooling.

When the SAT cools down to T_{end} without crystalizing, assuming that the specific heat of the supercooled SAT has the same properties as the liquid SAT, then the stored thermal energy in the supercooled PCM is:

$$E_{supercooled} = E_{heating} - c_p(l) \cdot (T_{\max} - T_{end}) \tag{6}$$

If T_{start} and T_{end} are equal, then $E_{heating}$ and $E_{cooling}$ are also equal. When the temperature of the supercooled SAT and the end temperature are the same, then the thermal energy stored at supercooled state is:

$$E_{supercooled} = L - (T_{melt} - T_{end}) \cdot [c_p(l) - c_p(s)] \tag{7}$$

The heat content measured by the heat loss method is theoretically $E_{supercooled}$ (Eq. (7)). Assuming that T_{end} is 20 °C, the latent heat of fusion is 264 kJ/kg, the heat capacity $c_p(l)$ and $c_p(s)$ are 2.8 kJ/(kg·K) and 1.9 kJ/(kg·K), respectively [14]. The theoretical heat content of SAT at 20 °C is calculated to 230 kJ/kg. The heat content at the supercooled state is lower than the latent heat of fusion due to the different heat capacities of the liquid and the solid state of the material and depends on the supercooled and end temperature of the SAT sample.

2.5. Error analysis

The error between measured heat content and the theoretical heat content mainly comes from two parts.

The first error is from the change of ambient temperature during the test. During one test, the variation of ambient temperature was within 0.5 K. The difference of the ambient temperature and thereby the sample temperature between summer and winter was up to 7 K. Assuming that $c_p(l)$ is the specific heat capacity of the supercooled SAT and $c_p(s)$ is the

specific heat capacity of SAT in solid state and the two heat capacities are constant when the ambient temperature changes 7 K. The theoretical heat content is 230 kJ/kg. The relative error of this term can be estimated as

$$\frac{\Delta Q}{E} = \frac{[c_p(l) - c_p(s)]\Delta T_{end}}{E} = \frac{(2.8 - 1.9)\cdot 7}{230} = 2.3\% \quad (8)$$

The second error comes from the temperature measurement method. The average temperature of three temperature sensors fixed outside of glass jar for representing the sample temperature was lower than the actural material temperature. The error can be estimated by the Biot number (*Bi*) for long cylinder heat exchange object which is shown in Eq. (9), in which h (W/m^2·K) is the surface heat loss coefficient, R is the cylinder diameter and λ (W/m·K) is the thermal conductivity of SAT/additives. h can be calculated by UA/A_s, where A_s is the surface area. Since UA is a function of temperature varying around 0.029-0.035 from 20 °C to 55 °C and λ has a value from literature with large variations 0.17-1.1[28], the Biot number can be calculated as a range of 0.04-0.34 which is shown in Eq. (9). In theory, only if the Biot number is smaller than 0.05, the outside average temperature can represent the whole sample temperature [30].

$$Bi = \frac{hR}{2\lambda} = \frac{UA/A_s \cdot R}{2\lambda} = \frac{(0.029 \sim 0.034)/0.01 \cdot 0.034}{2(0.17 \sim 1.1)} = 0.04 \sim 0.34 \quad (9)$$

However, the aim of using the heat loss method was to compare the heat contents of different SAT/additives samples and to find the additives which can best reduce phase separation. Therefore the precision of the heat loss method was assumed be sufficient. The heat loss method is simple regarding both test facility and calculation process. In addition, practical handling of the samples and additives at this scale is easy and phenomena which may happen in full size applications can be observed.

3. Results

The heat contents measured by the simple heat loss method for samples of SAT with extra water, SAT with thickening agents and SAT with polymer additives are presented in the following subsections. All results are shown in specific heat content values. The masses used in calculations are for total PCM mass including SAT and additives.

3.1. Heat content measurement of SAT with extra water

The 40%, 42%, 45% and 46% water content SAT-water samples were tested with different durations of the supercooled period: Less than 14 days, 41 days and 100 days. The tests with the period of less than 14 days were repeated three times. Fig. 4 shows the samples after 100 days of supercooling. It can be seen from the figure that both the 40% and 42% samples have a visible salt crystal layer at the lower part of the sample. The crystal layer of the 42% sodium acetate water mixture appeared looser compared to the 40% mixture. Both the mixtures of 45% and 46% were transparent without any visible segregation.

Fig. 4. The 40%, 42%, 45% and 46% salt water mixtures from right to left after 100 days supercooling

The measured heat contents are plotted in Fig. 5. It can be seen from the figure that:

- For the short supercooled periods, the 42% mixture had the highest heat content of 194 kJ/kg.
- With a supercooled period of 41 days, the heat content for the 42% mixture was reduced to 162 kJ/kg, while the heat content for the other mixtures were almost the same as for the short supercooled periods.
- For the samples which were supercooled for 100 days, the heat content of both the 40% and 42% mixtures were lower than for the short supercooled period. The heat content of the 45% and 46% mixtures were not further decreased.

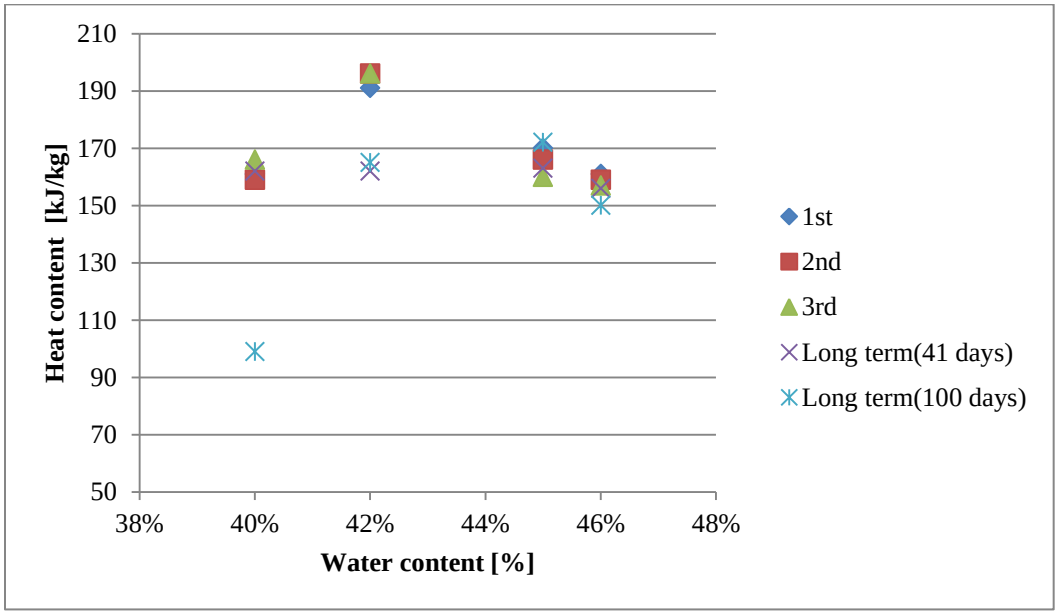

Fig. 5. Heat content of the 40%, 42%, 45% and 46% water salt mixtures

3.2. Heat content measurement of SAT with thickening agent

Table 1 and Table 2 show the measured heat content for SAT with different quantities of Xanthan Gum and CMC. The heat content of SAT with 0.1% and 0.2% Xanthan Gum was 183-195 kJ/kg.. SAT samples with 0.3% - 0.5% Xanthan Gum

had the highest heat contents with an average of 214 kJ/kg. Samples with 1% to 2% Xanthan Gum had heat contents of 204-208 kJ/kg

The heat contents of SAT with CMC were for all mixtures above 200 kJ/kg. Samples with 0.3% and 2% CMC had heat contents of 213-216 kJ/kg which was a slight improvement compared to SAT with 0.1% to 0.2% CMC.

Table 1. Heat content of SAT with different quantities of Xanthan Gum

SAT	Heat content (kJ/kg)				SAT	Heat content (kJ/kg)			
	1st	2nd	3rd	Average		1st	2nd	3rd	Average
+ 0.1% X-Gum	179	185	184	183	+ 0.5% X-Gum	213	216	214	214
+ 0.2% X-Gum	196	196	192	195	+ 1.0% X-Gum	205	214	205	208
+ 0.3% X-Gum	213	217	214	215	+ 1.5% X-Gum	205	208	204	206
+ 0.4% X-Gum	210	217	215	214	+ 2.0% X-Gum	208	206	206	207

Table 2. Heat content of SAT with different quantities of CMC

SAT	Heat content (kJ/kg)				SAT	Heat content (kJ/kg)			
	1st	2nd	3rd	Average		1st	2nd	3rd	Average
+ 0.1% CMC	194	201	206	200	+ 0.5% CMC	208	210	217	212
+ 0.2% CMC	208	212	209	210	+ 1.0% CMC	209	212	211	211
+ 0.3% CMC	210	215	214	213	+ 1.5% CMC	211	213	214	213
+ 0.4% CMC	216	216	207	213	+ 2.0% CMC	219	215	215	216

Table 3 shows the heat content of 42% SAT/water mixtures with 0.1% to 0.4% CMC. The average heat content was around 190 kJ/Kg which was similar to the heat content of 42% salt water mixture without additives and far below the heat content of SAT with 0.1% to 0.4% CMC.

Table 3. Heat contents of 42% water content salt water mixture with 0.1% to 0.4 % CMC

42% water content salt water mixture	Heat content (kJ/kg)		
	1st	2nd	3rd
+ 0.1% CMC	198	200	186
+ 0.2% CMC	187	193	192
+ 0.3% CMC	189	191	187
+ 0.4% CMC	188	189	195

3.3. Heat content measurement of SAT with polymer additives

It was found that glycerol, AquaKeep and tartaric acid had limited effect on increasing the heat content of SAT/additive mixtures, see Table 4. The heat content of SAT/glycerol, SAT/ AquaKeep and SAT/tartaric was up to 164 kJ/kg, 201 kJ/kg and 185 kJ/kg, respectively.

Table 4. Heat content of SAT with different quantities of Glycerol, Aquakeep and Tartaric acid

SAT	Heat content (kJ/kg)	SAT	Heat content (kJ/kg)
+1% Glycerol	161	+1.5%Aquakeep+3% H_2O	192
+2% Glycerol	161	+2%Aquakeep+3% H_2O	201
+2% Glycerol +1% H_2O	162	+1%Tartaric acid	166
+3% Glycerol +1% H_2O	164	+2%Tartaric acid	172
+0.5%Aquakeep	191	+1%Tartaric acid+4% H_2O	185
+1%Aquakeep	193	+2%Tartaric acid+2% H_2O	176
+0.5%Aquakeep+2% H_2O	188	+2%Tartaric acid+6% H_2O	162
+1%Aquakeep+3% H_2O	201	+4%Tartaric acid+6% H_2O	166

The solid additives EDTA, AMPS and the liquid polymer HD 200, HD 310 and HD 500 significantly increased the heat content of SAT/additive mixtures compared to SAT without additives. Typically an increase of 30% of heat content was observed. Through the heat content experiments with different compositions of SAT and additive mixtures it was found that SAT with 1% to 2% polymer additives had heat contents of up to 216 kJ/kg. Selected promising polymer additives and the results are listed in Table 5. Some samples of SAT with EDTA or HD had heat contents higher than 210 kJ/kg.

Table 5. Heat contents of SAT with 1% or 2% polymer additives

SAT	Heat content (kJ/kg)			
	1st	2nd	3rd	Average
+ 1% EDTA	214	215	218	216
+ 2% EDTA	213	212	221	215
+ 1% AMPS	205	207	206	206
+ 2% AMPS	205	204	205	205
+ 2% HD 200	217	216	216	216
+ 2% HD 310	215	215	217	216
+ 2% HD 500	212	212	215	213

Table 6 shows the heat contents of SAT with polymer additives and extra water. It can be seen from the table that the samples of SAT with polymer additives and extra water had lower heat contents than the samples of SAT with polymer additives in Table 5 but higher heat content compared to samples of SAT with phase separation and SAT with extra water.

Table 6. Heat contents of SAT with polymer additives with extra water

SAT	Heat content (kJ/kg)		
	1st	2nd	3rd
+3% EDTA + 4% H2O	203	203	-
+3%AMPS + 2% H2O	197	200	-
+2.6% HD200 +1.7% H2O	200	198	196
+2% HD310 +1.9% H2O	200	199	200
+2.6% HD500 +1.5% H2O	203	200	201

4. Discussion

Fig. 6 gives an overview of all results of heat content ranges for the SAT samples with different additives. The first column is the heat content of SAT suffering from phase separation, followed by SAT with extra water, thickening agents CMC and X-Gum, and the solid and liquid additives presented in section 2.1. Each column represents the heat contents of the tested samples. The blue part of the column is the lowest heat content and the red part is the measured heat content fluctuation which was caused by different quantities of additives in SAT.

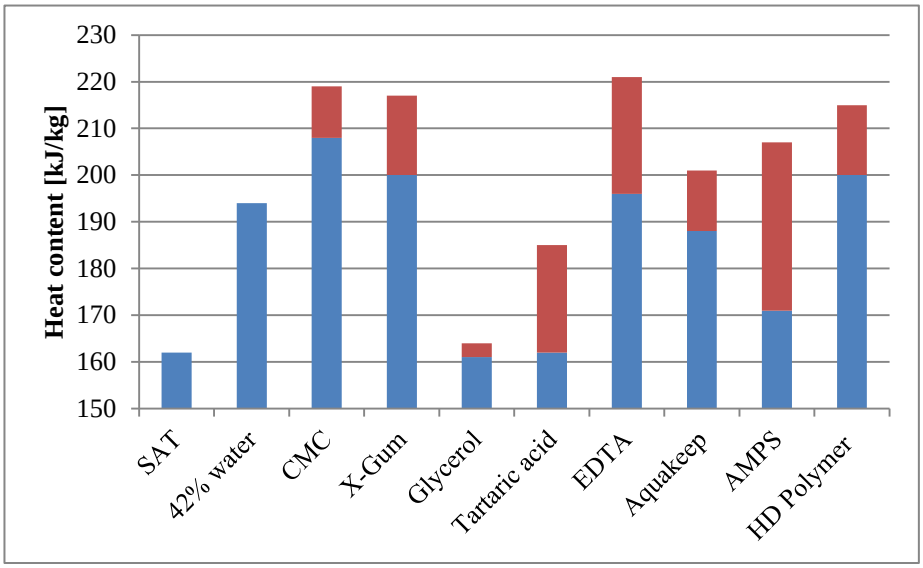

Fig. 6. Full scope of measured heat contents of SAT with and without different additives

Adding extra water into SAT is the easiest way to reduce phase separation since all the sodium acetate can be dissolved in water. However, in comparison of results it can be seen that the heat content of SAT-water (up to 194 kJ/kg) was lower compared to other SAT-additive compositions.

Adding thickening agents into SAT is an effective way of reducing phase separation by increasing the viscosity of SAT solution. The optimal ration of SAT and thickening agent should be investigated.

The solid and liquid polymer materials also showed to increase the heat content of SAT-polymer mixtures but the working principle is not clear. They do not increase the viscosity of the PCM as the thickening agents does. One theory is that the polymer materials increases the solubility of anhydrous sodium acetate in the water and in such a way that phase separation is avoided. Another theory could be that the chelating effect from EDTA which may keep anhydrous salt dissolved in the solution by its hexadentate (“six-toothed”) structure resulting in an increased solubility.

5. Conclusions

The heat content measurements for samples of SAT with a height of 5 cm in liquid phase with different additives have been carried out in order to elucidate how best to reduce the phase separation and maximize the heat content for SAT composites in supercooled state.

The theoretical heat content of supercooled SAT at 20 °C was calculated to be 230 kJ/kg by applying the latent heat of fusion of 264 kJ/kg, the liquid and solid heat capacity of 2.8 kJ/(kg·K) and 1.9 kJ/(kg·K). Based on heat content measurements, the heat released after solidification of a supercooled sample of SAT without additives was 162 kJ/kg. The lower value is due to the phase separation in the SAT.

For samples with extra water, the highest measured heat content of 194 kJ/kg was in the SAT-water mixture with 42% water. It was found that SAT and SAT-water mixtures with water contents lower than or equal to 42% suffered from phase separation. SAT-water mixtures with water contents higher than 42% did not suffer from the phase separation under the tested conditions. However, the heat content of SAT-water mixtures was decreased by the extra water and by a long supercooled period.

Adding thickening agents was an efficient way to reduce phase separation and thereby increase the energy released from heat storage material. SAT with 0.5-2% CMC and SAT with 0.3-0.5% Xanthan Gum properly dispersed in the sample are promising seasonal heat storage materials which had heat contents of about 30% higher than SAT with phase separation. Experiments showed that the heat contents of SAT with thickening agents were up to 216 kJ/kg.

The solid polymer materials EDTA and AMPS and the liquid polymer material HD series are also potential additives for SAT based heat storage materials since the SAT-polymer compositions had heat contents above 200 kJ/kg. The heat contents of SAT with 1% to 2% EDTA, AMPS, HD polymers were between 205-216 kJ/kg.

All in all, the optimal SAT and additive composite should be carefully selected and tested for cycling stability in order to find the best performing SAT composite for heat storage applications.

ACKNOWLEDGEMENT

This project was co-funded by the European Commission as part of the Seventh Framework Programme of the European Community for Research, Technological Development and Demonstration Activities under the funding scheme of “Collaborative Project” through the COMTES consortium and H.M. Heizkörper GmbH & Co. KG.

References

[1] W. van Helden, COMTES: Combined development of compact seasonal thermal energy storage technologies, RHC Conf. (2013).

[2] SAM.SSA, http://samssa.eu/.

[3] MERITS, http://www.merits.eu/.

[4] SOTHERCO, http://cordis.europa.eu/project/rcn/107960_en.html.

[5] COMTES, http://cordis.europa.eu/project/rcn/103641_en.html.

[6] IEA SHC Task 42, http://task42.iea-shc.org/.

[7] IEA ECES Annex 29, http://www.iea-eces.org/annexes/ongoing-annexes.html.

[8] B. Zalba, J.M. Marin, L.F. Cabeza, H. Mehling, Review on thermal energy storage with phase change: materials, heat transfer analysis and applications, Appl. Therm. Eng. 23 (2003) 251–283. doi:10.1016/s1359-4311(02)00192-8.

[9] T. Kousksou, P. Bruel, a. Jamil, T. El Rhafiki, Y. Zeraouli, Energy storage: Applications and challenges, Sol. Energy Mater. Sol. Cells. 120 (2014) 59–80. doi:10.1016/j.solmat.2013.08.015.

[10] T. Kousksou, F. Strub, J. Castaing Lasvignottes, a. Jamil, J.P. Bédécarrats, Second law analysis of latent thermal storage for solar system, Sol.

Energy Mater. Sol. Cells. 91 (2007) 1275–1281. doi:10.1016/j.solmat.2007.04.029.
[11] S. Furbo, J. Fan, E. Andersen, Z. Chen, B. Perers, Development of seasonal heat storage based on stable supercooling of a sodium acetate water mixture, Energy Procedia. 30 (2012) 260–269. doi:10.1016/j.egypro.2012.11.031.
[12] S. Furbo, S. Svendsen, Report on heat storage in a solar heating system using salt hydrates. Report no. 70. Thermal Insulation Laboratory, Technical University of Denmark., 1977. http://www.byg.dtu.dk/-/media/Institutter/Byg/publikationer/lfv/lfv/lfv_070.ashx?la=da.
[13] H. Kimura, J. Kai, Phase change stability of sodium acetate trihydrate and its mixtures, Sol. Energy. 35 (1985) 527–534. doi:10.1016/0038-092X(85)90121-5.
[14] N. Araki, M. Futamura, A. Makino, H. Shibata, Measurements of thermophysical properties of sodium acetate hydrate, Int. J. Thermophys. 16 (1995) 1455–1466.
[15] K. Kauffman, Y. Pan, Thermal Energy Storage in Sodium Sulfate Decahydrate Mixtures, University of Pennsylvania, 1972.
[16] M. Dannemand, W. Kong, J. Fan, J.B. Johansen, S. Furbo, Laboratory Test of a Prototype Heat Storage Module Based on Stable Supercooling of Sodium Acetate Trihydrate, Energy Procedia. 70 (2015) 172–181. doi:10.1016/j.egypro.2015.02.113.
[17] M. Dannemand, S. Furbo, Test of thermobattrie heat storage module. Report number R 308. Department of Civil Engineering, Technical University of Denmark, 2014. http://www.byg.dtu.dk/Publikationer/Byg_rapporter.
[18] P. Hu, D.J. Lu, X.Y. Fan, X. Zhou, Z.S. Chen, Phase change performance of sodium acetate trihydrate with AlN nanoparticles and CMC, Sol. Energy Mater. Sol. Cells. 95 (2011) 2645–2649. doi:10.1016/j.solmat.2011.05.025.
[19] B.M.L. Garay Ramirez, C. Glorieux, E.S. Martin Martinez, J.J. a Flores Cuautle, Tuning of thermal properties of sodium acetate trihydrate by blending with polymer and silver nanoparticles, Appl. Therm. Eng. 61 (2013) 838–844. doi:10.1016/j.applthermaleng.2013.09.049.
[20] L.F. Cabeza, G. Svensson, S. Hiebler, H. Mehling, Thermal performance of sodium acetate trihydrate thickened with different materials as phase change energy storage material, Appl. Therm. Eng. 23 (2003) 1697–1704. doi:10.1016/S1359-4311(03)00107-8.
[21] H.W. Ryu, S.W. Woo, B.C. Shin, S.D. Kim, Prevention of supercooling and stabilization of inorganic salt hydrates as latent heat storage materials, Sol. Energy Mater. Sol. Cells. 27 (1992) 161–172. doi:10.1016/0927-0248(92)90117-8.
[22] J.C. Choi, S.D. Kim, G.Y. Han, Heat transfer characteristics in low-temperature latent heat storage systems using salt-hydrates at heat recovery stage, Sol. Energy Mater. Sol. Cells. 40 (1996) 71–87. doi:10.1016/0927-0248(95)00084-4.
[23] G. Höhne, W. Hemminger, H.J. Flammersheim, Differential Scanning Calorimetry, Springer, 2003.
[24] Z. Yinping, J. Yi, J. Yi, A simple method, the -history method, of determining the heat of fusion, specific heat and thermal conductivity of phase-change materials, Meas. Sci. Technol. 10 (1999) 201–205. doi:10.1088/0957-0233/10/3/015.
[25] H. Hong, C.H. Park, J.H. Choi, J.H. Peck, Improvement of the T-history Method to Measure Heat of Fusion for Phase Change Materials, Int. J. Air-Conditioning Refrig. 11 (2003) 32–39.
[26] H. Hong, S.K. Kim, Y.S. Kim, Accuracy improvement of T-history method for measuring heat of fusion of various materials, Int. J. Refrig. 27 (2004) 360–366. doi:10.1016/j.ijrefrig.2003.12.006.
[27] J.H. Peck, J.J. Kim, C. Kang, H. Hong, A study of accurate latent heat measurement for a PCM with a low melting temperature using T-history method, Int. J. Refrig. 29 (2006) 1225–1232. doi:10.1016/j.ijrefrig.2005.12.014.
[28] M. Dannemand, J.B. Johansen, S. Furbo, Solidification behavior and thermal conductivity of bulk sodium acetate trihydrate composites with thickening agents and graphite, Sol. Energy Mater. Sol. Cells. 145 (2016) 287–295. doi:10.1016/j.solmat.2015.10.038.
[29] G.F.S., Latent heat of fusion, J. Franklin Inst. 193 (1922) 656. doi:10.1016/S0016-0032(22)90585-X.
[30] S. Yang, W. Tao, Heat transfer, 3rd ed., Higher Education Press, Beijing, 1998. (In Chinese).

Table and Figure captions

Paper 6 - Validation of a CFD model simulating charge and discharge of a small heat storage test unit based on a sodium acetate water mixture

Mark Dannemand, Jianhua Fan, Simon Furbo, Janko Reddi

ISES Solar World Congress 2013

Energy Procedia, 57 pp. 2451 – 2460, 2014

doi:10.1016/j.egypro.2014.10.254

Available online at www.sciencedirect.com

ScienceDirect

Energy Procedia 57 (2014) 2451 – 2460

Energy Procedia

2013 ISES Solar World Congress

Validation of a CFD model simulating charge and discharge of a small heat storage test module based on a sodium acetate water mixture

Mark Dannemand*, Jianhua Fan, Simon Furbo, Janko Reddi

Department of Civil Engineering, Technical University of Denmark, Brovej 118, Kgs. Lyngby, DK 2800, Denmark

Abstract

Experimental and theoretical investigations are carried out to study the heating of a 302 x 302 x 55 mm test box of steel containing a sodium acetate water mixture. A thermostatic bath has been set up to control the charging and discharging of the steel box. The charging and discharging has been investigated experimentally by measuring surface temperatures of the box as well as the internal temperature of the sodium acetate water mixture through a probe located in the center of the steel box. The temperature developments on the outer surfaces of the steel box are used as input parameters for a Computational Fluid Dynamics (CFD) model. The CFD calculated temperatures are compared to measured temperatures internally in the box to validate the CFD model. Four cases are investigated; heating the test module with the sodium acetate water mixture in solid phase from ambient temperature to 52˚C; heating the module starting with the salt water mixture in liquid phase from 72˚C to 95˚C; heating up the module from ambient temperature with the salt water mixture in solid phase, going through melting, ending in liquid phase at 78˚C/82˚C; and discharging the test module from liquid phase at 82˚C, going through the crystallization, ending at ambient temperature with the sodium acetate water mixture in solid phase. Comparisons have shown reasonable good agreement between experimental measurements and theoretical simulation results for the investigated scenarios.

Keywords: Seasonal heat storage; sodium acetare trihydrate, phase change materials; thermal behavior; experimants; computational fluid dynamics

* Corresponding author. Tel.: +45 45 25 18 87
E-mail address: markd@byg.dtu.dk.

doi:10.1016/j.egypro.2014.10.254

1. Introduction

Theoretical investigations have previously shown [1],[2],[3] that the solar fraction for solar heating systems can be improved significantly by the use of heat of fusion storages based on a sodium acetate water mixture with stable supercooling compared to solar heating systems with sensible and latent heat storages even under Danish climatic conditions. Calculations have shown that a solar heating system with a collector area of 36 m² can fully cover the yearly heat demand of a low energy house in Denmark if the solar heating system is equipped with a heat storage of 6 m^3 of sodium acetate water mixture which supercools in a stable way. Currently a development project is being carried out [4],[5],[6],[7] with the focus on developing such a heat storage. The storage is divided into a number of separate modules to optimize the system by allowing charge and discharge modules individually. The current module design is a flat steel tank with the salt water mixture enclosed in a chamber with heat exchangers integrated in the upper and lower surfaces. The inner height of the chamber containing the salt water mixture is 50-80 mm. In the current storage design each module contains 250-500 liters of salt water mixture. Previous experimental and theoretical Computational Fluid Dynamics investigations of prototype modules have shown deviations from the calculated to the measured values in some of the results [8].

This paper describes work done with a small 302 x 302 x 55 mm test steel box containing a sodium acetate water mixture. The focus is on the heating and cooling of the small test module and the behavior of the salt water mixture inside. The aim of this investigation is to compare theoretical CFD calculations to experimental measurements in order to validate the CFD model.

Nomenclature

C_p specific heat, J/kg·K
h sensible enthalpy, J
H enthalpy, J
k thermal conductivity, W/m·K
L latent heat, kJ/kg
S source term
t time, s
T temperature, K
β liquid fraction, -
ρ density, kg/m^3
μ dynamic viscosity, kg/m·s
ΔH latent heat, J

2. Experimental setup

Three different scenarios are tested for charging: investigating only solid state salt water mixture by heating the module from 22˚C to 52˚C; investigating only liquid state salt water mixture by heating the module from 72˚C to 95˚C and investigating heating both solid and liquid state salt water mixture as well as the melting by heating the module from 22˚C to 78˚C/82˚C. For discharge the scenario of cooling from liquid state 82˚C to 19˚C solid state is investigated including the crystallization of the salt water mixture.

One 302 x 302 x 55 mm steel box containing a sodium acetate (58 %wt) and water (42 %wt) mixture is heated up by placing it in a thermostatic bath containing water. The steel box is filled with a sodium acetate water mixture in hot liquid state to obtain a complete filling of the test module with no air inside.

The mass of the steel box is 4.626 kg and the mass of the salt water mixture filled into the box is 6.11 kg. The steel box has a material thickness of 2 mm. One side of the module has a filling neck for filling the module. Around the filling neck is a flange on which the lid is fixed. The filling neck has an inner diameter of approximately 40 mm. A brass container is located on the corner of the steel module which can be used to start crystallization of the salt water mixture if it supercools. The brass container is not relevant for this series of experiments and neglected.

Fig. 1. 302 x 302 x 55 mm steel module containing a salt water mixture.

In the center of lid a 170 mm long probe of stainless steel is fixed perpendicular to the plane of the lid. This places the tip of the probe in the center of the steel box when fastened. The probe has an outer diameter of 3 mm and a material thickness of 0.3 mm. A copper/constantan thermocouple (type TT) is placed inside the probe along with heat transfer compound to ensure maximum heat transfer from the probe to the thermocouple. A rubber gasket with a thickness of 4 mm is sealing the lid to the flange. 13 copper/constantan thermocouples (type TT) are fastened to the outer surfaces of the steel module with waterproof tape to measure the surface temperature of the steel module. Some inaccuracy of the surface temperature measurements are expected as the water temperature affects the measurements. Four sensors are placed on the top surface, two on the bottom surface, one on the side opposite from the lid and two on each of the remaining three sides. One last thermocouple is placed in the water. The measurements of the thermocouples are recorded every 2 seconds on an Agilent 34970A data logger.

A 600 mm x 400 mm x 215 mm plastic container constitutes the tub of the thermostatic bath. The tub is placed on 30 mm of Styrofoam insulation; the sides and top are covered with 75 mm of insulation to reduce heat losses and to keep a steady temperature inside the thermostatic bath. The water in the thermostatic bath is heated by a HETO Type 02 T 623 thermostat which includes a motor for stirring the water in the thermostatic bath to strive for uniform temperatures on all the surfaces of the steel module. Two pipes with valves are joined to the plastic container to work as inlet and outlet to allow for circulating cold water through the box to create an active discharge. The inlet and outlet are placed diagonally in the box for best circulation of water around the steel module during discharge. During charge the test module is covered with 35 mm of water and there is 60 mm of water from the bottom of the steel module to the bottom of the plastic container.

Fig. 2. Plastic tub for thermostatic bath with pipe connections and steel box.

To initialize the charge experiments the water in the thermostatic bath is heated to the desired end temperature; approximately 52˚C, 78˚C/82˚C and 95˚C without the steel module in the water. The steel module with the sensors attached is then placed in the hot water so that it is fully submerged. The module is placed on spikes to allow for water to be in contact with the entire bottom surface of the steel box. For the charge experiment with the salt water mixture only in liquid state the steel module is taken directly from an oven with a stable temperature of 72 ˚C. The charging runs until a stable temperature for the probe is reached in the center of the steel module. When a stable temperature is reached inside the module the thermostatic controller is turned off and the hot water in the thermostatic bath is emptied out and replaced with cold water from the tap. To simulate the discharge cold water is circulated through the plastic box with the lower pipe connection as the inlet and the pipe in the upper part of the thermostatic bath's box as an overflow outlet. During the discharge the steel module is covered with 20 mm of water. The discharge part of the experiment runs until the temperature measurement of the probe has stabilized.

Fig. 3 (a). Top view of thermostatic bath with steel box. (b) Thermostatic bath with lid and thermostatic controller.

Due to the temperature dependent density of the salt water mixture the steel module deforms as it is heated up and cooled down. In the initial cold solid state the box has a relatively uniform thickness of about 55 mm. In the hot melted state the salt water mixture has expanded and the thickness of the steel box at the center is increased to about 65 mm with 55 mm near the sides. It is assumed that the box is full in the hot liquid state without air inside and the liquid salt water mixture is incompressible. The volume reduction of the salt water mixture from 82˚C to 22˚C is estimated based on the densities of the salt water mixture at the different phases and temperatures with the formulas (1) and (2). The estimated volume reduction of the salt water mixture between 82˚C and 22˚C is larger than the estimated volume change of the steel box by the deformation. This indicates that a vacuum is formed inside the steel box when in the solid state which is the initial state of the heating up experiments starting from 22˚C. It is assumed that the vacuum is formed in the part of the module facing upwards during solidification due to gravity forces. If the module is placed horizontally when the crystallization is started the vacuum is formed under the top surface. If the module is placed vertical when the crystallization is started the vacuum is formed by the side facing upwards. The vacuum will work as a thermal resistance on the face it is located for the heating in the first period until the salt water mixture has expanded enough to fill the module. Experiments with charging the module after crystallization at horizontal and at vertical position are carried out.

3. CFD model

A simplified model of the steel box is built using the commercial CFD code Ansys (Fluent) 14.5. The filling neck and lid are neglected. The probe is modelled as solid and is fixed on one of the side walls. Only the steel box including the enclosure, the probe and the salt water mixture inside is simulated. The measured surface temperatures of the steel module are used as input parameters for the CFD model. The charge of the steel module is simulated by assigning averages of the measured surface temperatures to the respective surfaces of the steel box in the CFD model as boundary conditions. The surface temperatures are defined in the model as functions of time by user defined functions (UDF). The UDFs for the surfaces are compared to the measured temperatures to ensure good agreement. The model is initialized at a uniform temperature representing the starting temperature of the experiment.

The mesh is shown in figure 4b below with the salt hydrate and the top and bottom surfaces suppressed. The mesh is denser near the outer surfaces, the transition from the steel to the salt water mixture and around the probe. The mesh has 437,462 elements and average skewness of 0.123.

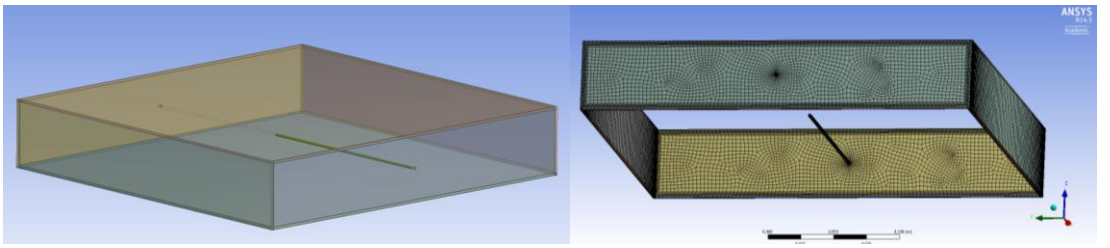

Fig. 4. (a) Geometry of the 302 x 302 x 55 mm steel box and probe in Ansys. (b) The mesh of the module with top and bottom surface and fluid suppressed.

Fluid flow in the box is calculated with a laminar model. Transient CFD calculations are performed with an initially standstill module (all fluid velocities are zero) and a uniform temperature. The PRESTO and second order upwind method are used for the discretization of the pressure and the momentum equations respectively. The SIMPLE algorithm is used to treat the pressure-velocity coupling.

During charge of the module, phase transitions of salt water mixture between solid and liquid phase will have a significant influence on the heat transfer in the module. The enthalpy-porosity method is used to calculate melting and crystallization of the salt water mixture. In the enthalpy-porosity method, the interface between the solid and liquid phase is not tracked explicitly. Instead, a quantity called the liquid fraction, which indicates the fraction of the cell volume that is in liquid form, is associated with each cell in the domain. The liquid fraction is computed every iteration, based on an enthalpy balance. The energy equation is written as

$$\frac{\delta}{\delta t}(\rho H) + \nabla \cdot (\rho \vec{v} H) = \nabla \cdot (k \nabla T) + S$$

Where ρ is density, kg/m^3; ν is fluid velocity vectors, m/s. S is Source term.
The enthalpy of the salt water mixture, H, consists of sensible enthalpy, h and latent heat, ΔH.

$$H = h + \Delta H$$
$$h = h_{ref} + \int_{T_{ref}}^{T} C_p dT$$

Where H is the enthalpy; C_p is the specific heat of salt water mixture; T is the temperature in K.
The latent heat is calculated by a product of the liquid fraction and the latent heat of the material.

$$\Delta H = \beta L$$

Where L is the latent heat of salt water mixture; β is the liquid fraction, -.
The liquid fraction is 1 when the salt water mixture temperature is higher than the melting point temperature, while it is 0 if the salt water mixture temperature is lower than the melting point temperature. In this way, melting and crystallization of salt water mixture during the charge of the module are considered.
The density of the mixture of 42% (weight) water and 58% (weight) sodium acetate is and its temperature dependency is adapted from Lane [9] and Fan [8]. Specific heat and thermal conductivity are adapted from Araki [10]. Dynamic viscosity is adapted from Inagaki [11]. Latent heat of the 42% (weight) water and 58% (weight) sodium acetate is assumed to L = 240 kJ/kg [12].

Density, [kg/m^3]: $\rho = 1523 - 0.780 \cdot T$ (1)

Thermal expansion coefficient, [1/K]: 0.000512

Specific heat, [J/(kgK)]: $C_p = 1594 + 4.33 \cdot T$

Thermal conductivity, [W/(mK)] $k = -2.72 + 0.0214 \cdot T - 3.63 \cdot 10^{-5} \cdot T^2$

Dynamic viscosity, [kg/(ms)] $\mu = 0.3673 - 0.001943 \cdot T + 2.592 \cdot 10^{-6} \cdot T^2$

where T is fluid temperature, [K].

The following properties of the solid salt water mixture and their dependences on temperature are used: Specific heat and thermal conductivity adapted from Araki [10]. Density from Lane [9].

Density, [kg/m^3]: 1450 (2)

Specific heat, [J/(kgK)]: $C_p = 1017 + 3.50 \cdot T$

Thermal conductivity, [W/(mK)] $k = 0.60$

where T is fluid temperature, [K].

The steel wall has a thermal conductivity of 60 W/K and a specific heat of 500 J/kgK. The density of the steel is assumed to be 9590 kg/m^3 based on the mass of the steel box and the volume of the steel in the CFD model.

For the heating up the solid salt water mixture from 22˚C to 52˚C a resistance of 0.0476 m^{2}K/W corresponding to a vacuum of 1/3 mm is assigned to the inner top surface of the steel box. This represents the vacuum related the contraction of the salt water mixture in the cold solid state. For the heating from 72˚C to 95˚C and from 22˚C to 78˚C/82˚C no resistances are assigned. The geometry of the steel box and the volume of the fluid are assumed to be constant regardless of the temperature level.

4. Results and discussion

The temperature measured in the center of the steel box by the probe is compared to the simulated temperature of the probe tip in the CFD model.

Figure 5 shows good agreement between the development of the measured probe temperature and the simulated temperature of the probe tip for the heating from 22°C to 52°C in the solid state. A contact thermal resistance for the heat transfer is applied to top inner surface of the steel box representing a small vacuum in the top of the box. Simulating the experiment without the contact resistance would lead a faster heating of the probe tip.

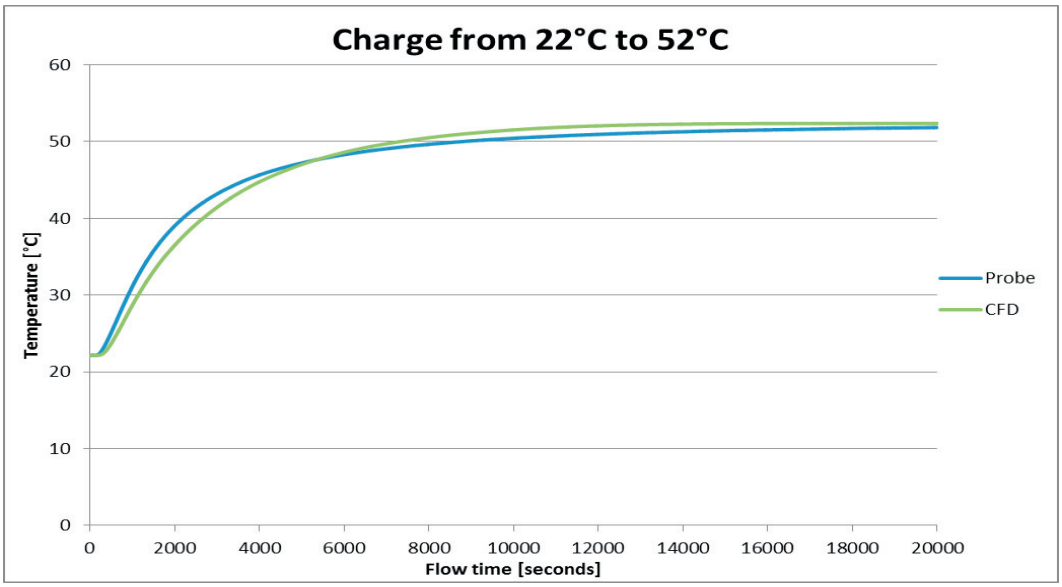

Fig. 5. Comparison of probe measurement and simulation tip temperature development for heating from 22°C to 52°C.

Figure 6 shows good agreement between the development of the measured probe temperature and the simulated temperature of the probe tip in the case of heating the liquid salt water mixture from 72°C to 95°C without any resistances applied.

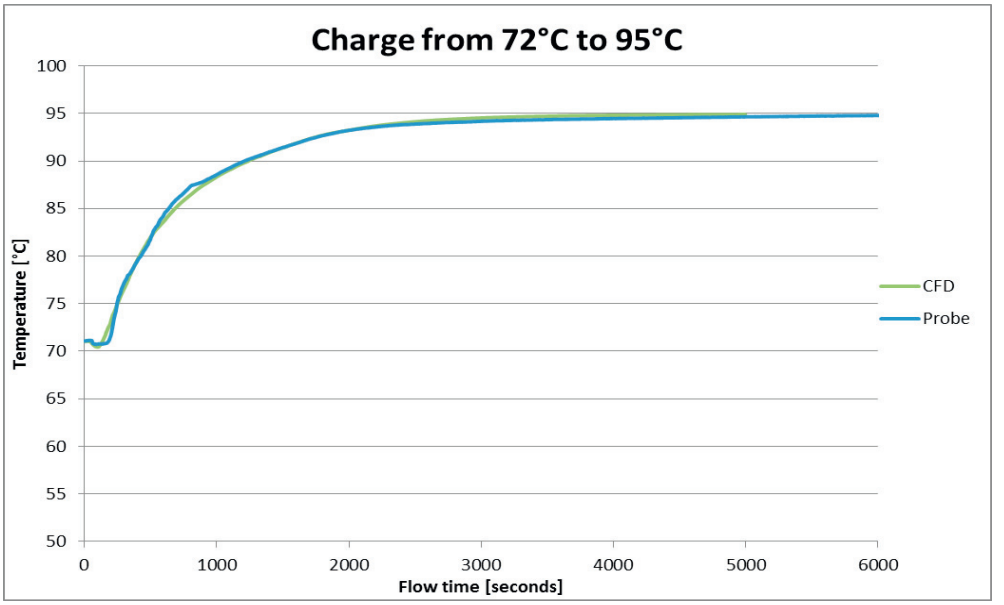

Fig. 6. Comparison of probe measurement and simulation tip temperature development for charging from 72°C to 95°C.

Figure 7 shows the temperature developments of the probe for the experimental setup compared to the simulated probe tip temperature development for two similar tests. (Probe1) Heating from 22°C to 78°C after crystallization of the salt water mixture with the module placed horizontally. (Probe2) Heating from 22°C to 82°C after crystallization of the salt water with the module placed vertical. It is assumed that for Probe1 a resistance caused by the vacuum on the top surface is reducing the heating rate compared to Probe2 where the vacuum is near the side and therefore has lower influence of the heating of the probe in the center. The end temperature for the two experiments differs with about 4K which partly causes the slower heating rate of Probe1 compared to Probe2. For each case the different boundary conditions are applied to the CFD model which gives the different results for the simulations CFD1 and CFD2. For both simulations no resistances are applied. The deviations between the experiment Probe1 and simulations CFD1 are much larger than the deviations between Probe2 and CFD 2. This supports the theory of vacuum forming inside the steel module resulting in a thermal resistance and reduced heating rate.

The deviations between the measured and simulated temperatures can also be influenced by the imprecise method of which the surface temperature of the box is measured. This can be an overestimation of the actual surface temperatures which are used as the boundary conditions for the CFD model.

It can be seen that the temperature of the sensor in the probe inside the steel box in the first part of the charging rises at a relative constant rate due to the thermal conduction in the salt water mixture from the hot outer surface through the salt hydrate to the probe. The curve flattens out and the heating rate of the probe decreases partly due to the thermal energy being absorbed by the phase change of the salt water mixture near the outer surfaces and partly because the temperature difference of the probe and the surface temperature of the steel box decrease. Considering no surface resistances on the upper surface, the last part of the salt water mixture that melts is in the middle part of the steel box where the sensor is located.

The last solid salt water mixture will be fixed in the center of the test module and not moving freely in the box because it surrounds the probe. When the part of the solid salt water mixture that is fixed to the probe comes loose it drops to the bottom of the steel box due to its higher density and the convection inside the steel box and around the probe is increased and the temperature of the probe increases rapidly when the warmer liquid near the surfaces are mixed with the just melted salt water mixture near the probe in the center.

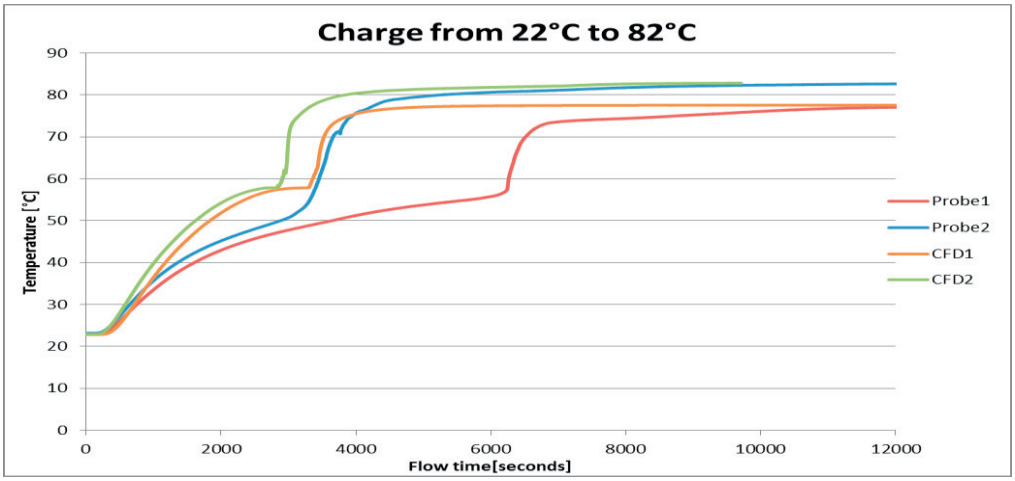

Fig. 7. Comparison of probe measurement and simulation tip temperature development for heating from 22°C to 82°C and 78°C.

Figure 8 shows the data for the discharge from 82°C to 19°C. The crystallization of the salt water mixture started spontaneous with only slight supercooling. The measured temperature development of the probe agrees well with the simulated probe tip temperature. The horizontal part of the curve indicates the release of the heat of fusion which for the measurement is slightly shorter than for the simulations. This can indicate that the latent heat of 240 kJ/kg used in the CFD model could be an over estimation.

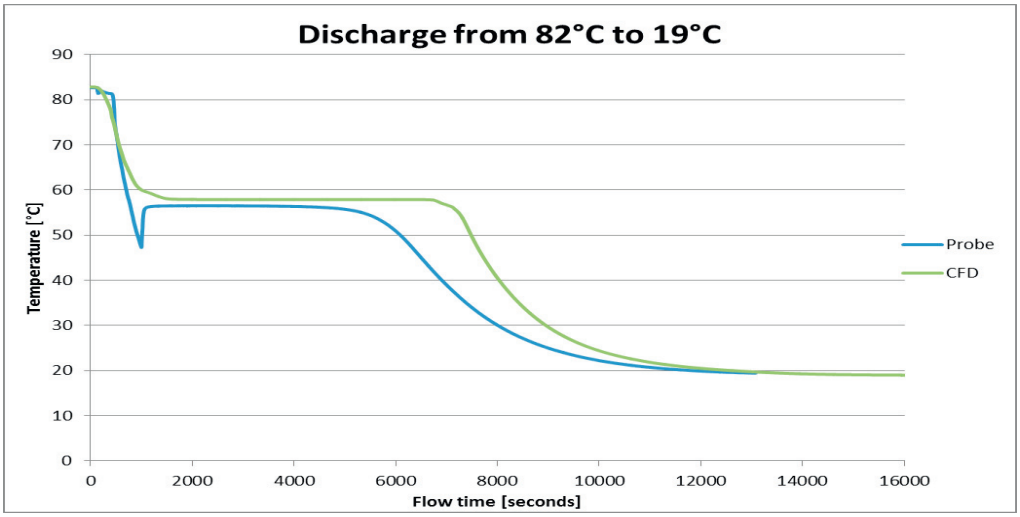

Fig. 8. Comparison of probe measurement and simulation tip temperature development for discharging from 82°C to 19°C.

5. Conclusion

Thermal experiments and CFD simulations have been carried out in order to investigate the behavior of a test steel module containing a salt water mixture and to validate the CFD model. Comparisons between measured temperatures for charging and discharging and temperatures calculated with a CFD model have shown good agreement. For heating of the salt water mixture without phase change the agreement between measurement and simulations are excellent. For the temperature developments through the phase change some deviations between measured and calculated temperatures are observed. The experimental investigations showed that orientation of the module when the salt water mixture crystalizes and the forming of vacuum in the rigid steel module can have a large effect on the heating rate of a module due to thermal resistances being created internally in the module by the vacuum. Considerations of rigidness and designs for full scale heat storages should be made to avoid lower heat transfer rates. Especially vacuum forming near the heat exchanger for the module can reduce the heat exchange capacity rate and reduce the efficiency of the storage system.

References

[1] J. Schultz and S. Furbo, “Solar heating systems with heat of fusion storage with 100% solar fraction for solar low energy buildings,” in ISES Solar World Congress 2007 Proceedings, 2007.

[2] S. Hirano and T. S. Saitoh, “Heat balance of long-term supercooled thermal energy storage,” Nihon Enerugi Gakkaishi/Journal of the Japan Institute of Energy, vol. 80, no. 11, pp. 1050–1059, 2001.

[3] S. Hirano and S. Takeo, “INFLUENCE OF OPERATING TEMPERATURE ON EFFICIENCY OF SUPERCOOLED THERMAL ENERGY STORAGE,” in IECEC 2002 Paper No. 20040, 2002, no. 20040, pp. 684–689.

[4] S. Furbo, J. Dragsted, J. Fan, E. Andersen, and B. Perers, “Experimental studies on seasonal heat storage based on stable supercooling of a sodium acetate water mixture,” ISES Solar World Congress 2011 Proceedings, 2011.

[5] S. Furbo, J. Fan, E. Andersen, Z. Chen, and B. Perers, “Development of Seasonal Heat Storage based on Stable Supercooling of a Sodium Acetate Water Mixture,” Energy Procedia, vol. 30, pp. 260–269, 2012.

[6] W. Van Helden, A. Hauer, S. Furbo, O. Skrylnyk, A. Ristić, S. Henninger, C. Rindt, F. Bruno, A. Lázaro, L. Luo, D. Basciotti, A. Heinz, R. Weber, I. Fernandez, J. Chiu, H. Zondag, R. Cuypers, J. Jänchen, and E. Lävemann, “Results of 4 years R & D in the IEA Task4224 on Compact Thermal Energy Storage : Materials Development for System Integration Task 4224.”

[7] T. Letz, E. Andersen, C. Bales, J. Bony, R. Heimrath, M. Haller, R. Haberl, J. Hadorn, D. Jaehnig, H. Kerskes, J. Schultz, R. Weber, and H. Zondag, “Performances of solar combisystems with advanced storage concepts Report A3 of Subtask A,” 2007.

[8] J. Fan, S. Furbo, E. Andersen, Z. Chen, B. Perers, and M. Dannemand, “Thermal Behaviour of a Heat Exchanger Module for Seasonal Heat Storage,” Energy Procedia, vol. 30, pp. 244–254, Jan. 2012.

[9] G. Lane, Solar heat storage latent heat material Vol 2. CRC, 1986.

[10] N. Araki, M. Futamura, A. Makino, and H. Shibata, “Measurements of Thermophysical Properties of Sodium Acetate Hydrate,” International Journal of Thermophysics, vol. 16, no. 6, pp. 1455–1466, 1995.

[11] T. Inagaki and T. Isshiki, “Thermal Conductivity and Specific Heat of Phase Change Latent Heat Storage Material Sodium Acetate Trihydrate and Heat Transfer of Natural Convection in a Horizontal Enclosed Rectangular Container,” Kagaku Kogaku Ronbunshu, vol. 39, no. 1, pp. 33–39, 2013.

[12] R. Tamme, “Low Temperature Thermal Storage Using Latent Heat and Direct Contact Heat Transfer,” in 21st Intersociety Energy Conversion Engineering Conference, 1986.

Paper 7 - Testing of PCM heat storage units with solar collectors as heat source

Gerald Englmair, Mark Dannemand, Jakob B. Johansen, Weiqiang Kong, Janne, Dragsted, Simon Furbo, Jianhua Fan

International Conference on Solar Heating and Cooling for Buildings and Industry, SHC 2015

Energy Procedia

Available online at www.sciencedirect.com

ScienceDirect

Energy Procedia 00 (2015) 000–000

Energy Procedia

www.elsevier.com/locate/procedia

SHC 2015, International Conference on Solar Heating and Cooling for Buildings and Industry

Testing of PCM Heat Storage Modules with Solar Collectors as Heat Source

Gerald Englmair*, Mark Dannemand, Jakob B. Johansen, Weiqiang Kong, Janne Dragsted, Simon Furbo, Jianhua Fan

Department of Civil Engineering, Technical University of Denmark, Brovej 118, DK-2800 Kgs. Lyngby, Denmark

Abstract

A latent heat storage based on the phase change material Sodium Acetate Trihydrate (SAT) has been tested as part of a demonstration system. The full heat storage consisted of 4 individual modules each containing about 200 kg of sodium acetate trihydrate with different additives. The aim was to actively utilize the ability of the material to supercool to obtain long storage periods. The modules were charged with solar heat supplied by 22.4 m^2 evacuated tubular collectors. The investigation showed that it was possible to fully charge one module within a period of 270 minutes with clear skies. In long periods with high level of irradiance several modules were charged in parallel due to the limited heat exchange capacity of the integrated heat exchanger of the modules. After the modules were heated to more than 80° C they were set to passively cool down. Modules reached 30°C in a period of parallel cool down without the sodium acetate trihydrate solidified in 3 of the 4 modules. Further tests showed that stable supercooling at ambient temperature is possible.

Peer-review by the scientific conference committee of SHC 2015 under responsibility of PSE AG.

Keywords: Phase change material; PCM; Seasonal heat storage; Sodium acetate trihydrate; Compact thermal energy storage; Stable supercooling;

1. Introduction

To integrate more solar energy into existing energy supply systems, long term heat storage is desired. The investigated heat storage concept is based on the principle of utilizing stable supercooling of a Phase Change Material (PCM). If Sodium Acetate Trihydrate (SAT), which has a melting point of 58 °C, has been fully melted, it

* Corresponding author. Tel.:+45 45251700;
E-mail address: gereng@byg.dtu.dk

Peer-review by the scientific conference committee of SHC 2015 under responsibility of PSE AG.

can cool down to ambient temperature in its liquid phase without releasing the heat of fusion. Having a PCM rest in supercooled state in temperature equilibrium with the ambient allows principally seasonal heat storage in compact systems [1]. To achieve stable supercooling in heat storage modules with SAT, a minimum material temperature of 80 °C must be achieved during the heating in all parts of the material volume, according to the experimental experience. The principle is shown in Fig.1.

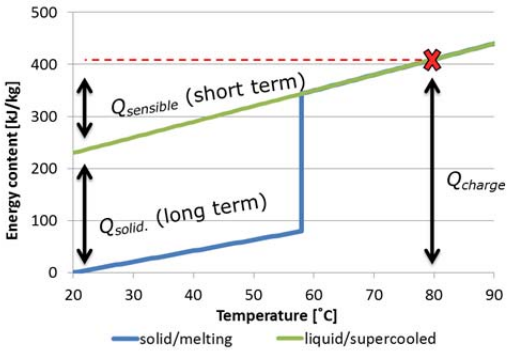

Fig. 1. Principle of stable supercooling with sodium acetate trihydrate.

The PCM heat storage can be used for short term heat storage by utilizing the sensible heat ($Q_{sensible}$) of the melted and supercooled PCM. The heat storage module can be left at ambient temperature with no heat loss until there is a heat demand (as long term heat storage). In that case solidification is activated, the heat of fusion ($Q_{solid.}$) is released, and the module temperature increases almost immediately to the melting temperature.

In this paper data from initial testing of heat storage modules, containing different mixtures of the PCM sodium acetate trihydrate, are presented. Modules in different material configurations have previously been tested under laboratory conditions to prove the concept [2]. The modules form a long term heat storage as a part of a solar combi-system including additionally a solar collector field and a water buffer storage. The solar combi-system was connected to an automated tapping system simulating domestic hot water tapping and space heating demands. The overall system design and its functionality were explained by J. B. Johansen et al. [3].

2. Method

Four modules were tested with different phase change materials based on SAT. The modules were assembled to a heat storage stack and charged via a plate heat exchanger by heat from the solar collector loop.

2.1. PCM modules

A schematic drawing of the PCM module is shown in Fig.2. The modules were fabricated with an internal height of 5 cm of a closed material chamber (volume: 150 litre) by Nilan A/S. Two of the modules were in stainless steel. The other two modules were in steel. The water volume in the heat exchanger of each module was 32 litres. An air expansion volume, connected to the expansion vessel, ensured limited change of pressure during material expansion (about 10%) from solid to liquid state. A PCM temperature sensor was placed in a probe on one end of the module.

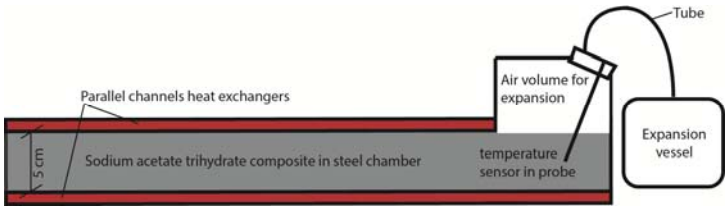

Fig. 2. Schematic module design with expansion vessel.

To overcome the problem of phase separation of the incongruently melting sodium acetate trihydrate, different PCM composites were filled into the modules. One proposed solution is to add a thickening agent to the PCM [4]. Therefore, CarboxyMethyl Cellulose (CMC) was used as thickening agent in two of the modules. One drawback of thickening agents is reduced heat transfer by convection because the thickness agents increase significantly viscosity of the PCM in its liquid phase. To counter balance this effect, a highly conductive graphite powder (C) was added in one module to increase thermal conductivity of the PCM composite.

Table 1. Configuration of the heat storage modules.

	Module 1	Module 2	Module 3	Module 4
Tank material	Carbon steel	Stainless steel	Carbon steel	Stainless steel
PCM composite	SAT + 1% CMC + 2% C + 5l Oil	SAT + 1% CMC	SAT + 1% H_2O + 1% EDTA	SAT + 2 % EDTA
PCM mass	202 kg	220 kg	202 kg	158 kg

Another factor that reduces heat transfer in solid SAT is insulating cavities formed during solidification and contraction of the PCM due to the density difference during phase change [5]. Adding Paraffin oil, which does not mix with SAT, was an attempt to increase heat transfer by having the oil filling in the cavities of the PCM [4].

Another possible solution for reducing the problem of phase separation is adding additives which increase the solubility of the crystal water in the melted and supercooled SAT mixture. Therefore SAT composites with Ethylenediaminetetraacetic Acid (EDTA) with and without extra water were tested. The actual PCM composites filled in modules are given in Table 1.

2.2. Heat storage

All modules were arranged separately, packed in 10 cm of foam insulation. The four modules were stacked in a 2 m high assembly (Fig.3-b). Motor valves (V1, V2, V3, or V4) were placed in front of each module, controlling flow through the module´s heat exchangers (Fig.3-a). The PCM heat storage was preferably charged module by module. Both, the upper and the lower heat exchanger of a module, were active during periods of charge.

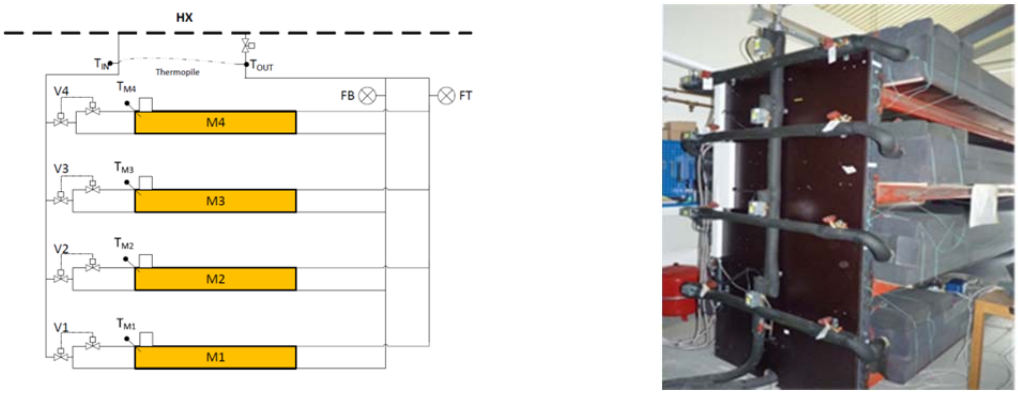

Fig. 3. (a) Hydraulic scheme of the PCM charging loop; (b) Photography of the front side of the heat storage.

In the PCM charging loop (Fig.3-a) the flow rates of the lower heat exchanges (FB) and the upper heat exchangers (FT) were measured separately. Two motor-valves per module were necessary to avoid natural circulation during cool down and unwanted backflows in inactive modules during charge. The charge of a module was stopped when it was considered to be melted i.e. the measured PCM temperature in the probe (T_{M1}, T_{M2}, T_{M3} or T_{M4}) was above 80°C. Inlet temperature (T_{IN}) and outlet temperature (T_{OUT}) were measured in the pipework to the heat exchanger (HX), where the heat was supplied from the collector loop.

Due to limited heat exchange capacity rates of the module´s heat exchangers, parallel module charge was optionally enabled. This means that it was possible to charge more than one module at the same time. In this way overheating of the heat transfer fluid was prevented.

2.3. Heat transfer from the collector field

As the heat source, a solar collector field, consisting of 7 modules of Kingspan HP450 evacuated tubular collectors with a total aperture area of 22.4 m^2, was utilized. The field was placed on a roof with an inclination angle of 45° and an azimuth angle of 13° towards east. The system was located at the solar heating test facility of the Technical University of Denmark (northern latitude of 55.6). As illustrated in Fig.4, the heat supplied by the collectors was transferred via a collector loop and a plate heat exchanger (HX) to the PCM charging loop (Fig.3 -a).

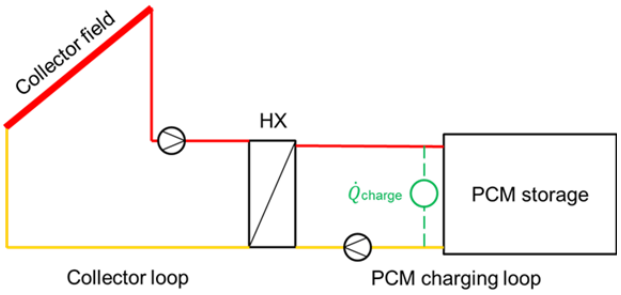

Fig. 4. Heat transfer during module charge (schematic).

The PCM modules needed to be operated with high inlet temperatures. Therefore, during PCM charge the collector loop as well as the PCM charging loop was circulated when the heat transfer fluid reached 70°C at the collector field outlet. Circulation was interrupted whenever this temperature level was undershot due to fluctuations of solar irradiance. A water volume flow rate of 16.5 l/min was realized in the PCM charging loop to ensure good heat transfer at the module´s heat exchangers. The set flow rate in the collector loop was 21 l/min during PCM storage charge.

2.4. Evaluation

Charging and cool down behaviour were evaluated by measurements of the PCM temperatures in the four modules.

Heat transfer rates in the PCM charging loop were calculated in the following way:

$$\dot{Q}_{charge} = \dot{V} \cdot c_p \cdot \rho \cdot \left(T_{IN} - T_{OUT}\right) \tag{1}$$

Where $\dot{V}$ is the measured volume flow rate of the heat transfer fluid, T_{IN} is the fluid temperature at the inlet to the modules, T_{OUT} is the fluid temperature at the outlet from the modules, c_p is the specific heat capacity of the heat transfer fluid at mean temperature between T_{IN} and T_{OUT}, ρ is the density of the heat transfer fluid at T_{OUT}, where the volume flow rates were measured.

The state of charge (*SOC*) of a module during single module charge was calculated based on the accumulated heat transferred to the PCM charging loop at a specific time *t* in relation to the total heat transferred to the module:

$$SOC(t) = \frac{\int_{start}^{t} \dot{Q}_{charge}}{\int_{start}^{end} \dot{Q}_{charge}} \tag{2}$$

The heat exchange capacity rate gives the power at the module´s heat exchanger per Kelvin of logarithmic temperature difference between the mean heat transfer fluid temperature in the PCM charging loop and the phase change material temperature (T_{PCM}):

$$HXCR = \dot{V} \cdot c_P \cdot \rho \cdot ln\left(\frac{T_{in} - T_{PCM}}{T_{out} - T_{PCM}}\right) \quad (3)$$

3. Results and discussion

Data from a single module charge, from a representative period of parallel module charge and from cool-down of the modules were evaluated. Supercooling was achieved by passive cool-down of modules to the ambient temperature. Although module no. 4 was frequently heated up to a probe temperature of about 85°C, no stable supercooling was achieved during the initial test period of the demonstration system.

3.1. Single module charge

In selected test runs modules have been charged individually. It was found that charging the modules in sunny afternoons matched well with the decreasing solar irradiance because the heat transfer rates during single module charge were falling with increasing PCM temperatures.

Module no. 1 was charged from ambient temperature (21°C) in solid state on the afternoon of the 8th of September. Fig.5 shows the measured solar radiation on the collector (grey curve) and the heat transferred to the modules (black, dotted curve).

Heat was transferred for 270 minutes to the heat storage, the charging (indicated by the heat transfer rate) stopped when the PCM temperature (orange curve in Fig.6) reached 80 °C. During this charge run 27.4 kWh of heat was transferred to the heat storage. The solar irradiance was fluctuating. The fluctuation of heat transfer happened with time delays. Heat transfer rates of up to 16 kW occurred at the beginning of the test. The heat transfer rates were dropping constantly until an operation time of 250 min.

In Fig.6 developments of the inlet temperature (grey curve) and the outlet temperature (black curve) were shown. As a consequence of the limited heat exchange capacity of the module, the charging loop was constantly heated up. At the end of the test, the inlet temperature dropped due to the decreasing solar irradiance (Fig.5). During the last 20 minutes the heat transfer rates were very low, since the inlet temperature, temperature of the module heat exchangers and the outlet temperature were almost the same.

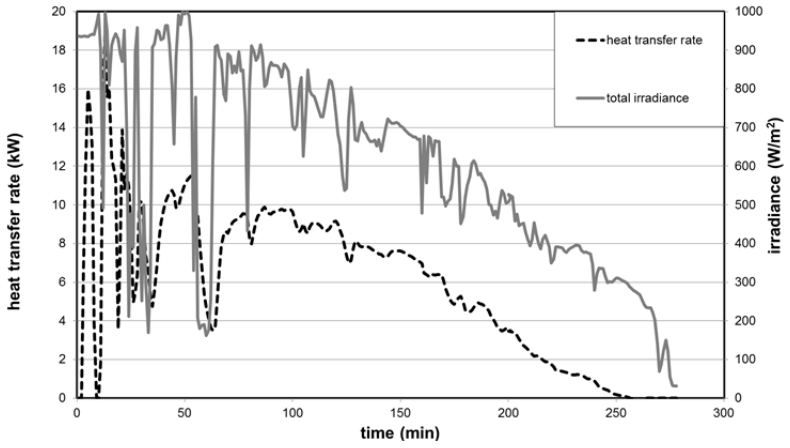

Fig. 5. Heat transfer rates during charge of module no. 1 and total irradiance development.

Until a state of charge of about 10% was reached, the heat exchange capacity rates (black dotted curve in Fig.6) were high because the heat transfer fluid in the module´s heat exchangers and the pipework including the temperature sensors were heated up. Therefore a sharp increase of the outlet temperature was observed.

In between 10% and 88% of the SOC, when 78% of the heat was transferred, the HXCR was around 250 W/K.

During the last 12% of charge a sharp increase of the PCM temperature was observed. This behaviour indicated liquid PCM state at the location of the temperature probe. Because sharp increase of PCM temperature occurs when a value below 58 °C was measured and because the temperatures were even lower before 88% of charge, it is very likely that the PCM temperature does not represent the mean material temperature in the chamber. Also a PCM temperature jump at 100% charge is a proof of this assumption.

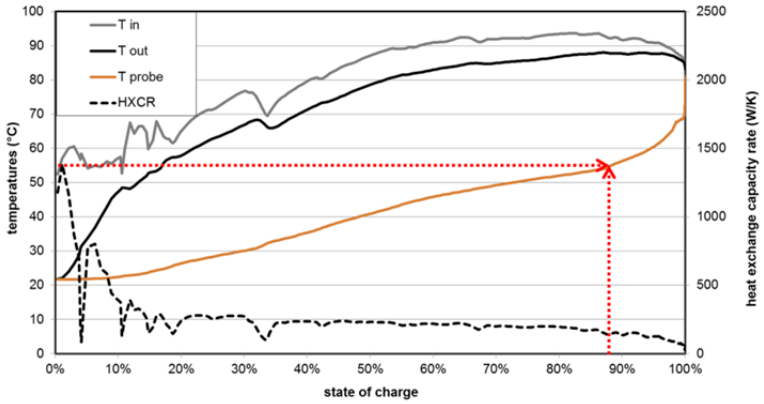

Fig. 6. Temperature developments during charge of module no. 1.

3.2. Parallel module charge

Fig.7 shows a representative period of parallel module charge in October 2015. Within two sunny days (2nd and 3rd of October), three modules were recharged by solar heat from an already supercooled state. Parallel charge at sunny days was necessary because of the limited heat exchange capacity rates of the modules. After charge, these three modules were cooled down for about five days to an equal temperature level of 30°C.

When parallel charge of modules was carried out, there were no heat transfer restrictions, due to the limited heat exchange capacity of PCM modules, occurring in the PCM charging loop. It was found that spontaneous solidification did not occur when applying heat to already supercooled modules.

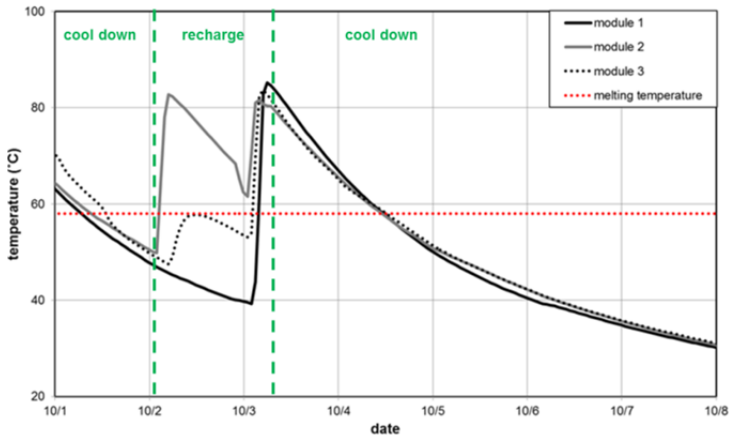

Fig. 7. PCM probe temperature developments.

3.3. Module cool-down

In two independent periods (5 days each) in August and October parallel cool down of modules showed comparable heat loss rates. Starting from a temperature of approximately 80 °C, the PCM was cooled down to a temperature of around 30 °C remaining in liquid state.

Individual module cool-down in longer periods proved that stable supercooling at ambient temperature can be achieved. In the initial test period module 2 was kept supercooled for 39 days before solidification was activated to discharge the heat of fusion [3].

The modules were installed in such a way that they could be tested individually and maintenance to each module was possible. Therefore the large surface-volume ratio of a single PCM module results in unfavourable fast cool-down. The specific heat losses of modules can be potentially, dramatically reduced by putting the flat modules together into a compact unit. In this way heat storage for short- and for long term application could be achieved.

4. Conclusions

Stable supercooling was achieved in three out of four modules after they were charged with solar collectors as a fluctuating heat source. Module no. 1, module no. 2 and module no. 3 have been successfully recharged and cooled down to 30°C in the same period. Recharge from supercooled state did not cause spontaneous solidification.

Single module charge showed that heat transfer rates allowed fast module charge from cold, solid state to melted state. Module no.1 can be charged within 270 minutes on a sunny afternoon. The development of heat transfer rates was strongly linked to the solar irradiance. During charge all pipework temperatures in the system were increasing due to the melting behavior of the PCM modules.

Because heat exchange capacity rates during charge of one module with solid PCM were only about 250 W/K, parallel module charge was necessary in long periods of sunshine. Therefore the heat storage must be designed for single and parallel module charge.

Long-term tests will show if spontaneous activation will appear during winter.

5. Acknowledgements

This research was funded by the European Commission (Grant Agreement N_ 295568) as part of the Seventh Framework Programme of the European Community for Research, Technological Development and Demonstration Activities under the funding scheme of “Collaborative Project” through the COMTES consortium. The work was also supported by the PhD program of the Sino Danish Center for Education and Research (SDC).

We thank our partners from Nilan A/S and the Graz University of Technology for sharing knowledge and discussions as well as the research technicians Troels V. Kristensen and Claus Aagaard for their practical support.

6. References

[1] B. Sandnes, J. Rekstad, Supercooling salt hydrates: Stored enthalpy as a function of temperature, Sol. Energy. 80 (2006) 616–625. doi:10.1016/j.solener.2004.11.014.

[2] M. Dannemand, W. Kong, J. Fan, J.B. Johansen, S. Furbo, Laboratory Test of a Prototype Heat Storage Module Based on Stable Supercooling of Sodium Acetate Trihydrate, Energy Procedia. 70 (2015) 172–181. doi:10.1016/j.egypro.2015.02.113.

[3] J. B. Johansen, G. Englmair, M. Dannemand, W. Kong, J. Fan, J. Dragsted, B. Perers, S. Furbo, Laboratory Testing of Solar Combi System with Compact Long Term PCM Heat Storage, presented at the International Conference on Solar Heating and Cooling for Buildings and Industry, SHC 2015, and pending publication.

[4] M. Dannemand, J.M. Schultz, J.B. Johansen, S. Furbo, Long term thermal energy storage with stable supercooled sodium acetate trihydrate, Appl. Therm. Eng. 91 (2015) 671–678. doi:10.1016/j.applthermaleng.2015.08.055.

[5] M. Dannemand, J.B. Johansen, S. Furbo, Solidification Behaviour and Thermal Conductivity of Bulk Sodium Acetate Trihydrate Mixtures with Thickening Agents and Graphite Powder, Sol. Energy Mater. Sol. Cells. (2015). doi:10.1016/j.solmat.2015.10.038.

The phase change material (PCM) sodium acetate trihydrate (SAT) melts at 58 °C. The melting process requires a significant amount of energy. SAT can cool down below the melting point and remain in liquid state. When the SAT remains in this supercooled state in temperature equilibrium with the ambient, the energy used for the melting is stored without additional heat losses. When the solidification of the SAT is started, the temperature of the SAT rises to the melting temperature and the stored heat is released. Utilizing this principle makes it possible to store heat seasonally.

DTU Civil Engineering
Technical University of Denmark

Brovej, Bygning 118
2800 Kongens Lyngby

www.byg.dtu.dk

ISBN 9788778774354
ISSN 1601-2917